

# Hydrogenation Catalyst and Anti-Microbial Material Synthesized from Vietnamese Rice Husk

PhD Thesis

for the Acquirement of the Degree

*Doctor rerum naturalium (Dr. rer. nat.)*

of the Faculty for Mathematics and Natural Sciences

of the University of Rostock

submitted by Felix Unglaube, born 12<sup>th</sup> December 1993 in Bad Saarow-Pieskow

Rostock, 12<sup>th</sup> May 2023

“You may ask what is the use of my deeds when they are proved useless.”

John Ronald Reuel Tolkien

## Statement of Authorship

Herewith I declare that this thesis is the result of my independent work. All sources and auxiliary materials used for this report are cited completely.

---

Rostock, 12th May 2023

This thesis was produced in the time from Dec. 2018 to Dec. 2021 in the group of Dr. habil. Esteban Mejia at the Leibniz Institute for Catalysis, Rostock.

**Erster Gutachter:** PD Dr. habil. Esteban Mejía  
Leibniz Institute for Catalysis  
Department Polymer Chemistry and Catalysis  
18059 Rostock, Germany

**Zweiter Gutachter:** Prof. Dr. Le Thanh Son  
VNU University of Science  
Faculty of Chemistry  
10999 Hanoi, Vietnam

**Eingereicht am:** 12.05.2023

**Datum der Verteidigung:** 07.11.2023



## Acknowledgements

Mein besonderer Dank gilt meinem Doktorvater PD Dr. habil. Esteban Mejia, einerseits für die Erstellung des Erstgutachtens dieser Arbeit, aber insbesondere für das in mich gesetzte Vertrauen, die jahrelange Zusammenarbeit, für jedes kreative und kritische Gespräch, für das Öffnen zahlloser Türen und für das Vorleben von wissenschaftlicher Neugierde, Leidenschaft und einer bewundernswerten Gelassenheit. Nichts davon war oder ist für mich je selbstverständlich gewesen, umso tiefer ist meine aufrichtige Dankbarkeit.

Bei Prof. Dr. Udo Kragl bedanken ich mich für die Aufnahme in den Arbeitskreis, Förderung und Ermutigung, an mir zu wachsen.

Ich danke der gesamten Abteilung für Analytik des Likats, für die zahllosen und wertvollen Gespräche, Hinweise und Diskussionen, sowie die zuverlässige Unterstützung. Mein besonderer Dank gilt: Carsten Robert Kreyenschulte, Hendrik Lund, Kathleen Schubert, Reinhard Eckelt, Hanan Atia, Stephan Bartling und Christine Fischer. Bei meinen zahlreichen Projekt- und Kooperationspartnern im Suvalig Projekt bedanke ich mich für die lehrreiche Zusammenarbeit. Darüber hinaus danke ich Alexander Lammers und Prof. Michael Lalk für die fruchtbare gemeinsame Arbeit.

I would like to thank all my Vietnamese colleagues and cooperation partners, especially, Prof. Le Minh Thang and Dr. Nguyen Ngoc Mai for their kind hospitality and for opening so many doors in a very different world, which I now feel much closer to.

Für die produktive Arbeitsatmosphäre im Likat möchte ich mich bei allen aktuellen und ehemaligen Mitgliedern des Arbeitskreis Mejia bedanken. Besonderer Dank an dieser Stelle gilt Rok und Swarup für so Vieles, was ich lernen durfte, Paul und Janina für die produktive Zusammenarbeit und Marc für die unermüdliche Hilfe.

Mein Dank gilt allen Freunden, die mich auf dem Weg zur Promotion begleitet haben. Ohne euch wäre die Zeit in Rostock deutlich langweiliger gewesen. Ich will an dieser Stelle nur eine Hand voll nennen (in order of appearance): Ronja, Erik, Alex, Felix und Isa. Besonders möchte ich mich bei meiner Partnerin Isa bedanken, für die gemeinsame Zeit, für alle Höhen und Tiefen, die ich mit dir erleben durfte.

Fabian, Julia, Ines und Memmel möchte ich für Jahre der bedingungslosen Unterstützung, Liebe und Hilfe danken. Ohne euch wäre diese Arbeit nicht zustande gekommen.

Vielen Dank.

## Abstract

This work presents the utilization of rice husk for the synthesis of catalytic as well as anti-microbially active materials. The rice husk was doped with salts or metal organic complexes, which acted as metal source and was consecutively chemically converted *via* pyrolysis. The prepared materials were composed of a carbon silica support doped with metal nanoparticles.

Ag-, Co- and Ni-doped systems were applied in catalytic hydrogenation reactions. Ag- and Co-based systems proved to be highly active in the selective conversion of nitro compounds to amines. For the Ag-based system,  $\text{AgNO}_3$  was used as metal source, while for the Co-based system, N-rich metal complexes were used. The catalyst synthesis was further improved by modifying the catalyst by base leaching. This led to a drastically improved catalytic performance. Furthermore, the scope of accessible hydrogenation reactions using rice husk-based catalysts was extended by applying the Ni-based catalyst (with Ni-salts as metal source) to the reductive conversion of epoxides to anti-Markovnikov alcohols in a highly selective manner. The prepared materials were characterized by microscopic techniques (SEM and STEM), spectroscopic methods (XPS, IR and EDX-mapping), thermal sorption analytics (TPx and BET-methods), TGA and DSC as well as XRD. The catalytic tests included reaction optimization, broad substrate screenings and kinetic as well as mechanistic studies.

Additionally, the Ag-doped material was tested as an anti-microbial agent against the ESKAPE pathogens (Enterococcus faecium, Staphylococcus aureus, Klebsiella pneumonia, Acinetobacter baumannii, Pseudomonas aeruginosa, Escherichia coli) and the pathogenic yeast Candida albicans. The tests proved activity against all pathogens using extremely low Ag-concentrations.

## Zusammenfassung

Diese Arbeit beschäftigt sich mit der Nutzung von Reisspelze für die Synthese von katalytisch- und anti-mikrobiell aktivem Material. Die Reisspelzen wurden mit Metallsalzen bzw. metallorganischen Komplexverbindungen imprägniert und anschließend durch Pyrolyseprozesse chemisch umgewandelt. Die hergestellten Materialien setzen sich aus einem Kohlenstoff/Silica Komposit-Trägermaterial dotiert mit Metall Nanopartikeln zusammen.

Mit Ag, Co und Ni dotierte Materialien konnten in katalytischen Hydrierreaktionen angewendet werden. Die Ag- und Co-basierten Katalysatoren zeigten hohe Aktivität in der selektiven Umwandlung von Nitro-Verbindungen zu Aminen. Während der Ag-basierte Katalysator  $\text{AgNO}_3$  als Metallquelle nutzt, wurde für den Co-basierten Katalysator auf N-reiche, metallorganische Komplexverbindungen zurückgegriffen. Dies führte zu einer deutlich verbesserten katalytischen Performance. Darüber hinaus wurde demonstriert, dass weitere Hydrierreaktionen zugänglich sind, indem der Ni-basierte Katalysator (basierend auf  $\text{NiNO}_3$ ) in der reduktiven Umwandlung von Epoxiden zu anti-Markovnikov Alkoholen angewendet wurde. Die hergestellten Materialien wurden mit einer Vielzahl von mikroskopischen (SEM und STEM) und spektroskopischen (XPS, IR and EDX-mapping) Techniken und durch thermale Sorption (TPx and BET-Methoden), TGA und DSC sowie XRD charakterisiert. Die katalytischen Untersuchungen umfassen neben der Optimierung der Reaktionsbedingungen und ausführlichem Substrate Screening auch kinetische und mechanistische Untersuchungen.

Außerdem wurde das Ag-basierte System auf seine anti-mikrobielle Wirkung gegen die ESKAPE Pathogene (*Enterococcus faecium*, *Staphylococcus aureus*, *Klebsiella pneumoniae*, *Acinetobacter baumannii*, *Pseudomonas aeruginosa*, *Escherichia coli*) und die pathogene Hefe *Candida albicans* untersucht. Die Untersuchungen demonstrierten eine starke Wirksamkeit des Materials gegen alle Pathogene, auch bei stark erniedrigtem Silbergehalt.

## Table of Contents

Preamble .....	1
Aim and sustainable development goals (SDG) .....	1
1 Introduction .....	1
1.1 Catalysis .....	2
1.1.1 General definition.....	2
1.1.2 Heterogeneous Catalysis .....	3
1.1.3 Hydrogenation Catalysis .....	4
1.2 Rice husk and agriculture waste .....	5
1.3 Utilization of rice husk and straw as bio-derived feedstock .....	9
1.3.1 General introduction .....	9
1.3.2 Non-catalytic applications .....	9
1.3.3 Catalytic application .....	11
1.4 Applications in Heterogeneous Catalysis.....	13
1.4.1 Hydrogenation of nitro compounds .....	13
1.4.2 Reductive synthesis of anti-Markovnikov alcohols from epoxides..	15
2 Results and Discussion .....	17
2.1 Preliminary Rice husk treatment .....	17
2.2 Silver containing materials .....	18
2.2.1 Preparation and characterization.....	18
2.2.2 Application as hydrogenation catalyst.....	20
2.2.3 Application as antimicrobial agent .....	24
2.3 Cobalt containing materials .....	27
2.3.1 Preparation and characterization.....	27
2.3.2 Application as hydrogenation catalyst.....	30
2.4 Nickel containing materials.....	34
2.4.1 Preparation and characterization .....	34
2.4.2 Application as hydrogenation catalyst .....	36
3 Conclusion and Outlook .....	39
Appendix .....	40
References.....	40
Original Publications.....	56
Development and Application of Efficient Ag-based Hydrogenation Catalysts Prepared from Rice Husk Waste .....	58
Preparation, Characterization and Antimicrobial Properties of Nanosized Silver-Containing Carbon/Silica Composites from Rice Husk Waste .....	68

Highly Active Heterogenous Hydrogenation Catalysts Prepared from Cobalt Complexes and Rice Husk Waste .....	76
Hydrogenation of Epoxides to Anti-Markovnikov Alcohols over a Nickel Heterogenous Catalyst Prepared from Biomass (Rice) Waste ...	91

## List of Abbreviations

<b>ABF</b>	annular bright field
<b>AIBN</b>	2-(azo(1-cyano-1-methylethyl))-2-methylpropane nitrile
<b>anti-MA</b>	anti-Markovnikov alcohol
<b>BET</b>	Brunauer-Emmett-Teller
<b>E<sub>a</sub></b>	activation energy
<b>ESKAPE</b>	<i>Acronym for Enterococcus faecium, Staphylococcus aureus, Klebsiella pneumoniae, Acinetobacter baumannii, Pseudomonas aeruginosa and Escherichia coli</i>
<b>HAADF</b>	high-angle annular dark-field imaging
<b>ICP-OES</b>	inductively coupled plasma optical emission spectroscopy
<b>IR</b>	infrared spectroscopy
<b>MCM-41</b>	Mobil Composition of Matter No. 41
<b>NP</b>	nanoparticles
<b>RH</b>	rice husk
<b>SDG</b>	sustainable development goals
<b>SEM</b>	scanning electron microscopy
<b>STEM</b>	scanning transmission electron microscope
<b>TEM</b>	transmission electron microscopy
<b>THF</b>	tetrahydrofuran
<b>TPD</b>	temperature programmed desorption
<b>XPS</b>	X-ray photoelectron spectroscopy
<b>XRD</b>	X-ray diffraction
<b>ZOI</b>	zone of inhibition
<b>ZSM-5</b>	Zeolite Socony Mobil-5

Units and element symbols are not included in the list of abbreviations.







## Preamble

### Aim and Sustainable Development Goals (SDG)

This work is a contribution to a more sustainable use of resources in the future. It is especially focused on the development of catalysts from rice husk for industrially relevant processes. The term “sustainability” is currently defined by the Oxford English Dictionary as “the degree to which a process or enterprise is able to be maintained or continued while avoiding the long-term depletion of natural resources”.<sup>1</sup> The term has been excessively used by various organizations since the beginning of the 21<sup>st</sup> century. This excessive use has led to dilution and unclear reinterpretations, in short: it has become a buzzword. Nevertheless, the concept of using resources and designing processes in a way that ensures the sustenance of resources for further generations and not maneuvering them into life-threatening shortages has proven to be the initiator for fundamental changes in almost every aspect of human cohabitation. The way we think about the production of energy, food and consumer products has been changed drastically. In view of the above definition of sustainability, the developments of this work are required to use a resource in a way that enables the developed processes to be maintained in the future.

Useful tools for the conceptualization of a sustainable development are the sustainable development goals (SDG) set by the general assembly of the United Nations in 2015. They are probably the most prominent example for using the concept of sustainability in a strategic plan for the future of mankind. The SDG are 17 objectives, which are referred to as “blueprints to achieve a [...] more sustainable future”.<sup>2</sup> The main reason for the emergence of plans like the SDG and the excessive use of the term “sustainability” is the increased awareness of the drastic changes of the environment (e.g. climate change and resource depletion) caused by industrialization within the last 200 years. The chemical industry, for example, is currently depending on fossil fuels to generate the required energy to conduct processes, and most of the produced organic structures originate from refined oil.<sup>3</sup> This is highly problematic since the use of fossil fuels is one of the main reasons for the mentioned drastic changes of the environment.<sup>4</sup> Thus, the chemical industry has to be transformed. This can be achieved by decreasing the required energy to maintain processes and by replacing chemicals that do not meet the definition of sustainability by the utilization of alternative resources.

This work, which aims to use the agricultural waste product rice husk, for the synthesis of catalytically active materials, does both: 1) utilizing a resource growing on fields and 2) lowering the energy requirements of chemical processes by using a catalyst.

# 1 Introduction

## 1.1 Catalysis

### 1.1.1 General Definition

The term “catalyst” (from greek “καταλύειν” – “to untie”) was defined by Ostwald in 1894<sup>5</sup> as a material that increases the speed of a chemical reaction without being consumed and without changing the final location of the thermodynamic reaction equilibrium. Sabatier later refined the term “catalysis” in what is today known as Sabatier’s law.<sup>6</sup> His key assumption is that the reaction educts are adsorbed onto the catalyst surface (1 in figure 1), are activated and form intermediates. These intermediates must be stable enough to be formed, but not stable enough to form a non-reactive compound. Through this, they enable rearrangement and recombination of the adsorbed species into the desired product, which is later on desorbed from the catalyst surface.

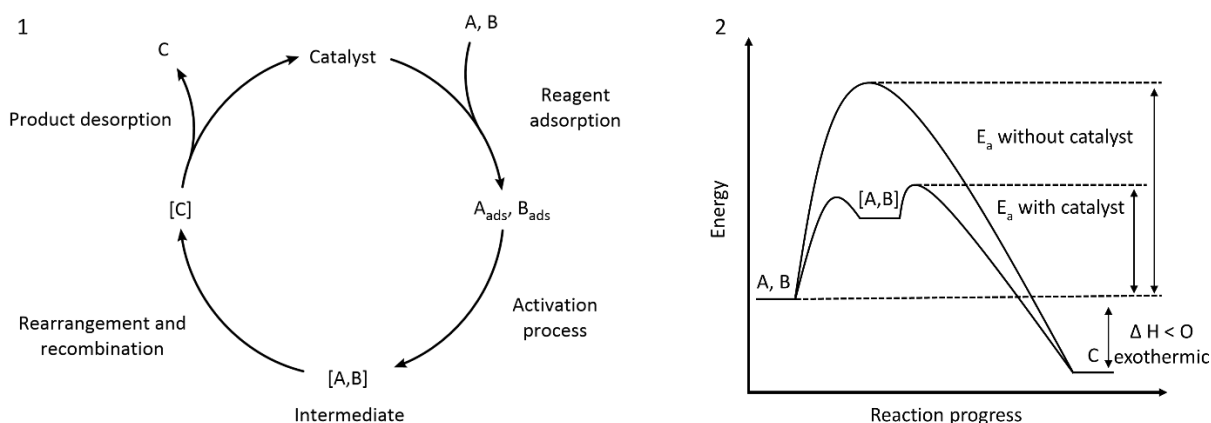


Figure 1 Representation of Sabatier’s law showing the cyclic nature of a catalytic heterogeneous reaction (A) and an energy scheme for a reaction with and without the use of a catalyst (B).<sup>6</sup>

The formation of the intermediates leads to a lower activation energy ( $E_a$ ) compared to the uncatalyzed reaction and, thus, catalysis is a purely kinetic phenomenon (2 in figure 1). With this definition, Sabatier established a view on catalysis that is the foundation for all work in the field and has been validated by many studies and modern methods. This fundamental principle can be applied to all types of catalyzed reactions, for example to reductions. Reduction reactions are among the most important transformations in synthetic chemistry and the use of hydrogen as reducing agent is extremely popular.<sup>7</sup> There are various industrially important reduction reactions that use hydrogen, e.g., the hydrotreating of the distilled fraction of crude oil. This treatment enables an easier removal of metal atoms and heteroatoms, especially of sulfur and nitrogen,<sup>8</sup> which is

important to ensure the quality of products derived from crude oil. Other examples for large scale applications are the hydrogenation of fats<sup>9</sup> or the reduction of adiponitrile to hexamethylenediamine.<sup>10</sup> Apart from the described large-scale applications, there are a number of small-scale transformations in organic chemistry used for the synthesis of chemicals with special applications, e.g. pharmaceuticals or platform chemicals.<sup>11</sup> Additionally, the utilization of hydrogen in the synthesis of energy carriers has become more and more important since the beginning of the 21<sup>st</sup> century, as it is a key step in the development of the so-called hydrogen economy.<sup>12</sup> Even though all described examples can be conducted with heterogeneous catalysts, it must be pointed out that homogeneous catalysts are also of great relevance in the chemical industry.<sup>13</sup> However, this chapter will only put further focus on heterogeneous systems, since this work only addresses the development of heterogeneous catalysts.

### 1.1.2 Heterogeneous Catalysis

The definition of a heterogeneous catalyst includes that the catalyst is present in a different phase than the reactants<sup>14</sup> while, in contrast, a homogeneous catalyst is present in the same phase as the reactants.<sup>15</sup> A heterogeneous catalyst is, in most cases, a solid material used in a gas- or liquid phase reaction. The solid catalyst is often composed of 1) the active centers/sites on which the chemical rearrangement and recombination of the reactants takes place and 2) the supporting material, which is the stable carrier of active centers. However, even though the support is usually a chemically inert material, it is of critical importance for the catalytic performance and contributes to the chemical transformation. Heterogeneous catalysts have considerable advantages over homogeneous systems (figure 2).

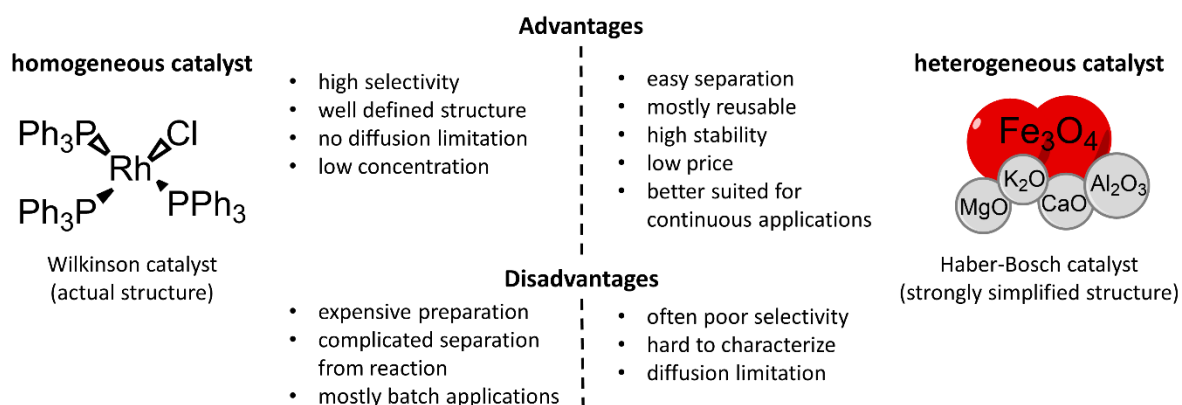


Figure 2 Comparison of homogeneous and heterogeneous catalysts.

They are usually more stable and, thus, tolerate extremely harsh reaction conditions. However, this aspect can be a disadvantage as well since high temperatures may be required for good catalyst activity. High temperatures are not tolerated by every

substrate. Furthermore, there are different possible deactivation mechanisms for heterogeneous catalysts associated with high temperatures, e.g. coking and particle migration.<sup>16</sup> Nevertheless, a major advantage in terms of downstream processing is the easy separation of the catalyst, consequently enabling, the possibility to recycle the catalyst. Despite these advantages, homogeneous catalysts are sometimes preferable, since they enable more precise control of the reaction selectivity. Hence, improvement of product selectivity is a major obstacle when designing a heterogeneous catalyst.

### 1.1.3 Hydrogenation Catalysis

When developing and designing a catalyst for a certain reaction, it is crucial to understand the mode under which catalysts operate. For that purpose, Sabatier's law<sup>6</sup> can be used as a blueprint to reach a comprehensive understanding of catalytic reactions, in this case hydrogenation reactions. The first step of a catalytic hydrogenation is the adsorption and activation of the reagents on the catalyst. The adsorption and activation of most organic molecules is achieved relatively easily, especially if the catalyst surface provides a form of attractive interaction, e.g.,  $\pi$ -stacking. Nevertheless, the selective activation of a certain targeted bond in an organic molecule can be challenging. Furthermore, as second step, the adsorption and consecutive activation of the reducing agent (i. e. hydrogen) must take place as well (not necessarily in this order; it is also possible that the catalyst surface is loaded with hydrogen first and is adsorbed onto the substrate in a second step). However, in most cases, this second step is the more critical one, since the bond dissociation energy of the strong, non-polarized H-H bond is high compared to more polar bonds, e.g. C-H bonds. The third step, the intermediate formation and recombination is, in most cases, a cascade of elementary surface reactions, which depend on the environment offered by the catalyst surface as well as on the energy states of possible reaction intermediates. For hydrogenation reactions, the transfer of a hydride species from the catalyst surface onto the targeted moiety is the critical step. Finally, the product desorption takes place, which is dependent on its physicochemical desorption equilibrium. This is very rarely a limitation for the reaction, unless an irreversible chemical adsorption of the product occurs.

Noble transition metals, especially those with not fully occupied d-orbitals, e.g., Pd or Pt, are suited for the activation of hydrogen and, thus, are frequently applied in hydrogenation reactions.<sup>6</sup> The activation takes place because their surface electrons can rapidly populate antibonding H<sub>2</sub> orbitals, facilitating H-H bond dissociation.<sup>17</sup> Hence, reduction catalysts like Pd on activated carbon have become standard systems in organic synthesis, especially for the hydrogenation of unsaturated C-C bonds.<sup>18</sup> These catalysts are reliable, easy to handle, and can usually be used at ambient conditions.<sup>19</sup> However,

their application also has decisive disadvantages, the foremost being that they are extremely expensive. Additionally, the high activity of noble metal catalysts in hydrogenation reactions can cause selectivity issues due to over-hydrogenation. For example, the reductive dehalogenation of substrates bearing aryl halide moieties or the dearomatization of phenyl groups are frequently reported problems.<sup>20</sup> Another socioeconomic and environmental drawback of noble metals is associated with their mining. Metal mining can have a drastic and mostly negative impact on many levels. The nature of the impact is often dependent on the mining form and can include high energy demand effecting significant CO<sub>2</sub> emissions,<sup>21</sup> use of potentially toxic compounds, metal discharge into the environment<sup>22</sup> and, last but not least, a negative social impact on people living in the mining area.<sup>23</sup> Nevertheless, a strong impact in terms of CO<sub>2</sub> emissions and environmental pollution is especially associated with rare elements like Pt, Pd, Ru or Au.<sup>21, 22, 23, 24</sup> Thus, there have been intensive efforts to develop catalytic systems that use more abundant metals as active centers in order to make catalytic process more sustainable.<sup>25, 26</sup>

## 1.2 Rice Husk and Agriculture Waste

Rice husk (RH), which is the main feedstock for the catalyst support preparation in this thesis, is the main waste product of rice production beside rice straw. Rice (*Oryza sativa*) or *paddy* is the third most produced crop on earth after wheat and corn, with an annual production of 498.3 million tons in absolute numbers (figure 3).<sup>27</sup> It is cultivated on an area of 1.6 million km<sup>2</sup>,<sup>27</sup> which is more than four times the area of Germany.

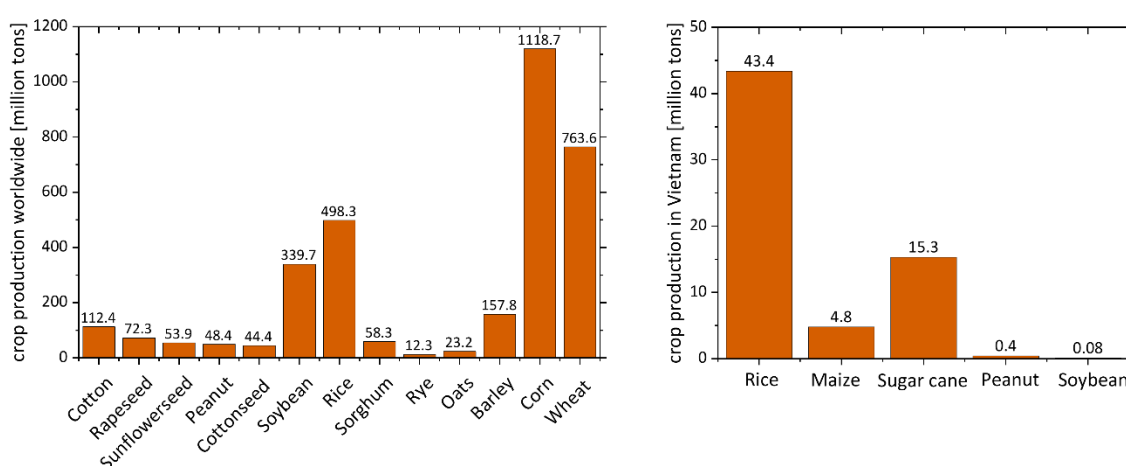


Figure 3 Production of crops worldwide<sup>27</sup> (left) and crop production in Vietnam<sup>28</sup> (right) in 2019.

The majority of rice is harvested on fields in Asia (approximately 443 million tons)<sup>27</sup> and it is considered the main source of calories for the two most populated countries in the

world, China and India, which alone harbor a third of the world population. Thus, rice production is vital for the nutrition of humanity. The scale on which it is produced is enormous and so is the amount of waste accruing due to its cultivation. The rice husk used for the work presented in this thesis was collected in Vietnam. Rice is the most important crop produced in Vietnam, which is depending on rice as nutrition source, like most Asian countries (figure 3).<sup>28</sup> The focus of this work is on rice husk, which is the protecting layer of the grain. It accumulates after the paddy ear is removed from the straw, dried and separated into grain and husk by milling in so-called husking machines. Around 20 to 25 wt% of the paddy ear is accounted to husk.<sup>29</sup> The overall amount of agricultural residues due to rice production is approximated with 800 million tons annually<sup>30</sup> and approximately 16 wt% of this waste is rice husk. Hence, the overall production of husk can be estimated to be around 135 million tons per year.<sup>31</sup>

The main purpose of the husk is to protect the rice grain. Thus, it has to be mechanically and biologically stable. The stability of rice husk is reflected in its composition. Rice husk is mainly composed of cellulose, lignin, hemicellulose and ash (figure 4). The share of hemicellulose (22 to 30 %) is low compared to softer natural fibers like bagasse (56 wt%).<sup>32</sup> A low hemicellulose share is often associated with more rigid plant parts like trunks or other supporting structures. However, the lignin and cellulose shares are surprisingly low, compared to other natural fibers that are designed by nature to protect the fruit body. For example: coconut coir, well known for being a mechanically resistant material has a lignin share of 32 wt%,<sup>33</sup> about 10 wt% higher than rice husk.

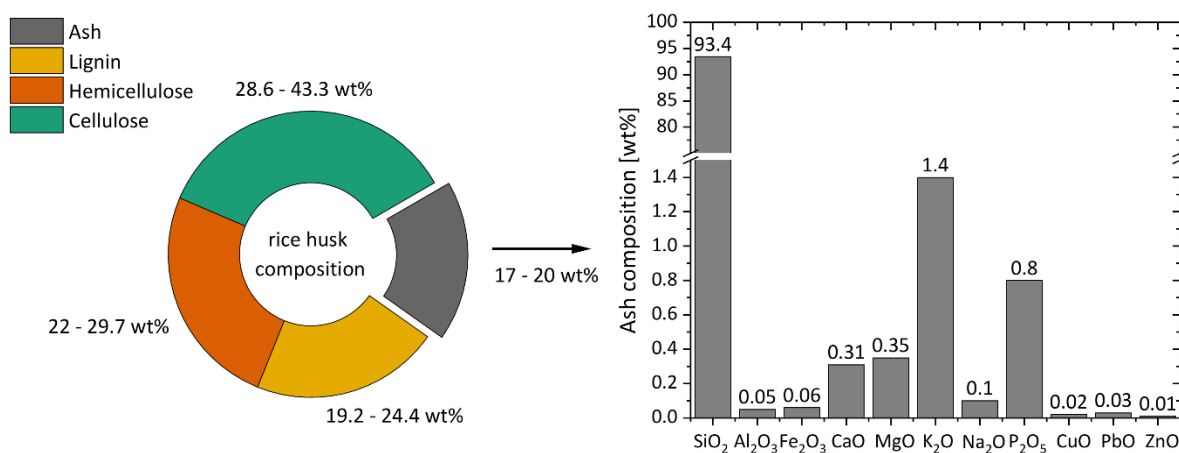


Figure 4 Rice husk (left) and rice husk ash (right) composition.<sup>32</sup>

Nevertheless, rice husk is well suited to protect the rice grain. This is due to the high content of what is usually referred to as ash. Ash is a collective term for everything that is left after the material is burned under atmospheric conditions. In the case of rice husk, most of the ash (93 wt%) is SiO<sub>2</sub> (figure 4). The remains are other nonflammable residues, especially oxides of alkaline- and alkaline earth metals, but also metal oxides like Al<sub>2</sub>O<sub>3</sub> and Fe<sub>2</sub>O<sub>3</sub> as well as phosphorus in oxidized form.

The fact that silica is found in living organisms and in plants in particular has been known to the scientific community since the beginning of the 19<sup>th</sup> century.<sup>34</sup> It is important to be aware of how and where nature incorporates silica into plants. This knowledge is the basis to be able to change the structure, and consequently, the properties, of materials derived from such plants can be changed, as described in this thesis.

The silica uptake by different species like diatoms<sup>35</sup> and terrestrial plants<sup>36</sup> from sediment always starts with the chemical dissolution of SiO<sub>2</sub> into orthosilicic acid (figure 5). The concentration of orthosilicic acid in marine and terrestrial water is in a range of 10<sup>-4</sup> to 10<sup>-3</sup> mol l<sup>-1</sup>.<sup>37</sup> This H<sub>4</sub>SiO<sub>4</sub> can move across plasma membranes of plant roots at biological pH.<sup>38</sup> Following the uptake in the roots,<sup>39</sup> the H<sub>4</sub>SiO<sub>4</sub> is transported to the shoots and distributed by the plant nodes. Finally, the H<sub>4</sub>SiO<sub>4</sub> reaches the panicles and starts to accumulate until concentrations of 2·10<sup>-3</sup> mol l<sup>-1</sup> are exceeded.<sup>40</sup> The orthosilicic acid starts to condensate into di-, tetracyclo- and polysilicic acid as a consequence of this high concentration (figure 5). The polysilicic acid forms colloidal silica and accumulates by eliminating water. The silica particles start to form a dense layer of 2.5 µm thickness beneath the cuticle layer<sup>41</sup> and the water leaves the plant by humidification. The amorphous silica particles lose more and more water over time, which increases mechanical stability.

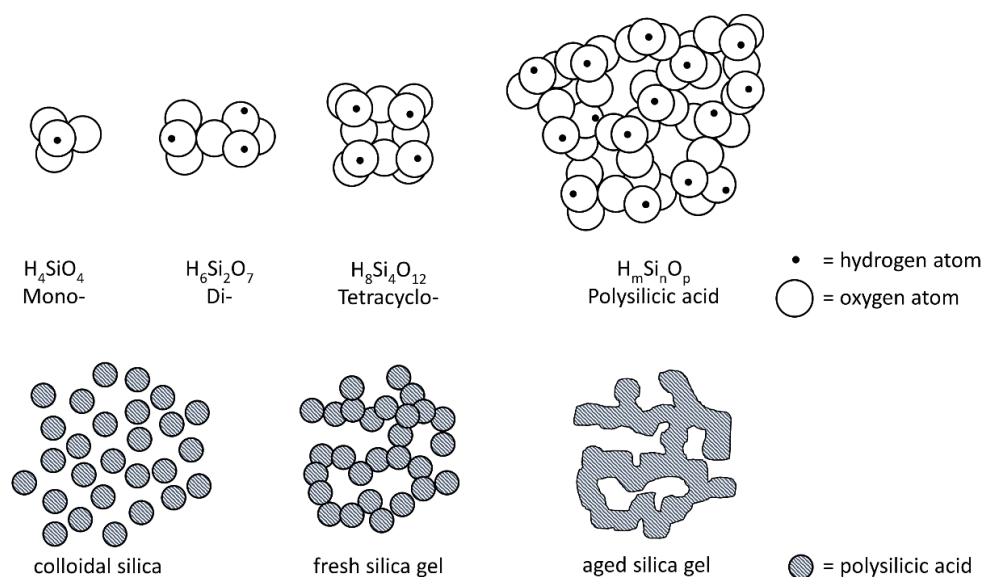
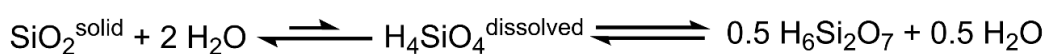


Figure 5 Conversion of SiO<sub>2</sub> into structures formed by silica gel.

The silica particles lower abiotic and biotic stressors by increasing mechanical stability and, thus, increase resistance of plants to pests and diseases.<sup>42</sup> Especially in the marine environment, several organisms rely on the utilization of Si in the form of SiO<sub>2</sub>. For example, diatoms sequester 240 Tmol of Si yr<sup>-1</sup>.<sup>43</sup> However, recent studies pointed out

that plants in the major terrestrial biomes also fix a total amount of  $84 \text{ Tmol Si yr}^{-1}$  and that most terrestrial Si is indeed fixed on cultivated land ( $29 \text{ Tmol Si yr}^{-1}$ ). The highest share of Si is considered to be fixed by members of the order of *Poales*, which includes i.e., grasses, sedges and the three main crops produced on Earth (figure 3).

However, beside the described advantages of a high silica content in rice husk, there are also disadvantages. They mainly lie at the end of the rice production chain: in the waste management. The high stability and stress resilience of the plant material entails a tendency for slow composting.<sup>44</sup> This is extremely problematic when taking into account the sheer amount of waste, because it would take too much time to compost the rice husk waste. Hence, composting of rice husk in the slow traditional way and reutilization as fertilizer is not practicable, even though the use as fertilizer would be generally beneficial for the rice production. Thus, the decomposition must be sped up or the rice husk must be transformed for repatriation in an exploitation chain. The current approach by rice farmers all over the world to deal with the plant waste is the open burning on the fields or the burning in furnaces, which is a form of faster decomposition (figure 6).



Figure 6 Burning of rice production residuals in Vietnam.<sup>45</sup>

The method is fairly straightforward because it does not require sophisticated machines and it is simply the fastest way to deal with the waste. Additionally, the resulting ash simultaneously acts as fertilizer, since it contains essential nutrients for the next generation of plant e.g. Si and P (as shown in figure 4). However, this practice is responsible for massive air pollution, drastically affecting the air quality in all rice growing regions such as China, India and Vietnam.<sup>46</sup> The pollution is a health risk for humans and has a negative environmental impact due to massive  $\text{CO}_2$  and particulate matter emission. Moreover, it affects the rice production itself, since recent studies indicated a correlation of high air pollution levels with low rice yields.<sup>47</sup> Hence, it is not only in the interest of human health and environmental conditions but also economically reasonable to find alternative ways of waste treatment in order to decrease the burden caused by rice production.



## 1.3 Utilization of Rice Husk and Straw as Bio-Derived Feedstock

### 1.3.1 General Introduction

The problem of dealing with RH as a waste product is not a new challenge. In fact, it is very old, since the origin of rice domestication can be dated back 8200<sup>48</sup> to 13500<sup>49</sup> years ago. Hence, it seems reasonable to assume that RH has been used for centuries for different purposes due to the fact that a separation of the husk from the grain was necessary at any given historic stage of rice consumption.<sup>50</sup> Generally, the use of RH can be divided into approaches that convert RH into a working material and approaches utilizing energy generated by burning RH or derivatives of it (figure 7).<sup>32</sup>

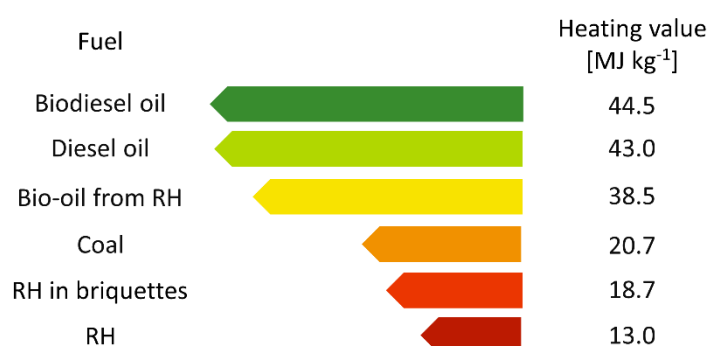


Figure 7 Heating value of RH compared to other fuels.<sup>32, 59, 60</sup>

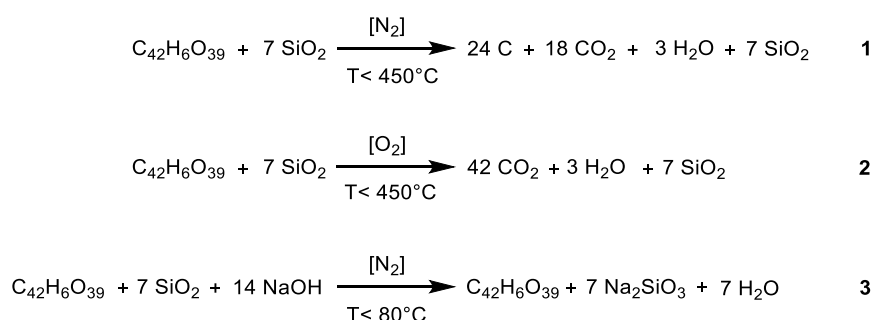
The earliest well-documented example of research on RH utilization is a German patent from 1924,<sup>51</sup> describing the use of RH as an additive for concrete.<sup>52</sup> This application has caught more and more attention in recent years due to its potential to replace the widespread Portland concrete.<sup>53, 54</sup> Besides, there are other uses that cannot be historically dated back accurately. The use of rice husk ash in ancient ceramic glazes is mentioned in literature.<sup>55</sup> Rice bran oil<sup>56</sup> (produced from RH through different extraction methodologies)<sup>57</sup> is produced since the 1950s on a large industrial scale, but was popular long before that.<sup>50</sup>

### 1.3.2 Non-Catalytic Applications

The burning of RH is an exothermic process and, therefore, energy is generated by it. Thus, burning for energy production is perhaps the most obvious way to deal with the RH waste, since it is common practice in the countryside. Nevertheless, the burning of pure RH is not favored from an energetical point of view, due to its low caloric value of 13 to 18.7 MJ kg<sup>-1</sup>.<sup>58</sup> Material synthesis from RH can be conducted 1) by separating RH into its constituents and consecutively utilizing them separately or 2) by using the RH as a whole.

The separation of RH into its main constituents carbon and silica is possible by various methods.<sup>61</sup> Most procedures start with pyrolysis of the RH under inert conditions (1 in scheme 1) or the burning of RH under aerobic conditions (2 in scheme 1), which leads to complete decarbonization of the material and mainly yields amorphous SiO<sub>2</sub> as residue. However, silica obtained by this approach is not directly used for application, since it contains impurities of other metal oxides.

One of the most popular down-stream treatment for unpurified silica from RH is etching (often also referred to as leaching, which is a more general term).<sup>1</sup> This process includes the selective removal of silica by converting it to a soluble form. This reverses, the natural silica deposition that was described above, is reversed. However, the conversion of SiO<sub>2</sub> into H<sub>4</sub>SiO<sub>4</sub> is very slow and, therefore, not suitable for technical application.<sup>40</sup> Hence, silica is usually removed by using base to convert it into the corresponding silicate, which can be extracted due to its good water solubility.<sup>62</sup> If a carbon-based material is to be synthesized, silica is removed in an analogous manner (3 in scheme 1). Nevertheless, a major drawback of this separation approach is its demand for high amounts of chemicals, energy and time, as well as the production of copious amounts of waste water.<sup>64-68</sup> The utilization approaches presented in this work use RH as a whole with two purposes: synthesis of 1) materials with antimicrobial activity and 2) hydrogenation catalysts.



Scheme 1 Reaction equations for 1) RH pyrolysis, 2) RH burning and 3) RH base leaching.<sup>63</sup>

The application of RH-derived materials as antimicrobial agents is mainly motivated by the fact that approximately 780 Million people (current state in 2014)<sup>69</sup> do not have access to clean drinking water. Beside chemical pollution, bacterial contamination is a major reason for poor drinking water quality. There are already several examples describing the loading of active carbon from RH with antimicrobial agents for water purification.<sup>66, 70</sup> Analogous to the RH-derived carbon materials, there are also examples of silica materials from RH, e.g. pseudowollastonite,<sup>64</sup> SiC,<sup>65</sup> pure silica<sup>66, 67</sup> or MCM-41<sup>68</sup>, which act as a carrier for antimicrobial agents, such as Ag nanoparticles (NP).

This thesis also presents the use of RH-derived material with Ag as an antimicrobial agent. The anti-microbial properties of Ag have been long known. Already Herodot<sup>71</sup> mentioned the use of Ag vessels for water storage by Romans and Persians to ensure the quality of

drinking water.<sup>72</sup> However, since the development of highly effective antibiotics, Ag has become less important as an antimicrobial agent. Nevertheless, the world is currently facing a global microbial resistance crisis due to intensive and inappropriate usage of antibiotics.<sup>73, 74</sup> The number of microbial strains in 2018 that developed resistance to the majority of antibiotics is increasing drastically and, approximately 700 000 people have died from infections caused by resistant pathogens.<sup>74</sup> It is estimated that, in 2050, this number will increase up to 10 000 000.<sup>73, 75</sup> Hence, there is a vital need for alternative antimicrobial agents like Ag, against which resistances are less likely to be developed.<sup>76</sup>

### 1.3.3 Catalytic Application

The amount of research with special focus on the catalytic application of RH-derived materials is rather small in terms of total number of research articles. According to the data-base Web of Science, only 4 %, of all reports regarding the use of RH (approx. 17.32 million articles), are related to catalysis.<sup>77</sup>

However, within these 710 000 publications, the use of silica as a support for heterogeneous catalysts is discussed many times. Thus, there are several examples of RH-derived silica matrices impregnated with a number of different metals and used as heterogeneous catalysts. Such catalysts are especially attractive for oxidation reactions, since silica supports tend to form highly active, dehydrated metal-oxo-species with metal oxides at high temperatures.<sup>78</sup> Prominent examples are the use of chromium on silica for styrene oxidation,<sup>79</sup> the ozonation of oxalic acid using RH after decarbonization,<sup>80</sup> oxidative degradation of CO and *p*-xylene from waste gas streams using Mn as active centers<sup>81</sup> or the partial methanol oxidation with copper on silica.<sup>82</sup> Additionally, other industrially relevant reaction types using silica from RH as carrier have been explored, e.g. the catalytic light naphtha cracking with ZSM-5,<sup>83</sup> MCM-41 loaded with Pd/Cu/Zn for methanol production from CO<sub>2</sub><sup>84</sup> or reduction of nitro compounds by Au NP.<sup>85</sup> Furthermore, there is a number of rather academic applications like TiO<sub>2</sub> on silica for photocatalytic applications,<sup>86</sup> iron for alkylation reactions<sup>87</sup> or even basic sodium silicate without further added metals for transesterification.<sup>88</sup> In contrast, the use of carbon from RH as support for catalysts is less explored. Only a hand full of examples are known in literature, e.g. the hydroxylation of phenol with Fe@C,<sup>89</sup> Fe/Cu@C for NO reduction with CO,<sup>90</sup> magnetic Ni/ferrite@C for nitrophenol reduction using NaBH<sub>4</sub> as reduction agent,<sup>91</sup> *Bacillus sp.* fixed on carbon as an oxidation catalyst<sup>92</sup> or activated carbon for NO, CO and toluene degradation.<sup>93</sup> Nevertheless, whether these examples will ever cross the boundary from academic research to applicable chemical processes is highly debatable as they do currently not outperform established catalytic systems.<sup>79, 83-86, 89, 91</sup> The only advantage they offer is the fact that the catalyst support is derived from a renewable

feedstock. However, all reported RH-based catalyst systems have two major pitfalls. First, all reported examples used silica or carbon from RH that can barely be distinguished from silica or carbon derived from any other sources.<sup>94</sup> Thus, all structural features of the RH are lost completely during the preparation process and do not contribute to the catalytic activity. Second, a high amount of energy is necessary for the separation of carbon and silica, which cannot be compensated by the energy saved due to the application of the catalyst in the targeted reactions. This critical point is intensified when considering that the recycling stability is only sufficiently evaluated for the minority of the above-mentioned catalysts. The lack of data concerning this critical parameter for a heterogeneous catalyst makes most catalysts based on RH-derived systems unattractive.

The use of RH-derived catalysts with a composite matrix of silica and carbon does not require the breakdown of RH. Thus, this approach eliminates the described major drawbacks in catalyst preparation by being straightforward and less energy-demanding. Nonetheless, this approach has rarely been explored and only few examples are reported in literature. These describe the use of sulfonated RH ash as an acid catalyst for the acylation of aldehydes<sup>95</sup> and esterification of glycerol,<sup>96</sup> waste cooking oil,<sup>97</sup> palm oil<sup>98</sup> or oleic acid with methanol.<sup>99</sup> The esterification of bio oils is a frequently described pathway towards bio fuels.<sup>100</sup> However, such catalysts made from RH ash could, in principle, also use pure carbon materials, since the sulfonation only takes place on the carbon surface.<sup>95-99</sup> Thus, there is no major advantage of using RH compared to other feedstocks.

Other examples for the direct use of RH as feedstock for catalyst supports concern biomass gasification into synthesis gas<sup>101, 102</sup> or hydrogen<sup>103</sup> by using *in situ* generated Ni<sup>101</sup> and Ni-Fe<sup>102, 103</sup> NP. In the described reactions, RH or rice straw also serves as the biomass, which is converted into synthesis gas.<sup>101, 102</sup> This means that RH can simultaneously be used as substrate and catalyst. Such catalysts are prepared by wet impregnation of RH with metals in an oxidized form.<sup>101-103</sup> Consecutively, catalytically active metal centers are generated via *in situ* carbothermal reduction in a reactor. Temperatures above 450 °C are required for the gasification.<sup>101-103</sup> This approach leads to a notable induction period but also enables a continuous process, which is preferred for large scale application from an engineering point of view. However, as described above, the conversion of RH in gas- or liquefaction reactions is economically not profitable.<sup>60</sup> This is also true for synthesis gas production from RH because it cannot compete economically with established approaches.<sup>104</sup>

## 1.4 Applications in Heterogeneous Catalysis

The following chapter will provide an overview on the conducted catalytic reactions using RH as feedstock for catalyst preparation: the reduction of nitro groups to the corresponding amines as well as the reductive conversion of epoxides to anti-Markovnikov alcohols (anti-MA). The current state of the art in catalyst development and known mechanistic modes of action will be introduced briefly to enable comprehension for the reactions presented in this thesis.

### 1.4.1 Hydrogenation of Nitro Compounds

The reduction of nitro groups is frequently used for the synthesis of amines in fine as well as bulk chemical synthesis<sup>25</sup> and it is a popular test reaction in catalyst development.<sup>25, 105</sup> The transformation was first reported by Béchamp more than 150 years ago.<sup>106</sup> Since this non-catalytic approach, the use of heterogeneous metal catalysts with hydrogen as reducing agent rapidly gained importance. Numerous metals have been employed as catalyst. Noble metals including Pd, Pt, Ir and Au<sup>107</sup> are popular as active sites, since they enable high turnover frequencies. Nevertheless, noble-metal-based catalysts often suffer from low selectivity.<sup>108, 109</sup> This is the case if the substrate molecule offers more than one potentially reducible group, e.g. alkyne, nitrile or carbonyl functions.<sup>107, 110, 111</sup> However, even with non-complex substrates like nitrobenzene or halogen-substituted nitrobenzene, selectivity issues can occur because noble-metal-based catalysts tend to catalyze dearomatization as well as dehalogenation.<sup>107, 108, 109</sup> Additionally, the use of noble metals comes with a significant financial burden.<sup>112</sup> Hence, it is reasonable to develop efficient replacements. This thesis presents alternative systems that use Ag and Co as active sites.

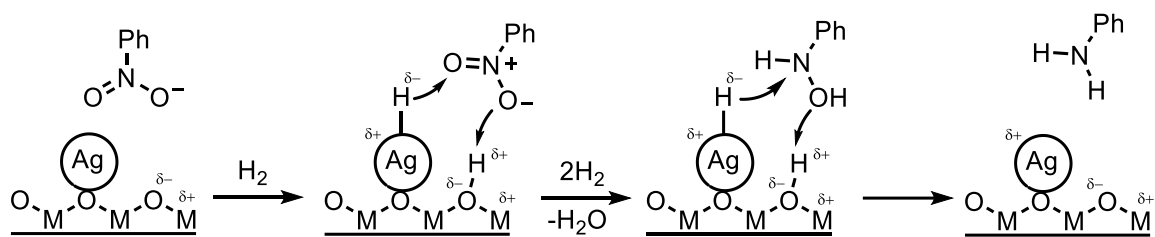


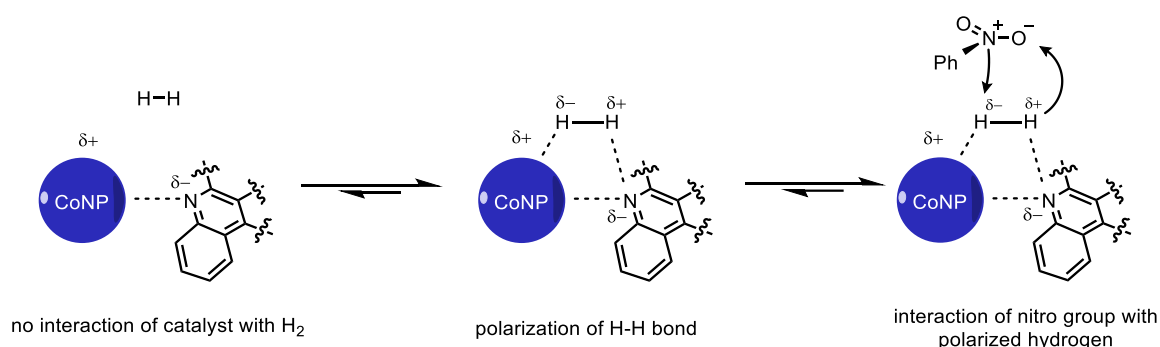
Figure 8 Mechanism of nitro hydrogenation by Ag NP on metal oxide support.<sup>115</sup>

Ag, which is by far the cheapest noble metal, has rarely been exploited for nitro reduction reactions, which can be explained by its unattractive inertness towards  $H_2$  dissociation at low temperatures.<sup>113</sup> However, the use of Ag NP on metal oxide support for selective hydrogenation of nitro groups has been reported.<sup>114, 115</sup> The mechanism is generally well understood and works via hydrogen dissociation on the highly polarized metal oxide

surface (figure 8).<sup>115</sup> The formed hydride species is transferred to the nitro group and the product is formed via water elimination. Unfortunately, the scope of most studies using Ag is very narrow and limited to nitrobenzene, chloronitrobenzenes, nitrophenol and other para-substituted nitro aromatics. So far, benzylic as well as aliphatic nitro compounds have been neglected.<sup>109, 116, 117, 118</sup>

Besides Ag, the use of Co as active center was also previously explored for the reduction of nitro compounds.<sup>25</sup> First reports in 1921,<sup>119</sup> 1937<sup>119</sup> and 1975<sup>120</sup> exclusively used CoS as active center for nitro group hydrogenation at high temperatures as well as high hydrogen pressure. No improvement was documented until 2005, when, Johnson *et al.*<sup>121</sup> presented metallic Co NP combined with a Co-Pd alloy as catalyst. The system achieved a turnover frequency of 23000 h<sup>-1</sup> at 80°C and 25 bar H<sub>2</sub>, which, to date, is still one of the highest ever reported values for this reaction. Nevertheless, the system is not attractive for application, since the recycling is insufficient and Pd is required. Thus, Co-based hydrogenation catalysts had to be improved further before being compatible with established noble metal systems. This happened in 2013, when Beller *et al.*<sup>122</sup> reported the development of Co NP with a Co<sub>3</sub>O<sub>4</sub> shell incorporated in a nitrogen-rich carbon environment by pyrolysis of nitrogen-rich Co complexes on silica. This approach led to a ligand-like interaction of the Co NP with pyridinic nitrogen moieties on the surface. This interaction facilitates charge polarization analogous to the mechanism proposed for Ag on metal oxide support and, thus, enables an easier H-H bond dissociation (Scheme 2).

122

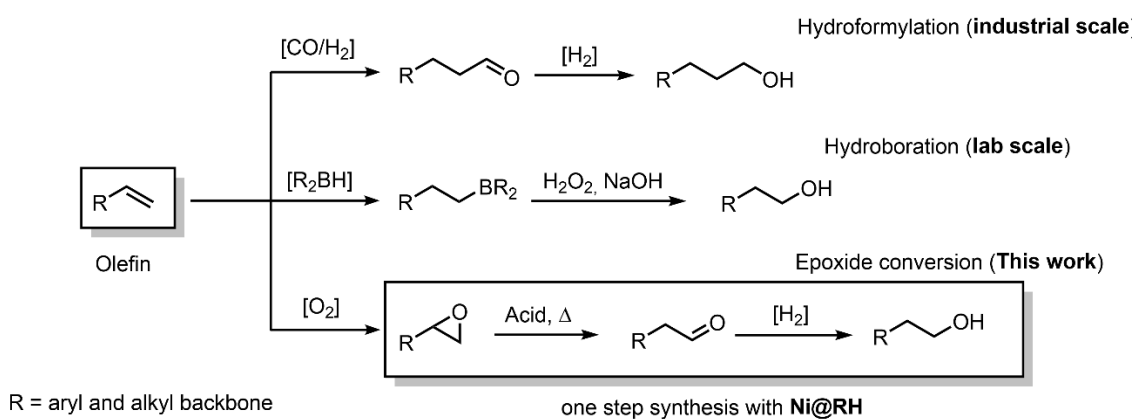


Scheme 2 Hydrogen activation via nitrogen Co NP interaction.<sup>123</sup>

The approach was used in many studies and led to a significant improvement of Co hydrogenation catalysts, even beyond the objective of nitrogen group reduction.<sup>123-128, 129, 130-132</sup> Studies showed that the use of the macrocyclic phthalocyanine, a chlorophyll and heme analogue, as Co source often achieved the best results in terms of catalytic performance.<sup>124-126</sup> Additionally, Beller *et al.*<sup>127</sup> established the impregnation of N-rich Co ligands on bio-derived chitosan for active nitro group reduction catalysts. However, the chitosan used in that study is a highly purified and processed industrial product and, thus, does not qualify as sustainable.

### 1.4.2 Reductive Synthesis of Anti-Markovnikov Alcohols from Epoxides

The second reaction presented in this thesis is the catalytic conversion of epoxides to the corresponding anti-MAs.<sup>133</sup> Currently, anti-MAs are synthesized on a small scale by hydroboration (scheme 3) but this approach is not suited for industrial scale, since borane agents are expensive, hard to recycle and required in stoichiometric amounts. The current pathway to anti-MAs used by industry is hydroformylation followed by carbonyl reduction (scheme 3). However, the synthesized alcohols always entail an additional C1 building block and, like many hydroformylations, the reaction often suffers from selectivity issues. Nonetheless, the approach is frequently used due to high turnover numbers of the applied Rh and Ru catalysts.<sup>134</sup> Despite this, a requirement for alternative synthetic pathways remains.

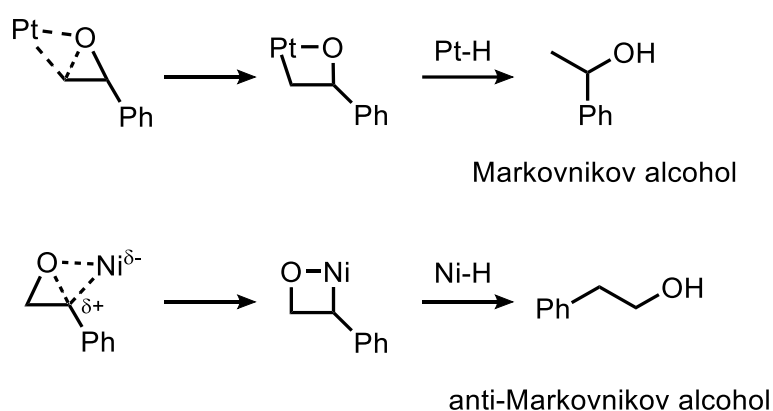


Scheme 3 Possible synthetic pathways to primary alcohols from terminal olefins.

The conversion of epoxides to anti-MAs has become an attractive third pathway at the beginning of the 21<sup>st</sup> century, the reason being that the selective synthesis of epoxide moieties has long been an unsolved challenge. However, when this changed and the synthesis of epoxides from olefins became possible on large scales,<sup>135</sup> their reduction to anti-MAs attracted more attention.<sup>136</sup> Additionally, olefins like styrene, which are key starting materials in these processes (scheme 3) are not only available via reforming from petroleum<sup>137</sup> but can also be produced from biomass on a large scale.<sup>138</sup>

Despite these more recent advances, the synthesis of anti-MAs from epoxides has already been known for a long time. In 1949, Renoll et al.<sup>133</sup> reported the synthesis using Raney-Ni with good selectivity but very harsh reaction conditions of 150 °C and 62 bar of H<sub>2</sub>. Furthermore, the synthesis was investigated in the early 1980s.<sup>133, 139, 140</sup> However, most of those early examples of selective systems did not operate under catalytic conditions, but used stoichiometric additives like chlorotrimethylsilane<sup>139</sup> or MgI<sub>2</sub>/AIBN.<sup>140</sup> Active catalytic systems like Pd/C<sup>110</sup> achieved only very poor selectivity towards the anti-MAs and the work of Renoll et al.<sup>133</sup> remained one of the few selective catalytic systems.

The mechanism for the catalytic ring opening and reduction was investigated in detail during the 1980s.<sup>141-143</sup> Especially the work of Bartók and Notheisz<sup>141</sup> pointed out that noble-metal-based systems (Pt or Pd/C) are only useful for the synthesis of Markovnikov products or for the conversion of symmetric epoxides when regioselectivity is not relevant. They used kinetic experiments to explain the high selectivity of Ni-based catalysts in comparison to Pt-based systems.<sup>141, 143</sup> They could show that the higher electron affinity of Ni causes a positively charged or strongly polarized intermediate with a positive charge/polarization that requires stabilization (Scheme 4). Thus, the C-O bond at the higher substituted carbon atom is cleaved. In comparison, Pt allows a non-charged intermediate through much faster metal-H insertion, causing the reaction to be more selective towards the Markovnikov product.



Scheme 4 Markovnikov selectivity using Pt or Ni catalysts. <sup>141, 143</sup>

Since the initial work by Renoll et al.,<sup>133</sup> epoxide conversion to anti-MAs was demonstrated with bulk Ni on different inorganic supporting materials<sup>144, 145</sup> like MgO-Al<sub>2</sub>O<sub>3</sub>,<sup>146</sup> MgO<sup>147</sup> or saponites.<sup>148</sup> However, the scope of the so far published systems is limited to 2-Phenylethan-1-ol and high Ni loadings are necessary. <sup>144-146 147, 148</sup> Additionally, catalysts like Raney-nickel have proven to be difficult to handle when wanting to avoid deactivation.<sup>149</sup> In general, epoxide-rings can be opened not only by coordination on a metal center, but also by several other techniques because the ring strain of the three-membered cycle causes high reactivity. Thus, epoxides are popular as intermediates in complex chemical transformations<sup>150</sup> as well as in polymer chemistry.<sup>151</sup>



## 2 Results and Discussion

The first step in the utilization of RH for the preparation of a hydrogenation catalyst was to modify its structure. This has to be done because the composition and surface structure of RH are not suitable for its direct application as a heterogeneous catalyst due to a lack of active sites and low thermal stability. Metal NP are frequently used as active sites in hydrogenation reactions and are, therefore, the most promising candidates to be introduced into RH to prepare a catalytically active material. In order to introduce metal NP onto the surface, two approaches can be considered: 1) previously prepared NP are deposited on the surface via impregnation techniques or 2) metal ions are deposited on the surface and subsequently converted into NP. The advantage of the first method is that the morphology and, consequently the reactivity of the NP can be controlled more precisely beforehand. This means that the supporting material only has the role of a mechanical stabilizer for the catalytically active species. The advantage of the second approach is that the reactivity of the generated NP is mainly dependent on the distribution and the chemical interaction with the supporting material. This means that, in the second approach, the nature of the support is much more important for the catalytic activity. In addition, the approach is far more explorative, since it is nearly impossible to precisely predict the interaction of a polymorphous natural fiber with metal ions. Thus, the second approach was chosen for this work.

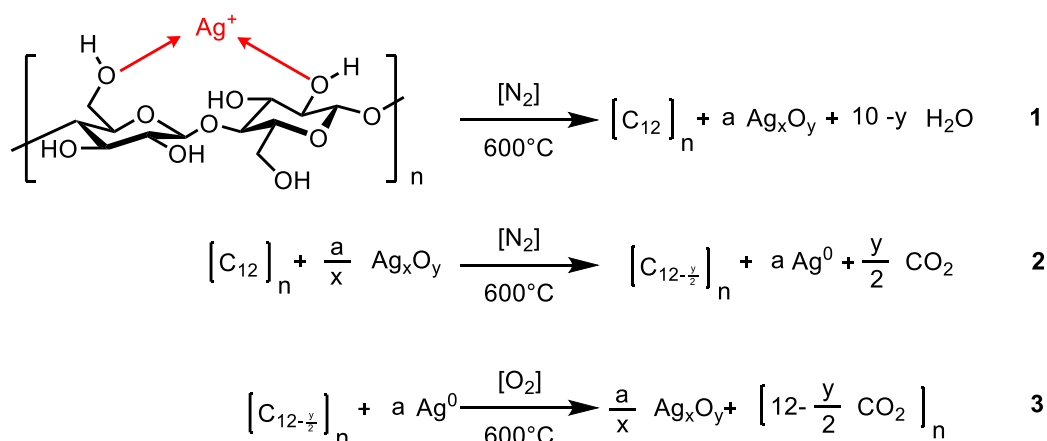
### 2.1 Preliminary Rice Husk Treatment

At the beginning of the preparation process, mechanical grinding of RH was conducted to generate small pieces of RH. This was achieved with a cutting mill using a 2 mm sieve followed by treatment with a ball mill in order to homogenize the RH and increase the accessible surface area. Additionally, acid leaching was applied to the homogenized RH using 10 mol% HCl, to eliminate trace metals, which are naturally present in RH. Such trace metals (like Mg, Ca, Mn, Co, Cu, Zn, Fe, Na and K) can negatively influence the material properties. However, control experiments revealed that the acid washing has no influence on the material performance. Thus, the step can be omitted, which avoids the production of approximately 300 liters of acidic wastewater per kilogram of prepared catalyst. This mechanical grinding was done equally for all materials presented in this work.

## 2.2 Silver-Containing Materials

### 2.2.1 Preparation and Characterization

The first developed system uses Ag NP as active centers. For the impregnation of RH with Ag ions, the RH was mixed with AgNO<sub>3</sub> in a methanolic solution for 24 h. This makes use of the ion coordination ability of carbohydrates for the fixation the Ag<sup>+</sup> ions on the surface (red in scheme 5).<sup>152</sup> Consecutively, the solvent was removed *in vacuo* and the material was dried for 24 h at 60°C at 60 mbar. Finally, the impregnated RH was pyrolyzed in a quartz tube furnace, resulting in the applied material, which is referred to as Ag@RH. The pyrolysis was performed under inert atmosphere (N<sub>2</sub>) in order to avoid the complete oxidation of the polysaccharide and lignin network to CO<sub>2</sub>. Furthermore, by using a N<sub>2</sub> atmosphere, the conversion of the Ag<sup>+</sup> ions to the corresponding oxides (**3** in scheme 5) is avoided. This is favoured, since in most reported cases completely oxidized metal NP are less active in hydrogenation reactions.<sup>153</sup> Nevertheless, this statement should not be generalized because contradicting examples are known.<sup>154</sup>



Scheme 5: Reaction equations for the conversion of coordinated Ag<sup>+</sup> ions (**1**) to Ag<sup>0</sup> (**2**) under nitrogen atmosphere and consecutive partial oxidation to Ag oxide (**3**).

Through the pyrolysis, the surface as well as the composition of the material has been drastically changed. The most significant change of the RH material under the applied conditions was the thermal decomposition of the contained hydrocarbons to a graphene-like structure in an autoxidative process. This structure was investigated with X-ray photoelectron spectroscopy (XPS) and infrared spectroscopy (IR) measurements, which showed a significant increase of sp<sup>2</sup> hybridized carbon and, simultaneously, a decreased amount of carbon oxygen bonds.

An indicator for the structural change was the highly increased surface area of the material. RH usually has a single-digit surface area<sup>155</sup> but the surface area of Ag@RH and

RH pyrolyzed without preliminary impregnation was determined to be  $260 \text{ m}^2\text{g}^{-1}$  and  $270 \text{ m}^2\text{g}^{-1}$ , respectively, which is significantly higher (B in figure 10). A type H3 hysteresis loop was identified, which is well known for silica-carbon-based materials<sup>156</sup> like clay<sup>157</sup>,<sup>158</sup> and silica-based catalysts prepared by sol-gel methods.<sup>159</sup> The hysteresis loop indicates the existence of slit pores and capillary condensation of adsorption gas in interstices between silica and carbon.<sup>158</sup>

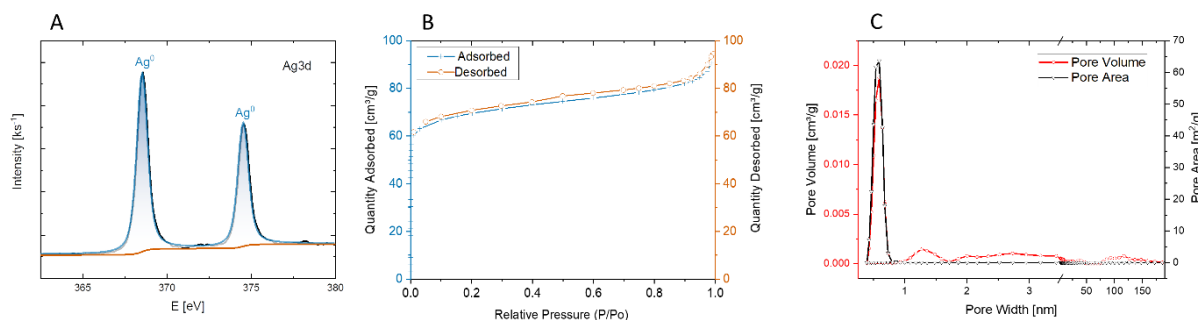


Figure 9 A) Ag3d<sub>5/2</sub> XPS signal, B) Brunauer-Emmett-Teller (BET) quantitative sorption of N<sub>2</sub> and C) pore volume and area distribution plotted against the pore width of Ag@RH.

Aside from the described changes, the Ag<sup>+</sup> ions were converted into their sterling oxidation state via carbothermal reduction (2 in scheme 5). The presence of Ag<sup>0</sup> in the sample was confirmed by X-ray diffraction (XRD) and XPS (A in figure 9) and the measured Ag3d<sub>5/2</sub> binding energy of 368.56 eV suggested NP with an average diameter of 6 nm. Interestingly, XRD peaks showed neither Pseudo-Voigt nor Lorentzian shape. The peak shape was interpreted to be a result of overlapping peaks from two or more crystallite fractions coexisting in the sample (Figure 10), a phenomenon known as bimodal crystallite size distribution.

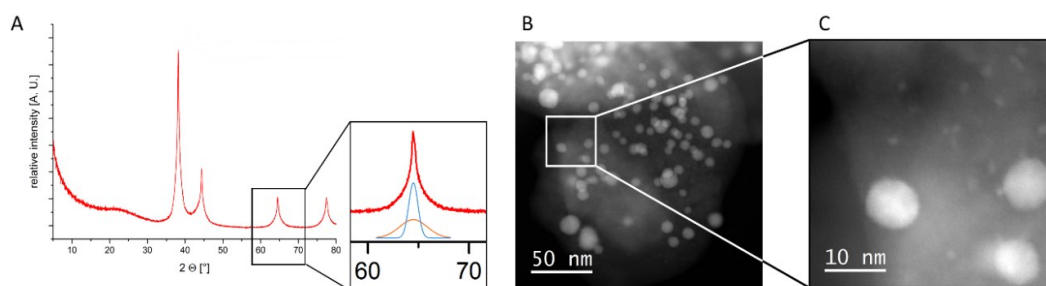


Figure 10 A) XRD pattern of Ag@RH with the schematic presentation of overlapping signals from different Ag particle size fractions. B) and C) annular bright field (ABF)-STEM of Ag@RH proving the presence of particle size fractions.

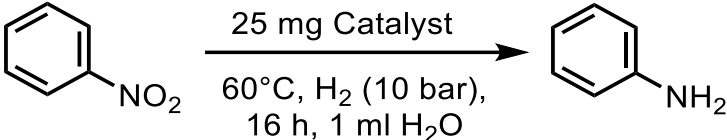
Thus, scanning transmission electron microscopy (STEM) was applied in order to prove the presence of more than one Ag crystallite size fraction (B and C in Figure 10). Indeed, STEM showed three crystallite fractions in the material. The smallest identified particle fraction had a diameter of 1 to 2 nm and was distributed all over the material. The second fraction, which consisted of particles of 6 to 10 nm, was the most widespread one and appeared to be fully monocrystalline. In contrast, the last identified fraction contained

larger particles of 70 to 200 nm and appeared to be the result of agglomeration of the smaller crystallites.

### 2.2.2 Application as Hydrogenation Catalyst

The catalytic activity of Ag@RH was tested in the hydrogenation of nitrobenzene to aniline. Additionally, other metals, e.g. Co, Cu and Ni were impregnated on RH with analogous methods and tested in the same reaction. Ag@RH clearly showed the best results with a yield of 47 % (table 1). In general, it is not surprising that Ag is active in the hydrogenation of nitro benzene, as described in the introduction.<sup>114, 115, 160</sup> Nevertheless, Co,<sup>127, 129</sup> Cu<sup>161</sup> and Ni<sup>162</sup>-based reduction catalysts are also known in the literature.<sup>25</sup> Thus, the observed clear differences in activity were unexpected. Another noteworthy result in the preliminary screening was the catalytic activity of the bare supporting material. The activity of the support can be explained by the metal impurities, e.g. Fe<sub>2</sub>O<sub>3</sub>, which are known to catalyze hydrogenation reactions.<sup>163</sup> These impurities were left in the material, even though it was leached with acid in the pretreatment. Additionally, it has to be pointed out that bare Ag particles fixed on silica and prepared through a similar process turned out to be catalytically inactive under the same reaction conditions. This result hints at the importance of the RH as support during the reaction as well as during the preparation process.

Table 1 Condition screening for the hydrogenation of nitrobenzene using pyrolyzed catalysts containing various metals (optimal conditions marked bold).



ii	Catalyst <sup>[a]</sup>	Pyrolysis temperature [°C]	Yield [%] <sup>[b]</sup>	Selectivity [%] <sup>[c]</sup>
1	RH	600	2.5	99
2	Co@RH	600	7.3	99
3	Cu@RH	600	4.8	78
4	Ni@RH	600	2.2	69
5	Ag@RH	600	47.3	99
<b>6</b>	<b>Ag@RH<sup>[d]</sup></b>	<b>600</b>	<b>47.3</b>	<b>99</b>
7	Ag@SiO <sub>2</sub>	600	-	-
8	Ag@RH	500	22	99
9	Ag@RH	700	29	99
10	Ag@RH	800	6	99

[a] Metal content of the catalysts is 13 wt-% of metal nitrate relative to dry mass of RH [b] Yields determined by GC using *n*-heptane as internal standard. [c] Selectivity towards aniline was calculated using GC with *n*-heptane as internal standard. [d] Catalyst prepared without acid leaching.

The pyrolysis temperature during preparation is a critical factor for the performance of heterogeneous catalysts.<sup>25, 130</sup> Thus, it is not surprising that a strong correlation of catalytic activity with this preparation parameter was found (Table 1). The achieved yield dropped drastically at both lower and higher temperatures. This can be explained with insufficient Ag reduction at lower temperatures and particle migration and/or thermal Ostwald ripening<sup>164</sup> leading to larger, less active particles at higher temperatures.<sup>165</sup>

Finally, all relevant reaction conditions, i.e. temperature, hydrogen pressure, reaction time and catalyst loading, were screened and optimized with regard to yield and selectivity. The system turned out to be highly selective towards the amine as reaction product and relevant side products like azo- or nitroso-components were not detected. The solvent screening revealed polar solvents as the best option and an equal voluminal mixture of methanol and water was chosen. Additionally, a base screening was done, since the addition of bases is often associated with higher yields in nitro reduction. Nevertheless, the screening showed that the addition of bases actually decreased the reaction yield and, thus, this step was not included. Finally, the catalyst loading was screened and it turned out that only 1.4 mol% of Ag with regard to the educt were sufficient for quantitative yield. The optimal conditions for the catalytic conversion of nitrobenzene to aniline are displayed in figure 12.

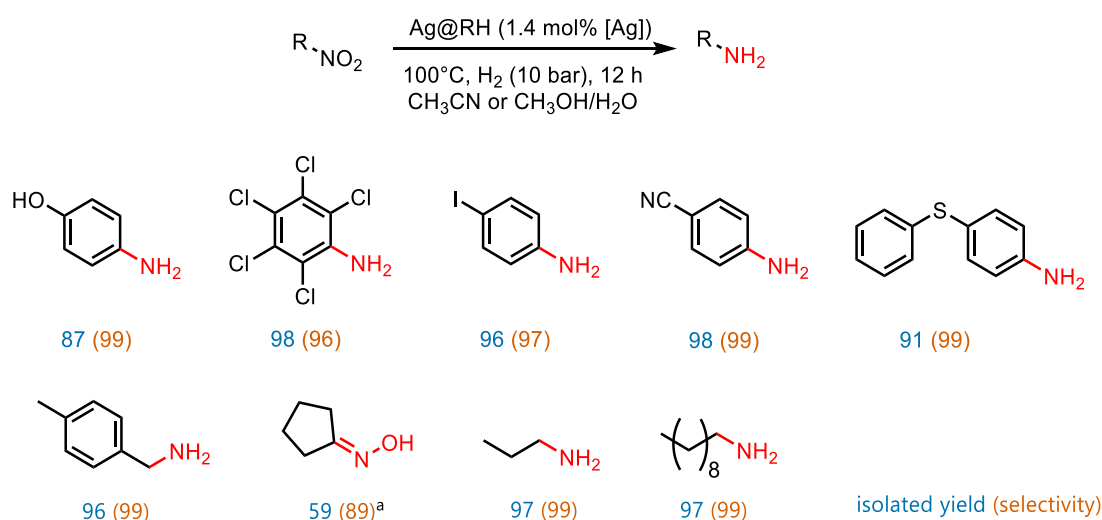


Figure 11 Selected products of the catalytic conversion of nitro compounds to amines using Ag@RH. [a] Isomeric mixture of nitrosocyclopentane and cyclopentanone oxime. Yield determined by GC.

In order to investigate the chemoselectivity and demonstrate the applicability of the synthesized catalyst, a substrate screening was performed (a selection of converted substrates is displayed in figure 11). An example of an industrially relevant educt converted with Ag@RH catalyst is 4-nitrophenol. The reduction of the nitro group to the corresponding amine is the first step in the synthesis of the globally used generic drug

paracetamol.<sup>118</sup> Even though the reaction was not optimized for this specific conversion, 4-aminophenol was produced in good yields of 87 %. Beside this example, a number of halogenated substrates were converted, providing evidence that reductive dehalogenation reactions do not limit the substrate scope. Additionally, other reduction sensitive groups like nitriles or sulfides did not seem to disturb the reaction selectivity. A number of aliphatic substrates were converted in excellent yields, as well. Nevertheless, it must be pointed out that the conversion of nitro groups bound to cyclic aliphatic carbon chains turned out to be difficult. At the given reaction conditions, the conversion stopped at the nitroso intermediate, which was stabilized by isomerization to the oxime. However, this limitation could be overcome by increasing the reaction temperature to 140°C and raising the H<sub>2</sub> pressure to 40 bar. Interestingly, this limitation was not found for non-cyclic aliphatic carbon backbones. This is particularly surprising, since these substrates also offer an acidic proton in alpha position, which can be assumed to be the reason for the isomerization.

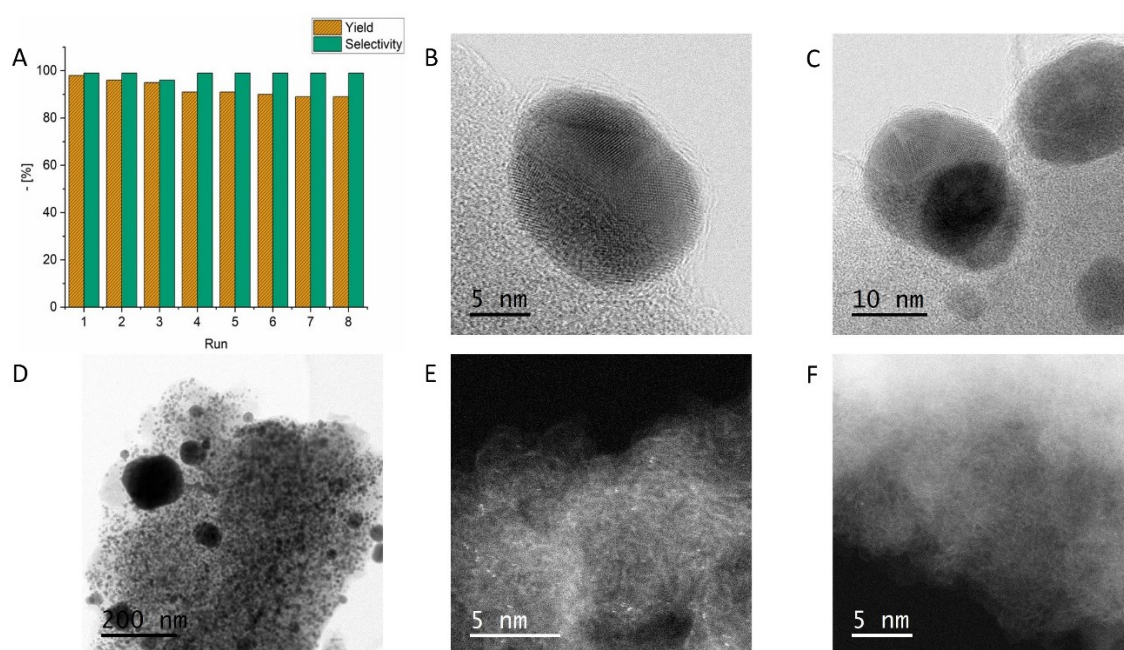


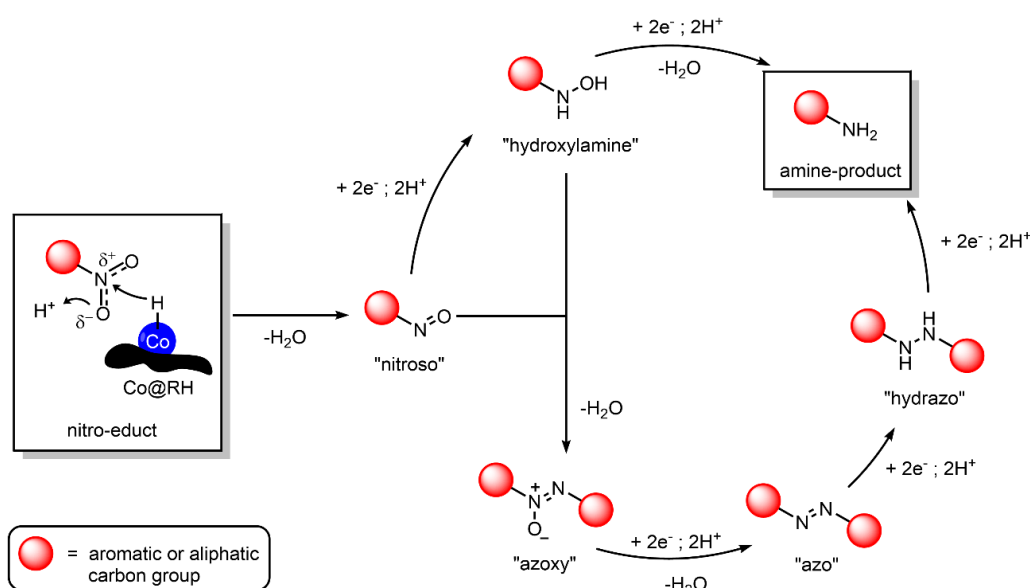
Figure 12 STEM images and recycling stability of Ag@RH. A) Catalyst recycling experiments for the hydrogenation of nitrobenzene using Ag@RH. B) ABF- high-angle annular dark-field imaging (HAADF)- STEM after first catalytic cycle. C) ABF- STEM after eight catalytic cycles. D) ABF-STEM after last catalytic cycle, E) HAADF- STEM after first catalytic cycle, F) HAADF- STEM after eight catalytic cycles.

Beside the chemoselectivity, the recycling stability is a key characteristic of heterogeneous catalysts. This is especially relevant, since it often justifies the favoured use of heterogeneous over homogeneous catalysts. Thus, the catalyst was recycled eight times using the conversion of nitro benzene to aniline as test reaction and the change of the Ag@RH catalyst was investigated with STEM. The yield decreased only marginally within the first four runs and then reached a stable plateau of around 91 % isolated yield

for the next four catalytic cycles (A in figure 12). The reaction selectivity remained stable at 99 % for the entire recycling experiment. The STEM revealed that the appearance of the catalyst did not change drastically on a macroscopic level (B to F in figure 12).

The slight decrease in yield can be explained by investigating the composition of the catalyst on a nm-scale (B and C in figure 12). While the main particle fraction of Ag particles with a diameter of 6 to 10 nm remained unchanged during the experiment, a strong change was visible for the smallest fraction of 1 to 2 nm particles. The smaller fraction almost entirely disappeared after four catalytic cycles. Thus, this suggests that the fraction of 6 to 10 nm NP is responsible for most of the materials' catalytic activity, which is in line with earlier studies.<sup>109, 116</sup> Additionally, the fact that the smallest fraction appears to leach from the surface raises the question if the reaction is purely heterogeneously catalyzed, since the leached Ag clusters could be responsible for activity, as well. However, a hot filtration experiment proved that the system acts only in a heterogeneous manner.

Finally, a reaction mechanism was proposed based on isolated intermediates and literature reports (scheme 6).<sup>25, 166</sup> The reaction starts with a hydride transfer from the Ag particles to the nitro educt, leading to a nitroso intermediate under the elimination of water. As described above, the nitroso intermediate is especially relevant for aliphatic substrates. There are two possible pathways from the nitroso intermediate, which are frequently described in literature.<sup>25, 166</sup> Those two pathways occur as competing processes: 1) the transfer of four more electrons and protons to a single nitroso benzene, leading to the amine via the hydroxylamine or 2) the condensation of a hydroxylamine with a nitroso group to an azoxy component, which is further reduced to the desired amine product.



Scheme 6 Proposed reaction mechanism for the reduction of nitro groups catalyzed by Ag@RH.

### 2.2.3 Application as Antimicrobial Agent

In cooperation with the Lalk group (Cellular Biochemistry & Metabolomics at the University of Greifswald), the antimicrobial behavior of Ag@RH against the ESKAPE pathogens (*Enterococcus faecium*, *Staphylococcus aureus*, *Klebsiella pneumoniae*, *Acinetobacter baumannii*, *Pseudomonas aeruginosa*, *Escherichia coli*) and the pathogenic yeast *Candida albicans* was tested. Preliminary tests gave positive results against all pathogens, using the exact same Ag@RH material used for the catalytic reduction of nitro compounds (figure 13).

The preliminary test as well as all following investigations on the antimicrobial behavior were conducted by determining the zone of inhibition (ZOI). Measuring the ZOI is since 1944<sup>167</sup> the most wide-spread method to examine anti-microbial properties offered by various materials.<sup>168</sup> In order to determine the ZOI Ag@RH was suspended in methanol (20 mg/ml) and 10  $\mu$ l of this suspension was transferred onto a cotton disc of 6 mm diameter with a syringe. The disc was placed on agar containing microbes. Finally, the sample was incubated, and the ZOI was measured after 24 h.

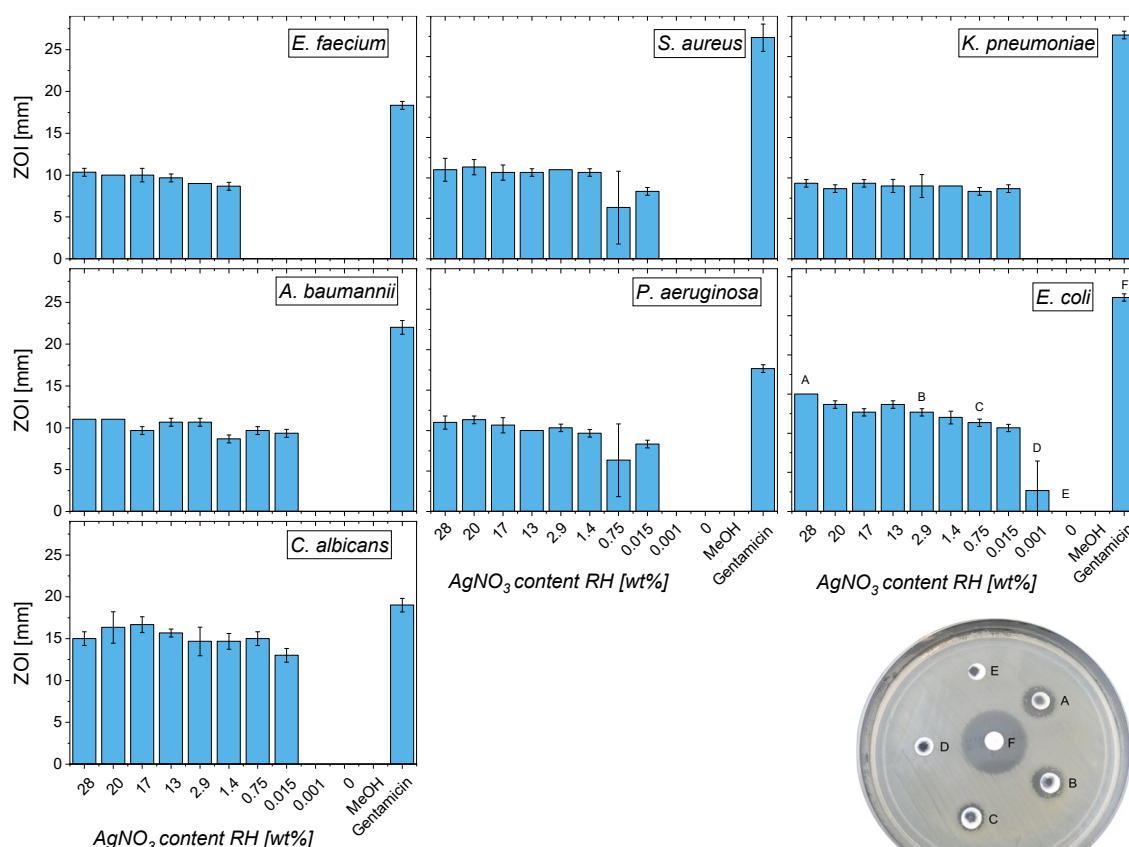


Figure 13 Antimicrobial effect of RH doped with Ag NP on *Enterococcus faecium*, *Staphylococcus aureus*, *Klebsiella pneumoniae*, *Acinetobacter baumannii*, *Pseudomonas aeruginosa*, *Escherichia coli* (ESKAPE pathogens) and *Candida albicans*.

The material prepared for the catalytic experiments contained 4.9 wt% of Ag, which is a relatively high amount. However, even though Ag cannot be considered a cheap



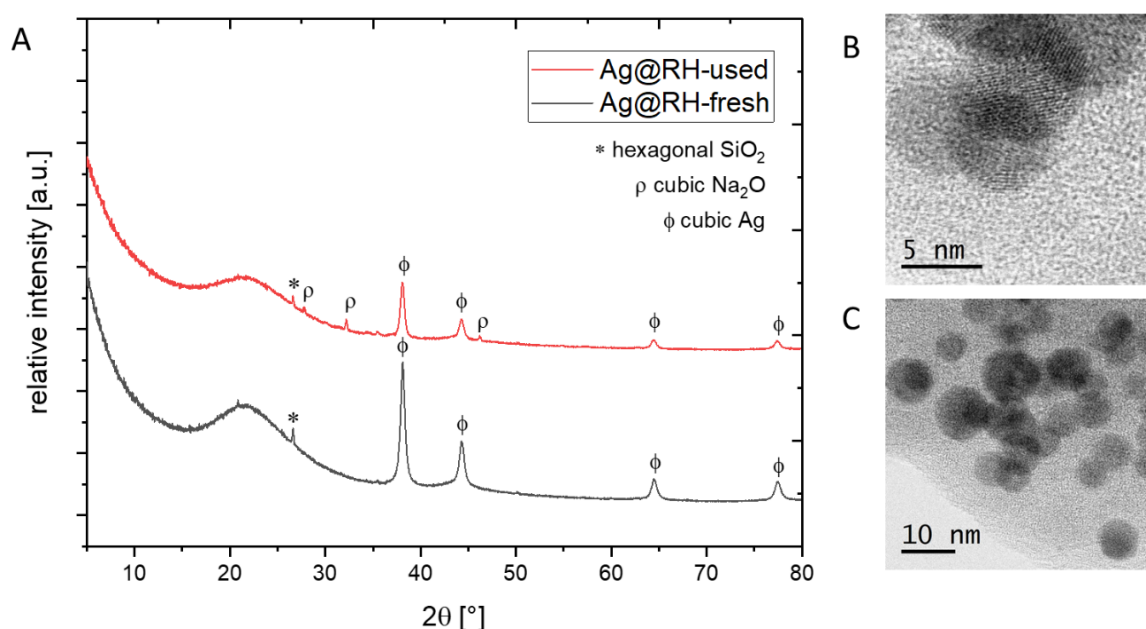
resource, it is cheaper than commonly used antibiotics. For example, 0.5 g of Cefuroxime, an antibiotic drug used against bronchitis, costs approximately 15 USD,<sup>169</sup> while the same amount of bulk Ag is available for approximately  $0.32 \pm 0.06$  USD. Furthermore, 0.5 g Ag NP of <100 nm particle size are available for 6 USD and 0.5 g AgNO<sub>3</sub> cost ~0.9 USD.<sup>170</sup> Nevertheless, it is reasonable to lower the amount of Ag as much as possible in order to decrease the product cost. Hence, a series of Ag-bearing materials were synthesized with AgNO<sub>3</sub> concentration in the non-pyrolyzed RH varying from 28 to 0.001 wt%. The material was consecutively tested for antimicrobial behavior (figure 13). The test revealed that the material was active against all strains. A significant loss of activity was observed down to a concentration of 0.015 wt% AgNO<sub>3</sub> in the non-pyrolyzed RH. This corresponds to an Ag concentration in the used Ag@RH material below the limit of quantification of the applied inductively coupled plasma optical emission spectrometry (ICP-OES) method, which is 0.001 wt% (table 2). Interestingly, a similar sensitivity of Gram-positive and -negative bacteria against the material was found.

Table 2 AgNO<sub>3</sub> content in raw material and Ag content in pyrolyzed material, on cotton disc and in agar.

ii	AgNO <sub>3</sub> in raw material [wt%] <sup>[a]</sup>	Ag in pyrolyzed material [wt%] <sup>[a]</sup>	Ag at cotton disc [wt%] <sup>[a]</sup>	Ag in agar [wt%] <sup>[a]</sup>
1	28	4.880(4)	0.069(3)	<0.001 <sup>[b]</sup>
2	20	3.472(8)	0.047(5)	<0.001 <sup>[b]</sup>
3	17	2.945(0)	0.033(4)	<0.001 <sup>[b]</sup>
4	13	2.241(3)	0.031(5)	<0.001 <sup>[b]</sup>
5	2.9	0.478(5)	<0.001 <sup>[b]</sup>	<0.001 <sup>[b]</sup>
6	1.4	0.10(2)	<0.001 <sup>[b]</sup>	<0.001 <sup>[b]</sup>
7	0.75	0.03(8)	<0.001 <sup>[b]</sup>	<0.001 <sup>[b]</sup>
8	0.015	<0.001 <sup>[b]</sup>	<0.001 <sup>[b]</sup>	<0.001 <sup>[b]</sup>
9	0.001	<0.001 <sup>[b]</sup>	<0.001 <sup>[b]</sup>	<0.001 <sup>[b]</sup>
10	0	<0.001 <sup>[b]</sup>	<0.001 <sup>[b]</sup>	<0.001 <sup>[b]</sup>
[a] Measured with ICP-OES [b] limit of quantification at 0.001 wt%				

Earlier works studying the interaction of bacteria with Ag NP have not shown a clear trend on this matter. On the one hand, Lara et al.<sup>171</sup> have reported less sensitivity of Gram-negative bacteria caused by their negatively charged outer lipopolysaccharide membrane, which prohibits the Ag<sup>+</sup> ions from entering the germs. On the other hand, Huang et al.<sup>172</sup> have reported the exact opposite and described the thinner cell wall of Gram-negative bacteria as the reason for the elevated sensitivity. Moreover, beside the high activity against bacteria, an antifungal behavior of the material against *Candida albicans* was also found.

Finally, the stability of Ag on the support surface was evaluated. This is an important parameter, since it is known that Ag can also have toxic effects on cells of higher animals. This has not only been proven in lab experiments, e.g., for zebra fish<sup>173</sup> and rats,<sup>174</sup> but also in a field study about infertility of *Macoma balthica* clams in the San Francisco Bay due to a massive Ag<sup>+</sup> discharge in the 1980s.<sup>175</sup> However, from the catalytic experiments it was already known that the NPs fraction of 6 to 10 nm is not leached from the surface under distinctly harsher conditions (B and C in figure 14). Thus, it can be assumed that the Ag NP were not removed from the surface in larger quantities. XRD measurements of the fresh and used Ag@RH material as well as determination of the Ag content in the agar with ICP-OES proved this assumption. It was shown that the Ag phase was neither significantly decreased nor changed during the antimicrobial experiments (A in figure 14). The ICP-OES measurements showed that even for the highest Ag loading, no leaching of Ag from Ag@RH into the agar ground could be detected (table 2).

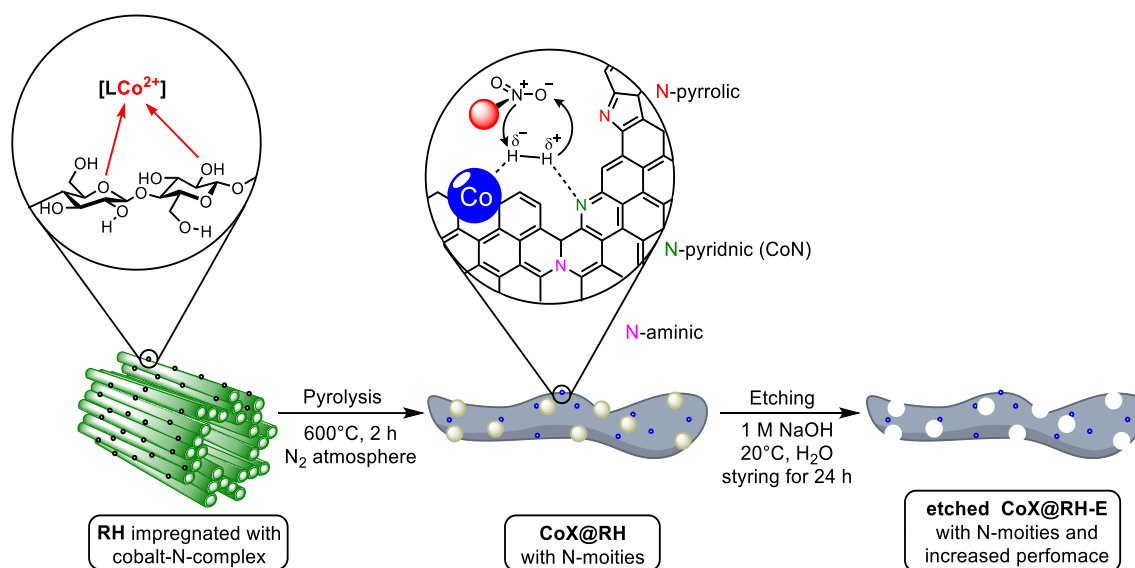


There are two general advantages of the developed system compared to literature-known antimicrobial agents mentioned in the introduction.<sup>64-68</sup> First, the required Ag concentration to enable antimicrobial activity is at least ten times lower than the known systems, lowering the production costs significantly. Secondly, the synthesis approach directly uses RH and not a preliminary processed derivative. Thus, a complete step of the upstream processing can be eliminated.

## 2.3 Cobalt-Containing Materials

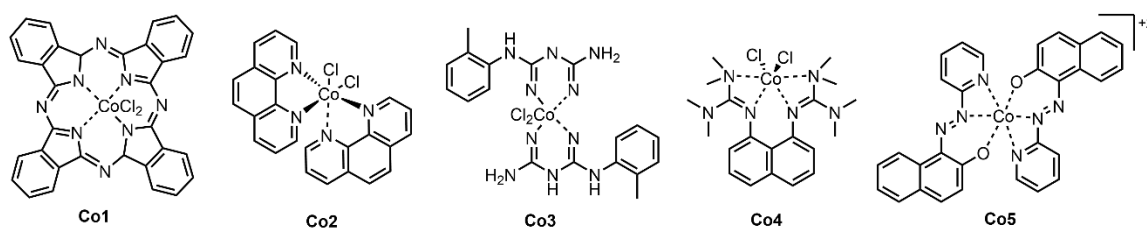
### 2.3.1 Preparation and Characterization

The general concept of generating metal NP on graphene via impregnation of the RH epidermis with metal ions followed by carbothermal reduction was shown successfully in the application of the Ag@RH system. Thus, the next step was to extend the scope of metals fixed on RH and optimize the preparation process by utilizing the unique composition of RH (scheme 7). Hence, two central points of the preparation approach were modified compared to the Ag@RH system. First, Co (instead of Ag) was impregnated on the RH epidermis. It was not applied as the inorganic salt but as a metal organic complex. Specifically, nitrogen-rich Co-complexes were used. Second, the material was further modified after the pyrolysis by etching of the silica from the material surface. This approach is based on the work of Zhang et al.<sup>126</sup> and Gascon et al.<sup>176</sup>, performed in 2017 and 2018, respectively. Both groups have showed drastically increased catalytic activity through etching of a Co-based hydrogenation catalyst with HF or NaOH. In both cases, the catalyst uses an artificial carbon-silica composite as support.



Scheme 7 Preparation approach for RH-based catalyst using N-rich Co-complexes tuned by base etching.

Five different N-rich Co-complexes were used for the impregnation of RH in order to generate catalytically active centers on the surface (scheme 8). The material impregnated with complex **Co1** gave the best results in terms of yield and selectivity in the consecutive catalytic studies, followed by complex **Co2**. Thus, this chapter on material preparation and characterization focuses on the materials derived from impregnation with these two ligands.



Scheme 8 N-rich Co complexes screened for catalyst preparation.

The technical procedure for catalyst preparation was barely changed compared to the Ag-based systems and was only extended by one step. The RH was impregnated in ethanol with the complex after the preliminary treatment (described in chapter 2.1). Consecutively, the obtained material was pyrolyzed under inert atmosphere and finally stirred in a Teflon® vessel containing NaOH for 24 h. The base concentration (in mol l<sup>-1</sup>) used for the etching is displayed as the last digit in the material name (e.g., 1 mol l<sup>-1</sup> NaOH was used for the preparation of Co1@RH-E1).

The drastic change of the RH surface morphology as well as its chemical composition during the preparation process was very much analogous to the changes described for Ag@RH (described in chapter 2.2.1). However, some dissimilarities, which can be explained by the different metal source and the base treatment, are noteworthy. Unlike for Ag@RH, the XPS measured C1s carbon binding of Co1@RH showed a drastically increased share of C-N bonding due to the used Co source, which contained such C-N bonds. Interestingly, neither the carbon nor the nitrogen binding situation was significantly changed by the etching process (A in figure 15). The main oxidation state of Co in Co1@RH was identified with XRD as being cubic Co with traces of cubic CoO (B in figure 15). However, the CoO phase disappeared in exchange for rhombohedral CoO(OH) in the freshly etched Co1@RH-E1 material and reappeared after the material had been washed. This leads to the assumption that the Co NP featured a so-called core shell structure, which has been previously described for Co-based catalytic systems.<sup>132, 177</sup>

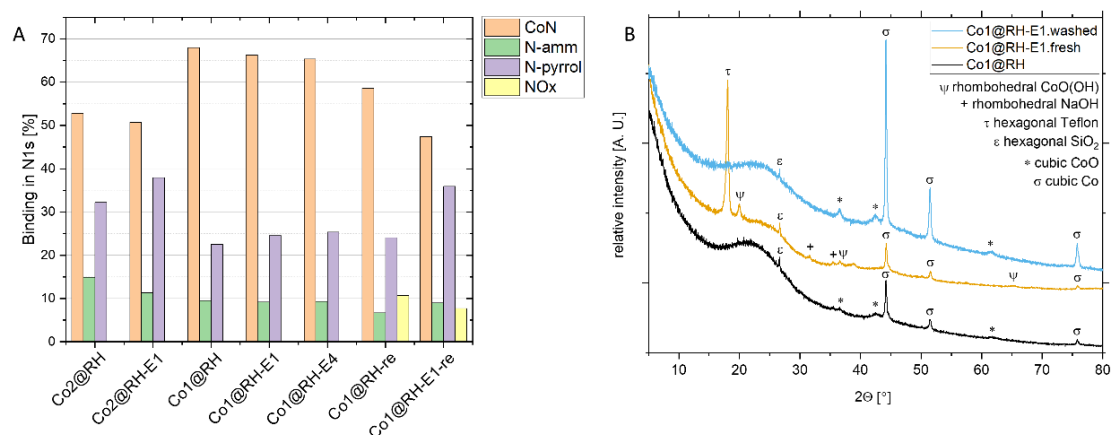


Figure 15 A) XPS measured nitrogen binding based on N1s peak and B) XRD pattern of Co1@RH (black), Co1@RH-E1.fresh (yellow) Co1@RH-E1.washed (blue) with different crystalline phases.

As expected, the amount of silicon in the material drastically decreased from 12 wt% to 3 wt% through the etching when using 1 mol l<sup>-1</sup> NaOH. Surprisingly, this had very little consequences for the microscopic surface structure of the material. BET measurements showed a slightly increased surface area of 347.13 m<sup>2</sup> g<sup>-1</sup> for Co1@RH-E1 compared to 323.63 m<sup>2</sup> g<sup>-1</sup> for Co1@RH. The micropore volume was nearly constant at 0.12 cm<sup>3</sup> g<sup>-1</sup>. When increasing the base concentration to 4 mol l<sup>-1</sup>, the silicon content was lowered to 1 wt% and the surface area was increased to 427 m<sup>2</sup> g<sup>-1</sup>. In addition, analogous to Ag@RH, an A type sorption loop was found. However, the loop showed stronger hysteresis.

Nevertheless, unlike the microscopic surface structure, the morphology of the material was drastically changed during the etching. The change was revealed by scanning electron microscopy (SEM) pictures (referred to in the following section as bold letters in brackets according to figure 16). The morphology of the untreated RH matched earlier studies (**A**), displaying silica dots that were strung together (black arrows).<sup>53, 63, 178</sup> After the pretreatment and the impregnation, the well-ordered surface morphology was disarrayed (**B**) but certain elements like fiber strands (black box) were still intact. The structure was not sustained during the pyrolysis (**C** and **D**) and the material then appeared to be mainly composed of nugget-like structures. From XPS measurements, it is known that these nuggets were composed of carbon and silica on the surface. Furthermore, small slits were visible on the material (red arrows). These slits did not disappear after the base etching (**E** and **F**) but instead were accompanied by certain areas with an almost sponge-like appearance (yellow arrows).

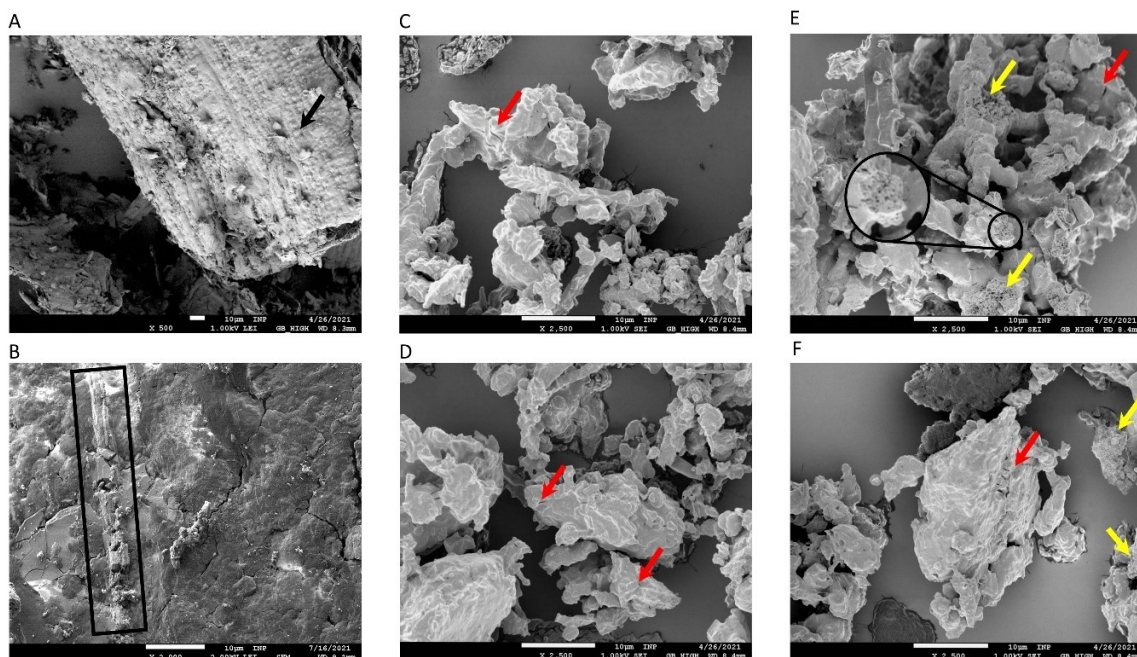


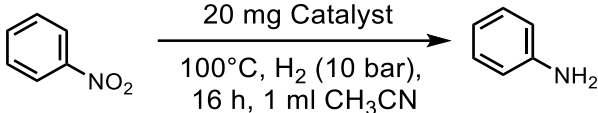
Figure 16 SEM pictures of untreated RH (**A**), RH+Co1 (**B**), Co1 (**C** and **D**), Co1@RH-E1 (**E** and **F**).

### 2.3.2 Application as Hydrogenation Catalyst

The prepared materials were tested in the hydrogenation of nitrobenzene to aniline. It turned out that all catalysts were catalytically active (table 3). However, drastic differences in activity were found. The use of  $\text{Co}(\text{NO}_3)_2$  as Co-source led to 5 % conversion, while catalysts prepared from metal organic Co-complexes (see ii 3-7 in table 3) showed higher activities. The only exception was the catalyst that was prepared using ligand Co5, which gave a conversion of only 1.3 %. Since Co5 was the only oxygen-bearing ligand, an inactivation of the Co by oxygen moieties during the pyrolysis seems a likely explanation for this result. The findings contradict a recent study by Beller et al.<sup>131</sup> In the study, Co salen complexes were pyrolyzed for the preparation of a highly active catalyst for reductive amination.

Base treatment of the catalyst increased the conversion in the tested nitrobenzene reduction. The achieved conversion was almost doubled in all cases (exemplarily shown for the Co1-catalysts in ii 2 and 3 in table 3). Again, the catalyst based on ligand Co5 was an exception and showed no increase in conversion if higher concentrated base ( $4 \text{ mol l}^{-1}$ ) was used for the etching (ii 3 and 4 in table 4). This result is surprising, since the catalyst Co1@RH-E4 offered a significantly higher surface area, which is usually associated with a higher number of active centers and, thus, with higher conversion. Nevertheless, the fact that the use of a more corrosive reaction solution was unnecessary is beneficial in terms of waste management and on-the-job safety. In conclusion, the catalyst used for all following experiments was based on Co1 and etched with  $1 \text{ mol l}^{-1}$  NaOH.

Table 3 Co source screening for the hydrogenation of nitrobenzene using pyrolyzed catalysts prepared by using N-rich Co complexes tuned by base etching.



ii	catalyst <sup>[a]</sup>	c(NaOH) [mol l <sup>-1</sup> ]	conversion [%] <sup>[b]</sup>
1	Co@RH	-	5
2	Co1@RH	-	39
<b>3</b>	<b>Co1@RH-E1</b>	<b>1</b>	<b>83</b>
4	Co1@RH-E4	4	85
5	Co2@RH-E1	1	38
5	Co3@RH-E1	1	29
6	Co4@RH-E1	1	16
7	Co5@RH-E1	1	1.3

[a] Metal content in the catalysts was 13 wt-% of metal nitrate relative to dry mass of RH  
 [b] Conversion determined by GC using *n*-heptane as internal standard.

Furthermore, 600 °C was found to be the pyrolysis temperature that gave the highest conversion of 83 % compared to approximately 50 % at 700 and 800 °C and 20 % at 500 °C. Thus, the pyrolysis temperature proved to be a critical preparation parameter, which is in line with the presented Ag-based catalyst and earlier studies.<sup>25, 123, 127, 130</sup> Additionally, it was demonstrated again that the use of a preliminary acid treatment of RH did not increase the catalytic activity of the prepared material and, thus, can be omitted.

In the next step, the reaction conditions were optimized for the reduction of nitrobenzene with aniline as reaction product. A temperature of 120 °C, 10 bar hydrogen pressure, 12 h reaction time and an equivoluminary isopropanol/water mixture were found as optimal conditions. Similar to the Ag-based system, polar and protic solvents showed the best performance for the hydrogenation and the addition of base lowered the yields significantly. Consecutively, the substrate scope was screened and 36 examples of successfully converted aliphatic and aromatic substrates demonstrated the versatility of the prepared catalyst (selection shown in figure 17). It is noteworthy that a selection of substrates was also screened with the non-etched catalyst and lower yields were obtained without exceptions.

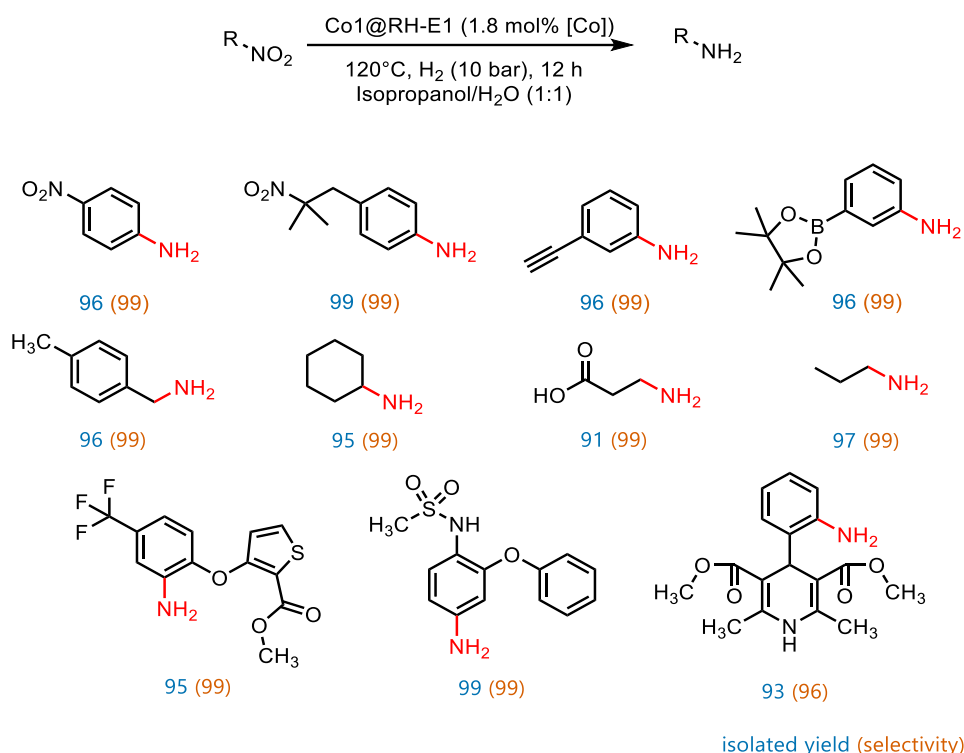


Figure 17 Selected products of the catalytic conversion of nitro compounds to amines using Co1@RH-E1 catalyst.

The high selectivity towards the nitro group was shown in the presence of various functional groups, e.g., aromatic carbon-halide bonds, nitriles, boron esters, acetylenes,



ketones, esters and imines. Furthermore, the catalyst was able to convert a number of aliphatic substrates into the corresponding amine at the given reaction conditions in good to excellent yields with perfect selectivity. Thus, the etched Co@RH catalyst was able to overcome the limitations of the Ag@RH catalyst, which required elevated reaction temperatures for the conversion of aliphatic substrates. Additionally, reaction selectivity was found in the conversion of beta-nitropropionic acid to the corresponding amine, since the catalyst did not cause any decarboxylation. The most remarkable feature of the prepared catalyst is its selectivity towards one nitro group, even if two are offered. All isomers of dinitrobenzene were converted into the corresponding nitroaniline with perfect selectivity. It was shown in the conversion of 2-nitro-2-(4-nitrobenzyl)propane that the catalyst seems to favour electron rich nitro groups. The use of harsher reaction conditions did not lead to the hydrogenation of both nitro groups, as demonstrated by an increase to 24 h reaction time, 50 bar hydrogen pressure and 150 °C temperature.

The number of materials able to catalyze the selective hydrogenation of one nitro group with hydrogen when two groups are offered by the same molecule is limited to five examples. However, four examples rely on kinetic product control, which is not the case for the catalyst presented in this work. Additionally, the known examples employ noble metals like Ru,<sup>179</sup> Pt-Pd alloys<sup>180</sup>, Au<sup>181</sup> and Ag.<sup>182</sup>

The prepared etched and non-etched catalysts were compared to established systems for the reduction of nitrobenzene by studying the reaction kinetics. The reaction followed a zero-order kinetic regardless if the etched or non-etched catalyst was used (figure 18), which was in line with previous studies.<sup>183, 184</sup>

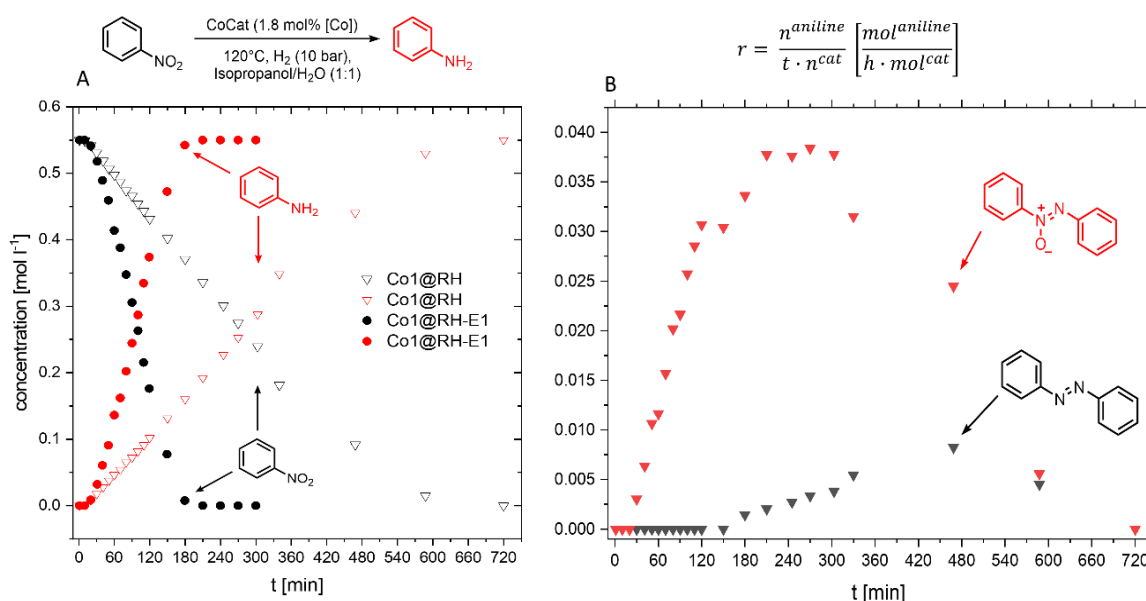


Figure 18 A) Concentration-time profile in kinetic experiments using Co1@RH-E1 (circles) and Co1@RH (triangles) and B) Concentration-time profile of reaction intermediates in kinetic experiments using Co1@RH.



However, it is visible in the concentration time profile (A in figure 18) that the reaction catalyzed by the etched material Co1@RH-E1 was complete after only 3 h, whereas the non-etched catalyst required a significantly longer reaction time of 10 h until full conversion was achieved.

The initial reaction rate ( $r$ ) (formula in B in figure 18) was used for a better comparison to literature-known systems. For Co1@RH-E1,  $r = 1938$  [ $\text{mol}^{\text{aniline}} / \text{mol}^{\text{Co}} \cdot \text{h}$ ] and for Co1@RH  $r = 290$  [ $\text{mol}^{\text{aniline}} / \text{mol}^{\text{Co}} \cdot \text{h}$ ] was determined. When these results are compared to the  $r$ -value of 473 [ $\text{mol}^{\text{aniline}} / \text{mol}^{\text{Co}} \cdot \text{h}$ ] of a Pd- $\text{Al}_2\text{O}_3$ -based system reported by Shi et al.<sup>183</sup>, it is evident that the etched Co-catalyst is superior to the noble-metal-based catalyst. The activation energy of Co1@RH-E1 was calculated based on Arrhenius' equation as being  $28.0 \pm 1.1$  [kJ / mol]. Hence, the activation energy is lower compared to benchmark systems, e.g., a HF-etched Co-catalyst by Zhou et al. ( $44.8$  [kJ / mol])<sup>125</sup> or an Au/ $\text{ZrO}_2$  catalyst by Gomez et al.<sup>185</sup> ( $67.2$  [kJ / mol]).

Finally, the recycling stability was evaluated and, once more, the etched and the non-etched catalyst were compared (figure 19). The yield decreased to  $\sim 70$  % after 3 reaction cycles when using Co1@RH and stabilized at this level for the next seven catalytic runs. The etched catalyst Co1@RH-E1 displayed superior behavior again, since no decrease in yield was observed after ten catalytic cycles. The reason for this difference in behavior was investigated by SEM studies (figure 19).

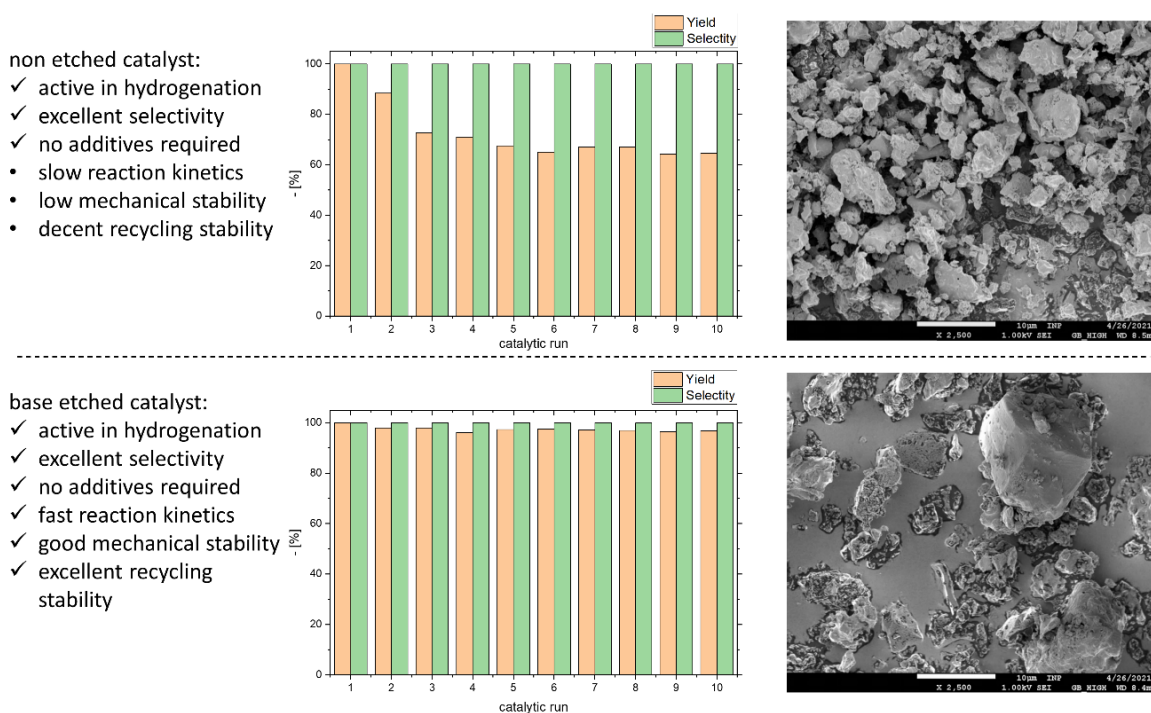


Figure 19 SEM picture of non etched catalyst and results of recycling experiments (top) as well as SEM pictures of etched catalyst and results of recycling experiments (bottom).

The etched catalyst appeared to be more mechanically stable. While Co1@RH disintegrated into small particles, Co1@RH-E1 remained structurally intact. Additionally, the increased stability coincides with a 4-fold lower oxygen/carbon ratio (measured with XPS) on the surface of Co1@RH-E1 after ten catalytic cycles. This suggests that the surface of the non-etched material is less stable towards oxidation and, thus, the active centers are more prone to deactivation by chemical transformation.

## 2.4 Nickel-Containing Materials

### 2.4.1 Preparation and Characterization

In the last step, a hydrogenation reaction with a different scope was conducted using a RH-derived catalyst. The conversion of epoxides to the corresponding anti-Markovnikov alcohols was chosen as test reaction. For this purpose, a Ni-containing material was prepared by a methodology similar to the Ag@RH synthesis (chapter 2.1).  $\text{Ni}(\text{NO}_3)_2$  was used for impregnation of RH and consecutively pyrolyzed at  $700^\circ\text{C}$ . The received supporting material had similar properties to the Ag@RH catalyst. Thus, XPS, XRD, IR and BET results will not be explained in detail. However, to understand how the material enabled the chosen test reaction, two features must be addressed: 1) the generated Ni particles and 2) the surface acidity.

The particles were examined with XRD, XPS, (temperature programmed desorption) TPD- $\text{H}_2$  and STEM. The XRD showed reflexes of cubic  $\text{Ni}^0$  at  $44$ ,  $51$  and  $76^\circ$  suggesting that most of the crystallites were coinage Ni. However, the XPS revealed that the composition of the particles was more complex (A in figure 21).

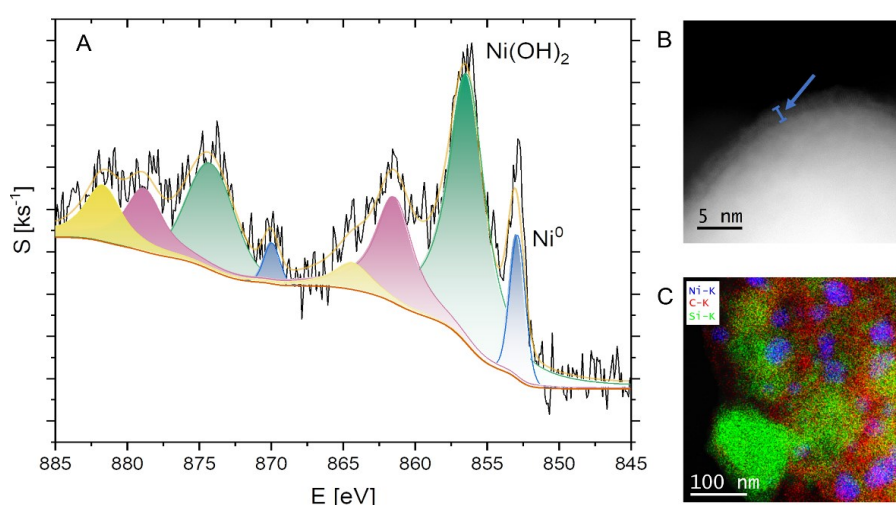


Figure 20 A) XPS measurement of Ni NP as well as B) HAADF STEM images of core shell structure and C) HAADF STEM with energy-dispersive X-ray spectroscopy mapping of Ni@RH.

The Ni 2p signals at 852.9 and 870.0 eV matched  $\text{Ni}^0$ <sup>186</sup> and, alongside a second Ni species could be identified by analyzing the Ni 2p<sub>3/2</sub> signal at 856.4 eV with corresponding satellite peaks at 861.4 eV and 864.3 eV. The second species appeared to be  $\text{Ni}(\text{OH})_2$ <sup>187</sup> indicating a core-shell-like structure of the Ni NP similar to the structure reported for the Co@RH catalyst, with a  $\text{Ni}^0$  core surrounded by a  $\text{Ni}^{2+}$  layer. The hypothesis of a core-shell-structure was proven by STEM, where a metal core with an oxide shell was visible (blue arrow in B in figure 20). The Ni-particle size varied strongly from 5 to 100 nm (C in figure 20). Interestingly, no carbon layer was observed on the particles, which was the case for the Ag@RH<sup>182</sup> and Co-based systems.<sup>131, 132</sup> However, the reducibility of the Ni NP was proven in TPD- $\text{H}_2$  measurements. The desorption curve showed two peaks with an offset at 188°C and 342°C. This indicates the presence of different active sites, which is a well-known phenomenon in hydrogenation catalysis using Ni NP.<sup>188</sup>

Finally, the acidity of the material was investigated. Firstly, a preliminary test with pH-indicators suggested a Brønsted acidic behavior of the catalyst. Hence, the material was further analyzed with  $\text{NH}_3$ -TPD and Corma's experiment.  $\text{NH}_3$ -TPD showed the presence of mainly strong acidic centers with a signal from 400 to 600 °C of Ni@RH, which was not present on the bare supporting material. However, the pyrolyzed RH only offered weak acidic sites with a peak around 160 °C. Additionally, the so-called Corma's experiment was done in order to test whether the catalyst offers Lewis acidity in addition to Brønsted acidity (table 4).

Thus, Corma's acetal was converted with both Ni@RH and the pyrolyzed RH and, based on the appearance of the products (**1**, **2** and **3** in table 4), the test revealed that the material was able to act as Lewis as well as Brønsted acid. However, the acidic activity in this experiment was mainly associated with the pyrolyzed RH since Ni@RH and the bare support gave very similar results.

Table 4 Results of Corma's acetal experiment for acidity assessment.

Corma's acetal		1	2	3
Catalyst	Conversion [%] <sup>[a]</sup>	Product distribution [%] <sup>[a]</sup>		
		Ketone 1	Ester 2	Dioxane 3
RH	65	40	-	60
Ni@RH	65	30	-	70

<sup>[a]</sup> Conversion was determined by GC using n-octane as internal standard <sup>[b]</sup> RH was prepared analogous to Ni@RH without the use of  $\text{Ni}(\text{NO}_3)_2$  salt Reaction conditions: 20 mg catalyst, 2 ml 1,2-dichlorobenzene, 1 mol l<sup>-1</sup> acetal, 180°C, 16 h, 1 bar  $\text{N}_2$ , reaction was conducted in steel autoclave

## 2.4.2 Application as Hydrogenation Catalyst

The prepared material was tested in the conversion of epoxides to anti-Markovnikov alcohols. For this, the synthesis of 2-phenylethan-1-ol from styrene oxide under hydrogen atmosphere was chosen as test reaction.

At this point it is noteworthy that a composite system is known using Ni NP on RH ash for furfural and leculinic acid hydrogenation.<sup>189</sup> This work by Kang et al. from 2020 is somewhat comparable to the results presented in this thesis as likewise, the potential of Ni NP for hydrogenation reactions was explored. Additionally, a number of parameters of evaluated catalytic performance were presented in the study<sup>189</sup> and the catalyst preparation was relatively similar. However, the Ni was not directly impregnated on RH but on already pyrolyzed RH ash and, therefore, an additional high temperature treatment is necessary to obtain the catalyst. Nevertheless, this example as well as well-established catalysts can be used as reference system for the herein presented catalysts.

Preliminary tests were successful since only the primary alcohol and never the secondary one was produced without exception. Thus, the reaction conditions were optimized (table 5). Interestingly, it was possible to fully control the reaction selectivity by choosing certain reaction conditions. A solvent screening revealed that the best alcohol yields could be achieved using an at least partially aquatic solvent mixture.

Table 5 Condition optimization of styrene oxide conversion to 2-phenylethan-1-ol.

ii	T [°C]	P [bar]	Solvent	Yield <sup>[b]</sup>		
				1	2	3
1	50	10	H <sub>2</sub> O:THF	93	4	-
2	50	25	H <sub>2</sub> O:THF	82	-	15
3	70	10	H <sub>2</sub> O:THF	-	86	12
<b>4</b>	<b>70</b>	<b>25</b>	<b>H<sub>2</sub>O:THF</b>	-	-	<b>99</b>
5	70 <sup>[c]</sup>	25 <sup>[c]</sup>	H <sub>2</sub> O:THF <sup>[c]</sup>	-	95 <sup>[c]</sup>	4 <sup>[c]</sup>

[a] Reaction conditions: 2 mmol of substrate, 2 ml solvent, 4 h reaction time, 20 mg catalyst (corresponding to 1.5 mol % Ni) [b] Yield was determined by GC using *n*-octane as internal standard [c] use of pyrolyzed RH not impregnated with Ni(NO<sub>3</sub>)<sub>2</sub>

The reaction temperatures and pressure could be used to control the reaction product as follows: 1) temperatures lower than 70 °C led to diol formation (**1** in table 5), 2)

pressure lower than 25 bar at elevated temperatures led to aldehyde formation (2 in table 5) and 3) the corresponding alcohol was synthesized in excellent selectivity and yields at 70 °C and 25 bar hydrogen pressure using a water: tetrahydrofuran (THF) solution (1:1 voluminal ratio) as solvent. Analogous to the Ag@RH and Co@RH systems, a screening was done for the optimal pyrolysis temperature during catalyst preparation and the required catalyst amount to obtain maximum yield. An optimal pyrolysis temperature of 700°C was found to give best catalytic performance, which is 100 °C higher than the preparation temperature for the Ag@RH and Co@RH catalysts.

The substrate scope was investigated after optimizing the reaction conditions (figure 21). Thus, a number of epoxides was successfully converted to the corresponding anti-MAs, including terminal and non-terminal epoxides. This is an advantage over comparable heterogenous or homogeneous systems since the substrate scopes of those systems are often limited to terminal epoxides.<sup>149, 190</sup> A number of halogenated epoxides were converted without any dehalogenation and, furthermore, nitril groups remained unchanged during the reduction with the Ni@RH catalyst.

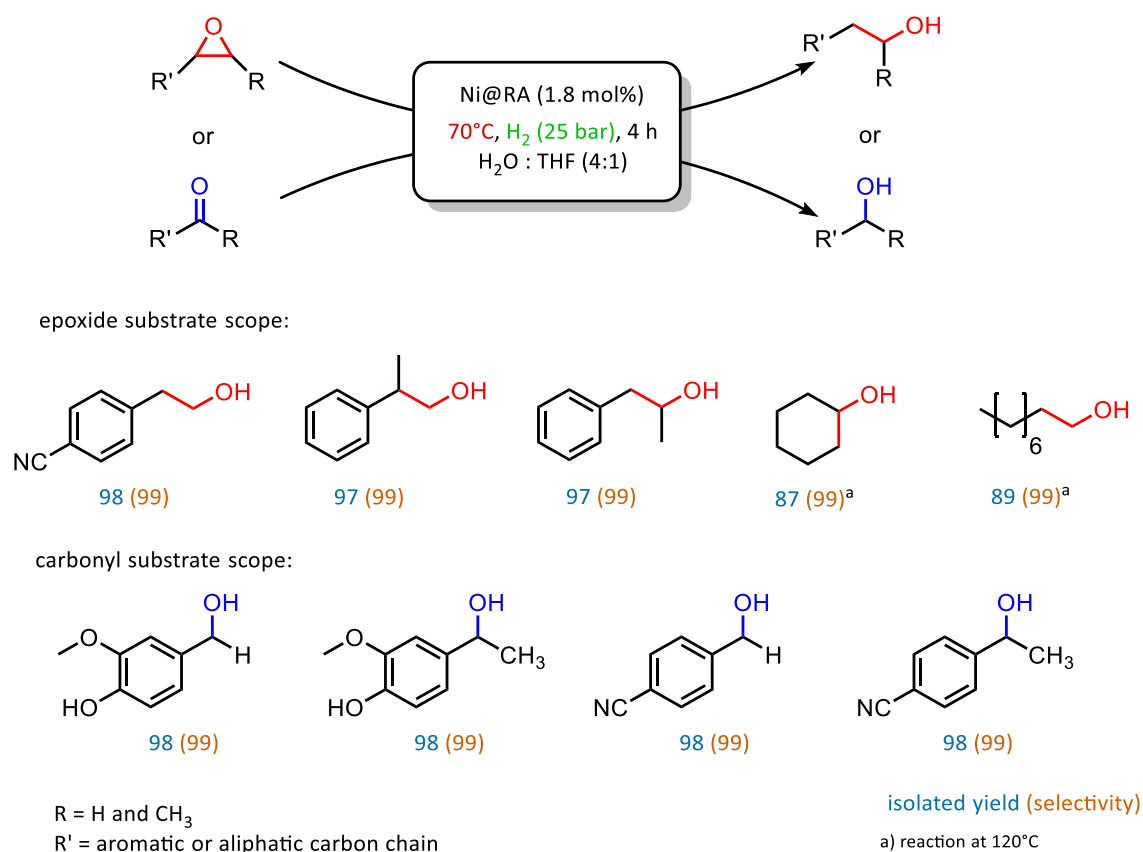


Figure 21 Products of substrate screening using leached Ni catalyst. Conditions: 120 °C, 10 bar H<sub>2</sub>, 1 mmol substrate, 12 h, in 1 ml of Isopropanol/H<sub>2</sub>O, 20 mg catalyst (1.8 mol% of Ni).

Furthermore, beside aromatic epoxides, aliphatic epoxides were also converted. However, the reaction temperature needed to be elevated to 120 °C in order to achieve

reasonable yields as they, dropped drastically when converting aliphatic epoxies at 70 °C. In addition to the epoxide based scope, a number of carbonyl compounds were converted to the corresponding alcohols to investigate the hydrogenation ability of the catalyst. Again, excellent selectivity towards the desired alcohol was observed, proving that the catalyst can also be used in “pure” hydrogenation reaction.

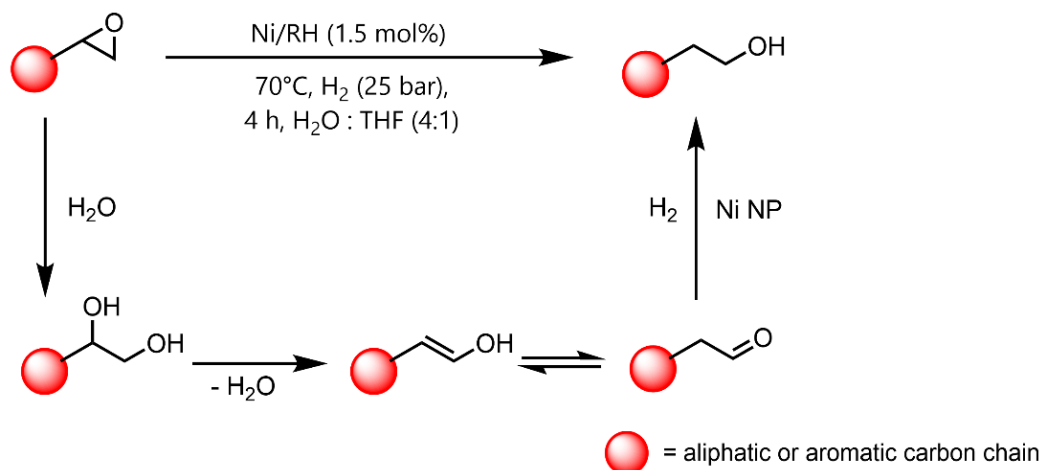


Figure 22: Proposed reaction mechanism for the conversion of terminal epoxides to anti-Mas.

Finally, a reaction mechanism was proposed based on literature as well as isolated and NMR-characterized reaction intermediates (figure 22). The reaction can be divided into three allocable steps: 1) the conversion of the epoxide to a diol, 2) diol conversion to the corresponding aldehyde or ketone and 3) the hydrogenation of the carbonyl to an alcohol. All intermediates can be isolated (table 5).

The catalyst activates epoxides by solid Brønsted-acid-catalyzed formation of diols similar to the epoxide opening promoted by water acting as weak acid at high temperatures.<sup>191</sup> The diols are further converted to the corresponding aldehyde or ketone via Lewis-acid-catalyzed rearrangement.<sup>191, 192</sup> Finally, the carbonyl group is reduced to an alcohol moiety by Ni NP. The hydrogenation of carbonyl groups by Ni NP is the last reaction step and works through a well described and understood hydride transfer mechanism<sup>145</sup> analogous to the already described Ag and Co systems.<sup>25, 193</sup>

### 3 Conclusion and Outlook

In conclusion, this thesis described the utilization of RH for the development of hydrogenation catalysts. The preparation of the **Ag@RH** catalyst for nitro group reduction showed that it is generally possible to fix metal ions on RH and convert them into catalytically active particles via carbothermal reduction. It was further demonstrated that the methodology can be transferred to the use of other metals as active centers. The Co-based catalyst **Co@RH-E1** was prepared with the literature known approach of generating catalytically active Co centers by introducing Co in form of N-rich Co complexes. Furthermore, the catalytic properties as well as the recycling stability of the prepared catalysts were improved by base etching of the carbon silica composite structure of the RH support. The Co catalyst was likewise used for the reduction of nitro groups. Finally, **Ni@RH** derived from RH was used for the reductive conversion of epoxides to anti-MAs. The catalytic performance of the three model systems was evaluated by reaction optimization, an extensive substrate screening and kinetic studies. Furthermore, the structure-activity relationships of the prepared catalysts were investigated with several characterization methods e.g., XRD, XPS, TPD, BET surface area analysis, EA, IR and the microscopy techniques SEM and STEM. In doing so, the catalytically active centers were identified, and the mode of action could be disclosed.

Additionally, the prepared Ag-containing material **Ag@RH** was successfully tested for the application as antimicrobial agent. It was shown that the Ag NP on pyrolyzed RH are antimicrobially active in extremely low amounts against the ESKAPE pathogens and pathogenic yeast. The presented method benefits from the well-known anti-microbial mode of action of Ag NP and combines it with an easy and straightforward synthesis approach.

In summary, the alternative ways of RH utilization presented in this thesis can be applied to different hydrogenation reactions by using different metals and to the preparation of sanitary materials. However, such alternative ways of treatment must first and foremost gain the trust and acceptance from the people most affected: the rice farmers. Otherwise the traditional method of open burning will remain the solution of dealing with the waste, since it secures a smooth rice production and, consequently, the basis of existence for approximately 4 million people in Vietnam alone.<sup>28</sup> Thus, it is of utter importance that research as presented here is not only discussed and presented within the scientific community but also introduced to authorities and workers in the affected communities.

## Appendix

### References

- (1) Stevenson, A. *Oxford dictionary of English*; Oxford University Press, USA, 2010.
- (2) General Assembly, U. N. *Resolution adopted by the General Assembly on 6 July 2017*; A/RES/71/313, 2017.
- (3) Weissermel, K.; Arpe, H.-J. *Industrial organic chemistry*; John Wiley & Sons, 2008. Schobert, H. *Chemistry of fossil fuels and biofuels*; Cambridge University Press, 2013.
- (4) Hoel, M.; Kverndokk, S. Depletion of fossil fuels and the impacts of global warming. *Resource and energy economics* **1996**, 18 (2), 115-136. Martins, F.; Felgueiras, C.; Smitkova, M.; Caetano, N. Analysis of fossil fuel energy consumption and environmental impacts in European countries. *Energies* **2019**, 12 (6), 964.
- (5) Hassler, F. Die Katalyse und ihre Anwendung in der Technik. *Angewandte Chemie* **1904**, 17 (41), 1540-1544.
- (6) Van Santen, R. A. *Modern heterogeneous catalysis: an introduction*; John Wiley & Sons, 2017.
- (7) Chiusoli, G. P.; Maitlis, P. M. *Metal-catalysis in industrial organic processes*; Royal Society of Chemistry, 2019.
- (8) Rana, M. S.; Sámano, V.; Ancheyta, J.; Diaz, J. A review of recent advances on process technologies for upgrading of heavy oils and residua. *Fuel* **2007**, 86 (9), 1216-1231. Mederos, F. S.; Elizalde, I.; Ancheyta, J. Steady-State and Dynamic Reactor Models for Hydrotreatment of Oil Fractions: A Review. *Catalysis Reviews* **2009**, 51 (4), 485-607.
- (9) List, G. R.; King, J. W. *Hydrogenation of fats and oils: theory and practice*; Elsevier, 2016.
- (10) Werner, J. Amination by reduction. Unit processes review. *Industrial & Engineering Chemistry* **1961**, 53 (1), 77-78.
- (11) Bonrath, W.; Medlock, J.; Schütz, J.; Wüstenberg, B.; Netscher, T.; Wüstenberg, B.; Netscher, T. *Hydrogenation in the vitamins and fine chemicals industry—an overview*; InTech Rijeka, 2012.
- (12) McDowall, W.; Eames, M. Forecasts, scenarios, visions, backcasts and roadmaps to the hydrogen economy: A review of the hydrogen futures literature. *Energy policy* **2006**, 34 (11), 1236-1250.
- (13) Chaloner, P. A.; Esteruelas, M. A.; Joó, F.; Oro, L. A. *Homogeneous hydrogenation*; Springer Science & Business Media, 2013.
- (14) Thomas, J. M.; Thomas, W. J. *Principles and practice of heterogeneous catalysis*; John Wiley & Sons, 2014.
- (15) Behr, A.; Neubert, P. *Applied homogeneous catalysis*; John Wiley & Sons, 2012.
- (16) Argyle, M. D.; Bartholomew, C. H. Heterogeneous catalyst deactivation and regeneration: a review. *Catalysts* **2015**, 5 (1), 145-269.
- (17) Baetzold, R. Calculated model for metal cluster catalysis: H<sub>2</sub> dissociation. *Surface Science* **1975**, 51 (1), 1-13.



- (18) Delbecq, F.; Sautet, P. Competitive  $C\equiv C$  and  $C\equiv O$  Adsorption of  $\alpha$ - $\beta$ -Unsaturated Aldehydes on Pt and Pd Surfaces in Relation with the Selectivity of Hydrogenation Reactions: A Theoretical Approach. *Journal of Catalysis* **1995**, *152* (2), 217-236. Boitiaux, J.; Cosyns, J.; Vasudevan, S. Hydrogenation of highly unsaturated hydrocarbons over highly dispersed palladium catalyst: part I: behaviour of small metal particles. *Applied Catalysis* **1983**, *6* (1), 41-51.
- (19) Takale, B. S.; Thakore, R. R.; Gao, E. S.; Gallou, F.; Lipshutz, B. H. Environmentally responsible, safe, and chemoselective catalytic hydrogenation of olefins: ppm level Pd catalysis in recyclable water at room temperature. *Green Chemistry* **2020**, *22* (18), 6055-6061. Kuai, L.; Chen, Z.; Liu, S.; Kan, E.; Yu, N.; Ren, Y.; Fang, C.; Li, X.; Li, Y.; Geng, B. Titania supported synergistic palladium single atoms and nanoparticles for room temperature ketone and aldehydes hydrogenation. *Nature communications* **2020**, *11* (1), 1-9.
- (20) Bao, M.; Nakamura, H.; Yamamoto, Y. Facile allylative dearomatization catalyzed by palladium. *Journal of the American Chemical Society* **2001**, *123* (4), 759-760.
- (21) Farjana, S. H.; Huda, N.; Mahmud, M. P. Life cycle assessment of cobalt extraction process. *Journal of Sustainable Mining* **2019**, *18* (3), 150-161.
- (22) Eckelman, M. J.; Graedel, T. Silver emissions and their environmental impacts: a multilevel assessment. *Environmental science & technology* **2007**, *41* (17), 6283-6289. Kalavrouziotis, I.; Koukoulakis, P. The environmental impact of the platinum group elements (Pt, Pd, Rh) emitted by the automobile catalyst converters. *Water, air, and soil pollution* **2009**, *196* (1), 393-402.
- (23) Tsurukawa, N.; Prakash, S.; Manhart, A. Social impacts of artisanal cobalt mining in Katanga, Democratic Republic of Congo. *Öko-Institut eV, Freiburg* **2011**.
- (24) Monai, M.; Melchionna, M.; Fornasiero, P. From metal to metal-free catalysts: Routes to sustainable chemistry. *Advances in catalysis* **2018**, *63*, 1-73.
- (25) Formenti, D.; Ferretti, F.; Scharnagl, F. K.; Beller, M. Reduction of nitro compounds using 3d-non-noble metal catalysts. *Chemical reviews* **2018**, *119* (4), 2611-2680.
- (26) Liu, J. Catalysis by supported single metal atoms. *Acs Catalysis* **2017**, *7* (1), 34-59.
- (27) Tetrault, R. *World Agricultural Production - World Production, Markets, and Trade Report*; U.S. Department of Agriculture, online, 2021.
- (28) Vietnam, G. Statistical Yearbook of Vietnam 2019. Statistics Publishing House, Hanoi: 2020.
- (29) Chand, N.; Fahim, M. *Tribology of natural fiber polymer composites*; Woodhead publishing, 2020.
- (30) Domínguez-Escribá, L.; Porcar, M. Rice straw management: the big waste. *Biofuels, Bioproducts and Biorefining* **2010**, *4* (2), 154-159.
- (31) Quispe, I.; Navia, R.; Kahhat, R. Energy potential from rice husk through direct combustion and fast pyrolysis: a review. *Waste management* **2017**, *59*, 200-210.
- (32) Soltani, N.; Bahrami, A.; Pech-Canul, M.; González, L. Review on the physicochemical treatments of rice husk for production of advanced materials. *Chemical engineering journal* **2015**, *264*, 899-935.
- (33) Rencoret, J.; Ralph, J.; Marques, G.; Gutiérrez, A.; Martínez, A. n. T.; del Río, J. C. Structural characterization of lignin isolated from coconut (*Cocos nucifera*) coir fibers. *Journal of agricultural and food chemistry* **2013**, *61* (10), 2434-2445.
- (34) de Saussure, N. T. *Recherches chimiques sur la vegetation*; Nyon, 1804.

- (35) Hildebrand, M.; Higgins, D. R.; Busser, K.; Volcani, B. E. Silicon-responsive cDNA clones isolated from the marine diatom *Cylindrotheca fusiformis*. *Gene* **1993**, *132* (2), 213-218. Hildebrand, M.; Volcani, B. E.; Gassmann, W.; Schroeder, J. I. A gene family of silicon transporters. *Nature* **1997**, *385* (6618), 688-689.
- (36) Kaur, H.; Greger, M. A review on si uptake and transport system. *Plants* **2019**, *8* (4), 81.
- (37) Wiberg, E. *Lehrbuch der anorganischen Chemie*; Walter de Gruyter GmbH & Co KG, 2019.
- (38) Raven, J. Silicon transport at the cell and tissue level. In *Studies in plant science*, Vol. 8; Elsevier, 2001; pp 41-55.
- (39) Ma, J. F.; Yamaji, N.; Mitani, N.; Tamai, K.; Konishi, S.; Fujiwara, T.; Katsuhara, M.; Yano, M. An efflux transporter of silicon in rice. *Nature* **2007**, *448* (7150), 209-212.
- (40) Schué, F. *Water soluble polymers: solution properties and applications*. ; Wiley Online Library, 1998.
- (41) Ma, J. F.; Yamaji, N. Silicon uptake and accumulation in higher plants. *Trends in plant science* **2006**, *11* (8), 392-397.
- (42) Epstein, E. The anomaly of silicon in plant biology. *Proceedings of the National Academy of Sciences* **1994**, *91* (1), 11-17. Ma, J. F. Role of silicon in enhancing the resistance of plants to biotic and abiotic stresses. *Soil science and plant nutrition* **2004**, *50* (1), 11-18. Richmond, K. E.; Sussman, M. Got silicon? The non-essential beneficial plant nutrient. *Current opinion in plant biology* **2003**, *6* (3), 268-272.
- (43) Treguer, P.; Nelson, D. M.; Van Bennekom, A. J.; DeMaster, D. J.; Leynaert, A.; Queguiner, B. The silica balance in the world ocean: a reestimate. *Science* **1995**, *268* (5209), 375-379.
- (44) Lim, S. L.; Wu, T. Y.; Sim, E. Y. S.; Lim, P. N.; Clarke, C. Biotransformation of rice husk into organic fertilizer through vermicomposting. *Ecological Engineering* **2012**, *41*, 60-64.
- (45) Pictures taken and processed by Felix Unglaube all rights reserved.
- (46) Lasko, K.; Vadrevu, K. Improved rice residue burning emissions estimates: Accounting for practice-specific emission factors in air pollution assessments of Vietnam. *Environmental Pollution* **2018**, *236*, 795-806.
- (47) Wahid, A.; Maggs, R.; Shamsi, S.; Bell, J.; Ashmore, M. Effects of air pollution on rice yield in the Pakistan Punjab. *Environmental Pollution* **1995**, *90* (3), 323-329. Ishii, S.; Marshall, F. M.; Bell, J.; Abdullah, A. M. Impact of ambient air pollution on locally grown rice cultivars (*Oryza sativa* L.) in Malaysia. *Water, Air, and Soil Pollution* **2004**, *154* (1-4), 187-201.
- (48) Molina, J.; Sikora, M.; Garud, N.; Flowers, J. M.; Rubinstein, S.; Reynolds, A.; Huang, P.; Jackson, S.; Schaal, B. A.; Bustamante, C. D. Molecular evidence for a single evolutionary origin of domesticated rice. *Proceedings of the National Academy of Sciences* **2011**, *108* (20), 8351-8356.
- (49) Higham, C.; Lu, T. L.-D. The origins and dispersal of rice cultivation. *Antiquity* **1998**, *72* (278), 867-877. Liu, L.; Lee, G.-A.; Jiang, L.; Zhang, J. Evidence for the early beginning (c. 9000 cal. BP) of rice domestication in China: a response. *The Holocene* **2007**, *17* (8), 1059-1068.
- (50) Lai, O.-M.; Jacoby, J. J.; Leong, W.-F.; Lai, W.-T. Nutritional studies of rice bran oil. *Rice Bran and Rice Bran Oil* **2019**, 19-54.

- (51) Beagle, E. C. *Rice-husk conversion to energy*; FAO, Roma (Italia), 1978.
- (52) Ghosal, S.; Moulik, S. Use of rice husk ash as partial replacement with cement in concrete-A review. *International Journal of Engineering Research* **2015**, 4 (9), 506-509.
- (53) Malhotra, V. Fly ash, slag, silica fume, and rice husk ash in concrete: A review. *Concrete International* **1993**, 15 (4), 23-28.
- (54) Raman, S. N.; Ngo, T.; Mendis, P.; Mahmud, H. High-strength rice husk ash concrete incorporating quarry dust as a partial substitute for sand. *Construction and Building Materials* **2011**, 25 (7), 3123-3130. Singh, B. Rice husk ash. In *Waste and Supplementary Cementitious Materials in Concrete*, Elsevier, 2018; pp 417-460. He, J.; Kawasaki, S.; Achal, V. The utilization of agricultural waste as agro-cement in concrete: a review. *Sustainability* **2020**, 12 (17), 6971.
- (55) Tichane, R. *Ash glazes*; Krause Pubns Inc, 1998.
- (56) Shahidi, F. *Bailey's Industrial Oil and Fat Products, Edible Oil and Fat Products: Processing Technologies*; John Wiley & Sons, 2005.
- (57) Sohail, M.; Rakha, A.; Butt, M. S.; Iqbal, M. J.; Rashid, S. Rice bran nutraceuticals: A comprehensive review. *Critical Reviews in Food Science and Nutrition* **2017**, 57 (17), 3771-3780.
- (58) Deshannavar, U. B.; Hegde, P. G.; Dhalayat, Z.; Patil, V.; Gavas, S. Production and characterization of agro-based briquettes and estimation of calorific value by regression analysis: An energy application. *Materials Science for Energy Technologies* **2018**, 1 (2), 175-181.
- (59) Bakar, M. S. A.; Titiloye, J. O. Catalytic pyrolysis of rice husk for bio-oil production. *Journal of analytical and applied pyrolysis* **2013**, 103, 362-368. Dey, P.; Ray, S.; Newar, A. Defining a waste vegetable oil-biodiesel based diesel substitute blend fuel by response surface optimization of density and calorific value. *Fuel* **2021**, 283, 118978. Thao, P. T. M.; Kurisu, K. H.; Hanaki, K. Greenhouse gas emission mitigation potential of rice husks for An Giang province, Vietnam. *biomass and bioenergy* **2011**, 35 (8), 3656-3666.
- (60) Huang, H.-j.; Yuan, X.-z.; Zeng, G.-m.; Liu, Y.; Li, H.; Yin, J.; Wang, X.-l. Thermochemical liquefaction of rice husk for bio-oil production with sub-and supercritical ethanol as solvent. *Journal of analytical and applied pyrolysis* **2013**, 102, 60-67. Liu, Y.; Yuan, X.-z.; Huang, H.-j.; Wang, X.-l.; Wang, H.; Zeng, G.-m. Thermochemical liquefaction of rice husk for bio-oil production in mixed solvent (ethanol–water). *Fuel processing technology* **2013**, 112, 93-99.
- (61) Hu, S.; Hsieh, Y.-L. Preparation of activated carbon and silica particles from rice straw. *ACS Sustainable Chemistry & Engineering* **2014**, 2 (4), 726-734.
- (62) Okamoto, G.; Okura, T.; Goto, K. Properties of silica in water. *Geochimica et Cosmochimica Acta* **1957**, 12 (1-2), 123-132.
- (63) Liou, T.-H. Preparation and characterization of nano-structured silica from rice husk. *Materials Science and Engineering: A* **2004**, 364 (1-2), 313-323.
- (64) Shamsudin, R.; Ng, M. H.; Ahmad, A.; Akbar, M. A. M.; Rashidbenam, Z. Silver-doped pseudowollastonite synthesized from rice husk ash: Antimicrobial evaluation, bioactivity and cytotoxic effects on human mesenchymal stem cells. *Ceramics International* **2018**, 44 (10), 11381-11389.
- (65) Biswas, M. C.; Tiimob, B. J.; Abdela, W.; Jeelani, S.; Rangari, V. K. Nano silica-carbon-silver ternary hybrid induced antimicrobial composite films for food packaging application. *Food Packaging and Shelf Life* **2019**, 19, 104-113.

- (66) Cui, J.; Yang, Y.; Hu, Y.; Li, F. Rice husk based porous carbon loaded with silver nanoparticles by a simple and cost-effective approach and their antibacterial activity. *Journal of colloid and interface science* **2015**, *455*, 117-124.
- (67) Cui, J.; Liang, Y.; Yang, D.; Liu, Y. Facile fabrication of rice husk based silicon dioxide nanospheres loaded with silver nanoparticles as a rice antibacterial agent. *Scientific reports* **2016**, *6* (1), 1-10.
- (68) Jafari, L.; Pourahmad, A.; Asadpour, L. Rice husk based MCM-41 nanoparticles loaded with Ag<sub>2</sub>S nanostructures by a green and room temperature method and its antimicrobial property. *Inorganic and Nano-Metal Chemistry* **2017**, *47* (11), 1552-1559.
- (69) Supply, W. U. J. W.; Programme, S. M. *Progress on drinking water and sanitation: 2014 update*; World Health Organization, 2014.
- (70) Naqvi, S. A. Z.; Irfan, A.; Zaheer, S.; Sultan, A.; Shajahan, S.; Rubab, S. L.; Ain, Q.; Acevedo, R. Proximate composition of orange peel, pea peel and rice husk wastes and their potential use as antimicrobial agents and antioxidants. *Vegetos* **2021**, *34* (2), 470-476.
- (71) Medici, S.; Peana, M.; Nurchi, V. M.; Zoroddu, M. A. Medical uses of silver: history, myths, and scientific evidence. *Journal of medicinal chemistry* **2019**, *62* (13), 5923-5943.
- (72) Alexander, J. W. History of the medical use of silver. *Surgical infections* **2009**, *10* (3), 289-292.
- (73) Banin, E.; Hughes, D.; Kuipers, O. P. Bacterial pathogens, antibiotics and antibiotic resistance. *FEMS microbiology reviews* **2017**, *41* (3), 450-452.
- (74) European Centre for Disease Prevention and Control. Surveillance of antimicrobial resistance in Europe 2018. Stockholm: ECDC; 2019.
- (75) O'Neill, J. Tackling drug-resistant infections globally: final report and recommendations. **2016**.
- (76) Robinson, T. P.; Bu, D.; Carrique-Mas, J.; Fèvre, E. M.; Gilbert, M.; Grace, D.; Hay, S. I.; Jiwakanon, J.; Kakkar, M.; Kariuki, S. Antibiotic resistance is the quintessential One Health issue. *Transactions of the Royal Society of Tropical Medicine and Hygiene* **2016**, *110* (7), 377-380. Schulman, L. S. Bacterial resistance to antibodies: a model evolutionary study. *Journal of theoretical biology* **2017**, *417*, 61-67.
- (77) source "web of science", <https://www.webofscience.com/wos/woscc/basic-search>, search keyword: "rice husk, utilization or use" and "rice husk, utilization or use, catalysis or catalyst" used date 07.02.2022.
- (78) Jehng, J.-M.; Hu, H.; Gao, X.; Wachs, I. E. The dynamic states of silica-supported metal oxide catalysts during methanol oxidation. *Catalysis Today* **1996**, *28* (4), 335-350.
- (79) Adam, F.; Fook, C. L. Chromium modified silica from rice husk as an oxidative catalyst. *Journal of Porous Materials* **2009**, *16* (3), 291-298. Adam, F.; Iqbal, A. The oxidation of styrene by chromium–silica heterogeneous catalyst prepared from rice husk. *Chemical Engineering Journal* **2010**, *160* (2), 742-750.
- (80) Wu, J.; Chen, S.; Muruganandham, M. Catalytic ozonation of oxalic acid using carbon-free rice husk ash catalysts. *Industrial & engineering chemistry research* **2008**, *47* (9), 2919-2925.
- (81) Van Nguyen, T. T.; Nguyen, T.; Nguyen, P. A.; Pham, T. T. P.; Mai, T. P.; Truong, Q. D.; Ha, H. K. P. Mn-Doped material synthesized from red mud and rice husk ash

- as a highly active catalyst for the oxidation of carbon monoxide and p-xylene. *New Journal of Chemistry* **2020**, 44 (46), 20241-20252.
- (82) Chen, W.-S.; Chang, F.-W.; Roselin, L. S.; Ou, T.-C.; Lai, S.-C. Partial oxidation of methanol over copper catalysts supported on rice husk ash. *Journal of Molecular Catalysis A: Chemical* **2010**, 318 (1-2), 36-43.
  - (83) Khoshbin, R.; Oruji, S.; Karimzadeh, R. Catalytic cracking of light naphtha over hierarchical ZSM-5 using rice husk ash as silica source in presence of ultrasound energy: Effect of carbon nanotube content. *Advanced Powder Technology* **2018**, 29 (9), 2176-2187.
  - (84) Siriworarat, K.; Deerattrakul, V.; Dittanet, P.; Kongkachuichay, P. Production of methanol from carbon dioxide using palladium-copper-zinc loaded on MCM-41: Comparison of catalysts synthesized from flame spray pyrolysis and sol-gel method using silica source from rice husk ash. *Journal of Cleaner Production* **2017**, 142, 1234-1243.
  - (85) Li, Y.; Lan, J. Y.; Liu, J.; Yu, J.; Luo, Z.; Wang, W.; Sun, L. Synthesis of gold nanoparticles on rice husk silica for catalysis applications. *Industrial & engineering chemistry research* **2015**, 54 (21), 5656-5663.
  - (86) Artkla, S.; Kim, W.; Choi, W.; Wittayakun, J. Highly enhanced photocatalytic degradation of tetramethylammonium on the hybrid catalyst of titania and MCM-41 obtained from rice husk silica. *Applied Catalysis B: Environmental* **2009**, 91 (1-2), 157-164.
  - (87) Franco, A.; De, S.; Balu, A. M.; Romero, A. A.; Luque, R. Integrated Mechanochemical/Microwave-Assisted Approach for the Synthesis of Biogenic Silica-Based Catalysts from Rice Husk Waste. *ACS Sustainable Chemistry & Engineering* **2018**, 6 (9), 11555-11562.
  - (88) Roschat, W.; Siritanon, T.; Yoosuk, B.; Promarak, V. Rice husk-derived sodium silicate as a highly efficient and low-cost basic heterogeneous catalyst for biodiesel production. *Energy Conversion and Management* **2016**, 119, 453-462.
  - (89) Zhang, X.; Li, Y.; Li, G.; Hu, C. Preparation of Fe/activated carbon directly from rice husk pyrolytic carbon and its application in catalytic hydroxylation of phenol. *RSC advances* **2015**, 5 (7), 4984-4992.
  - (90) Teng, Z.; Huang, S.; Fu, L.; Xu, H.; Li, N.; Zhou, Q. Study of a catalyst supported on rice husk ash for NO reduction with carbon monoxide. *Catalysis Science & Technology* **2020**, 10 (5), 1431-1443.
  - (91) Han, F.; Xu, X.; Fu, Y.; Wang, X. Synthesis of rice-husk-carbon-supported nickel ferrite catalyst for reduction of nitrophenols. *Journal of nanoscience and nanotechnology* **2019**, 19 (9), 5838-5846.
  - (92) Kennedy, L. J.; Sekaran, G. Integrated biological and catalytic oxidation of organics/inorganics in tannery wastewater by rice husk based mesoporous activated carbon—*Bacillus* sp. *Carbon* **2004**, 42 (12-13), 2399-2407.
  - (93) Lu, C.-Y.; Wey, M.-Y.; Chuang, K.-H. Catalytic treating of gas pollutants over cobalt catalyst supported on porous carbons derived from rice husk and carbon nanotube. *Applied Catalysis B: Environmental* **2009**, 90 (3-4), 652-661.
  - (94) Liu, Y.; Guo, Y.; Gao, W.; Wang, Z.; Ma, Y.; Wang, Z. Simultaneous preparation of silica and activated carbon from rice husk ash. *Journal of Cleaner Production* **2012**, 32, 204-209.
  - (95) Shirini, F.; Mamaghani, M.; Seddighi, M. Sulfonated rice husk ash (RHA-SO<sub>3</sub>H): A highly powerful and efficient solid acid catalyst for the chemoselective

- preparation and deprotection of 1, 1-diacetates. *Catalysis Communications* **2013**, *36*, 31-37.
- (96) Galhardo, T. S.; Simone, N. I.; Gonçalves, M.; Figueiredo, F. v. C.; Mandelli, D.; Carvalho, W. A. Preparation of sulfonated carbons from rice husk and their application in catalytic conversion of glycerol. *ACS Sustainable Chemistry & Engineering* **2013**, *1* (11), 1381-1389.
- (97) Li, M.; Zheng, Y.; Chen, Y.; Zhu, X. Biodiesel production from waste cooking oil using a heterogeneous catalyst from pyrolyzed rice husk. *Bioresource technology* **2014**, *154*, 345-348.
- (98) Balan, W. S.; Janaun, J.; Chung, C. H.; Semilin, V.; Zhu, Z.; Haywood, S. K.; Touhami, D.; Chong, K. P.; Yaser, A. Z.; Lee, P. C. Esterification of residual palm oil using solid acid catalyst derived from rice husk. *Journal of hazardous materials* **2021**, *404*, 124092.
- (99) Li, M.; Chen, D.; Zhu, X. Preparation of solid acid catalyst from rice husk char and its catalytic performance in esterification. *Chinese Journal of Catalysis* **2013**, *34* (9), 1674-1682.
- (100) Magar, S.; Mohanraj, G. T.; Jana, S. K.; Rode, C. V. Synthesis and characterization of supported heteropoly acid: Efficient solid acid catalyst for glycerol esterification to produce biofuel additives. *Inorganic and Nano-Metal Chemistry* **2020**, *50* (11), 1157-1165. Mallesham, B.; Sudarsanam, P.; Reddy, B. M. Production of biofuel additives from esterification and acetalization of bioglycerol over SnO<sub>2</sub>-based solid acids. *Industrial & Engineering Chemistry Research* **2014**, *53* (49), 18775-18785.
- (101) Shen, Y.; Yoshikawa, K. Tar conversion and vapor upgrading via in situ catalysis using silica-based nickel nanoparticles embedded in rice husk char for biomass pyrolysis/gasification. *Industrial & Engineering Chemistry Research* **2014**, *53* (27), 10929-10942.
- (102) Shen, Y.; Zhao, P.; Shao, Q.; Ma, D.; Takahashi, F.; Yoshikawa, K. In-situ catalytic conversion of tar using rice husk char-supported nickel-iron catalysts for biomass pyrolysis/gasification. *Applied Catalysis B: Environmental* **2014**, *152*, 140-151.
- (103) Xu, X.; Li, Z.; Tu, R.; Sun, Y.; Jiang, E. Hydrogen from Rice Husk Pyrolysis Volatiles via Non-Noble Ni-Fe Catalysts Supported on Five Differently Treated Rice Husk Pyrolysis Carbon Supports. *ACS Sustainable Chemistry & Engineering* **2018**, *6* (7), 8325-8339.
- (104) Spath, P. L.; Dayton, D. C. *Preliminary screening--technical and economic assessment of synthesis gas to fuels and chemicals with emphasis on the potential for biomass-derived syngas*; National Renewable Energy Lab., Golden, CO.(US), 2003.
- (105) Orlandi, M.; Brenna, D.; Harms, R.; Jost, S.; Benaglia, M. Recent developments in the reduction of aromatic and aliphatic nitro compounds to amines. *Organic Process Research & Development* **2016**, *22* (4), 430-445.
- (106) Béchamp, A. De l'action des protosels de fer sur la nitronaphtaline et la nitrobenzine;: nouvelle méthode de formation des bases organiques artificielles de zinin. *Annales de chimie et de physique* **1854**, *42*, 186-196.
- (107) Blaser, H.-U.; Steiner, H.; Studer, M. Selective Catalytic Hydrogenation of Functionalized Nitroarenes: An Update. *ChemCatChem* **2009**, *1* (2), 210-221. DOI: 10.1002/cctc.200900129.

- (108) Boronat, M.; Concepción, P.; Corma, A.; González, S.; Illas, F.; Serna, P. A Molecular Mechanism for the Chemoselective Hydrogenation of Substituted Nitroaromatics with Nanoparticles of Gold on TiO<sub>2</sub> Catalysts: A Cooperative Effect between Gold and the Support. *Journal of the American Chemical Society* **2007**, *129* (51), 16230-16237. DOI: 10.1021/ja076721g. Corma, A.; Concepción, P.; Serna, P. A Different Reaction Pathway for the Reduction of Aromatic Nitro Compounds on Gold Catalysts. *Angewandte Chemie International Edition* **2007**, *46* (38), 7266-7269. DOI: 10.1002/anie.200700823.
- (109) Shimizu, K.-i.; Miyamoto, Y.; Kawasaki, T.; Tanji, T.; Tai, Y.; Satsuma, A. Chemoselective Hydrogenation of Nitroaromatics by Supported Gold Catalysts: Mechanistic Reasons of Size- and Support-Dependent Activity and Selectivity. *The Journal of Physical Chemistry C* **2009**, *113* (41), 17803-17810. DOI: 10.1021/jp906044t.
- (110) Accrombessi, G.; Geneste, P.; Olivé, J.-L.; Pavia, A. Hydrogénolyse en phase liquide sur Pd/C des époxydes du carvomenthène et du limonène. *Tetrahedron* **1981**, *37* (18), 3135-3140.
- (111) Corma, A.; Serna, P. Chemoselective Hydrogenation of Nitro Compounds with Supported Gold Catalysts. *Science* **2006**, *313* (5785), 332-334. DOI: 10.1126/science.1128383.
- (112) Gebbink, R. J. K.; Moret, M.-E. *Non-Noble Metal Catalysis: Molecular Approaches and Reactions*; John Wiley & Sons, 2019.
- (113) Montoya, A.; Schlunke, A.; Haynes, B. S. Reaction of Hydrogen with Ag(111): Binding States, Minimum Energy Paths, and Kinetics. *The Journal of Physical Chemistry B* **2006**, *110* (34), 17145-17154. DOI: 10.1021/jp062725g. Mohammad, A. B.; Yudanov, I. V.; Lim, K. H.; Neyman, K. M.; Rösch, N. Hydrogen Activation on Silver: A Computational Study on Surface and Subsurface Oxygen Species. *The Journal of Physical Chemistry C* **2008**, *112* (5), 1628-1635. DOI: 10.1021/jp0765190.
- (114) Jiang, J.-X.; Li, Y.; Wu, X.; Xiao, J.; Adams, D. J.; Cooper, A. I. Conjugated microporous polymers with rose bengal dye for highly efficient heterogeneous organo-photocatalysis. *Macromolecules* **2013**, *46* (22), 8779-8783. Mei, D.; Neurock, M.; Smith, C. M. Hydrogenation of acetylene–ethylene mixtures over Pd and Pd–Ag alloys: First-principles-based kinetic Monte Carlo simulations. *Journal of Catalysis* **2009**, *268* (2), 181-195. Wang, S.; Huang, H.; Tsareva, S.; Bruneau, C.; Fischmeister, C. Silver-Catalyzed Hydrogenation of Ketones under Mild Conditions. *Advanced Synthesis & Catalysis* **2019**, *361* (4), 786-790. Xie, Y.; Hu, P.; Bendikov, T.; Milstein, D. Heterogeneously catalyzed selective hydrogenation of amides to alcohols and amines. *Catalysis Science & Technology* **2018**, *8* (11), 2784-2788. Steffan, M.; Jakob, A.; Claus, P.; Lang, H. Silica supported silver nanoparticles from a silver (I) carboxylate: Highly active catalyst for regioselective hydrogenation. *Catalysis Communications* **2009**, *10* (5), 437-441. Bron, M.; Teschner, D.; Knop-Gericke, A.; Jentoft, F. C.; Kröhnert, J.; Hohmeyer, J.; Volckmar, C.; Steinhauer, B.; Schlögl, R.; Claus, P. Silver as acrolein hydrogenation catalyst: intricate effects of catalyst nature and reactant partial pressures. *Physical Chemistry Chemical Physics* **2007**, *9* (27), 3559-3569.
- (115) Wen, C.; Yin, A.; Dai, W.-L. Recent advances in silver-based heterogeneous catalysts for green chemistry processes. *Applied Catalysis B: Environmental* **2014**, *160-161*, 730-741. DOI: <https://doi.org/10.1016/j.apcatb.2014.06.016>.

- (116) Shimizu, K.-i.; Miyamoto, Y.; Satsuma, A. Size- and support-dependent silver cluster catalysis for chemoselective hydrogenation of nitroaromatics. *Journal of Catalysis* **2010**, *270* (1), 86-94.
- (117) Shimizu, K.-i.; Satsuma, A. Silver cluster catalysts for green organic synthesis. *Journal of the Japan Petroleum Institute* **2011**, *54* (6), 347-360. Paun, C.; Słowik, G.; Lewin, E.; Sá, J. Flow hydrogenation of p-nitrophenol with nano-Ag/Al<sub>2</sub>O<sub>3</sub>. *RSC Advances* **2016**, *6* (90), 87564-87568, 10.1039/C6RA17512K. DOI: 10.1039/C6RA17512K. Khan, S. R.; Farooqi, Z. H.; Waheed uz, Z.; Ali, A.; Begum, R.; Kanwal, F.; Siddiq, M. Kinetics and mechanism of reduction of nitrobenzene catalyzed by silver-poly(N-isopropylacryl amide-co-allylacetic acid) hybrid microgels. *Materials Chemistry and Physics* **2016**, *171*, 318-327. DOI: <https://doi.org/10.1016/j.matchemphys.2016.01.023>. Zhao, B.; Dong, Z.; Wang, Q.; Xu, Y.; Zhang, N.; Liu, W.; Lou, F.; Wang, Y. Highly Efficient Mesoporous Core-Shell Structured Ag@SiO<sub>2</sub> Nanosphere as an Environmentally Friendly Catalyst for Hydrogenation of Nitrobenzene. *Nanomaterials* **2020**, *10*, 883. Naik, B.; Hazra, S.; Prasad, V. S.; Ghosh, N. N. Synthesis of Ag nanoparticles within the pores of SBA-15: An efficient catalyst for reduction of 4-nitrophenol. *Catalysis Communications* **2011**, *12* (12), 1104-1108. DOI: <https://doi.org/10.1016/j.catcom.2011.03.028>. Cárdenas-Lizana, F.; de Pedro, Z. M.; Gómez-Quero, S.; Keane, M. A. Gas phase hydrogenation of nitroarenes: A comparison of the catalytic action of titania supported gold and silver. *Journal of Molecular Catalysis A: Chemical* **2010**, *326* (1), 48-54. DOI: <https://doi.org/10.1016/j.molcata.2010.04.006>. Mohamed, M. M.; Al-Sharif, M. S. One pot synthesis of silver nanoparticles supported on TiO<sub>2</sub> using hybrid polymers as template and its efficient catalysis for the reduction of 4-nitrophenol. *Materials Chemistry and Physics* **2012**, *136* (2), 528-537. DOI: <https://doi.org/10.1016/j.matchemphys.2012.07.021>. Chen, Y.; Wang, C.; Liu, H.; Qiu, J.; Bao, X. Ag/SiO<sub>2</sub>: a novel catalyst with high activity and selectivity for hydrogenation of chloronitrobenzenes. *Chemical Communications* **2005**, (42), 5298-5300, 10.1039/B509595F. DOI: 10.1039/B509595F.
- (118) Attia, Y. A.; Mohamed, Y. M. Silicon-grafted Ag/AgX/rGO nanomaterials (X= Cl or Br) as dip-photocatalysts for highly efficient p-nitrophenol reduction and paracetamol production. *Applied Organometallic Chemistry* **2019**, *33* (3), e4757.
- (119) Griffiths, F.; Brown, O. The Catalytic Activity of Cobalt Sulfide for the Gas-phase Reduction of Nitro benzene to Aniline. *Journal of Physical Chemistry* **1937**, *41* (3), 477-484.
- (120) R. Braden, H. K., H. Ziemann. . Process for preparing unsaturated amino compounds. DE2362780A1. German Patent. Germany 1975.
- (121) Raja, R.; Golovko, V. B.; Thomas, J. M.; Berenguer-Murcia, A.; Zhou, W.; Xie, S.; Johnson, B. F. Highly efficient catalysts for the hydrogenation of nitro-substituted aromatics. *Chemical communications* **2005**, (15), 2026-2028.
- (122) Westerhaus, F. A.; Jagadeesh, R. V.; Wienhöfer, G.; Pohl, M.-M.; Radnik, J.; Surkus, A.-E.; Rabeah, J.; Junge, K.; Junge, H.; Nielsen, M.; et al. Heterogenized cobalt oxide catalysts for nitroarene reduction by pyrolysis of molecularly defined complexes. *Nature chemistry* **2013**, *5* (6), 537-543.
- (123) Formenti, D.; Ferretti, F.; Topf, C.; Surkus, A.-E.; Pohl, M.-M.; Radnik, J.; Schneider, M.; Junge, K.; Beller, M.; Ragaini, F. Co-based heterogeneous



- catalysts from well-defined  $\alpha$ -diimine complexes: Discussing the role of nitrogen. *Journal of Catalysis* **2017**, *351*, 79-89.
- (124) Formenti, D.; Topf, C.; Junge, K.; Ragaini, F.; Beller, M. Fe<sub>2</sub>O<sub>3</sub>/NGr@C-and Co<sub>3</sub>O<sub>4</sub>/NGr@C-catalysed hydrogenation of nitroarenes under mild conditions. *Catalysis Science & Technology* **2016**, *6* (12), 4473-4477.
- (125) Zhou, P.; Jiang, L.; Wang, F.; Deng, K.; Lv, K.; Zhang, Z. High performance of a cobalt–nitrogen complex for the reduction and reductive coupling of nitro compounds into amines and their derivatives. *Science advances* **2017**, *3* (2), e1601945.
- (126) Zhang, F.; Zhao, C.; Chen, S.; Li, H.; Yang, H.; Zhang, X.-M. In situ mosaic strategy generated Co-based N-doped mesoporous carbon for highly selective hydrogenation of nitroaromatics. *Journal of Catalysis* **2017**, *348*, 212-222.
- (127) Sahoo, B.; Formenti, D.; Topf, C.; Bachmann, S.; Scalone, M.; Junge, K.; Beller, M. Biomass-Derived Catalysts for Selective Hydrogenation of Nitroarenes. *ChemSusChem* **2017**, *10* (15), 3035-3039.
- (128) Jagadeesh, R. V.; Banerjee, D.; Arockiam, P. B.; Junge, H.; Junge, K.; Pohl, M.-M.; Radnik, J.; Brückner, A.; Beller, M. Highly selective transfer hydrogenation of functionalised nitroarenes using cobalt-based nanocatalysts. *Green Chemistry* **2015**, *17* (2), 898-902. Li, W.; Artz, J.; Broicher, C.; Junge, K.; Hartmann, H.; Besmehn, A.; Palkovits, R.; Beller, M. Superior activity and selectivity of heterogenized cobalt catalysts for hydrogenation of nitroarenes. *Catalysis Science & Technology* **2019**, *9* (1), 157-162.
- (129) Sahoo, B.; Surkus, A. E.; Pohl, M. M.; Radnik, J.; Schneider, M.; Bachmann, S.; Scalone, M.; Junge, K.; Beller, M. A biomass-derived non-noble cobalt catalyst for selective hydrodehalogenation of alkyl and (hetero) aryl halides. *Angewandte Chemie* **2017**, *129* (37), 11394-11399. Scharnagl, F. K.; Hertrich, M. F.; Ferretti, F.; Kreyenschulte, C.; Lund, H.; Jackstell, R.; Beller, M. Hydrogenation of terminal and internal olefins using a biowaste-derived heterogeneous cobalt catalyst. *Science advances* **2018**, *4* (9), eaau1248.
- (130) Formenti, D.; Mocci, R.; Atia, H.; Dastgir, S.; Anwar, M.; Bachmann, S.; Scalone, M.; Junge, K.; Beller, M. A State-of-the-Art Heterogeneous Catalyst for Efficient and General Nitrile Hydrogenation. *Chemistry—A European Journal* **2020**, *26* (67), 15589-15595.
- (131) Senthamarai, T.; Chandrashekhar, V. G.; Gawande, M. B.; Kalevaru, N. V.; Zbořil, R.; Kamer, P. C.; Jagadeesh, R. V.; Beller, M. Ultra-small cobalt nanoparticles from molecularly-defined Co–salen complexes for catalytic synthesis of amines. *Chemical Science* **2020**, *11* (11), 2973-2981.
- (132) Murugesan, K.; Chandrashekhar, V. G.; Kreyenschulte, C.; Beller, M.; Jagadeesh, R. V. A General Catalyst Based on Cobalt Core–Shell Nanoparticles for the Hydrogenation of N-Heteroarenes Including Pyridines. *Angewandte Chemie* **2020**, *132* (40), 17561-17565.
- (133) Newman, M. S.; Underwood, G.; Renoll, M. The reduction of terminal epoxides. *Journal of the American Chemical Society* **1949**, *71* (10), 3362-3363.
- (134) Takahashi, K.; Yamashita, M.; Ichihara, T.; Nakano, K.; Nozaki, K. High-Yielding Tandem Hydroformylation/Hydrogenation of a Terminal Olefin to Produce a Linear Alcohol Using a Rh/Ru Dual Catalyst System. *Angewandte Chemie* **2010**, *122* (26), 4590-4592.

- (135) Panke, S.; Held, M.; Wubbolts, M. G.; Witholt, B.; Schmid, A. Pilot-scale production of (S)-styrene oxide from styrene by recombinant *Escherichia coli* synthesizing styrene monooxygenase. *Biotechnology and bioengineering* **2002**, *80* (1), 33-41.
- (136) Yang, Z.; Zhang, S.; Zhao, H.; Li, A.; Luo, L.; Guo, L. Subnano-FeO<sub>x</sub> Clusters Anchored in an Ultrathin Amorphous Al<sub>2</sub>O<sub>3</sub> Nanosheet for Styrene Epoxidation. *ACS Catalysis* **2021**, *11* (18), 11542-11550.
- (137) Heusch, R.; Leverkusen, B. *Ullmann's Encyclopedia of Industrial Chemistry*; 2000. James, D. H.; Castor, W. M. *Ullmann's encyclopedia of industrial chemistry*; 2011.
- (138) McKenna, R.; Nielsen, D. R. Styrene biosynthesis from glucose by engineered *E. coli*. *Metabolic engineering* **2011**, *13* (5), 544-554. Lian, J.; McKenna, R.; Rover, M. R.; Nielsen, D. R.; Wen, Z.; Jarboe, L. R. Production of biorenewable styrene: utilization of biomass-derived sugars and insights into toxicity. *Journal of Industrial Microbiology and Biotechnology* **2016**, *43* (5), 595-604. Fujiwara, R.; Noda, S.; Tanaka, T.; Kondo, A. Styrene production from a biomass-derived carbon source using a coculture system of phenylalanine ammonia lyase and phenylacrylic acid decarboxylase-expressing *Streptomyces lividans* transformants. *Journal of bioscience and bioengineering* **2016**, *122* (6), 730-735. Ortuño, M. A.; Dereli, B. s. r.; Cramer, C. J. Mechanism of Pd-catalyzed decarbonylation of biomass-derived hydrocinnamic acid to styrene following activation as an anhydride. *Inorganic chemistry* **2016**, *55* (9), 4124-4131.
- (139) Vankar, Y. D.; Arya, P. S.; Rao, C. T. 2Inc/Chlorotrimethins Ilane: A Mild Reducing System for the Conversion of Epoxides into Alcohols. *Synthetic Communications* **1983**, *13* (10), 869-872.
- (140) Bonini, C.; Di Fabio, R.; Sotgiu, G.; Cavagnero, S. Oxirane rings: studies and applications of a new chemo and regio selective reductive opening of epoxides. *Tetrahedron* **1989**, *45* (10), 2895-2904.
- (141) Bartók, M.; Notheisz, F.; Zsigmond, A.; Smith, G. The mechanism of hydrogenolysis and isomerization of oxacycloalkanes on metals: III. Effect of partial pressure of hydrogen on the selectivity of hydrogenolysis of oxacycloalkanes on Pt. *Journal of Catalysis* **1986**, *100* (1), 39-44.
- (142) Makriyannis, A.; Knittel, J. Conformational analysis of amphetamine in solution based on unambiguous assignment of the diastereotopic benzylic protons in the <sup>1</sup>H NMR spectra. *Tetrahedron Letters* **1981**, *22* (46), 4631-4634.
- (143) Bartók, M.; Notheisz, F. Stereochemistry of the hydrogenolysis of oxacycloalkanes on metal catalysts. *Journal of the Chemical Society, Chemical Communications* **1980**, (14), 667-668.
- (144) Vicente, I.; Salagre, P.; Cesteros, Y. Ni nanoparticles supported on microwave-synthesised saponite for the hydrogenation of styrene oxide. *Applied clay science* **2011**, *53* (2), 212-219.
- (145) Kanojiya, S. K.; Shukla, G.; Sharma, S.; Dwivedi, R.; Sharma, P.; Prasad, R.; Satalkar, M.; Kane, S. Hydrogenation of Styrene Oxide to 2-Phenylethanol over Nanocrystalline Ni Prepared by Ethylene Glycol Reduction Method. *International Journal of Chemical Engineering* **2014**, 2014.
- (146) Bergadà, O.; Salagre, P.; Cesteros, Y.; Medina, F.; Sueiras, J. E. High-selective Ni-MgO catalysts for a clean obtention of 2-phenylethanol. *Applied Catalysis A: General* **2004**, *272* (1-2), 125-132.

- (147) Sasu, A.; Dragoi, B.; Ungureanu, A.; Royer, S.; Dumitriu, E.; Hulea, V. Selective conversion of styrene oxide to 2-phenylethanol in cascade reactions over non-noble metal catalysts. *Catalysis Science & Technology* **2016**, 6 (2), 468-478.
- (148) Vicente, I.; Salagre, P.; Cesteros, Y. Ni nanoparticles supported on microwave-synthesised hectorite for the hydrogenation of styrene oxide. *Applied Catalysis A: General* **2011**, 408 (1-2), 31-37.
- (149) Liu, W.; Li, W.; Spannenberg, A.; Junge, K.; Beller, M. Iron-catalysed regioselective hydrogenation of terminal epoxides to alcohols under mild conditions. *Nature Catalysis* **2019**, 2 (6), 523-528.
- (150) Heravi, M. M.; Lashaki, T. B.; Poorahmad, N. Applications of Sharpless asymmetric epoxidation in total synthesis. *Tetrahedron: Asymmetry* **2015**, 26 (8-9), 405-495. Ahmad, A.; Burtoloso, A. C. Total Synthesis of ( $\pm$ )-Brussonol and ( $\pm$ )-Komaroviquinone via a Regioselective Cross-Electrophile Coupling of Aryl Bromides and Epoxides. *Organic letters* **2019**, 21 (15), 6079-6083.
- (151) Herzberger, J.; Niederer, K.; Pohlit, H.; Seiwert, J.; Worm, M.; Wurm, F. R.; Frey, H. Polymerization of ethylene oxide, propylene oxide, and other alkylene oxides: synthesis, novel polymer architectures, and bioconjugation. *Chemical reviews* **2016**, 116 (4), 2170-2243.
- (152) Burger, J.; Kettenbach, G.; Klüfers, P. Coordination equilibria in transition metal based cellulose solvents. In *Macromolecular Symposia*, 1995; Wiley Online Library: Vol. 99, pp 113-126.
- (153) Scholten, J.; Pijpers, A.; Hustings, A. Surface characterization of supported and nonsupported hydrogenation catalysts. *Catalysis Reviews* **1985**, 27 (1), 151-206.
- (154) Dasireddy, V. D.; Likoza, B. The role of copper oxidation state in Cu/ZnO/Al<sub>2</sub>O<sub>3</sub> catalysts in CO<sub>2</sub> hydrogenation and methanol productivity. *Renewable Energy* **2019**, 140, 452-460. Bodnar, Z.; Mallat, T.; Bakos, I.; Szabo, S.; Zsoldos, Z.; Schay, Z. Oxidation state of germanium promoter on a palladium/carbon catalyst and its role in hydrogenation reactions. *Applied Catalysis A: General* **1993**, 102 (2), 105-123.
- (155) Alvarez, J.; Lopez, G.; Amutio, M.; Bilbao, J.; Olazar, M. Physical activation of rice husk pyrolysis char for the production of high surface area activated carbons. *Industrial & Engineering Chemistry Research* **2015**, 54 (29), 7241-7250.
- (156) Sing, K.; Everett, D.; Haul, R.; Moscou, L.; Pierotti, R.; Rouquerol, J.; Siemieniewska, T. Physical and biophysical chemistry division commission on colloid and surface chemistry including catalysis. *Pure Appl. Chem* **1985**, 57 (4), 603-619.
- (157) Carrado, K. A.; Csencsits, R.; Thiyagarajan, P.; Seifert, S.; Macha, S. M.; Harwood, J. S. Crystallization and textural porosity of synthetic clay minerals. *Journal of Materials Chemistry* **2002**, 12 (11), 3228-3237.
- (158) Qian, Z.; Hu, G.; Zhang, S.; Yang, M. Preparation and characterization of montmorillonite-silica nanocomposites: A sol-gel approach to modifying clay surfaces. *Physica B: Condensed Matter* **2008**, 403 (18), 3231-3238.
- (159) Adam, F.; Muniandy, L.; Thankappan, R. Ceria and titania incorporated silica based catalyst prepared from rice husk: adsorption and photocatalytic studies of methylene blue. *Journal of colloid and interface science* **2013**, 406, 209-216.
- (160) Wei, H.; Gomez, C.; Liu, J.; Guo, N.; Wu, T.; Lobo-Lapidus, R.; Marshall, C. L.; Miller, J. T.; Meyer, R. J. Selective hydrogenation of acrolein on supported silver

- catalysts: A kinetics study of particle size effects. *Journal of catalysis* **2013**, 298, 18-26.
- (161) Ipatieff, V. N.; Corson, B. B.; Kurbatov, I. D. Copper as Catalyst for the Hydrogenation of Benzene. *The Journal of Physical Chemistry* **1939**, 43 (5), 589-604. DOI: 10.1021/j150392a004. Watari, R.; Kayaki, Y. Copper Catalysts Unleashing the Potential for Hydrogenation of Carbon–Oxygen Bonds. *Asian Journal of Organic Chemistry* **2018**, 7 (10), 2005-2014. DOI: 10.1002/ajoc.201800436.
- (162) Adkins, H.; Cramer, H. I. The use of nickel as a catalyst for hydrogenation. *Journal of the American Chemical Society* **1930**, 52 (11), 4349-4358. DOI: 10.1021/ja01374a023. Ryabchuk, P.; Agostini, G.; Pohl, M.-M.; Lund, H.; Agapova, A.; Junge, H.; Junge, K.; Beller, M. Intermetallic nickel silicide nanocatalyst—A non-noble metal–based general hydrogenation catalyst. *Science advances* **2018**, 4 (6), eaat0761.
- (163) Stein, M.; Wieland, J.; Steurer, P.; Tölle, F.; Mülhaupt, R.; Breit, B. Iron Nanoparticles Supported on Chemically-Derived Graphene: Catalytic Hydrogenation with Magnetic Catalyst Separation. *Advanced Synthesis & Catalysis* **2011**, 353 (4), 523-527. Hudson, R.; Riviere, A.; Cirtiu, C. M.; Luska, K. L.; Moores, A. Iron-iron oxide core–shell nanoparticles are active and magnetically recyclable olefin and alkyne hydrogenation catalysts in protic and aqueous media. *Chemical Communications* **2012**, 48 (27), 3360-3362.
- (164) Hansen, T. W.; DeLaRiva, A. T.; Challa, S. R.; Datye, A. K. Sintering of catalytic nanoparticles: particle migration or Ostwald ripening? *Accounts of chemical research* **2013**, 46 (8), 1720-1730.
- (165) Lu, Y.; Chen, W. Size effect of silver nanoclusters on their catalytic activity for oxygen electro-reduction. *Journal of Power Sources* **2012**, 197, 107-110.
- (166) Torbina, V. V.; Vodyankin, A. A.; Ten, S.; Mamontov, G. V.; Salaev, M. A.; Sobolev, V. I.; Vodyankina, O. V. Ag-based catalysts in heterogeneous selective oxidation of alcohols: a review. *Catalysts* **2018**, 8 (10), 447.
- (167) Heatley, N. A method for the assay of penicillin. *Biochemical Journal* **1944**, 38 (1), 61-65.
- (168) Barnard, R. T. The zone of inhibition. *Clinical chemistry* **2019**, 65 (6), 819-819. Bauer, A. W.; PERRY, D. M.; KIRBY, W. M. Single-disk antibiotic-sensitivity testing of staphylococci: An analysis of technique and results. *AMA archives of internal medicine* **1959**, 104 (2), 208-216.
- (169) Patel, D.; Thiyagu, R.; Surulivelrajan, M.; Patel, H.; Pandey, S. Price variability among the oral antibiotics available in a south Indian tertiary care hospital. *J Clin Diagn Res* **2009**, 3 (6), 1871-1875.
- (170) Web page of Merck KGaA, accessed at 20.10.2021, "Silber nanopowder, <100 nm particle size, contains PVP as dispersant, 99.5% trace metals basis" URL: <https://www.sigmaaldrich.com/DE/de/product/aldrich/576832>. 2021. (accessed).
- (171) Lara, H. H.; Ayala-Núñez, N. V.; Turrent, L. d. C. I.; Padilla, C. R. Bactericidal effect of silver nanoparticles against multidrug-resistant bacteria. *World Journal of Microbiology and Biotechnology* **2010**, 26 (4), 615-621.
- (172) Huang, L.; Dai, T.; Xuan, Y.; Tegos, G. P.; Hamblin, M. R. Synergistic combination of chitosan acetate with nanoparticle silver as a topical antimicrobial: efficacy against bacterial burn infections. *Antimicrobial agents and chemotherapy* **2011**, 55 (7), 3432-3438.

- (173) Asharani, P.; Lian, W. Y.; Gong, Z.; Valiyaveetil, S. *Toxicity of silver nanoparticles in zebrafish models Nanotechnology* **2008**, *19* (25), 255102.
- (174) Sung, J. H.; Ji, J. H.; Yoon, J. U.; Kim, D. S.; Song, M. Y.; Jeong, J.; Han, B. S.; Han, J. H.; Chung, Y. H.; Kim, J. Lung function changes in Sprague-Dawley rats after prolonged inhalation exposure to silver nanoparticles. *Inhalation toxicology* **2008**, *20* (6), 567-574. Kim, Y. S.; Kim, J. S.; Cho, H. S.; Rha, D. S.; Kim, J. M.; Park, J. D.; Choi, B. S.; Lim, R.; Chang, H. K.; Chung, Y. H. Twenty-eight-day oral toxicity, genotoxicity, and gender-related tissue distribution of silver nanoparticles in Sprague-Dawley rats. *Inhalation toxicology* **2008**, *20* (6), 575-583.
- (175) Brown, C. L.; Parchaso, F.; Thompson, J. K.; Luoma, S. N. Assessing toxicant effects in a complex estuary: A case study of effects of silver on reproduction in the bivalve, *Potamocorbula amurensis*, in San Francisco Bay. *Human and Ecological Risk Assessment* **2003**, *9* (1), 95-119.
- (176) Sun, X.; Olivos-Suarez, A. I.; Osadchii, D.; Romero, M. J. V.; Kapteijn, F.; Gascon, J. Single cobalt sites in mesoporous N-doped carbon matrix for selective catalytic hydrogenation of nitroarenes. *Journal of catalysis* **2018**, *357*, 20-28.
- (177) Zhang, C.; Guo, X.; Yuan, Q.; Zhang, R.; Chang, Q.; Li, K.; Xiao, B.; Liu, S.; Ma, C.; Liu, X. Ethyne-reducing metal-organic frameworks to control fabrications of core/shell nanoparticles as catalysts. *ACS Catalysis* **2018**, *8* (8), 7120-7130.
- (178) Zou, Y.; Yang, T. Rice husk, Rice husk ash and their applications. In *Rice Bran and Rice Bran Oil*, Elsevier, 2019; pp 207-246.
- (179) Hou, J.; Ma, Y.; Li, Y.; Guo, F.; Lu, L. Selective partial hydrogenation of dinitrobenzenes to nitroanilines catalyzed by Ru/C. *Chemistry letters* **2008**, *37* (9), 974-975.
- (180) Vile, G.; Almora-Barrios, N.; López, N. r.; Perez-Ramirez, J. Structure and reactivity of supported hybrid platinum nanoparticles for the flow hydrogenation of functionalized nitroaromatics. *ACS Catalysis* **2015**, *5* (6), 3767-3778.
- (181) Liu, S.-S.; Liu, X.; Yu, L.; Liu, Y.-M.; He, H.-Y.; Cao, Y. Gold supported on titania for specific monohydrogenation of dinitroaromatics in the liquid phase. *Green Chemistry* **2014**, *16* (9), 4162-4169. Torres, C. C.; Jiménez, V. A.; Campos, C. H.; Alderete, J. B.; Dinamarca, R.; Bustamente, T. M.; Pawelec, B. Gold catalysts supported on TiO<sub>2</sub>-nanotubes for the selective hydrogenation of p-substituted nitrobenzenes. *Molecular Catalysis* **2018**, *447*, 21-27.
- (182) Unglaube, F.; Kreyenschulte, C. R.; Mejia, E. Development and Application of Efficient Ag-based Hydrogenation Catalysts Prepared from Rice Husk Waste. *ChemCatChem* **2021**, *13* (11), 2583-2591.
- (183) Wu, H.; Zhuo, L.; He, Q.; Liao, X.; Shi, B. Heterogeneous hydrogenation of nitrobenzenes over recyclable Pd (0) nanoparticle catalysts stabilized by polyphenol-grafted collagen fibers. *Applied Catalysis A: General* **2009**, *366* (1), 44-56.
- (184) Relvas, J.; Andrade, R.; Freire, F. G.; Lemos, F.; Araújo, P.; Pinho, M. J.; Nunes, C. P.; Ribeiro, F. R. Liquid phase hydrogenation of nitrobenzene over an industrial Ni/SiO<sub>2</sub> supported catalyst. *Catalysis today* **2008**, *133*, 828-835. Rode, C.; Vaidya, M.; Jaganathan, R.; Chaudhari, R. Hydrogenation of nitrobenzene to p-aminophenol in a four-phase reactor: reaction kinetics and mass transfer effects. *Chemical engineering science* **2001**, *56* (4), 1299-1304.

- (185) Gomez, S.; Torres, C.; Garcia Fierro, J. L.; Apesteguia, C. R.; Reyes, P. Hydrogenation of nitrobenzene on Au/ZrO<sub>2</sub> catalysts. *Journal of the Chilean Chemical Society* **2012**, *57* (2), 1194-1198.
- (186) Bihani, M.; Bora, P. P.; Nachtegaal, M.; Jasinski, J. B.; Plummer, S.; Gallou, F.; Handa, S. Microballs containing Ni (0) Pd (0) nanoparticles for highly selective micellar catalysis in water. *ACS Catalysis* **2019**, *9* (8), 7520-7526.
- (187) Danilovic, N.; Subbaraman, R.; Strmcnik, D.; Chang, K. C.; Paulikas, A.; Stamenkovic, V.; Markovic, N. M. Enhancing the alkaline hydrogen evolution reaction activity through the bifunctionality of Ni (OH)<sub>2</sub>/metal catalysts. *Angewandte Chemie* **2012**, *124* (50), 12663-12666.
- (188) Zieliński, M.; Wojcieszak, R.; Monteverdi, S.; Mercy, M.; Bettahar, M. Hydrogen storage in nickel catalysts supported on activated carbon. *International journal of hydrogen energy* **2007**, *32* (8), 1024-1032.
- (189) Madduluri, V. R.; Mandari, K. K.; Velpula, V.; Varkolu, M.; Kamaraju, S. R. R.; Kang, M. Rice husk-derived carbon-silica supported Ni catalysts for selective hydrogenation of biomass-derived furfural and levulinic acid. *Fuel* **2020**, *261*, 116339.
- (190) Gansäuer, A.; Fan, C. A.; Keller, F.; Karbaum, P. Regiodivergent epoxide opening: a concept in stereoselective catalysis beyond classical kinetic resolutions and desymmetrizations. *Chemistry—A European Journal* **2007**, *13* (29), 8084-8090. Gansäuer, A.; Fan, C.-A.; Piester, F. Sustainable radical reduction through catalytic hydrogen atom transfer. *Journal of the American Chemical Society* **2008**, *130* (22), 6916-6917. Gansäuer, A.; Klatte, M.; Brändle, G. M.; Friedrich, J. Nachhaltige stereoselektive Radikalreduktion durch katalytischen H-Atom-Transfer (HAT). *Angewandte Chemie* **2012**, *124* (35), 9021-9024. Zaccheria, F.; Psaro, R.; Ravasio, N.; Sordelli, L.; Santoro, F. Mono and bifunctional catalysts for styrene oxide isomerization or hydrogenation. *Catalysis letters* **2011**, *141* (4), 587-591.
- (191) Wang, Z.; Cui, Y.-T.; Xu, Z.-B.; Qu, J. Hot water-promoted ring-opening of epoxides and aziridines by water and other nucleophiles. *The Journal of organic chemistry* **2008**, *73* (6), 2270-2274.
- (192) Wang, J.-L.; Li, H.-J.; Wang, H.-S.; Wu, Y.-C. Regioselective 1, 2-Diol Rearrangement by Controlling the Loading of BF<sub>3</sub>·Et<sub>2</sub>O and Its Application to the Synthesis of Related Nor-Sesquiterene-and Sesquiterene-Type Marine Natural Products. *Organic letters* **2017**, *19* (14), 3811-3814. Pandey, A. K.; Ghosh, A.; Banerjee, P. Lewis-acid-catalysed tandem Meinwald rearrangement/intermolecular [3+ 2]-cycloaddition of epoxides with donor-acceptor cyclopropanes: synthesis of functionalized tetrahydrofurans. *Eur. J. Org. Chem* **2015**, *2517*, 2523. Bah, J.; Naidu, V. R.; Teske, J.; Franzén, J. Carbocations as Lewis acid catalysts: Reactivity and scope. *Advanced Synthesis & Catalysis* **2015**, *357* (1), 148-158. Davies, T. E.; Kondrat, S. A.; Nowicka, E.; Kean, J. L.; Harris, C. M.; Socci, J. M.; Apperley, D. C.; Taylor, S. H.; Graham, A. E. Nanoporous alumino-and borosilicate-mediated Meinwald rearrangement of epoxides. *Applied Catalysis A: General* **2015**, *493*, 17-24.
- (193) Zhang, Y.; Yang, H.; Chi, Q.; Zhang, Z. Nitrogen-Doped Carbon-Supported Nickel Nanoparticles: A Robust Catalyst to Bridge the Hydrogenation of Nitriles and the Reductive Amination of Carbonyl Compounds for the Synthesis of Primary Amines. *ChemSusChem* **2019**, *12* (6), 1246-1255. Heitbaum, M.; Glorius, F.;

Escher, I. Asymmetric heterogeneous catalysis. *Angewandte Chemie International Edition* **2006**, 45 (29), 4732-4762.

## Original Publications

The author contributions are stated for each paper.

**Publication 1:** F. Unglaube, C. R. Kreyenschulte and E. Mejia. ChemCatChem (2021), 13, 11, 2583-2591.

*"Development and Application of Efficient Ag-based Hydrogenation Catalysts Prepared from Rice Husk Waste."*

I conceptualized this work, planned and conducted all experiments, except for the STEM measurements. The manuscript was prepared by me and Esteban Mejia. My overall contribution to this work is approximately 90 %.

**Publication 2:** F. Unglaube, A. Lammers, C. R. Kreyenschulte, M. Lalk and E. Mejia. ChemistryOpen (2021), 10, 1244-1250.

*"Preparation, Characterization and Antimicrobial Properties of Nanosized Silver-Containing Carbon/Silica Composites from Rice Husk Waste."*

I conceptualized this work, planned all experiments, and prepared the investigated materials. The manuscript was prepared by me, Alexander Lammers and Esteban Mejia. My overall contribution to this work is approximately 50 %.

**Publication 3:** F. Unglaube, J. Schlapp, A. Quade, J. Schäfer and E. Mejia. Catal. Sci. Technol. (2022), 12, 3123-3136.

*" Highly active heterogeneous hydrogenation catalysts prepared from cobalt complexes and rice husk waste "*

I conceptualized this work, planned and conducted the majority of the experiments, except for the SEM and XPS measurements. The manuscript was prepared by me and Esteban Mejia. My overall contribution to this work is approximately 85 %.



**Publication 4:** F.Unglaube, H. Atia, S. Bartling, C. Kreyenschulte and E. Mejia. *Helv. Chim. Acta* (2023), 106. Jg., Nr. 2, S. e202200167.

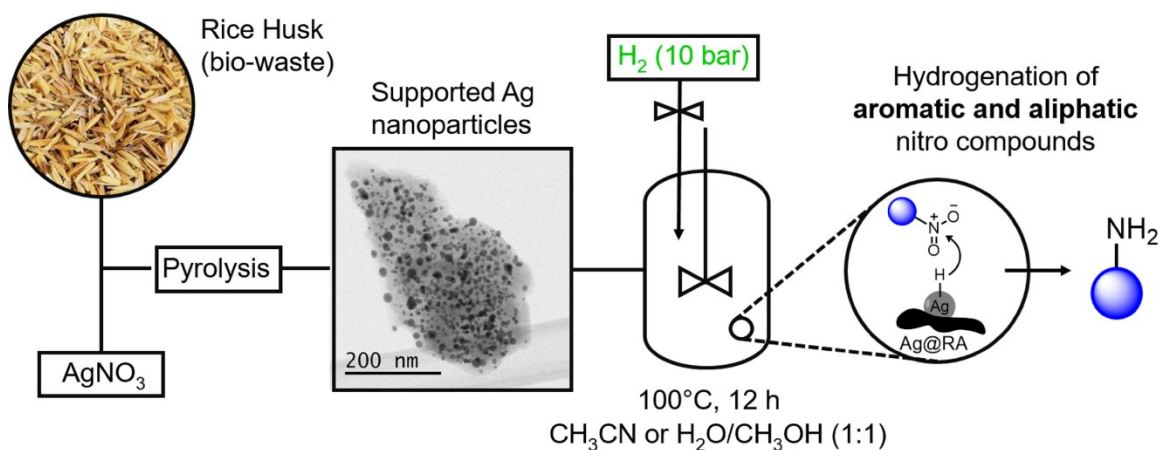
*"Hydrogenation of Epoxides to Anti-Markovnikov Alcohols over a Nickel Heterogenous Catalyst Prepared from Biomass (Rice) Waste"*

I conceptualized this work, planned and conducted the majority of the experiments, except for the SEM and XPS measurements. The manuscript was prepared by me and Esteban Mejia. My overall contribution to this work is approximately 90 %.

## Development and Application of Efficient Ag-based Hydrogenation Catalysts Prepared from Rice Husk Waste

F. Unglaube, C. R. Kreyenschulte and E. Mejia. ChemCatChem (2021), 13, 11, 2583-2591.

DOI: 10.1002/cctc.202100045



**Abstract:** The development of strategies for the sustainable management and valorization of agricultural waste is of outmost importance. With this in mind, we report the use of rice husk (RH) as feedstock for the preparation of heterogeneous catalysts for hydrogenation reactions. The catalysts were prepared by impregnating the milled RH with a silver nitrate solution followed by carbothermal reduction. The composition and morphology of the prepared catalysts were fully assessed by IR, AAS, ICP-MS, XPS, XRD and STEM techniques. This novel bio-genic silver-based catalysts showed excellent activity and remarkable selectivity in the hydrogenation of nitro groups in both aromatic and aliphatic substrates, even in the presence of reactive functionalities like halogens, carbonyls, borate esters or nitriles. Recycling experiments showed that the catalysts can be easily recovered and reused multiple times without significant drop in performance and without requiring re-activation.



# Development and Application of Efficient Ag-based Hydrogenation Catalysts Prepared from Rice Husk Waste

Felix Unglaube,<sup>[a]</sup> Carsten Robert Kreyenschulte,<sup>[a]</sup> and Esteban Mejía<sup>\*[a]</sup>

The development of strategies for the sustainable management and valorization of agricultural waste is of utmost importance. With this in mind, we report the use of rice husk (RH) as feedstock for the preparation of heterogeneous catalysts for hydrogenation reactions. The catalysts were prepared by impregnating the milled RH with a silver nitrate solution followed by carbothermal reduction. The composition and morphology of the prepared catalysts were fully assessed by IR,

AAS, ICP-MS, XPS, XRD and STEM techniques. This novel bio-genic silver-based catalysts showed excellent activity and remarkable selectivity in the hydrogenation of nitro groups in both aromatic and aliphatic substrates, even in the presence of reactive functionalities like halogens, carbonyls, borate esters or nitriles. Recycling experiments showed that the catalysts can be easily recovered and reused multiple times without significant drop in performance and without requiring re-activation.

## 1. Introduction

Rice or *padi* is by far the most important food crop for human consumption and the primary food source for more than a third of the world's population.<sup>[1]</sup> Padi fields account for more than 10% of the world's cultivated land, resulting in an estimated worldwide production of more than 500 million metric tons in 2020.<sup>[2]</sup> Thus, the management and disposal of the non-edible rice by-products, mainly rice husk (RH) and straw, presents environmental challenges, as traditionally vast amounts of these products are burned in the open after harvesting. This practice, even though convenient for the farmers, releases in the atmosphere large amounts of greenhouse gases and particulate matter.<sup>[3]</sup> Hence, the development of strategies for the sustainable management and valorization of rice agricultural waste is of high relevance.

Due to the high amount of silica present in RH (up to 25 wt-%),<sup>[4]</sup> many research efforts have been devoted to the extraction and use of this bio-genic silica as supporting material of heterogeneous catalyst. A number of publications have demonstrated the utility of such systems in esterification,<sup>[5]</sup> hydrogenation,<sup>[6]</sup> C–C coupling, and oxidation reactions,<sup>[7]</sup> as well as in bio-mass gasification.<sup>[8]</sup> Different approaches for the isolation of bio-genic silica and carbon from RH are known, including microwave, or Soxhlet-assisted extractions, commonly combined with several washing steps with NaClO<sub>2</sub> and KOH solutions. The direct extraction using concentrated alkali

hydroxides requires large excesses of base,<sup>[9]</sup> while carbothermal reductive approaches (as developed by Laine et al.) demand stoichiometric amounts of carbon or Na<sub>2</sub>CO<sub>3</sub>.<sup>[10]</sup> In all these separation methods the natural structure of the RH epidermis is completely destroyed,<sup>[11]</sup> especially if basic or acidic treatments are necessary.<sup>[12]</sup> Therefore, the organic functional groups at the husk surface (in hemicellulose, cellulose, and lignin) are not involved in the subsequent building of the catalyst active centers.

The coordination capabilities of carbohydrates and other donor groups at the surface of bio-derived lignocellulosic or chitosan waste materials (Figure 1) have been exploited before for the synthesis of nanostructured heterogeneous catalysis.<sup>[13]</sup> For instance, Beller and co-workers used this approach for the

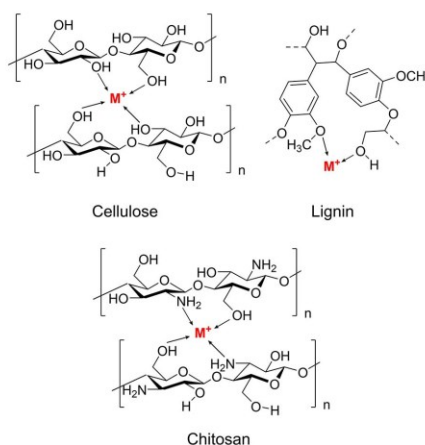


Figure 1. Exemplary coordination of metal ions with relevant bio polymers found in bio-waste materials.

[a] F. Unglaube, Dr. C. R. Kreyenschulte, Dr. E. Mejía  
Leibniz-Institut für Katalyse e.V.  
Albert-Einstein-Straße 29 A  
18059, Rostock (Germany)  
E-mail: Esteban.Mejia@catalysis.de

Supporting information for this article is available on the WWW under <https://doi.org/10.1002/cctc.202100045>

© 2021 The Authors. ChemCatChem published by Wiley-VCH GmbH. This is an open access article under the terms of the Creative Commons Attribution Non-Commercial NoDerivs License, which permits use and distribution in any medium, provided the original work is properly cited, the use is non-commercial and no modifications or adaptations are made.

preparation of N-doped Co/Co<sub>3</sub>O<sub>4</sub>-containing carbocatalysts for hydrodehalogenation reactions. These materials were easily obtained by pyrolysis of chitosan pre-treated by impregnation of a Co(II) solution.<sup>[14]</sup> Pioneering works of Shen and Yoshikawa report the use of pyrolyzed RH as support for nickel particles and their use as catalysts in gasification reactions. They impregnated RH directly with a NiNO<sub>3</sub> solution and used carbothermal reduction under N<sub>2</sub> atmosphere to generate supported metal nano particles.<sup>[8]</sup> Interestingly, this direct impregnation approach of RH has not been further extended, neither to other metals, nor to other reactions, despite the excellent activities displayed by other bio-derived heterogeneous catalysis, especially in hydrogenation reactions.<sup>[14–15]</sup>

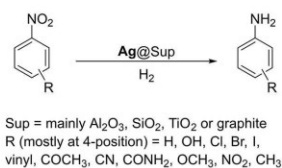
The selective hydrogenation of nitro groups is an important reaction, as it has found many applications in industry and academia since the first industrial application was reported by Béchamp more than 150 years ago.<sup>[16]</sup> Starting from this non-catalytic approach, the use of hydrogen as reducing agent rapidly became the method of choice. Numerous homogenous as well as heterogeneous metal catalyst have been successfully employed in the hydrogenation of nitro groups. These systems are commonly based on expensive noble metals including Pd, Pt, Ir and Au,<sup>[17]</sup> and more rarely, on base metals like Fe, Ni and Co.<sup>[13c,18]</sup> Most of these catalysts display high turn-over frequencies (TOF) but generally suffer from limited selectivity towards easily reducible groups, although important advances towards selectivity have been made, especially with gold-based systems.<sup>[19]</sup>

Silver, the cheapest noble metal, has been relatively less exploited than its congeners for hydrogenation reactions, perhaps due to the virtual inertness of silver surfaces towards H<sub>2</sub> dissociation at low temperatures.<sup>[20]</sup> However, silver-based hydrogenation catalysts have proven to be very active and selective in both heterogeneous and homogeneous systems.<sup>[21]</sup> Remarkably, there are only few accounts on the activity of silver catalysts for the hydrogenation of nitro compounds and the available reports have a very narrow substrate scope. Most of them describe only the conversion of nitrobenzene, chloronitrobenzenes, nitrophenol and other *para*-substituted nitro aromatics,<sup>[19d,22]</sup> while benzylic and aliphatic nitro compounds have been so far neglected (Scheme 1).

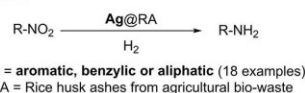
Interestingly, there is a broad variety of “green” methodologies to prepare silver nano particles (AgNP) by using so-called biogenic reduction solutions, typical consistent of plant extracts.<sup>[23]</sup> The resulting AgNP are exclusively used as bactericides, while catalytic applications of these materials remain unexplored.

Therefore, we decided to investigate the preparation and application of a heterogeneous bio-derived silver-based catalyst by simple impregnation of waste rice husk with silver ions, subsequently converted into supported nanoparticles by carbothermal reduction (Ag@RA, Scheme 1). This approach differs significantly from established methods for the reductive generation of AgNPs by adding stoichiometric reductants like NaBH<sub>4</sub><sup>[24]</sup> or organoalkoxysilanes,<sup>[25]</sup> photochemical deposition<sup>[26]</sup> or the so called auto-reduction.<sup>[27]</sup> The carbothermal reduction is made possible by the metal coordination with the donor

Previous works:



This work:



**Scheme 1.** Hydrogenation of nitro compounds using silver-based heterogeneous catalysts.

groups of the plant's biopolymers (Figure 1), an approach which is similar to the fixation of silver ions using dopamine.<sup>[28]</sup>

Moreover, in this way we also exploit the naturally occurring nanostructured silica particles at the RH epidermis to obtain hybrid silica-carbon supports, otherwise difficult to prepare. The obtained catalysts have been successfully employed in the hydrogenation of both aromatic and aliphatic nitro groups with excellent activity and selectivity (Scheme 1). This contribution represents, to the best of our knowledge, not only the silver-based catalysts for nitro reduction with the broadest substrate scope, but also the first silver-based hydrogenation catalysts from bio-waste.

## 2. Results and Discussion

### 2.1. Catalyst Preparation and Characterization

In order to avoid interferences and background reactions in the hydrogenation experiments, the metal ions naturally present in the RH have to be removed, for which an acidic leaching method was applied as reported.<sup>[29]</sup> After leaching, the amount of Mg, Ca, Mn, Co, Cu and Zn dropped below detection limits of the used analytic methods (atomic absorption spectrometry, AAS and inductively coupled plasma mass spectrometry, ICP-MS). Moreover, the amount of Fe, Na and K was reduced by more than 95 wt% (Table S1).

The attenuated total reflection infrared (ATR-IR) spectra of raw RH (Figure S20) show strong peaks at cm<sup>-1</sup> = 3330, 2916, 1627, 1319, 1036, and 460. These values changed significantly after pyrolysis at 600 °C (Figure S21). The peaks related to C–C, C–H, C–O and C=O bond stretching (i.e., all peaks at wave numbers higher than 1550 cm<sup>-1</sup>) disappeared completely (Figure S21). The peaks at 455 and 1066 cm<sup>-1</sup> can be attributed to the symmetric and asymmetric Si–O–Si stretching vibrations. Another peak attributable to SiO<sub>2</sub> can be found at 797 cm<sup>-1</sup>, corresponding to a Si–O deformation vibration.<sup>[30]</sup> The broad peak around 1552 cm<sup>-1</sup> cannot be unambiguously assigned,



but could be the result of overlapping C=O and C=C stretching vibrations.<sup>[30a]</sup> This indicates that the majority of biopolymers' structures from the RH were destroyed during the thermal treatment and the remaining material is a composite of amorphous SiO<sub>2</sub> and graphene-like carbon.

X-ray photoelectron spectroscopy (XPS) analysis of the catalyst prepared by pyrolysis at 600 °C (Ag@RA600) suggests that silicon occurs at the surface only as SiO<sub>2</sub>, with a Si2p signal at 103.43 eV (Figure S7) which can be correlated to the main O1s signal at 532.9 eV (Figure S9). The most common carbon bonds at the surface are C–C, with a signal at 284.8 eV. Smaller carbon moieties are visible at 286.19 eV and 287.93 eV and can be attributed to C–O or O–C–O bonds, respectively (Figure S8). The C–O bond is visible as small shoulder in the O1s signal at 530.79 eV (Figure S9), the appearance of these signals suggests that acetal and hemiacetal functions from the lignocellulose are not completely destroyed through the pyrolysis. The surface area and pore structure of the catalyst was investigated by Brunauer-Emmett-Teller (BET) surface area analysis. It was observed that the surface area decreased slightly from 273.9 m<sup>2</sup>g<sup>−1</sup> to 260.7 m<sup>2</sup>g<sup>−1</sup> when the RH was doped with silver (Ag@RA600) compared to the RH pyrolyzed at the same temperature without metal doping (RA600). A majority of nanopores was found on Ag@RA600 with a maximum of pore volume and area at a pore size of 0.6 nm (Figure 2).

The X-ray diffraction pattern of RA shows a broad reflection from 15 to 40° which can be attributed amorphous silica, the main silicon species in the sample.<sup>[30b]</sup> Additionally, reflections, of hexagonal SiO<sub>2</sub> (quartz) at 20.8, 26.6, 36.4 and 39.4° were also observed. There were three Bragg peaks that could not be clearly assigned to any structure, although those at 31.6° and 35.7° could be attributed to a Magnetite structure. Alas, the reflexes are too weak to provide an unambiguous statement.<sup>[31]</sup> Conversely, the reflection at 33.2° remains puzzling. It can be assumed that the observed diffraction peaks result from the naturally inhomogeneous composition of the RH, containing (along with silica) traces of several inorganic materials. Importantly, all the described reflections observed in RA can be found as well in the silver-containing Ag@RA600 catalyst. Additionally, reflections of cubic silver could be observed at 38.1°, 44.3°, 64.4° and 77.4° for the same sample, although unusually shaped. The Bragg peaks are neither Lorentzian, nor Pseudo-Voigt-shaped, but very sharp around the center and broad at the base (Figure 3). This shape can be explained by the peak overlapping resulting from the presence of two or more fractions of different-sized crystallites coexisting in the sample (schematically displayed in Figure 3).

While such bimodal crystallite size distributions are a common phenomenon in the field of materials science, they remain rarely reported in catalysis using silver. To prove that the peaks are not caused by the overlapping of silver signals with signals of a different non-silver crystallite, an extensive XPS survey was performed. No other element (apart from silver) was found in relevant amounts. The measured Ag3d<sub>5/2</sub> and Ag3d<sub>3/2</sub> binding energies were at 368.56 eV and 374.56 eV, respectively (Figure 4).

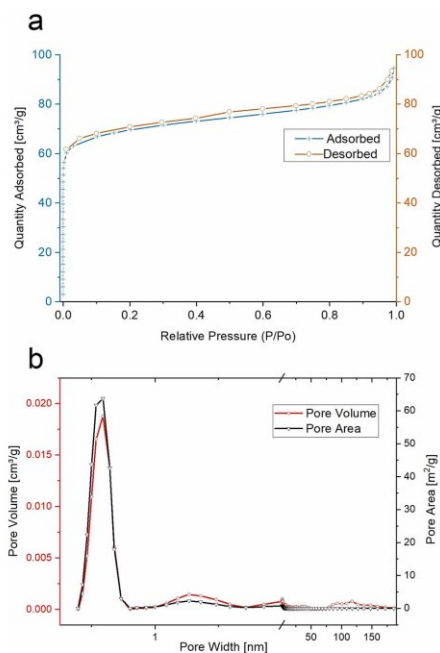


**Figure 2.** Surface characterization of Ag@RA600 (obtained by pyrolysis at 600 °C). a) BET quantitative adsorption and desorption of nitrogen. b) Pore volume and Area distribution plotted against the pore width.

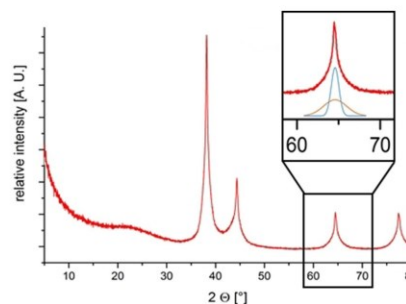


**Figure 3.** XRD pattern for Ag@RA600. In the insert there is the schematic presentation of overlapping signals from different silver particle size fractions, giving the diffraction peaks its unusual shape.

It is well known that binding energies are influenced by the particle size. Kim et al. showed a correlation of core bindings energies with the partial size of silver nano particles on pyrolytic graphite.<sup>[32]</sup> According to their observations, the measured

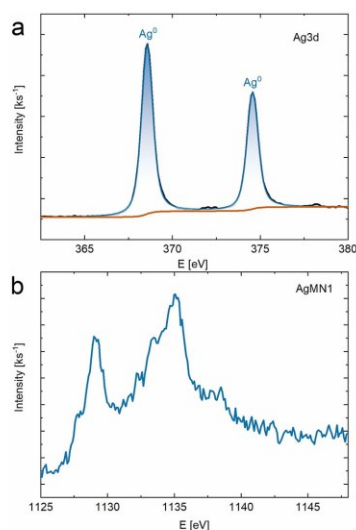


Figure 4. a)  $\text{Ag}3d_{5/2}$  XPS signal and b)  $\text{Ag}4d_{5/2}$  XPS signal of  $\text{Ag@RA600}$

binding energies of  $\text{Ag}3d_{5/2}$  at 368.56 eV are caused by particles of 6 nm in diameter. Such a straightforward correlation via XPS cannot be done in the present case where a triple size distribution of the silver particles was observed (see microscopic characterization below). Especially the characterization of the smallest particles can be problematic since it cannot be asserted whether they are metallic, and their lack of crystallinity strongly influences their electronic properties. Thus, microscopic analysis (STEM) was performed to assess the size of the silver particles. The images show three particle size fractions. Particles of 6–10 nm in diameter occurred as the main fraction (Figure 5 and Figure S1), while smaller particles of 1 to 2 nm in diameter have been found all over the material (Figure 5, right side). The bigger fraction appeared to be fully monocrystalline (Figure S1). Along with these two fractions, bigger particles (70–200 nm)

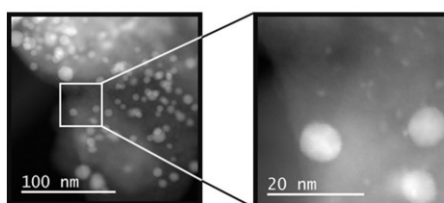


Figure 5. HAADF-STEM of  $\text{Ag@RA600}$ . In the picture, two of the three size fractions (around 1 nm, 6–10 nm) of silver nano particles can be observed at the catalyst surface.

resulting from the agglomeration of smaller crystallites could also be observed (Figure S2).

## 2.2. Catalytic Experiments

In a preliminary screening, heterogeneous catalyst containing different metals have been prepared by wet impregnation of the support with a solution of the corresponding nitrate followed by pyrolysis at 600 °C (see Experimental section). The choice of metals to be tested was based mainly on their availability (low price) and known hydrogenation activity in other systems.<sup>[33]</sup> These metals included silver,<sup>[21]</sup> cobalt,<sup>[14–15,34]</sup> nickel,<sup>[35]</sup> and copper.<sup>[36]</sup> The obtained materials have been tested in the hydrogenation of nitro compounds, for which nitrobenzene was selected as model substrate. The outcome of these hydrogenation reactions (under non-optimized conditions) is summarized in Table 1. From the tested catalysts, the one containing silver NP supported on RH ( $\text{Ag@RA}$ , Table 1, Entry 1), showed by far the best activity. Other metal-containing catalyst with the same support (Entries 3–7) only showed poor conversions. Interestingly, a silver-based catalyst prepared with commercial silica as support ( $\text{Ag@SiO}_2$ , Entry 2) did not showed any hydrogenation activity, attesting the important role played by the hybrid silica/carbon nature of RA. To assess this effect, the XRD pattern of  $\text{Ag@RA}$  and  $\text{Ag@SiO}_2$  were analyzed using Scherrer's method by whole powder pattern fitting. It was shown that the average particle size in  $\text{Ag@SiO}_2$  is with 54 nm, significantly higher than the particle size in  $\text{Ag@RA}$  which displayed two fractions with an average size of 3 nm and 16 nm, respectively (Table S1). This suggests a strong correlation of Ag particle size and catalytic activity, being the smaller particles more active, which is in a line with previous reports.<sup>[22a,37]</sup> Also noteworthy is the small hydrogenation activity displayed by the undoped rice husk ash (RA, Entry 8). This could be attributed to the eventual traces of  $\text{Fe}_2\text{O}_3$  present in the RA, (even after the acidic leaching treatment made to the starting RH), as this compound is well known for its ability to act as hydrogenation catalyst.<sup>[38]</sup>

Table 1. Preliminary screening for the hydrogenation of nitrobenzene using pyrolyzed catalysts.

Entry	Catalyst <sup>[a]</sup>	Yield [%] <sup>[b]</sup>	Selectivity [%] <sup>[c]</sup>
1	$\text{Ag@RA}$	47.3	99
2	$\text{Ag@SiO}_2$	–	–
3	$\text{Co@RA}$	7.3	99
4	$\text{Cu@RA}$	4.8	78
5	$\text{Ni@RA}$	2.2	69
6	$\text{Co/Cu@RA}^d$	6.5	93
7	$\text{Co/Ni@RA}^d$	5.9	81
8	RA600	2.5	99

Reaction Conditions: 60 °C, 10 bar  $\text{H}_2$ , 1 mmol nitrobenzene, 1 ml  $\text{H}_2\text{O}$ , 16 h, 25 mg catalyst [a] Metal content in the catalysts is 13 wt-% of metal nitrate relative to dry mass of RH [b] Yields determined by GC using n-heptane as internal standard. [c] Selectivity towards aniline was calculated using GC with n-heptane as internal standard. [d] Metal salts in a stoichiometric ratio of 1:1

The silver-containing catalyst Ag@RA was chosen for further optimization. Pyrolysis temperatures from 400 to 800 °C have been tested in the catalyst preparation, as it has been shown to be a critical factor in the subsequent performance of heterogeneous catalysts.<sup>[39]</sup> With these materials in hand, we tested their catalytic activity in the hydrogenation of nitrobenzene (Table 2). It turned out that the catalysts synthesized at 600 °C displayed the highest activity (Entries 3 and 4). Higher pyrolysis temperatures (Entries 5 and 6) resulted in lower activities, probably due to thermal Ostwald ripening and/or particle migration of the silver particles at the catalyst surface,<sup>[40]</sup> leading to bigger, less active particles.<sup>[37a]</sup>

The screening also revealed that the acid leaching pre-treatment had no influence on the catalytic performance, neither in terms of activity nor in selectivity (Entry 4). Hence, since the acidic pre-treatment of the RH is not necessary in this case, a significant amount of waste can be avoided since the acidic washing water is the main waste product of the catalyst synthesis. Moreover, the silver loading used in the catalyst preparation was also investigated (Figure S32). It was found that a catalyst loading corresponding to 1.4 mol% of silver was the minimum amount necessary to achieve full yield. A small solvent survey for the same reaction showed that acetonitrile and a mixture of methanol/water (ratio 1:1), resulted in quantitative yields and selectivity (Table S4). The effect of the reaction temperature was also assessed, resulting that the best results were obtained at 100 °C (Figure S33). Further screening revealed a pressure of at least 10 bar of hydrogen is necessary to achieve full yield. Decreasing the reaction pressure to 5 bar significantly lowered the yield to 11%. Extending the reaction time to 48 h with at this pressure led only to a yield of 45%. Nevertheless, the selectivity towards aniline remained at 99% (Table S3). Importantly, our hydrogenation catalyst shows excellent activity without the necessity of a base, a common additive in hydrogenation systems. On the contrary, addition of inorganic or organic bases has a detrimental effect on the catalyst performance (Figure S34).

Once the optimal reaction conditions for the hydrogenation of nitro groups using Ag@RA600 were defined, the substrate scope was investigated (Scheme 2). To our delight, almost quantitative yields and selectivity were obtained in all the tested substrates, both aromatic and aliphatic. Nitrobenzene

derivatives bearing either electron donor (i.e., methoxy, alkyl) or electron-withdrawing groups (i.e., halide, cyano, carbonyl) were equally converted to their corresponding anilines in excellent yields. Only a small steric influence was observed in the hydrogenation of methyl 2-nitrobenzoate, which gave slightly lower yields (86%) than the less sterically hindered methyl 4-nitrobenzoate (93%). Interestingly, the hydrogenation of 1,4-dinitrobenzene resulted in the quantitative formation of the singly reduced 1-amino-4-nitrobenzene, attesting the mild nature of the newly developed hydrogenation catalyst. Furthermore, the reaction remained selective towards single reduction even if harsher reaction conditions were applied (140 °C, 40 bar H<sub>2</sub> and 24 h).

This feature was further exploited for the reduction of nitroaromatics bearing groups that might undergo reduction or are labile under hydrogenations conditions. For instance, aromatic halogen-carbon bonds readily undergo reductive dehalogenation with different metal catalysts,<sup>[14,41]</sup> but remained untouched by our system. Even with the fully halogenated pentachloronitrobenzene and the highly sensitive 1-iodo-4-nitrobenzene the reaction selectivity did not dropped below 96%. Importantly, the catalyst showed to be robust against acidic phenolic groups, as it was shown with the successful reduction of 4-nitrophenol, a precursor for the drug Paracetamol.<sup>[22b]</sup> Thioethers are not cleaved under our reaction conditions and do not poison the catalyst. Likewise, C–B and B–O bonds of borate esters remain untouched through the hydrogenation, which is an important requirement in the design of late-stage derivatization methodologies in the synthesis of bio-active molecules and pharmaceuticals.<sup>[42]</sup> Importantly, benzylic, and aliphatic nitro compounds were also successfully hydrogenated. Interestingly, the reduction of secondary aliphatic substrates under the standard reaction conditions proved to be challenging, yielding the corresponding nitroso intermediate as the main products. Applying harsher reaction conditions was thus necessary to fully reduce nitro-cyclopentane, nitrocyclohexane as well as 2-nitropropane to the desired amines.

Finally, the recyclability of the catalyst was assessed for the reduction of nitrobenzene to aniline. After each reaction, the solid catalyst was simply recovered by centrifugation and re-used (Figure 6). After 4 runs the yield decreased only marginally and stabilizes around 91% through four further runs. Importantly, the selectivity remained stable (99%) through the eight recycling experiments, surpassing the performance of other reported hydrogenation silver catalyst which have to be reactivated to avoid drastic loss of activity.<sup>[21e]</sup>

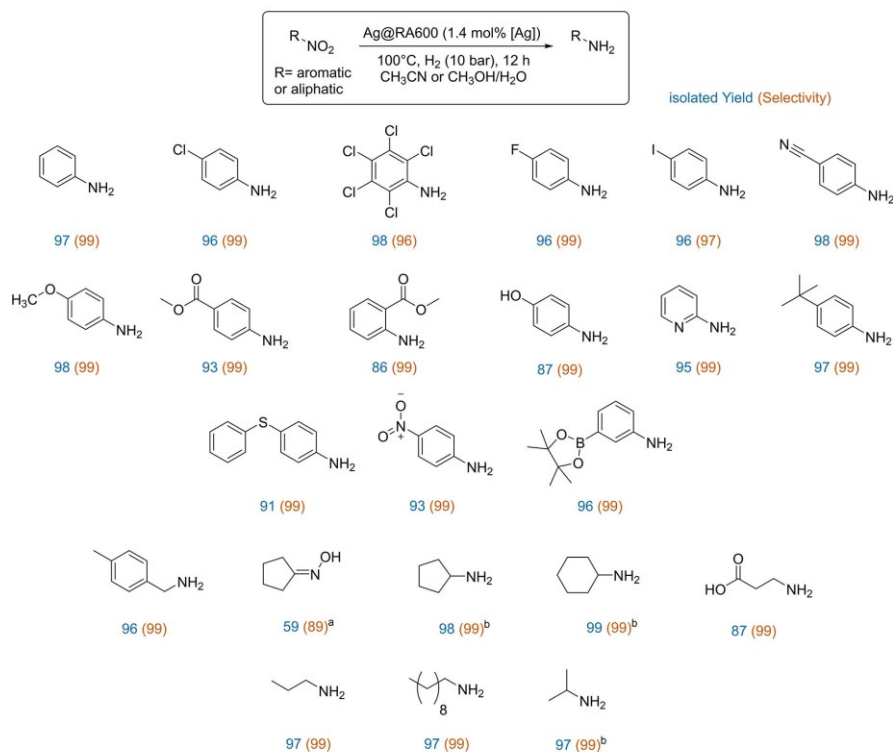
To verify the stability of the catalyst and to confirm that its activity is only due to silver sites at the catalyst surface (and not due to leached metal species in solution) a “hot filtration” experiment was conducted (for details, see Experimental Section). In this experiment the heterogeneous catalyst is removed from the reaction mixture during a catalytic run and the substrate conversion is constantly followed. After filtration of the hot reaction mixture, the conversion virtually stopped, as only an additional 3% of product was detected in the following 11 h. Hence, since silver NP are known to be highly active

**Table 2.** Preliminary screening for the hydrogenation of nitrobenzene using the silver-containing catalyst Ag@RA.

Entry	Pyrolysis temperature	Yield [%] <sup>[a]</sup>	Selectivity [%] <sup>[b]</sup>
1	400	21	99
2	500	22	99
3	600	47	99
4 <sup>[c]</sup>	600	47	99
5	700	29	99
6	800	6	99

Reaction Conditions: 60 °C, 10 bar H<sub>2</sub>, 1 mmol substrate, 12 h, 1 ml H<sub>2</sub>O, 20 mg catalyst (corresponding to 1.4 mol% Ag). [a] Yields determined by GC using n-heptane as internal standard [b] Selectivity towards aniline was calculated using GC with n-heptane as internal standard. [c] Catalyst prepared without acid leaching.





**Scheme 2.** Reaction products for the hydrogenation of nitro groups using Ag@RA600 as catalyst. Reaction Conditions if not stated differently: 100 °C, 10 bar H<sub>2</sub>, 1 mmol substrate, 12 h, 1 ml solvent (see supporting information), 20 mg catalyst (1.4 mol% of Ag). [a] In acetonitrile. Isomeric mixture of nitrosocyclopentane and cyclopentanone oxime (shown). Yield determined by GC (see supporting information) [b] Reaction conditions: 140 °C, 40 bar H<sub>2</sub>, 24 h in CH<sub>3</sub>OH/ H<sub>2</sub>O (1:1).

hydrogenation catalysts,<sup>[21f,22b,e,g,i]</sup> the loss of reactivity of the filtered solution suggests that no silver NP are leached from the catalyst surface. However, the small yield drop in the recycling experiments and the background reactivity observed in the filtered reaction mixture suggest that a minute fraction of unsupported silver species (ions, atoms, clusters or particles) is washed off from the catalyst during the first runs.<sup>[21d]</sup>

STEM imaging revealed that after the first recycling run the fraction of NP with the smaller size (1 to 2 nm) were significantly depleted from the catalyst surface, and by the last recycling run were completely vanished. This goes in hand with the initial small activity loss and subsequent stabilization of the catalyst's performance throughout the successive recycling experiments. This observation also places the mid-sized fraction of NP (6 to 10 nm particles) as the main contributors to the catalytic activity.

In addition, a Scherrer analysis of the XRD pattern indicates a growth of the NP after the catalysis, where the small particles increased their average crystallite size from 3 nm (in the fresh catalyst) to 4 nm (after the last run), which is not significant due to the accuracy of the measurement. The bigger particles increased their average size from 16 to 25 nm, respectively (Table S1). Interestingly, STEM images also showed that the silver particles developed a carbon coating after the first catalytic cycle, not thicker than one or two layers (Figure S3d). The layer seems to preserve its thickness and appearance during the recycling experiments and does not affect the catalyst activity (Figure S4d).

Based on these observations and in literature reports,<sup>[33,43]</sup> we proposed the reaction mechanism presented in Scheme 3. At the reaction onset, hydrides are generated at the surface of the silver particles<sup>[21b]</sup> while protons attack the partially positively charged oxygen of the nitro group.<sup>[22a]</sup> A subsequent



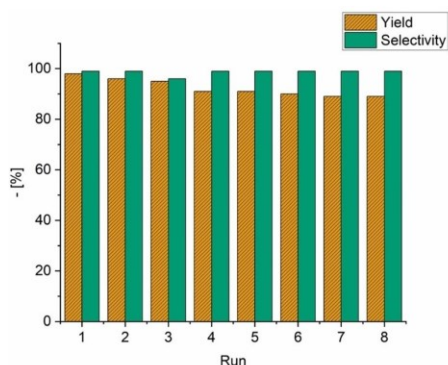


**Figure 6.** Catalyst recycling experiments for the hydrogenation of nitrobenzene using Ag@RA600. Details can be found in the Experimental Section.

hydride transfer and water elimination leads to the formation of nitroso species, which can be reduced further to the corresponding hydroxylamine and ultimately to the amine product. The hydroxylamine and the nitroso species can condensate in an alternative pathway to form an azoxy intermediate, which is consecutively reduced to the azo and the hydro-azo products. This intermediates are usually detected if bases are used in the reaction.<sup>[33]</sup> Interestingly, the azo compounds were the only detected side-products in our reaction (by GC-MS, see Fig. S80).

### 3. Conclusion

Herein we report the synthesis and application of a heterogeneous catalyst consisting of silver nanoparticles supported on a hybrid silica/carbon support derived from agricultural bio-waste. The catalyst was prepared by simple carbothermal reduction of milled rice husk impregnated with a silver nitrate solution, without the need of additional pre-treatment like acid

leaching of the rice husk ashes. The prepared catalysts were fully characterized by IR, AAS, ICP-MS, XPS, XRD and STEM techniques. These materials showed to be highly active in the hydrogenation nitro groups in both aliphatic and aromatic substrates. They also showed to be highly selectivity towards the nitro group, even in the presence of easily reducible or labile groups, giving almost quantitative yields and selectivity in most cases. This is, to the best of our knowledge, the first Ag-based hydrogenation catalysts prepared from agricultural bio-waste, as well as the silver catalysts for nitro reduction with the broadest substrate scope.

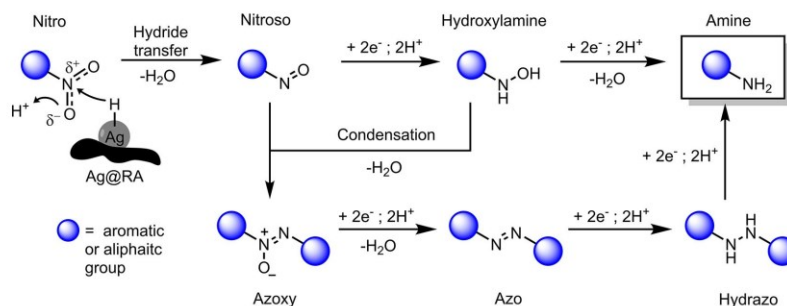
Importantly, with the present results, we establish an alternative route for the valorization of agricultural rice bio-waste, resulting in high added-value products (the catalysts) with potential immediate impact in the chemical industry.

## Experimental Section

### Catalyst Preparation

The RH was sun-dried at the harvesting sites by Vietnamese farmers. The samples were then shredded with a cutting mill SM 200 (rotation and speed 1000 rpm, 2 mm sieve sizes) and milled to a fine powder in a ball mill PM 200 (in steel cups with steel balls at 400 rpm for 3 h). Subsequently, the milled RH samples were subjected to steps "a" (acidic leaching pre-treatment) and "b" (metal impregnation), or only "b", before the pyrolysis step "c".

- samples of 10 g of RH were washed under reflux conditions with 50 ml of a 10 mol% HCl solution for 24 h to remove all traces of metals and mud. Afterwards, the samples were filtrated through a G4 glass filter and washed with distilled water until neutral pH value was reached. The wet samples were dried under vacuum (10 mbar) at 70 °C for 24 h.
- the dry samples were mixed with 13 wt% of metal nitrates (relative to dry mass of rice husk) in 50 ml of ethanol and stirred for 24 h at 21 °C. The solvent was removed in vacuo with a rotary evaporator.
- the samples were placed in an aluminum oxide crucible inside a quartz tube furnace and heated at 400, 500, 600, 700 or 800 °C at a rate of 10 °C/min, and the temperature was maintained for 1 h. The furnace was continuously flushed with nitrogen (50 ml/



**Scheme 3.** Proposed reaction mechanism for the reduction of nitro groups catalysed by Ag@RA600.

min). After cooling to 25 °C the catalysts were stored under ambient conditions.

### Catalytic experiments

For the catalytic experiments 1 mmol of the substrate, 25 mg catalyst and acetonitrile (32 mmol, 1 ml) were added together in a 12 ml vial, equipped with a Teflon-coated magnetic stirrer and a steel cannula (0.45 × 12 mm) pierced through the cap to equalize pressure. The closed vial was placed in an autoclave and flushed three times with hydrogen at a pressure of 10 bar and subsequently the reaction pressure was adjusted. The stirred reaction vessel was heated for a given reaction time in an aluminum block. The autoclave was then cooled down in an ice bath and 2 ml ethyl acetate was added to the reaction mixture. The crude mixture was filtered through a syringe filter, and the vial was washed two more times with ethyl acetate and filtered. After performing TLC, the product was fixed on silica and purified by column chromatography.

### Recycling and hot filtration experiment

For the recycling experiment 200 mg of catalyst, nitrobenzene (816 µl, 8 mmol) and acetonitrile (8 ml, 256 mmol) were added together as described in the general procedure. The catalyst was recovered using a centrifuge. For the hot filtration experiment 50 mg of catalyst, nitrobenzene (204 µl, 2 mmol) and acetonitrile (2 ml, 64 mmol) were added together like described in the general procedure. The reaction was stopped after 5 h, the autoclave was cooled down to 55 °C and degassed. The reaction mixture was filtrated through a preheated syringe filter and a Celite plug and a sample for GC analysis was taken. The filtrated reaction mixture was placed back into an autoclave and the reaction time was completed under the conditions described above.

### Acknowledgements

We would like to thank all the Vietnamese farmers and local authorities at the sample collection sites for their help and hospitality. Also, thanks to Dr. Hendrik Lund, Dr. Stephan Bartling as well as Reinhard Eckelt for performing the XRD, XPS and BET-surface measurements (respectively), and for their helpful comments and discussions. Furthermore, we would like to acknowledge the funding for the SUVALIG project from the German Federal Ministry of Education and Research (BMBF, 031B0707B) and the RoHan SDG Graduate School funded by the German Academic Exchange Service (DAAD, 57315854) and the German Federal Ministry for Economic Cooperation and Development (BMZ) inside the framework "SDG Bilateral Graduate school program". Open access funding enabled and organized by Projekt DEAL.

### Conflict of Interest

The authors declare no conflict of interest.

**Keywords:** Biomass · Rice Husk · Heterogeneous Catalysis · Silver · Hydrogenation · Nitro groups · Amines

- [1] G. S. Kush, *Origin, dispersal, cultivation and variation of rice*. In *Oryza: From Molecule to Plant*, Springer Netherlands, Dordrecht, 1997.
- [2] „World Rice Production 2020/2021“, can be found under, <http://www.worldagriculturalproduction.com/crops/rice.aspx>, 2020.
- [3] C. A. Moraes, I. J. Fernandes, D. Calheiro, A. G. Kieling, F. A. Brehm, M. R. Rigon, J. A. Berwanger Filho, I. A. Schneider, E. Osorio, *Waste Manage. Res.* **2014**, *32*, 1034–1048.
- [4] L. Sun, K. Gong, *Ind. Eng. Chem. Res.* **2001**, *40*, 5861–5877.
- [5] J. Janaun, N. Safie, N. Siambun, in *AIP Conference Proceedings*, Vol. 1756, AIP Publishing, **2016**, p. 090007.
- [6] Y. Li, J. Y. Lan, J. Liu, J. Yu, Z. Luo, W. Wang, L. Sun, *Ind. Eng. Chem. Res.* **2015**, *54*, 5656–5663.
- [7] A. Franco, S. De, A. M. Balu, A. A. Romero, R. Luque, *ACS Sustainable Chem. Eng.* **2018**, *6*, 11555–11562.
- [8] Y. Shen, K. Yoshikawa, *Ind. Eng. Chem. Res.* **2014**, *53*, 10929–10942.
- [9] D. Li, X. Zhu, *Mater. Lett.* **2011**, *65*, 1528–1530.
- [10] a) J. C. Marchal, D. J. Krug III, P. McDonnell, K. Sun, R. M. Laine, *Green Chem.* **2015**, *17*, 3931–3940; b) R. M. Laine, J. C. Furgal, P. Doan, D. Pan, V. Popova, X. Zhang, *Angew. Chem.* **2016**, *128*, 1077–1081; *Angew. Chem. Int. Ed.* **2016**, *55*, 1065–1069.
- [11] S. Yamanaka, H. Takeda, S. Komatsubara, F. Ito, H. Usami, E. Togawa, K. Yoshino, *Appl. Phys. Lett.* **2009**, *95*, 123703.
- [12] a) M. Si, X. Yan, M. Liu, M. Shi, Z. Wang, S. Wang, J. Zhang, C. Gao, L. Chai, Y. Shi, *ACS Sustainable Chem. Eng.* **2018**, *6*, 7969–7978; b) L. Chen, R. Chen, S. Fu, *ACS Sustainable Chem. Eng.* **2015**, *3*, 1794–1800.
- [13] a) B. Gyurcsik, L. Nagy, *Coord. Chem. Rev.* **2000**, *203*, 81–149; b) K. M. Kim, S. C. Song, S. B. Lee, H. C. Kang, Y. S. Sohn, *Inorg. Chem.* **1998**, *37*, 5764–5768; c) J. H. Advani, K. Ravi, D. R. Naikwadi, H. C. Bajaj, M. B. Gawande, A. V. Biradar, *Dalton Trans.* **2020**, *49*, 10431–10440.
- [14] B. Sahoo, A. E. Surkus, M. M. Pohl, J. Radnik, M. Schneider, S. Bachmann, M. Scalone, K. Junge, M. Beller, *Angew. Chem.* **2017**, *129*, 11394–11399; *Angew. Chem. Int. Ed.* **2017**, *56*, 11242–11247.
- [15] a) B. Sahoo, D. Formenti, C. Topf, S. Bachmann, M. Scalone, K. Junge, M. Beller, *ChemSusChem* **2017**, *10*, 3035–3039; b) F. K. Scharnagl, M. F. Hertrich, F. Ferretti, C. Kreyenschulte, H. Lund, R. Jackstell, M. Beller, *Sci. Adv.* **2018**, *4*, eaau1248.
- [16] A. Béchamp, *Ann. Chim. Phys.* **1854**, *42*, 186–196.
- [17] H.-U. Blaser, H. Steiner, M. Studer, *ChemCatChem* **2009**, *1*, 210–221.
- [18] a) P. Veerakumar, I. Panneer Muthuselvan, C.-T. Hung, K.-C. Lin, F.-C. Chou, S.-B. Liu, *ACS Sustainable Chem. Eng.* **2016**, *4*, 6772–6782; b) Y. Gao, K. Liu, C. Wu, H. Zhang, Q. Zhang, *Appl. Catal. A* **2020**, *592*, 117434.
- [19] a) M. Boronat, P. Concepción, A. Corma, S. González, F. Illas, P. Serna, *J. Am. Chem. Soc.* **2007**, *129*, 16230–16237; b) A. Corma, P. Concepción, P. Serna, *Angew. Chem. Int. Ed.* **2007**, *46*, 7266–7269; *Angew. Chem.* **2007**, *119*, 7404–7407; c) A. Corma, P. Serna, *Science* **2006**, *313*, 332–334; d) K.-i. Shimizu, Y. Miyamoto, T. Kawasaki, T. Tanji, Y. Tai, A. Satsuma, *J. Phys. Chem. C* **2009**, *113*, 17803–17810.
- [20] a) A. Montoya, A. Schlunke, B. S. Haynes, *J. Phys. Chem. B* **2006**, *110*, 17145–17154; b) A. B. Mohammad, I. V. Yudanov, K. H. Lim, K. M. Neyman, N. Rösch, *J. Phys. Chem. C* **2008**, *112*, 1628–1635.
- [21] a) J.-X. Jiang, Y. Li, X. Wu, J. Xiao, D. J. Adams, A. I. Cooper, *Macromolecules* **2013**, *46*, 8779–8783; b) C. Wen, A. Yin, W.-L. Dai, *Appl. Catal. B* **2014**, *160*–161, 730–741; c) D. Mei, M. Neurock, C. M. Smith, *J. Catal.* **2009**, *268*, 181–195; d) S. Wang, H. Huang, S. Tsareva, C. Bruneau, C. Fischmeister, *Adv. Synth. Catal.* **2019**, *361*, 786–790; e) Y. Xie, P. Hu, T. Bendikov, D. Milstein, *Catal. Sci. Technol.* **2018**, *8*, 2784–2788; f) M. Steffan, A. Jakob, P. Claus, H. Lang, *Catal. Commun.* **2009**, *10*, 437–441; g) M. Bron, D. Teschner, A. Knop-Gericke, F. C. Jentoft, J. Kröhnert, J. Hohmeyer, C. Volckmar, B. Steinhauer, R. Schlögl, P. Claus, *Phys. Chem. Chem. Phys.* **2007**, *9*, 3559–3569; h) H. Wei, C. Gomez, J. Liu, N. Guo, T. Wu, R. Lobo-Lapidus, C. L. Marshall, J. T. Miller, R. J. Meyer, *J. Catal.* **2013**, *298*, 18–26.
- [22] a) K.-i. Shimizu, Y. Miyamoto, A. Satsuma, *J. Catal.* **2010**, *270*, 86–94; b) C. Paun, G. Slowik, E. Lewin, J. Să, *RSC Adv.* **2016**, *6*, 87564–87568; c) S. R. Khan, Z. H. Farooqi, Z. Waheed uz, A. Ali, R. Begum, F. Kanwal, M. Siddiq, *Mater. Chem. Phys.* **2016**, *171*, 318–327; d) B. Zhao, Z. Dong, Q. Wang, Y. Xu, N. Zhang, W. Liu, F. Lou, Y. Wang, *Nanomaterials* **2020**, *10*, 883; e) B. Naik, S. Hazra, V. S. Prasad, N. N. Ghosh, *Catal. Commun.* **2011**, *12*, 1104–1108; f) F. Cárdenas-Lizana, Z. M. de Pedro, S. Gómez-Quero, M. A. Keane, *J. Mol. Catal. A* **2010**, *326*, 48–54; g) R. Rajesh, R.

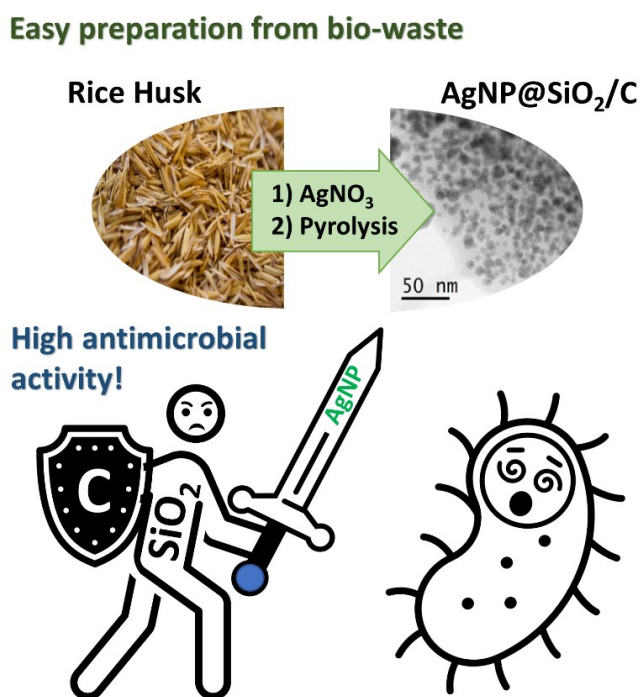
- Venkatesan, *J. Mol. Catal. A* **2012**, 359, 88–96; h) Y. A. Attia, Y. M. Mohamed, *Appl. Organomet. Chem.* **2019**, 33, e4757; i) M. M. Mohamed, M. S. Al-Sharif, *Mater. Chem. Phys.* **2012**, 136, 528–537; j) Y. Chen, C. Wang, H. Liu, J. Qiu, X. Bao, *Chem. Commun.* **2005**, 5298–5300.
- [23] M. S. Akhtar, J. Panwar, Y.-S. Yun, *ACS Sustainable Chem. Eng.* **2013**, 1, 591–602.
- [24] X. Lan, Y. Li, C. Du, T. She, Q. Li, G. Bai, *Chem. Eur. J.* **2019**, 25, 8560–8569.
- [25] H. J. Hah, S. M. Koo, S. H. Lee, *J. Sol-Gel Sci. Technol.* **2003**, 26, 467–471.
- [26] a) H. Huang, X. Ni, G. Loy, C. Chew, K. Tan, F. Loh, J. Deng, G. Xu, *Langmuir* **1996**, 12, 909–912; b) M. Zaarour, M. El Roz, B. Dong, R. Retoux, R. Aad, J. Cardin, C. Dufour, F. Goubilleau, J.-P. Gilson, S. Mintova, *Langmuir* **2014**, 30, 6250–6256.
- [27] X. Lan, Q. Li, L. Cao, C. Du, L. Ricardez-Sandoval, G. Bai, *Appl. Surf. Sci.* **2020**, 508, 145220.
- [28] K. Wang, R. Chen, X. Zhu, Q. Liao, D. Ye, G. Chen, M. Liu, *Ind. Eng. Chem. Res.* **2020**, 59, 16205–16216.
- [29] A. Chakraverty, P. Mishra, H. Banerjee, *J. Mater. Sci.* **1988**, 23, 21–24.
- [30] a) S. Hu, Y.-L. Hsieh, *ACS Sustainable Chem. Eng.* **2014**, 2, 726–734; b) B. J. Saikia, G. Parthasarathy, N. Sarmah, *Bull. Mater. Sci.* **2008**, 31, 775–779.
- [31] S. Janbroers, J. Louwen, H. Zandbergen, P. Kooyman, *J. Catal.* **2009**, 268, 235–242.
- [32] I. Lopez-Salido, D. C. Lim, Y. D. Kim, *Surf. Sci.* **2005**, 588, 6–18.
- [33] D. Formenti, F. Ferretti, F. K. Scharnagl, M. Beller, *Chem. Rev.* **2018**, 119, 2611–2680.
- [34] F. A. Westerhaus, R. V. Jagadeesh, G. Wienhöfer, M.-M. Pohl, J. Radnik, A.-E. Surkus, J. Rabeah, K. Junge, H. Junge, M. Nielsen, A. Brückner, M. Beller, *Nat. Chem.* **2013**, 5, 537–543.
- [35] a) H. Adkins, H. I. Cramer, *J. Am. Chem. Soc.* **1930**, 52, 4349–4358; b) P. Ryabchuk, G. Agostini, M.-M. Pohl, H. Lund, A. Agapova, H. Junge, K. Junge, M. Beller, *Sci. Adv.* **2018**, 4, eaat0761.
- [36] a) V. N. Ipatieff, B. B. Corson, I. D. Kurbatov, *J. Phys. Chem.* **1939**, 43, 589–604; b) R. Watairi, Y. Kayaki, *Asian J. Org. Chem.* **2018**, 7, 2005–2014.
- [37] a) Y. Lu, W. Chen, *J. Power Sources* **2012**, 197, 107–110; b) N. R. Jana, T. K. Sau, T. Pal, *J. Phys. Chem. B* **1999**, 103, 115–121; c) P. Claus, H. Hofmeister, *J. Phys. Chem. B* **1999**, 103, 2766–2775.
- [38] a) M. Stein, J. Wieland, P. Steurer, F. Tölle, R. Mülhaupt, B. Breit, *Adv. Synth. Catal.* **2011**, 353, 523–527; b) R. Hudson, A. Riviere, C. M. Cirtiu, K. L. Luska, A. Moores, *Chem. Commun.* **2012**, 48, 3360–3362.
- [39] D. Formenti, R. Mocci, H. Atia, S. Dastgir, M. Anwar, S. Bachmann, M. Scalone, K. Junge, M. Beller, *Chem. Eur. J.* **2020**, 26, 15589–15595.
- [40] T. W. Hansen, A. T. DeLaRiva, S. R. Challa, A. K. Datye, *Acc. Chem. Res.* **2013**, 46, 1720–1730.
- [41] a) F. Alonso, I. P. Beletskaya, M. Yus, *Chem. Rev.* **2002**, 102, 4009–4092; b) T. Vincent, S. Spinelli, E. Guibal, *Ind. Eng. Chem. Res.* **2003**, 42, 5968–5976; c) Y. Mitoma, S. Nagashima, C. Simion, A. M. Simion, T. Yamada, K. Mimura, K. Ishimoto, M. Tashiro, *Environ. Sci. Technol.* **2001**, 35, 4145–4148.
- [42] a) M. T. Mandal, Haifeng; Xiao, Li; Su, Jing; Li, Guoqing; Yang, Shu-Wei; Pan, Weidong; Tang, Haiqun; Dejesus, Reynalda; Hicks, Jacqueline; Lombardo, Matthew; Chu, Hong; Hagmann, William; Pasternak, Alex; Gu, Xin; Jiang, Jinlong; Dong, Shuzhi; Ding, Fa-Xiang; London, Clare; Biswas, Dipshikha; Young, Katherine; Hunter, David N.; Zhao, Zhiqiang; Yang, Dexi, Vol. WO 2015112441 (Ed.: M. S. D. Corp.), USA, **2015**; b) G. Li, S. Azuma, H. Minegishi, H. Nakamura, *J. Organomet. Chem.* **2015**, 798, 189–195.
- [43] V. V. Torbina, A. A. Vodyankin, S. Ten, G. V. Mamontov, M. A. Salaev, V. I. Sobolev, O. V. Vodyankina, *Catalysts* **2018**, 8, 447.

Manuscript received: January 11, 2021  
 Revised manuscript received: February 24, 2021  
 Accepted manuscript online: March 11, 2021  
 Version of record online: April 6, 2021

## Preparation, Characterization and Antimicrobial Properties of Nanosized Silver-Containing Carbon/Silica Composites from Rice Husk Waste

F. Unglaube, A. Lammers, C. R. Kreyenschulte, M. Lalk and E. Mejia. ChemistryOpen (2021)., 10(12), 1244.

DOI: 10.1002/open.202100239



**Abstract:** Rice Husk, one of the main side products in the rice production, and its sustainable management represents a challenge in many countries. Herein we describe the use of this abundant agricultural bio-waste as feedstock for the preparation of silver-containing carbon/silica nano composites with antimicrobial properties. The synthesis was performed using a fast and cheap methodology consisting of wet impregnation followed by pyrolysis, yielding C/SiO<sub>2</sub> composite materials doped with varying amounts of silver from 28 to 0.001 wt-% (Ag@RHA). The materials were fully characterized and their antimicrobial activity against ESKAPE pathogens, namely *E. faecium*, *S. aureus*, *K. pneumoniae*, *A. baumannii*, *P. aeruginosa*, and *E. coli*, and the pathogenic yeast *C. albicans* was investigated. Sensitivities of these strains against the prepared materials were demonstrated, even with exceptional low amounts of 0.015 m% silver. Hence, this work introduces a straightforward method for the synthesis of antimicrobial agents from abundant sources and tackles urgent questions like bio-waste valorization and affordable alternatives to increasingly fewer effective antibiotics.



# Preparation, Characterization and Antimicrobial Properties of Nanosized Silver-Containing Carbon/Silica Composites from Rice Husk Waste

Felix Unglaube,<sup>[a]</sup> Alexander Lammers,<sup>[b]</sup> Carsten Robert Kreyenschulte,<sup>[a]</sup> Michael Lalk,<sup>\*,[b]</sup> and Esteban Mejía<sup>\*,[a]</sup>

Rice husk, one of the main side products in the rice production, and its sustainable management represent a challenge in many countries. Herein, we describe the use of this abundant agricultural bio-waste as feedstock for the preparation of silver-containing carbon/silica nano composites with antimicrobial properties. The synthesis was performed using a fast and cheap methodology consisting of wet impregnation followed by pyrolysis, yielding C/SiO<sub>2</sub> composite materials doped with varying amounts of silver from 28 to 0.001 wt%. The materials were fully characterized and their antimicrobial activity against

ESKAPE pathogens, namely *E. faecium*, *S. aureus*, *K. pneumoniae*, *A. baumannii*, *P. aeruginosa*, and *E. coli*, and the pathogenic yeast *C. albicans* was investigated. Sensitivities of these strains against the prepared materials were demonstrated, even with exceptional low amounts of 0.015 m% silver. Hence, we report a straightforward method for the synthesis of antimicrobial agents from abundant sources which addresses urgent questions like bio-waste valorization and affordable alternatives to increasingly fewer effective antibiotics.

## Introduction

Rice is among the most widely spread food crops on earth, as the current world production is estimated at around 500 million tons annually.<sup>[1]</sup> Importantly, along with the produced food, approximately 800 million tons of production residues annually arise, which are mainly rice straw and rice husk (RH).<sup>[2]</sup> The common practice to “manage” the post-harvest waste is the open burning after the plant material has been left and dried on the fields, as it is cheap and straightforward, and the resulting ashes serve as fertilizer. However, studies demonstrated that the use of rice husk ashes for plant nutrition is not especially beneficial since other fertilizing techniques, for example incorporation of rice straw in soil, have similar or better effects.<sup>[3]</sup> Additionally, this practice causes massive air pollution in all rice-growing regions including China, India, Philippines and Vietnam.<sup>[4]</sup> This pollution poses not only a health risk for humans,<sup>[5]</sup> but also has a negative environmental impact due to the massive emissions of CO<sub>2</sub> and particulate matter. Yet, to

worsen things, studies also indicated a correlation between high air pollution levels and low rice yields.<sup>[6]</sup> Hence, it is necessary to find alternative methodologies of waste treatment in order to decrease the significant health and environmental burden caused by rice production. Beside solving major challenges in logistics and political implementation, a valid and useful alternative must be presented in order to obtain acceptance from the most affected persons, the rice farmers, and convince them to abandon traditional methods.

For almost one century, there have been efforts to develop and demonstrate applicable methods of utilization of waste from the rice production chain.<sup>[7]</sup> A vast majority of these approaches are dealing with the use of rice husk ash (RHA), which is the product of the often incomplete burning of RH. The calorific value of RH is approx. 18.7 MJ kg<sup>-1</sup>,<sup>[8]</sup> which is less than half of biodiesel.<sup>[9]</sup> The burning is, therefore, unsatisfactory in terms of energy efficiency and produces significant amounts of CO<sub>2</sub>, fine particles and silicon-containing waste.<sup>[10]</sup> Nevertheless, it has to be noted that RHA can be used as an additive in concrete due to its high silica content. Even though it increases the water demand of the resulting raw material, this approach has already been demonstrated to be applicable.<sup>[11]</sup> In recent years, many rather complicated methods have been developed to separate the two main compounds of RH, carbon and silica, in order to use them as bio-derived feedstock for silicon-based technologies. The obtainable products are solar-grade silicon,<sup>[12]</sup> alkoxysilanes or orthosilicates (important building blocks in the semiconductors and silicone industry),<sup>[13]</sup> electrode materials<sup>[14]</sup> or light-emitting amorphous SiO<sub>2</sub> nanophosphors.<sup>[15]</sup> Carbon from rice husk can further be used as catalyst for production of biofuel additives,<sup>[16]</sup> but the main potential lies in the use as absorbent for waste water treatment,<sup>[17]</sup> due to its high surface area and good adsorption

[a] F. Unglaube, Dr. C. R. Kreyenschulte, Dr. E. Mejía  
Leibniz-Institut für Katalyse e.V. (LIKAT)  
18059 Rostock (Germany)  
E-mail: Esteban.Mejia@catalysis.de

[b] A. Lammers, Prof. Dr. M. Lalk  
Institut für Biochemie  
Universität Greifswald  
17489 Greifswald (Germany)  
E-mail: lalk@uni-greifswald.de

Supporting information for this article is available on the WWW under <https://doi.org/10.1002/open.202100239>

© 2021 The Authors. Published by Wiley-VCH GmbH. This is an open access article under the terms of the Creative Commons Attribution Non-Commercial NoDerivs License, which permits use and distribution in any medium, provided the original work is properly cited, the use is non-commercial and no modifications or adaptations are made.

properties. An advantage of this approach is that the carbon must not necessarily be isolated from RHA, as it can be modified or used directly. The removable compounds span from organic pollutants to inorganic molecules like phosphate,<sup>[18]</sup> nitrate<sup>[19]</sup> or various relevant heavy metal ions like  $\text{Cu}^{2+}$ ,  $\text{Ni}^{2+}$ ,  $\text{Cd}^{2+}$ ,  $\text{Mn}^{2+}$ ,  $\text{Co}^{2+}$ ,  $\text{Hg}^{2+}$ ,  $\text{Pb}^{2+}$  or  $\text{Cr}^{6+}$ .<sup>[20]</sup>

Next to the removal of organic and inorganic compounds from wastewater, the removal of microbial pathogens to weaken the antimicrobial resistance crisis might be a promising usage of rice husks in future. Even though highly active antibiotics have been a tool to efficiently control bacterial infection since the commercial introduction of Penicillin in the 1940s, we are currently facing a global antimicrobial resistance crisis, caused by the intense and wrong usage of antibiotics in combination with the lack of novel compounds.<sup>[21]</sup> Every year, approximately 700,000 people die of infections caused by resistant pathogens in contrast to 8,200,000 by cancer and 1,200,000 by traffic accidents. It has been estimated that there will be around 10,000,000 deaths caused by resistant pathogens in 2050.<sup>[21a,22]</sup> Whether novel classes of antibiotics should be in investigation or rather alternative methods, is debatable.<sup>[23]</sup>

An alternative approach to commonly used antibiotics is the usage of silver nanoparticles (AgNP), since they are known to have antimicrobial properties.<sup>[24]</sup> Every infection which can be avoided makes the use of "old-school" antibiotics obsolete and therefore lowers the risk of pathogens evolving resistances.<sup>[25]</sup> In aqueous solutions, AgNP release silver ions ( $\text{Ag}^+$ ) which have numerous antimicrobial activities.<sup>[26]</sup> Even though AgNPs themselves have antimicrobial properties, it is preferable to use silver ions instead as they are active in trace amounts, which is beneficial since silver can indeed be toxic in higher concentrations to cells of higher animals as well.<sup>[27]</sup> They interact with the membrane and cell wall proteins of the microorganisms, resulting in damage to those structures along with a disturbed proton gradient, leading to cell death.<sup>[28]</sup> If the silver ions reach the cytoplasm, they can inhibit the electron transport chain, damage DNA and RNA, inhibit DNA replication, denature the 30S ribosomal subunit resulting in inhibited protein synthesis and induce the formation of reactive oxygen species (ROS).<sup>[28,29]</sup> The numerous mechanisms of action result in a wide spectrum of target organisms, including (drug-resistant) bacteria, fungi and viruses. In addition, silver nanoparticle resistance of microorganisms is rarely reported.<sup>[26b]</sup> Moreover, it has been shown that the combination of silver nanoparticles and antibiotics significantly improves the antimicrobial effect of the antibiotics.<sup>[29,30]</sup> The wide spectrum of target organisms and the low risk of resistance development have made silver nanoparticles promising targets in current research.<sup>[24a,b,26,31]</sup> The combination of an antimicrobial material like AgNPs and a material with excellent ability to adsorb pollutants, like RHA, leads to a composite which offers multifunctionality as a filter material. The need of cheap and easily manufacturable materials for both water and air sanitation is undeniably a key aspect to secure the health of millions of humans, since on the one hand, approx. 780 million people do not have access to clean water on a daily basis (status 2014),<sup>[32]</sup> while, on the other hand, air pollution and airborne pathogens are extremely

problematic, like recently demonstrated by the devastating COVID-19 pandemic,<sup>[33]</sup> in both private households and indoor working places,<sup>[34]</sup> as well as in professional healthcare environments.<sup>[35]</sup> Fortunately, AgNPs can be and are applied against pathogens in water or on surfaces as well as against airborne pathogens.<sup>[36]</sup> Moreover, since ancient times, the use of silver has not been associated with health risks (when not used in disproportionate amounts).<sup>[37]</sup>

State of the art in AgNP preparation is the reduction of an oxidized silver source by chemical, physical, biological or photochemical techniques,<sup>[38]</sup> requiring an external reduction agent which reacts with  $\text{Ag}^+$  species. This approach leads to the production of stoichiometric amounts of waste which need to be removed after the synthesis. The AgNPs prepared in such a way can be used as colloids, in solution or can be fixed on a solid supporting material which enables easier separation from the treated subject and recycling.

The preparation of supported AgNPs (fixed on a solid supporting material) commonly involves generation of the particles followed by deposition on a previously prepared suitable support, resulting in a multistep process that produces significant amounts of waste.

In this work, we present a straightforward method which combines preparation of support and AgNPs in one step, resulting in an excellent atom economy. The direct application of  $\text{Ag}^+$  ions on the lignocellulosic framework offered by RH is followed by carbothermal reduction yielding carbon/silica composites doped with AgNPs (Ag@RHA). This is, to the best of our knowledge, the simplest yet reported method for the preparation of antimicrobial systems with AgNPs as active agent and rice husk as support precursor. This presents a more sustainable alternative to previous reports on the preparation of "bio-derived" antimicrobial agents. Usually, RH is only used as the feedstock for the preparation of supporting material like active carbon,<sup>[39]</sup> pseudowollastonite,<sup>[40]</sup> silica-carbon nanoparticles,<sup>[41]</sup> pure silica or MCM-41 nanoparticles. In all the previously reported methodologies, silver is impregnated on the prepared support in a subsequent step, therefore producing significant amounts of waste during the preparation.

## Results and Discussion

All tested Ag@RHA were prepared by wet impregnation of previously shredded RH with different amounts of  $\text{AgNO}_3$  followed by pyrolysis at 600 °C. The resulting pyrolyzed material is made mainly of carbon, silicon, oxygen and contains low amounts of nitrogen and phosphorus as well as sulfur and iron (Table S1 and Figure S1, Supporting Information). X-ray diffraction (XRD) analysis (Figure S1) revealed a broad peak from 15 to 30° suggesting the existence of an amorphous silica phase and/or carbon phase. Additionally, reflexes at 26.6° and 50.1° fitting to a crystalline hexagonal  $\alpha\text{-SiO}_2$  phase are also present. The peak shapes for cubic silver reflexes at 38.1°, 44.3°, 64.5° and 77.5° match those of similar materials previously reported by our group,<sup>[42]</sup> which indicates the existence of a bimodal Ag crystallite phase. Beside these three phases, two weak peaks at

35.6° and 62.7° indicate the existence of cubic  $\text{Fe}_2\text{O}_3$ , which can commonly be observed in RHA due to the high iron content in the plant.<sup>[43]</sup> The average silver crystallite size was calculated using whole powder pattern fitting-Scherrer methodology for the raw material, containing 20 m% of silver and was found to be 14 nm. The surface area was investigated using Brunauer-Emmett-Teller (BET) isotherm analysis; a BET surface area of  $260.7 \text{ m}^2 \text{ g}^{-1}$  was found (Figure 1A) with a small hysteresis for the desorption. The cumulative volume of pores between 2 nm and 100 nm width is with  $0.05 \text{ cm}^3 \text{ g}^{-1}$ , only half of the t-Plot micropore volume of  $0.104 \text{ cm}^3 \text{ g}^{-1}$  from 0.25 to 2 nm pore

width. The clearly visible pore volume and area maximum around 0.6 nm underlines the microporous character of the prepared material.

IR measurements (Figure S2) revealed vibrations at 454, 571, 798 and  $1067 \text{ cm}^{-1}$  which can be correlated with Si–O bonds, confirming the presence of high amounts of silica in the material.<sup>[44]</sup> A broad signal around  $1543 \text{ cm}^{-1}$  corresponding to carbon-carbon double bond vibrations was observed, which is a common feature in RHA.<sup>[45]</sup>

Moreover, the morphology of the AgNPs was investigated with scanning transmission electron microscopy (STEM), since previous studies suggested a correlation of the particle shape and antimicrobial activity, even though the reported particle size was up to 20-fold higher.<sup>[46]</sup> The STEM images of Ag@RHA with the highest silver concentration revealed a spherical shape (Figure 2A, Figures S3A and 3B) with a diameter of about 10 nm with a few outliers reaching 50 nm and a full crystalline structure of the AgNPs (Figure 2B and Figure S3C).

A series of composites (Ag@RHA) containing different amounts of silver was prepared to evaluate the minimal amount of metal needed to get a significant antimicrobial activity (Table 1). Nine samples have been prepared, starting from 28 wt % of  $\text{AgNO}_3$  in the RH (which correspond to 4.880(4) wt % of Ag in the pyrolyzed material), to 0.001 wt % of  $\text{AgNO}_3$  which corresponds to an Ag amount lower than the limit of detection (and quantification) of the applied inductively coupled plasma-optical emission spectrometry (ICP-OES) method.

For the antimicrobial activity assessment, the pyrolyzed material (Ag@RHA) was suspended in methanol ( $20 \text{ mg ml}^{-1}$ ) and 10  $\mu\text{l}$  of the suspension were transferred on a cotton disc (6 mm diameter) which was placed on the agar containing the microbes (Figure S4). Interestingly, no detectable amounts of Ag were found in agar after the antimicrobial tests, suggesting that leaching and diffusion of silver did take place only in minute quantities (Table 1).

The antimicrobial test results revealed a high sensitivity of all Gram-positive bacteria (*Enterococcus faecium*, *Staphylococcus aureus*), Gram-negative bacteria (*Klebsiella pneumoniae*, *Acinetobacter baumannii*, *Pseudomonas aeruginosa*, *Escherichia coli*), and the yeast (*Candida albicans*) whose growth were inhibited (Figure 3). The activity is clearly related to the silver content on

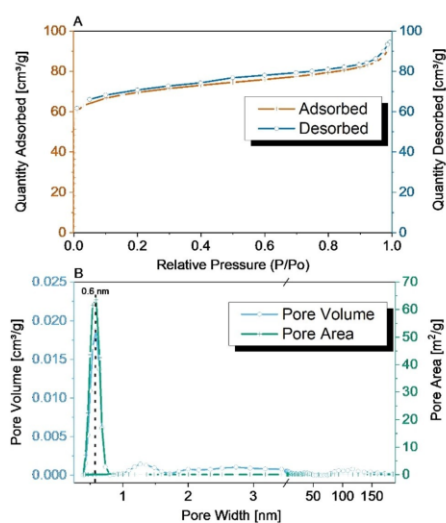


Figure 1. A) BET-isotherm quantity ad and desorption plot and B) plot of pore volume and area vs. pore width.

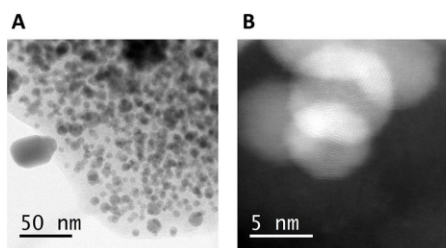
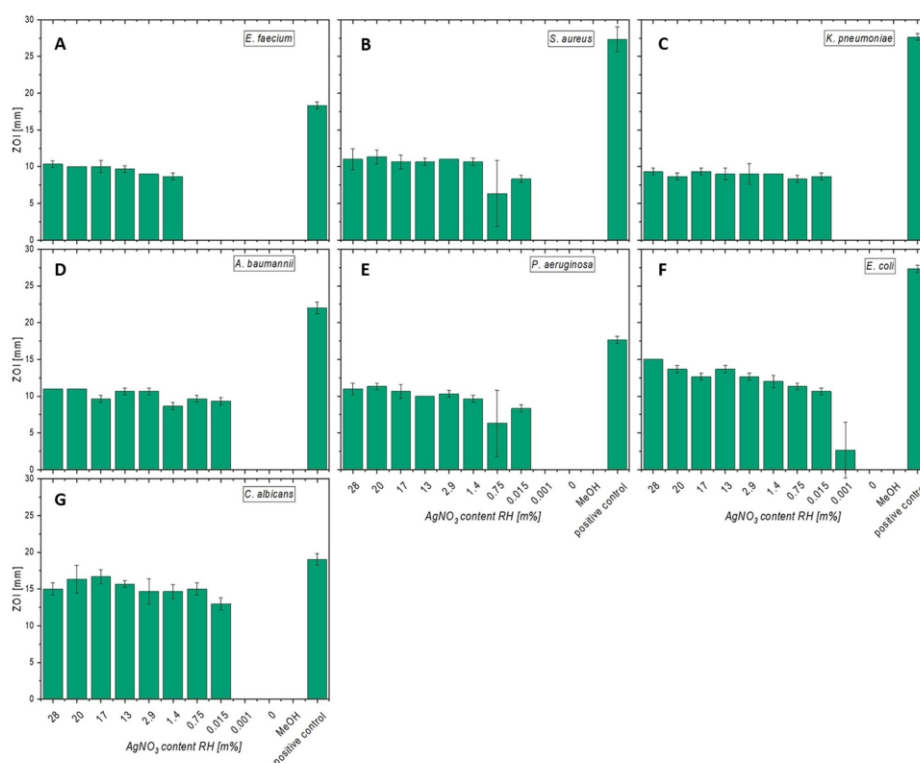


Figure 2. Microscopy images of Ag@RHA with highest silver concentration: A) Annular bright field STEM image of spherical shaped AgNPs and B) high-angle annular dark field STEM image displaying the crystalline character of AgNPs.

ii	$\text{AgNO}_3$ added to RH [wt %] <sup>[a]</sup>	Ag after pyrolysis [wt %] <sup>[a]</sup>	Ag at cotton disc [wt %] <sup>[a]</sup>	Ag in agar [wt %] <sup>[a]</sup>
1	28	4.880(4)	0.069(3)	< 0.001 <sup>[b]</sup>
2	20	3.472(8)	0.047(5)	< 0.001 <sup>[b]</sup>
3	17	2.945(0)	0.033(4)	< 0.001 <sup>[b]</sup>
4	13	2.241(3)	0.031(5)	< 0.001 <sup>[b]</sup>
5	2.9	0.478(5)	< 0.001 <sup>[b]</sup>	< 0.001 <sup>[b]</sup>
6	1.4	0.10(2)	< 0.001 <sup>[b]</sup>	< 0.001 <sup>[b]</sup>
7	0.75	0.03(8)	< 0.001 <sup>[b]</sup>	< 0.001 <sup>[b]</sup>
8	0.015	< 0.001 <sup>[b]</sup>	< 0.001 <sup>[b]</sup>	< 0.001 <sup>[b]</sup>
9	0.001	< 0.001 <sup>[b]</sup>	< 0.001 <sup>[b]</sup>	< 0.001 <sup>[b]</sup>
10	0	< 0.001 <sup>[b]</sup>	< 0.001 <sup>[b]</sup>	< 0.001 <sup>[b]</sup>

[a] Measured with ICP-OES [b] limit of quantification at 0.001 m%.



**Figure 3.** Antimicrobial effect of Ag@RHA to bacterial and yeast test strains. The bar charts show the zones of inhibition (ZOI) induced by different silver concentrations against (A) *Enterococcus faecium*, (B) *Staphylococcus aureus*, (C) *Klebsiella pneumoniae*, (D) *Acinetobacter baumannii*, (E) *Pseudomonas aeruginosa*, (F) *Escherichia coli*, and (G) *Candida albicans*. MeOH was used as negative control. Gentamicin was used as positive control for bacterial cells and Amphotericin B for the yeast. The cotton discs had a diameter of 6 mm. The error bars show the standard deviation  $n=3$ .

the material and not the pure support, since no inhibition was detected when biochar without silver was used (prepared from RH under the same conditions). Most microorganisms were sensitive against the AgNPs made with an initial AgNO<sub>3</sub> content of 0.015 wt% (Table 1, entry 8). *E. faecium* was sensitive to a lesser extent, but clearly inhibited in growth at an initial Ag content of 1.4 wt% (Figure 3A). Two different strains of *E. coli* (DSM 498 and 787) have been tested, but only the 498-strain showed clear sensitivity against the AgNPs (Figure 3G). The 787-strain showed a slight decrease in cell density but no clear zone of inhibition (not shown). The analyzed Ag contents in the cotton discs and agar were in every case  $<0.001$  wt% as measured by ICP-OES (Table 1), showcasing the low amounts of silver necessary to achieve antimicrobial activity of the prepared material.

The antimicrobial activity of AgNPs against the ESKAPE pathogens (*E. faecium*, *S. aureus*, *K. pneumoniae*, *A. baumannii*, *P. aeruginosa*, and *E. coli*) as well as *C. albicans* has been shown by several studies.<sup>[40,47]</sup> Salouti and colleagues showed a decreased number of colony forming units of a wound infected with *S. aureus* after treatment with AgNPs on a mouse model.<sup>[48]</sup> The combination of rifampicin with AgNPs was shown to increase the antimicrobial activity against methicillin-resistant *S. aureus* and *K. pneumoniae* as compared to rifampicin alone.<sup>[49]</sup> Furthermore, the antibacterial effect of AgNPs was shown against methicillin-resistant *S. aureus*.<sup>[50]</sup> Transmission electron microscopy imaging revealed a thinning and permeabilization of the cell wall causing cell lysis.

Importantly, our Ag@RHA materials display antimicrobial activities at much lower silver concentrations compared to



other studies. For instance, Azam and colleagues produced silver-doped  $\text{CaSiO}_3$  (synthesized from rice husk ash as a limestone precursor) and showed good antimicrobial activity against *E. coli* and *S. aureus* with Ag contents between 1–5 wt%.<sup>[40]</sup> In contrast, we showed clear zones of inhibition with Ag contents below 0.001 wt% in the agar indicating a much higher bioactivity of the RHA-supported AgNPs.

The antimicrobial test results revealed a similar sensitivity of Gram-positive and -negative bacteria against Ag@RHA. Due to a thinner cell wall, it can be argued that Gram-negative bacteria might be more sensitive against AgNPs.<sup>[51]</sup> Other studies argue that Gram-negative bacteria are less sensitive against AgNPs because of the negatively charged lipopolysaccharides of their outer membrane which very likely interact with the positively charged silver ions and prevent the ions from entering the cells.<sup>[28b]</sup>

Next to bacterial pathogens, the Ag@RHA showed clear antifungal effects against *C. albicans* (Figure 3F). This result is supported by other studies showing similar results. Kim and colleagues showed, by transmission electron microscopy imaging, that AgNPs result in a damage of the cell membrane of *C. albicans*.<sup>[47b]</sup> Using flow cytometry, they demonstrated that the cells got stuck in the G2/M phase of the cell cycle. Next to yeasts, the antifungal effect of Ag@RHA was also shown against several fungi, for example *Aspergillus niger*, *Aspergillus fumigatus* and *Fumigatus soleni*, indicating a wide antifungal spectrum.<sup>[47a]</sup>

Additionally, the conditions during the antimicrobial test have been reproduced with 50 mg of Ag@RHA to assess the stability of the prepared material and to investigate its applicability. The recovered Ag@RHA sample was analyzed by XRD. The average crystallite size was calculated at 12 nm using Scherrer's method (Table S2), showing no change compared to the freshly prepared material. Notable is the appearance of reflexes at 27.8°, 32.2°, 46.2°, 54.7° and 62.9°, relating to a cubic  $\text{Na}_2\text{O}$  phase (Figure S1), which is most likely the result of the contact with the aqueous agar at 37°C for 24 h rather than the result of using methanol in the preparation of the suspension.

## Conclusion

In summary, we have successfully developed a simple method for obtaining highly antimicrobial silver nanoparticles supported on carbon/silica composites derived from agricultural (rice) bio-waste. The high antimicrobial activity was demonstrated by the good results obtained even when extremely low amounts of silver were loaded on the support. The materials were characterized before and after the antimicrobial tests, where no significant change was detected by X-ray diffraction analyses. This suggests a possible long-term stability and recycling potential. In conclusion, the herein described silver-containing rice husk-based antimicrobial materials are suitable for tackling some of the challenges discussed above, as they can be used as multifunctional filters or coating materials in water sanitation and medicinal applications, thanks to its stability and good antimicrobial activity, even with minimal amounts of silver deposited on the surface.

## Experimental Section

### General Preparation Procedure

The RH samples were received from Vietnamese farmers at the Red River Delta (Nam Dinh Province, 20°23'27.7"N 106°15'34.7"E) and Mekong Delta (An Giang Province, 10°24'55.0"N 105°11'52.3"E). The RH was received pre-dried, and was shredded with a cutting mill SM 200 (rotation and speed 1000 rpm, 2 mm sieve sizes) and milled to a fine powder in a ball mill PM 200 (in steel cups with steel balls at 400 rpm for 3 h). The samples were mixed with different amounts of  $\text{AgNO}_3$ , 50 ml ethanol and stirred for 24 h at 21°C. The solvent was removed with a rotary evaporator and the sample was placed in an aluminium oxide crucible which was placed inside a quartz tube furnace. The samples were heated to 600°C with 10°C min<sup>-1</sup>, respectively, and the temperature was maintained for 1 h. The furnace was continuously flushed with nitrogen (50 ml min<sup>-1</sup>); after cooling to 25°C, the material was stored under ambient conditions.

### General Agar Diffusion Test Procedure

The material was not soluble in any common solvent. Therefore, suspensions with MeOH were prepared (20 mg ml<sup>-1</sup>) and homogenized using FastPrep™ (Lysing Matrix D, 20 s, 6 ms<sup>-1</sup>; MP Biomedicals, Santa Ana, California, USA). The antimicrobial activity of the suspensions was tested using the antimicrobial disc diffusion test. We used the ESKAPE pathogens *Enterococcus faecium* (DSM 20477), *Staphylococcus aureus* (DSM 799), *Klebsiella pneumoniae* (DSM 30104), *Acinetobacter baumannii* (DSM 30008), *Pseudomonas aeruginosa* (DSM 1117), *Escherichia coli* (DSM 498 and 787) and the yeast *Candida albicans* (DSM 10697) as test organisms. All strains were purchased at the German Collection of Microorganisms and Cell Cultures (DSMZ, Braunschweig, Germany).

The strains were pre-cultured before use overnight at 37°C on Mueller Hinton Agar II (2.0 g L<sup>-1</sup> beef heart infusion, 17.5 g L<sup>-1</sup> acid casein hydrolysate, 1.5 g L<sup>-1</sup> starch, 17.0 g L<sup>-1</sup> agar; Becton Dickinson, Franklin Lakes, New Jersey, USA). For each organism, a solution with an absorbance of OD600 0.125 was prepared. The whole surface of a Mueller Hinton agar II plate was covered with the cell solution using a soaked cotton swab. 10 µl of the test suspension was transferred to the cotton discs (6 mm diameter) and the discs were transferred to the agar plate after the MeOH was evaporated. The negative controls were cotton discs with MeOH only, the positive controls were Gentamicin (10 µg, Sensi-Disc™ GM-10, Becton Dickinson, Franklin Lakes, New Jersey, USA) for bacterial strains and Amphotericin B (ROTI®Antibiotika Disks Amphotericin B (AP) 100 Units, Carl Roth, Karlsruhe, Germany) for the yeast. Organisms were incubated for 24 h as described above and the zones of inhibition were measured.

## Acknowledgements

We would like to thank all the Vietnamese farmers and local authorities at the rice husk sample collection sites (Nam Dinh and An Giang provinces) for their help and hospitality. Also, thanks go to Dr. Hendrik Lund and Reinhard Eckelt for performing the XRD and BET surface measurements, respectively, and for their helpful comments and discussions. Furthermore, we would like to acknowledge the funding for the SUVALIG project from the German Federal Ministry of Education and Research (BMBF, 031B0707B) and the RoHan SDG Graduate School funded by the

German Academic Exchange Service (DAAD, 57315854) and the German Federal Ministry for Economic Cooperation and Development (BMZ) inside the framework "SDG Bilateral Graduate school programme". Financial support from the Leibniz Society and the Leibniz Science Campus ComBioCat is also gratefully acknowledged.

### Conflict of Interest

The authors declare no conflict of interest.

### Data Availability Statement

The data that support the findings of this study are available in the supplementary material of this article.

**Keywords:** antimicrobial resistance · antimicrobial surface · ESKAPE pathogens · rice husk · silver

- [1] a) B. Singh, *Waste and Supplementary Cementitious Materials in Concrete*, Elsevier, Amsterdam (Netherlands) **2018**, pp. 417–460; b) M. Simone, K. Menzie, S. MacDonald, S. Haley, S. Shagam, S. Shagam, S. Meyer for United States Department of Agriculture, Report: "WASDE – 616" **2021**, ISSN: 1554–9089.
- [2] L. Domínguez Escribá, M. Porcar, *Biofuels Bioprod. Biorefin.* **2010**, *4*, 154–159.
- [3] a) P. Ly, Q. D. Vu, L. S. Jensen, A. Pandey, A. de Neergaard, *Paddy Water Environ.* **2015**, *13*, 465–475; b) E. M. Hanafi, H. El Khadrawy, W. Ahmed, M. Zaabal, *World Appl. Sci. J.* **2012**, *16*, 354–361; c) M. Gummert, N. V. Hung, P. Chivenge, B. Douthwaite, *Sustainable Rice Straw Management*, Springer Nature, Basingstoke (UK) **2020**, p. 102; d) G. Singh, S. Jalota, B. Sidhu, *Soil Use Manage.* **2005**, *21*, 17–21; e) H. Pathak, R. Singh, A. Bhatia, N. Jain, *Paddy Water Environ.* **2006**, *4*, 111–117.
- [4] K. Lasko, K. Vadvreva, *Environ. Pollut.* **2018**, *236*, 795–806.
- [5] a) M. F. Khan, M. T. Latif, W. H. Saw, N. Amil, M. Nadzir, M. Sahani, N. Tahir, J. Chung, *Atmos. Chem. Phys.* **2016**, *16*, 597–617; b) S. You, Y. W. Tong, K. G. Neoh, Y. Dai, C.-H. Wang, *Environ. Pollut.* **2016**, *218*, 1170–1179.
- [6] a) A. Wahid, R. Maggs, S. Shamsi, J. Bell, M. Ashmore, *Environ. Pollut.* **1995**, *90*, 323–329; b) S. Ishii, F. M. Marshall, J. Bell, A. M. Abdullah, *Water Air Soil Pollut.* **2004**, *154*, 187–201.
- [7] E. C. Beagle, *Rice-husk Conversion to Energy*, FAO, Roma (Italy), **1978**, p. 184.
- [8] U. B. Deshannavar, P. G. Hegde, Z. Dhalayat, V. Patil, S. Gavas, *Mater. Sci. Technol.* **2018**, *1*, 175–181.
- [9] P. Dey, S. Ray, A. Newar, *Fuel* **2021**, *283*, 118978.
- [10] T. Chungsangunsit, S. H. Gheewala, S. Patumsawad, *Int. J. Eng.* **2005**, *6*.
- [11] a) S. N. Raman, T. Ngo, P. Mendis, H. Mahmud, *Constr. Build. Mater.* **2011**, *25*, 3123–3130; b) V. Malhotra, *Concr. Int.* **1993**, *15*, 23–28; c) X. Liu, X. Chen, L. Yang, H. Chen, Y. Tian, Z. Wang, *Res. Chem. Intermed.* **2016**, *42*, 893–913; d) Y. Zou, T. Yang, *Rice Bran and Rice Bran Oil*, Elsevier, Amsterdam (Netherlands) **2019**, p. 207–246.
- [12] J. C. Marchal, D. J. Krug III, P. McDonnell, K. Sun, R. M. Laine, *Green Chem.* **2015**, *17*, 3931–3940.
- [13] a) M. Asuncion, I. Hasegawa, J. Kampf, R. Laine, *J. Mater. Chem. A* **2005**, *15*, 2114–2121; b) R. M. Laine, J. C. Furgal, P. Doan, D. Pan, V. Popova, X. Zhang, *Angew. Chem. Int. Ed.* **2016**, *55*, 1065–1069; *Angew. Chem.* **2016**, *128*, 1077–1081.
- [14] a) S.-S. Huang, M. T. Tung, C. D. Huynh, B.-J. Hwang, P. M. Bieker, C.-C. Fang, N.-L. Wu, *ACS Sustainable Chem. Eng.* **2019**, *7*, 7851–7861; b) L. Wang, J. Xue, B. Gao, P. Gao, C. Mou, J. Li, *RSC Adv.* **2014**, *4*, 64744–64746.
- [15] a) L. L. Devi, C. Basavapoornima, V. Venkatramu, P. Babu, C. Jayasankar, *Ceram. Int.* **2017**, *43*, 16622–16627; b) M. K. Chhina, K. Singh, *Ceram. Int.* **2020**, *46*, 9370–9379.
- [16] T. S. Galhardo, N. I. Simone, M. Gonçalves, F. v. C. Figueiredo, D. Mandelli, W. A. Carvalho, *ACS Sustainable Chem. Eng.* **2013**, *1*, 1381–1389.
- [17] Z. Shamsollahi, A. Partovinia, *J. Environ. Manage.* **2019**, *246*, 314–323.
- [18] S. Mor, K. Chhoden, K. Ravindra, *J. Cleaner Prod.* **2016**, *129*, 673–680.
- [19] N. D. Suzaimi, P. S. Goh, N. A. N. N. Malek, J. W. Lim, A. F. Ismail, *J. Environ. Chem. Eng.* **2019**, *7*, 103235.
- [20] L. Joseph, B.-M. Jun, J. R. Flora, C. M. Park, Y. Yoon, *Chemosphere* **2019**, *229*, 142–159.
- [21] a) E. Banin, D. Hughes, O. P. Kuipers, *FEMS Microbiol. Rev.* **2017**, *41*, 450–452; b) European Centre for Disease Prevention and Control, Report: "Surveillance of antimicrobial resistance in Europe" **2018**. Stockholm (Sweden).
- [22] J. O'Neill for the Government of the United Kingdom, Report: "Tackling drug-resistant infections globally: final report and recommendations." **2016**. London (UK).
- [23] a) L. Czaplewski, R. Bax, M. Clokie, M. Dawson, H. Fairhead, V. A. Fischetti, S. Foster, B. F. Gilmore, R. E. Hancock, D. Harper, *Lancet Infect. Dis.* **2016**, *16*, 2, 239–251; b) J.-M. Rolain, C. Abat, M.-T. Jimeno, P.-E. Fournier, D. Raoult, *Clin. Microbiol. Infect.* **2016**, *22*, 408–415.
- [24] a) B. Jamil, H. Bokhari, M. Imran, *Curr. Drug Targets* **2017**, *18*, 363–373; b) M. Kumar, A. Curtis, C. Hoskins, *Pharmaceutica* **2018**, *10*, 11; c) K. Whitehead, M. Vaidya, C. Liauw, D. Brownson, P. Ramalingam, J. Kamieniak, S. Rowley-Neale, L. Tetlow, J. Wilson-Nieuwenhuis, D. Brown, *Int. Biodeterior. Biodegrad.* **2017**, *123*, 182–190.
- [25] a) T. P. Robinson, D. Bu, J. Carrique-Mas, E. M. Fèvre, M. Gilbert, D. Grace, S. I. Hay, J. Jiwakanon, M. Kakkar, S. Kariuki, *Trans. R. Soc. Trop. Med. Hyg.* **2016**, *110*, 377–380; b) L. S. Schulman, *J. Theor. Biol.* **2017**, *417*, 61–67.
- [26] a) A. Hamad, K. S. Khashan, A. Hadi, *J. Inorg. Organomet. Polym. Mater.* **2020**, *30*, 4811–4828; b) R. Y. Pelgrift, A. J. Friedman, *Adv. Drug Delivery Rev.* **2013**, *65*, 1803–1815.
- [27] a) P. Asharani, W. Lian, *Nanotechnology* **2008**, *19*, 255102; b) J. H. Sung, J. H. Ji, J. U. Yoon, D. S. Kim, M. Y. Song, J. Jeong, B. S. Han, J. H. Han, Y. H. Chung, J. Kim, *Inhalation Toxicol.* **2008**, *20*, 567–574; c) Y. S. Kim, J. S. Kim, H. S. Cho, D. S. Rha, J. M. Kim, J. D. Park, B. S. Choi, R. Lim, H. K. Chang, Y. H. Chung, *Inhalation Toxicol.* **2008**, *20*, 575–583.
- [28] a) M. L. Knetsch, L. H. Koole, *Polymer* **2011**, *3*, 340–366; b) H. H. Lara, N. V. Ayala-Núñez, L. d. C. I. Turrent, C. R. Padilla, *World J. Microbiol. Biotechnol.* **2010**, *26*, 615–621.
- [29] K. Blecher, A. Nasir, A. Friedman, *Virulence* **2011**, *2*, 395–401.
- [30] J. G. Leid, A. J. Ditto, A. Knapp, P. N. Shah, B. D. Wright, R. Blust, L. Christensen, C. Clemons, J. Wilber, G. W. Young, *J. Antimicrob. Chemother.* **2012**, *67*, 138–148.
- [31] D. McShan, P. C. Ray, H. Yu, *J. Food Drug Anal.* **2014**, *22*, 116–127.
- [32] W. U. J. W. Supply, S. M. for World Health Organization & United Nations Children's Fund (UNICEF). Report: "Progress on drinking water and sanitation": **2014**.
- [33] G. E. Mena, P. P. Martinez, A. S. Mahmud, P. A. Marquet, C. O. Buckee, M. Santillana, *Science* **2021**, *372*, 6545.
- [34] S. Fujiyoshi, D. Tanaka, F. Maruyama, *Front. Microbiol.* **2017**, *8*, 2336.
- [35] W. Hiwar, M. F. King, F. Shuweihdi, L. A. Fletcher, S. J. Dancer, C. J. Noakes, *Indoor Air* **2021**, *31*, 1308–1322.
- [36] a) S. P. Deshmukh, S. Patil, S. Mullani, S. Delekar, *Mater. Sci. Eng. C* **2019**, *97*, 954–965; b) A. Ali, M. Pan, T. B. Tilly, M. Zia, C. Y. Wu, *Air Qual. Atmos. Health* **2018**, *11*, 1233–1242; c) C. Pokhum, V. Intasanta, W. Yaipimai, N. Subjalearndee, C. Srisithirathkul, V. Pongsorarith, N. Phanomkate, C. Chawengkijwanich, *Atmospheric Pollut. Res.* **2018**, *9*, 172–177.
- [37] S. Medici, M. Peana, V. M. Nurchi, M. A. Zoroddu, *J. Med. Chem.* **2019**, *62*, 5923–5943.
- [38] A. Haider, I.-K. Kang, *Adv. Mater. Sci. Eng.* **2015**, *11*, 8, 1165–1188.
- [39] J. Cui, Y. Yang, Y. Hu, F. Li, *J. Colloid Interface Sci.* **2015**, *455*, 117–124.
- [40] R. Shamsudin, M. H. Ng, A. Ahmad, M. A. M. Akbar, Z. Rashidbenam, *Ceram. Int.* **2018**, *44*, 11381–11389.
- [41] M. C. Biswas, B. J. Tiimob, W. Abdela, S. Jeelani, V. K. Rangari, *Food Packag. Shelf Life* **2019**, *19*, 104–113.
- [42] F. Unglaube, C. R. Kreyenschulte, E. Mejía, *ChemCatChem* **2021**, *13*, 2583–2591.
- [43] H. Chen, W. Wang, J. C. Martin, A. J. Oliphant, P. A. Doerr, J. F. Xu, K. M. DeBora, C. Chen, L. Sun, *ACS Sustainable Chem. Eng.* **2013**, *1*, 254–259.
- [44] B. J. Saikia, G. Parthasarathy, N. Sarmah, *Bull. Mater. Sci.* **2008**, *31*, 775–779.
- [45] S. Hu, Y.-L. Hsieh, *ACS Sustainable Chem. Eng.* **2014**, *2*, 726–734.
- [46] A. Alshareef, K. Laird, R. Cross, *Appl. Surf. Sci.* **2017**, *424*, 310–315.
- [47] a) T. Khan, A. Yasmin, H. E. Townley, *Colloids Surf. B* **2020**, *194*, 111156; b) K.-J. Kim, W. S. Sung, B. K. Suh, S.-K. Moon, J.-S. Choi, J. G. Kim, D. G. Lee, *BioMetals* **2009**, *22*, 235–242; c) H.-J. Park, S. Park, J. Roh, S. Kim, K.

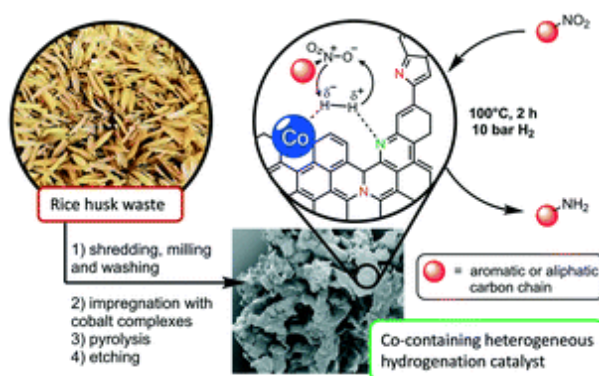
- Choi, J. Yi, Y. Kim, J. Yoon, *Ind. Eng. Chem. Res.* **2013**, *19*, 614–619; d) G. Rahimi, F. Alizadeh, A. Khodavandi, *Trop. J. Pharm. Res.* **2016**, *15*, 371–375; e) M. Y. Vaidya, A. J. McBaln, J. A. Butler, C. E. Banks, K. A. Whitehead, *Sci. Rep.* **2017**, *7*, 1–9.
- [48] M. Salouti, F. Mirzaei, R. Shapouri, A. Ahangari, *Jundishapur J. Microbiol.* **2016**, *9*.
- [49] U. Farooq, T. Ahmad, A. Khan, R. Sarwar, J. Shafiq, Y. Raza, A. Ahmed, S. Ullah, N. U. Rehman, A. Al-Harrasi, *Int. J. Nanomed.* **2019**, *14*, 3983.
- [50] D. G. Romero-Urbina, H. H. Lara, J. J. Velázquez-Salazar, M. J. Arellano-Jiménez, E. Larios, A. Srinivasan, J. L. Lopez-Ribot, M. J. Yacamán, *Beilstein J. Nanotechnol.* **2015**, *6*, 2396–2405.
- [51] L. Huang, T. Dai, Y. Xuan, G. P. Tegos, M. R. Hamblin, *Antimicrob. Agents Chemother.* **2011**, *55*, 3432–3438.

Manuscript received: October 21, 2021  
Revised manuscript received: November 24, 2021

## Highly Active Heterogeneous Hydrogenation Catalysts Prepared from Cobalt Complexes and Rice Husk Waste

F. Unglaube, J. Schlapp, A. Quade, J. Schafer and E. Mejia. *Catalysis Science & Technology* (2022) 12, 3123-3136

DOI: 10.1039/D2CY00005A



**Abstract:** The utilization and valorization of agricultural waste is a key strategy for the implementation of a sustainable economy to lessen the environmental footprint of human activities on Earth. This work describes the use of rice husk (RH) from agricultural waste to prepare a highly active catalyst for the reduction of nitro compounds. RH was impregnated with various cobalt complexes bearing N-donor ligands, then pyrolyzed and the resulting composite was etched with a base to remove the silica domains. The composition and morphology of the prepared materials were investigated by IR, AAS, ICP-OES, XRD, BET, XPS and SEM technics. The material showed excellent activity and selectivity in the hydrogenation of nitro groups in aromatic and aliphatic substrates. A remarkable selectivity towards nitro groups was found in the presence of various reactive functionalities, including halogens, carbonyls, borates, and nitriles. Apart from their excellent activity and selectivity, these catalysts showed remarkable stability, allowing their easy recovery and multiple reuse without requiring re-activation.

Cite this: *Catal. Sci. Technol.*, 2022, 12, 3123Received 3rd January 2022,  
Accepted 3rd February 2022

DOI: 10.1039/d2cy00005a

rsc.li/catalysis

# Highly active heterogeneous hydrogenation catalysts prepared from cobalt complexes and rice husk waste†

Felix Unglaube,<sup>a</sup> Janina Schlapp,<sup>a</sup> Antje Quade,<sup>b</sup>  
Jan Schäfer<sup>b</sup> and Esteban Mejía<sup>✉\*</sup>

The utilization and valorization of agricultural waste is a key strategy for the implementation of a sustainable economy to lessen the environmental footprint of human activities on Earth. This work describes the use of rice husk (RH) from agricultural waste to prepare a highly active catalyst for the reduction of nitro compounds. RH was impregnated with various cobalt complexes bearing N-donor ligands, then pyrolyzed and the resulting composite was etched with a base to remove the silica domains. The composition and morphology of the prepared materials were investigated by IR, AAS, ICP-OES, XRD, BET, XPS and SEM techniques. The material showed excellent activity and selectivity in the hydrogenation of nitro groups in aromatic and aliphatic substrates. A remarkable selectivity towards nitro groups was found in the presence of various reactive functionalities, including halogens, carbonyls, borates, and nitriles. Apart from their excellent activity and selectivity, these catalysts showed remarkable stability, allowing their easy recovery and multiple reuse without requiring re-activation.

## Introduction

The sustainable development goals (SDGs), set by the UN general assembly in 2015, are referred to as “blueprints to achieve a [...] more sustainable future”.<sup>1</sup> Overall the SDGs comprise 17 objectives which are supposed to be achieved by 2030 to improve the quality of human cohabitation and sustain the Earth as habitat for humans. The utilization of agricultural waste can meet many of the SDGs by promoting sustainable agriculture (SDG 2), economic growth (SDG 8), and industrialization (SDG 9), as well as by improving production patterns (SDG 12) and reducing the emission of atmospheric pollutants (SDG 13).<sup>2,3</sup> In this context, utilization can mean recirculation of inedible by-products of agricultural processes, including the use of bio-waste as fodder for livestock,<sup>4</sup> or for the production of fertilizers.<sup>5,6</sup> Utilization can also mean the use of waste in non-related economic sectors, which had caught much attention due to the broad palette of agricultural wastes and their growing amount worldwide.<sup>7</sup> For instance, “energy-dense” wastes like manure

are suitable for the production of bio fuels,<sup>8</sup> (importantly bio gas), contributing to the energy and transport sector.<sup>9,10</sup> Fibrous plant bio-waste like straw or bagasse can be used in the production of much needed materials like concrete,<sup>11</sup> or filters for water purification.<sup>12</sup> The synthesis of more advanced materials like supercapacitors,<sup>13,14</sup> fluorescent carbon nanotubes,<sup>15</sup> or catalysts has been part of research efforts as well, alas, to a lesser extent.

The preparation of catalysts from bio-waste has proven to be a promising approach thanks to the diversity offered by bio-waste in terms of structure and composition.<sup>16</sup> Recent examples include the use of catalysts made from banana peels,<sup>17</sup> or oyster shells,<sup>18</sup> for transesterification reactions, or the use of heterogeneous catalysts from rice husk (RH) for the epoxidation of limonene,<sup>19</sup> and the reduction of nitro groups.<sup>20</sup>

Hydrogenation reactions are among the most important catalytic transformations in the chemical industry, as illustrated by the widely applied reduction of nitro compounds to amines. This reaction is a key transformation in the industrial-scale production of amines,<sup>21,22</sup> as well as in the synthesis of active pharmaceutical ingredients like the widely used paracetamol.<sup>23</sup> The most popular systems used to catalyze this transformation are metal-based, including Ni-RANEY®,<sup>24</sup> NiS,<sup>25</sup> Pd and Pt (Adams’ catalyst),<sup>26</sup> Cu–Mn–Fe or Cu@SiO<sub>2</sub>.<sup>27</sup> These catalysts, as applied on an industrial scale, normally require harsh reaction conditions (e.g. temperatures above 200 °C), except for Pd–Pt alloys. However, high temperatures are not tolerated by most functionalized

<sup>a</sup> Leibniz-Institut für Katalyse e. V. an der Universität Rostock, Albert-Einstein-Straße 29a, 18059 Rostock, Germany. E-mail: Esteban.Mejia@catalysis.de

<sup>b</sup> Leibniz-Institut für Plasmaforschung und Technologie e.V., Felix-Hausdorff-Str. 2, 17489 Greifswald, Germany

† Electronic supplementary information (ESI) available. See DOI: 10.1039/d2cy00005a





## Paper

## Catalysis Science &amp; Technology

organic substrates and highly active systems suffer from insufficient selectivity towards amines. Among the few exceptions are the cobalt<sup>28</sup> and nickel<sup>29</sup> based systems reported independently by the groups of Zou and Beller, which display excellent activities even at room temperature.

It is possible to modify catalysts with either Fe or VO(acac)<sub>3</sub> to improve the tolerance towards sensitive moieties like alkenes, alkynes, nitriles or carbonyl functions.<sup>30</sup> However, most systems are able to catalyze to some extent undesired side reactions like dearomatization or reductive dehalogenation. The latter is especially problematic since relevant substrates are often bearing halogens. The use of 3d non-noble metals as catalysts has become more prevalent in the last decade since they are able to overcome selectivity issues, and being fairly abundant in the Earth crust, their mining has less environmental impact.<sup>31</sup>

During the last decade, cobalt has played an important role in the development of heterogeneous catalysts for amine synthesis *via* hydrogenation with 3d-metal catalysts (Scheme 1), even though the first catalytic system was published already in 1937 by Griffiths and Brown using CoS.<sup>32</sup> Almost 80 years later, Beller *et al.* reported a significant improvement in the catalytic performance by supporting cobalt on a SiO<sub>2</sub> carrier with the aid of nitrogen-donor ligands. They described the formation of coordinative interactions between cobalt species and nitrogen at the support's surface, allowing an easier activation of hydrogen.<sup>33</sup>

Based on this approach, Gascon *et al.* reported in 2018 a system containing Co<sub>3</sub>O<sub>4</sub> improved by etching with HF, leaching the silica domains, which leads to higher surface area and more active sites.<sup>34</sup>

Further improvements have been made to these Co-based catalytic systems, especially regarding the reaction conditions for the hydrogenation of nitro aromatics, as recently reported by the group of Palkovits, among others.<sup>35–37</sup> Furthermore, a number of studies have shown the feasibility of other reduction reactions using heterogeneous cobalt catalysts, including reductive amination of carbonyl compounds,<sup>38</sup> and the reduction of O<sub>2</sub> to H<sub>2</sub>O<sub>2</sub>.<sup>39</sup>

The vast majority of these processes are carried out with catalysts containing highly sophisticated supporting materials which require laborious and energy-intensive synthetic procedures. Thus, the use of inexpensive bio-waste as a feedstock for the catalyst preparation (as showcased above) offers an appealing alternative, not only in economic terms, but also due to its intrinsic sustainability. However, the direct impregnation of a bio-derived feedstock with cobalt precursors for the synthesis of catalytically active materials has been rarely reported. In 2017, Beller *et al.* reported the preparation of a Co-based catalyst using chitosan, and its use in hydrodehalogenation reactions,<sup>40</sup> and hydrogenation of nitroarenes (40 bar H<sub>2</sub> and 110 °C).<sup>41</sup> Additionally, in 2018 Yang *et al.* prepared a catalyst by impregnation of bamboo with CoCl<sub>2</sub> for hydrogenation reactions (at 110 °C and 50 bar H<sub>2</sub>).<sup>42</sup>

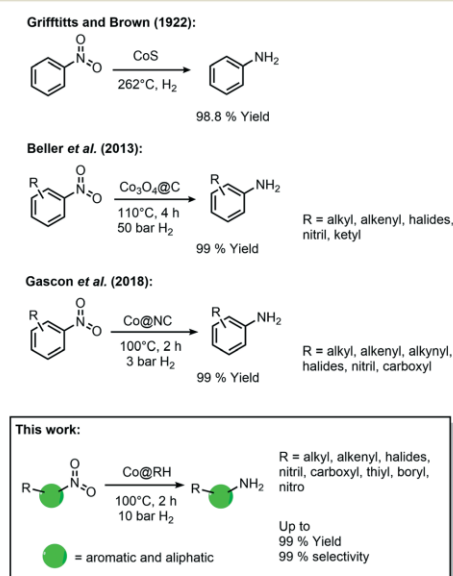
Rice husk (RH) is, besides rice straw, the main by-product of rice production, and is considered to be one of the most abundant agricultural waste on earth, with over 40 million tons produced in 2015 in China alone.<sup>43</sup> Its unique structure is made up of a lignocellulose matrix decorated with silica nanoparticles (up to 20 wt% silica) and, unlike other bio-derived feedstocks like chitosan, RH does not need to be isolated or purified in a complicated manner for its utilization.

Herein, we report the use of RH as a feedstock for the preparation of cobalt-containing materials with remarkable activities as a catalyst in hydrogenation reactions. Our synthetic approach consists of a) impregnating the milled plant material (RH) with cobalt complexes bearing N-donor ligands, b) thermal treatment to generate catalytic active cobalt centers on the surface of the biogenic waste, and c) leaching of the silica domains by base etching, increasing the material's porosity and surface area, boosting the catalytic performance (Fig. 1). We demonstrate that our catalyst outperforms other "classic" and bio-derived catalysts, not only in terms of general activity under milder conditions, but also in other relevant aspects like reaction rate, recycling stability, and substrate scope including the commonly neglected aliphatic substrates.

## Results and discussion

### Catalyst preparation and characterization

The crude, sun-dried rice husk (RH) is first chopped into small particles and ground in a ball mill to increase the



**Scheme 1** Historical development of cobalt-catalyzed synthesis of amines by hydrogenation of nitro compounds.

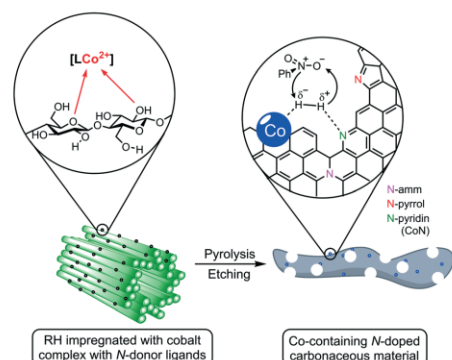


Fig. 1 Schematic representation of the surface structure and coordinative interactions in rice husk (RH) and its conversion into a hydrogenation catalyst containing cobalt species on a porous, N-doped, carbonaceous support. For a detailed description see the text below.

accessible surface area. Subsequently, the material was washed with water and added to an ethanolic solution of an *in situ* prepared cobalt complex bearing nitrogen-donor ligands (Scheme 2).<sup>44–47</sup> After removing the solvent *in vacuo*, the dried material was pyrolyzed at 600 °C under an inert atmosphere. Finally, the resulting ashes were etched with a base. To understand the changes underwent by the RH during this process, the surface after each step was analyzed using X-ray and microscopy techniques (see below and in the ESI†). XPS revealed that the surface of crude RH offers mainly  $sp^3$  hybridized carbon in C–C bonds with a high content of C–O bonds (Fig. 2), in accordance with the expected composition of RH being cellulose and lignocellulose.

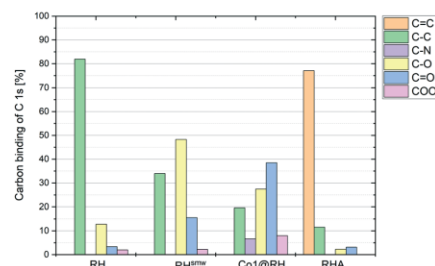
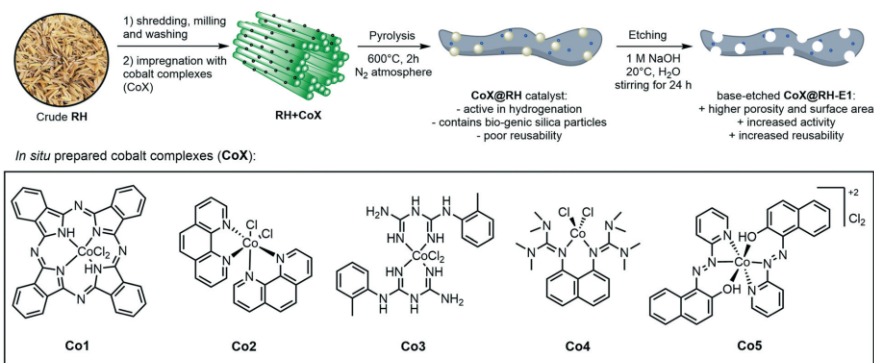


Fig. 2 Carbon bonds in the different stages of catalyst processing, measured by XPS.

After shredding, milling and washing (RH<sup>RMW</sup> in Fig. 2) the amount of C–C bonds on the surface is decreased from 82% to 34% and the amount of oxidized carbon (C–O and C=O in Fig. 2) increased significantly. This is most likely caused aerobic oxidation promoted by the kinetic energy supplied by the ball mill. Next, the ground RH was impregnated with cobalt complexes of five different N-containing ligands (Co1–5, Scheme 2). All the employed cobalt complexes are chelates containing multi-dentate N-donor ligands. However, they differ in the Co:N ratio (from 1:4 to 1:10) and can be distinguished by the “chemical nature” of the N atoms: Co1–2 are aromatic and Co3–4 are non-aromatic, while Co5 is the only complex containing oxygen. After the impregnation with Co1–5 in alcoholic solution the amount of oxygenated carbon increased and new C–N bonds appear, as expected. Not surprisingly, the major change on the surface was observed after the pyrolysis process. Nearly all of the oxygenated carbons, as well as the  $sp^3$  hybridized carbons were converted



## Paper

## Catalysis Science &amp; Technology

into  $sp^2$  hybridized carbons. This suggests a transformation of the hydrocarbon network (mainly composed of cellulose) to a surface mainly composed of graphene, barely decorated with oxygenated groups.

This thermal transformation of homopolysaccharides has been qualitatively described before for RH (Tulliani *et al.*),<sup>48</sup> and for chitosan (Beller *et al.*).<sup>40</sup>

Optical and electronic microscopy studies (SEM, Fig. S1†) of crude RH have been thoroughly reported.<sup>43,49,50</sup> The fibrous RH epidermis is characterized by the presence of small particles of silica (red arrow Fig. 3A). These features are not observable after mechanical treatment (chopping and milling) and impregnation, after which the material only shows vestiges of fibrous domains (yellow box Fig. 3B) along with smooth and crystalline bodies (red arrow in Fig. 3B), most likely corresponding to Co1-5 complexes deposited on the ground RH epidermis.

The use of HF as an etching agent for the removal of  $SiO_2$  from cobalt catalysts supported on silica/carbon composites has shown to boost its catalytic performance.<sup>51,52</sup> However, the toxicity and safety concerns inherent in the use of HF discouraged us to use it for the treatment of our catalysts.

Instead, we decided to subject our materials to simple etching with NaOH 1 M. As expected, the silicon content in all prepared catalysts, regardless of the ligand used, is markedly reduced if the material is etched with an aqueous hydroxide base. The use of higher concentrations of NaOH further reduces the silica content but only to a limited extent; the use of 1 M NaOH decreases the Si in Co1@RH from 11.77 wt% to 3.02 wt% while the use of 2 or 4 M NaOH solution yields lower Si contents of 2.07 wt% and 1.46 wt%, respectively (Table S1†). The same trend is observed for the specific surface area of the samples: base etching of Co1@RH with 1 M NaOH increases its surface area from 323.63  $m^2 g^{-1}$

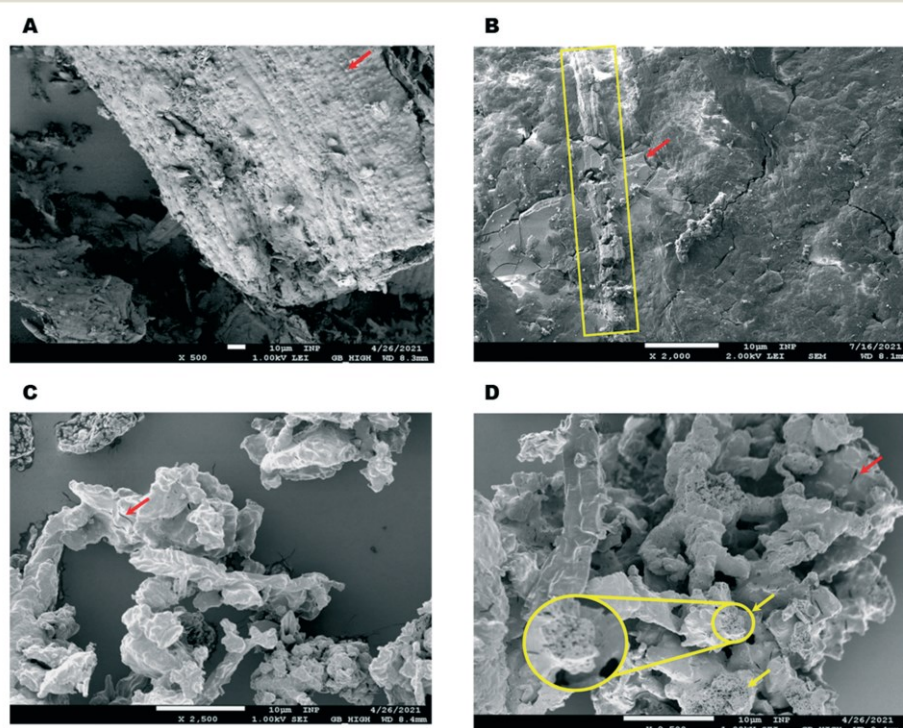


Fig. 3 SEM pictures of the different stages of catalyst preparation. (A) Milled and ground RH. The red arrow indicates silica nanoparticles on the plant epidermis. (B) Material after impregnation with an ethanolic solution of complex Co1. The yellow box highlights the presence of residual fibrous domains. The red arrow shows the deposited metal complex. (C) Material after pyrolysis at 600 °C under nitrogen. The red arrow shows small crevices at the surface. (D) Final product after etching with a base. The red arrow shows small crevices at the surface. The yellow arrows and the zoomed circled area highlight the new, highly porous pumice-like structure.





to 347.13 m<sup>2</sup> g<sup>-1</sup> (Co1@RH-E1), while the material treated with 4 M NaOH (Co1@RH-E4) displays a much higher surface area of 427.87 m<sup>2</sup> g<sup>-1</sup> (Co1@RH-E4, Table S2†).

Pyrolysis leads to a further significant change in morphology, resulting in irregular aggregates of smaller particles without any defined shape and brittle appearance (Fig. 3C). Interestingly, after removing the silica domains by base etching the morphology does not change greatly; the particles show a similar shape, but the etched material is clearly more porous (Fig. 3D). While a number of crevices are visible at both non-etched and the etched materials (red arrows Fig. 3C and D), a pumice-like structure is clearly present in the etched sample (yellow arrows and zoomed circled area in Fig. 3D). This change in porosity is clearly reflected in the surface measurements (Table S2†). Upon etching, the cumulative pore volume (of pores between 2 and 100 nm width) is doubled, increasing from 0.11 cm<sup>3</sup> g<sup>-1</sup> (for Co1@RH) to 0.27 cm<sup>3</sup> g<sup>-1</sup> (Co1@RH-E1). The main increase in pore volume is associated with a pore width of 1.1 to 1.4 nm and 2.7 to 3.4 nm for etching with 1 M NaOH (Fig. S44 and S46†). Interestingly, for etching with 4 M NaOH a drastic increase in pore volume is also visible from 4 to 15 nm pore width (Fig. S48†).

Importantly, the cobalt content at the catalysts' surface did not change significantly after the etching processes, as determined by ICP-OES (Table S1†). The nature of the crystalline phases in different samples was investigated by XRD (Fig. 4): in Co1@RH, a freshly etched sample without washing the sample to remove the excess base (Co1@RH-E1.fresh) and a washed sample like the one used in catalytic experiments (Co1@RH-E1.washed). The diffraction patterns showed broad reflections from 16 to 30° correlating with amorphous silica and a small peak at 26.6° from hexagonal SiO<sub>2</sub>.<sup>20</sup> The main cobalt phases in both Co1@RH and Co1@RH-E1.washed are cubic Co and cubic CoO (σ and \*, respectively). The CoO phase disappears after the etching while the main phase of cubic Co remains and three additional reflections appear: rhombohedral NaOH, which is the

remaining base from the etching, hexagonal Teflon (impurity from the preparation) and rhombohedral CoO(OH) (ψ).

The appearance of Co(III) is in line with the known facile oxidation of Co(II) at high pH values,<sup>53</sup> resulting in the oxidation of CoO to CoO(OH) during base etching. The fact that Co(0) remains unchanged during the etching procedure suggest that a Co core covered by a CoO layer is formed. This core-layer structure has been observed in other catalytically active cobalt particles.<sup>54</sup>

To better understand the nature of nitrogen atoms at the material surface and their role in the catalytic activity, their surface was investigated using XPS (for details, see section 1 in the ESI†). The validity and usefulness of this approach has been demonstrated in previous studies.<sup>41,54,55</sup> Co1@RH shows a significantly higher share of cobalt–nitrogen (CoN) bonding (67%) compared to Co2@RH (52%) while the share of N-pyrrol and N-amm bonding (see Fig. 1 and 4) is significantly lower (Fig. 5). The etched material shows a very similar bonding distribution compared to the untreated material for both Co2@RH-E1 with CoN (51%), N-pyrrol (38%) and N-amm (11%) and for Co1@RH-E1 with CoN (66%), N-pyrrol (24%) and N-amm (9%). The use of a base of higher concentration (4 M) does not change the bonding situation. Interestingly, the nitrogen to cobalt ratio (N/Co) differs significantly from the trends found in the nitrogen bonding distribution. The ratio increases from 1.5 for Co2@RH to 3.8 for Co2@RH-E1, while drops drastically in the series Co1@RH (5.1), Co1@RH-E1 (2.7) and Co1@RH-E4 (1.3) (Fig. S13†). An inverted but analogous trend is visible in the oxygen to carbon ratio (O/C) which is higher for Co2@RH (2.6) than for Co2@RH-E1 (7.1) and increasing in the series Co1@RH (6.5), Co1@RH-E1 (9.5), and Co1@RH-E4 (15.3) (Fig. S14†).

#### Catalytic hydrogenation of nitro compounds

The hydrogenation of nitrobenzene to aniline was chosen as a model reaction to test and optimize the catalytic activity of

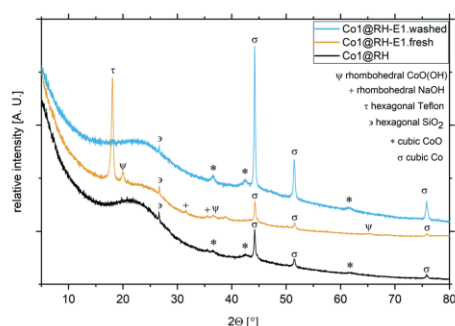


Fig. 4 XRD patterns and different crystalline phases from cobalt catalysts at different preparation stages. Co1@RH (black), Co1@RH-E1.fresh (yellow) and Co1@RH-E1.washed (blue).

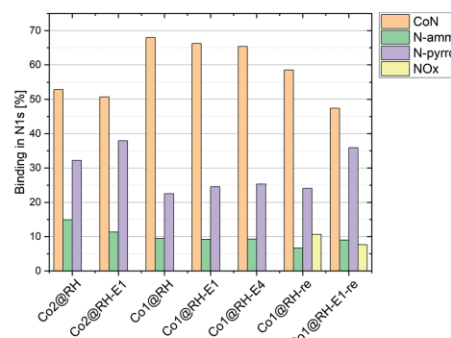
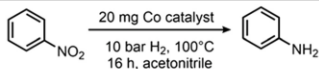


Fig. 5 Nitrogen bonding measured by XPS in different catalysts at different stages; "re" stands for "recycled".



**Table 1** Catalytic activity for the hydrogenation of nitrobenzene for the different cobalt-based catalysts prepared from RH using different ligands before and after etching with NaOH

		
Catalyst	$c(\text{NaOH})^a$ [mol L <sup>-1</sup> ]	Yield of aniline <sup>b</sup> [%]
Co@RH	—	5
Co1@RH	—	39
Co1@RH-E1	1	83
Co1@RH-E2	2	83
Co1@RH-E4	4	85
Co2@RH	—	22
Co2@RH-E1	1	38
Co3@RH	—	16
Co3@RH-E1	1	29
Co4@RH	—	12
Co4@RH-E1	1	16
Co5@RH	—	1.3
Co5@RH-E1	1	1.3

Reaction conditions: 10 bar H<sub>2</sub>, 100 °C, 16 h, in acetonitrile (1 ml) and 20 mg catalyst. <sup>a</sup> Base concentration used for etching. <sup>b</sup> Yield was determined by GC using *n*-octane as an internal standard.

all prepared materials (Table 1). The use of catalysts prepared in the absence of N-donor ligands (Co@RH) leads to lower catalytic activity compared to those catalysts made using cobalt complexes of N-donor ligands Co1–5 (Table 2). Co1@RH showed the best performance with 39% yield of aniline, followed by Co2@RH (22%), Co3@RH (16%), Co4@RH (12%) and Co5@RH (1.2%). It is noteworthy that the best results were obtained with catalysts prepared from complexes containing aromatic N-heterocycles without oxygen (Co1–3). The significant reduction of yield using Co5, the only oxygen-bearing ligand, is in marked contrast with recent data reported by Beller *et al.* who used cobalt–salen

complexes to generate catalytically active Co nanoparticles.<sup>56</sup> Moreover, cobalt phthalocyanines (like in Co1) are known to form active reduction catalysts after pyrolysis.<sup>57–60</sup> Thus, the high activity of Co1@RH is in line with this precedent.

The surface area is another parameter which must be considered when comparing the catalytic activity of the prepared materials (Table S2†). While the micropore and BET surface area are within a similar range for all catalysts, there are differences in the cumulative pore volume. Therefore, Co1@RH-E1, the most active catalyst, shows the highest macropore volume (0.27 cm<sup>3</sup> g<sup>-1</sup>), while all other catalysts have similar macropore volumes. Additionally, Co1@RH-E4,

**Table 2** Screening of reaction conditions for the hydrogenation of nitrobenzene using Co1@RH (with and without base pre-treatment) as a catalyst

Catalyst	$T$ [°C]	$p\text{H}_2$ [bar]	Solvent <sup>a</sup>	Base additive	Yield of aniline <sup>b</sup> [%]
Co1@RH-E1	120	10	Heptane	—	56
Co1@RH-E1	120	10	Ethanol	—	65
Co1@RH-E1	120	10	H <sub>2</sub> O	—	86
Co1@RH-E1	120	10	Ethanol/H <sub>2</sub> O	—	97
Co1@RH-E1	120	10	<i>i</i> -PrOH/H <sub>2</sub> O	—	99
Co1@RH	120	10	<i>i</i> -PrOH/H <sub>2</sub> O	—	89
Co1@RH-E1	120	5	<i>i</i> -PrOH/H <sub>2</sub> O	—	43
Co1@RH	120	5	<i>i</i> -PrOH/H <sub>2</sub> O	—	19
Co1@RH-E1	90	10	<i>i</i> -PrOH/H <sub>2</sub> O	—	85
Co1@RH-E1	100	10	<i>i</i> -PrOH/H <sub>2</sub> O	—	92
Co1@RH	100	10	<i>i</i> -PrOH/H <sub>2</sub> O	—	27
Co1@RH-E1	110	10	<i>i</i> -PrOH/H <sub>2</sub> O	—	95
Co1@RH	110	10	<i>i</i> -PrOH/H <sub>2</sub> O	—	43
Co1@RH-E1	130	10	<i>i</i> -PrOH/H <sub>2</sub> O	—	96
Co1@RH-E1	120	10	<i>i</i> -PrOH/H <sub>2</sub> O	Pyridine	87
Co1@RH	120	10	<i>i</i> -PrOH/H <sub>2</sub> O	Pyridine	84
Co1@RH-E1	120	10	<i>i</i> -PrOH/H <sub>2</sub> O	NaOH	89
Co1@RH-E1	120	10	<i>i</i> -PrOH/H <sub>2</sub> O	NEt <sub>3</sub>	83
Co1@RH-E1	120	10	<i>i</i> -PrOH/H <sub>2</sub> O	NaCO <sub>3</sub>	71
Co1@RH	120	10	<i>i</i> -PrOH/H <sub>2</sub> O	NaCO <sub>3</sub>	50

<sup>a</sup> *i*-PrOH/H<sub>2</sub>O have been used in an equal volume ratio. <sup>b</sup> Yield of aniline was determined by GC using *n*-octane as an internal standard.



which has the highest surface area ( $428 \text{ m}^2 \text{ g}^{-1}$ ) but a similar macropore volume ( $0.25 \text{ cm}^3 \text{ g}^{-1}$ ), shows no significant increase in catalytic activity.

A screening of the pyrolysis temperature for the preparation of **Co1@RH** revealed that the material prepared at  $600^\circ\text{C}$  was the most active in nitrobenzene conversion. Significantly lower yields were achieved using the catalyst prepared at  $500$ ,  $700$ ,  $800$  or  $900^\circ\text{C}$ , respectively (Fig. S58†).

When RH is used as a feedstock for the synthesis of silica, silicon, carbon or their composites, it is common practice to wash the raw plant material with an aqueous acid to remove eventual traces of heavy metals.<sup>61</sup> In our case, we observed that an acidic washing of the RH prior to impregnation does not improve the catalytic activity. Thus, skipping the acidic pre-treatment altogether, we could avoid the generation of approximately 30 liters of acidic wastewater per kg of catalyst produced.

The reaction conditions have been optimized for the nitrobenzene conversion to aniline using **Co1@RH** and **Co1@RH-E1** to determine the differences of both catalysts resulting from base etching. The screening revealed that the etched catalyst outperformed the untreated material in every case. For instance, assessment of the optimal catalyst loading showed that **Co1@RH-E1** achieved quantitative yields of aniline with only 20 mg of catalyst (corresponding to 1.8

mol% cobalt) while 41 mg of **Co1@RH** (corresponding to 4 mol% cobalt) was required (Fig. S60†). A similar trend was observed in the pressure screening, with full yield at 10 bar  $\text{H}_2$  using **Co1@RH-E1** and 20 bar  $\text{H}_2$  pressure using **Co1@RH**. The temperature screening showed a maximum performance at  $120^\circ\text{C}$ , while at  $130^\circ\text{C}$  the yield decreased, most likely caused by the lower hydrogen solubility at higher temperatures (Fig. S63†). The use of polar protic solvents has shown to give the highest yields, a water and isopropanol 1 : 1 mixture being the one with the best results (Fig. S59†).<sup>62,63</sup>

Since previous studies have shown that the addition of bases has a positive effect on the hydrogenation of nitro groups (by promoting the deprotonation of azoxy intermediates),<sup>64</sup> we performed a small base screening in our model reaction (Fig. S62†). Surprisingly, the addition of bases to our system (whether organic or inorganic) appears to be detrimental (Table 2), a phenomenon which we observed in other RH-based systems before.<sup>20</sup>

When comparing the catalytic performance of the prepared materials with literature reports, they have shown to be better than, or at least comparable with most reported catalysts.<sup>64,65</sup> Some superior systems include those developed by the teams of Palkovits and Beller, operating at  $40^\circ\text{C}$ ,<sup>36</sup> and those by Zou and co-workers, which are very active even at room temperature.<sup>28</sup>

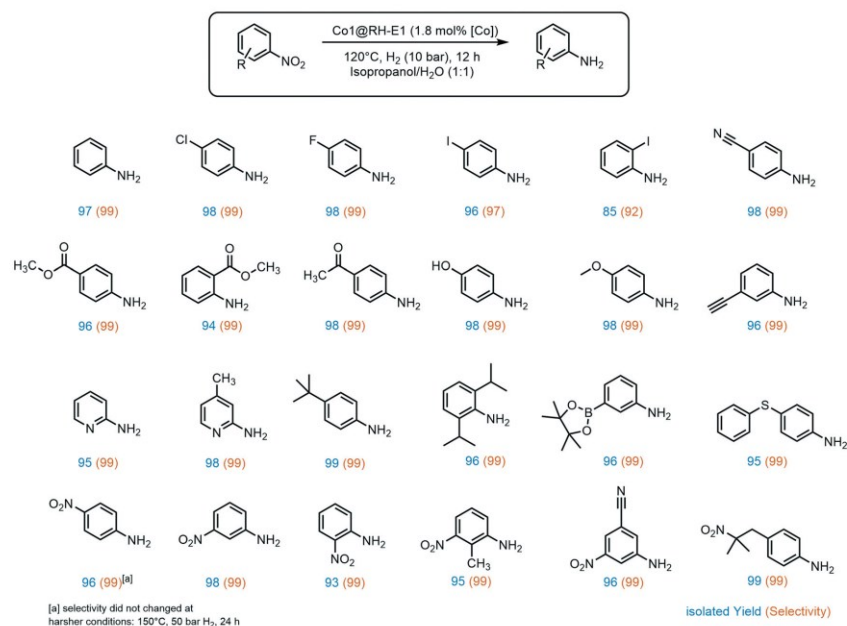


**Fig. 6** Products of the hydrogenation of aromatic nitro compounds using **Co1@RH-E1**. Reaction conditions:  $120^\circ\text{C}$ , 10 bar  $\text{H}_2$ , 1 mmol substrate, 12 h, in 1 ml of isopropanol/ $\text{H}_2\text{O}$ , 20 mg catalyst (1.8 mol% of Co).



## Paper

## Catalysis Science &amp; Technology

A broad substrate screening was done to determine the extent and limits of the prepared hydrogenation catalyst. A series of aromatic nitro compounds were tested, obtaining in almost all cases quantitative yields and 99% selectivity towards the reduction of the nitro group (Fig. 6). The catalysis has shown to be highly chemoselective, reducing only the nitro groups even in the presence of other potentially reactive groups, including nitriles, ketones, aldehydes and alkynes. The inertness of our system towards nitrile groups came as a surprise, since very similar cobalt based systems are known to be excellent catalyst for the hydrogenation of these functionalities.<sup>54</sup> Importantly, halogen-containing substrates are also well tolerated; *i.e.* the high yield of 4-iodoaniline (96%) suggests that dehalogenation of the nitro-precursor hardly takes place, which is a well-known side reaction in the hydrogenation of iodine-containing compounds with highly active catalysts.<sup>40,66</sup> Moreover, sterically demanding groups in the *ortho* position to the nitro group lead to slightly decreased yields, as observed for methyl-4-aminobenzoate (96% yield) *versus* methyl-2-aminobenzoate (94% yield). Additionally, the lower yield of 85% of 2-iodoaniline is an indicator for the negative impact of good leaving groups in the *ortho* position on the reaction while aliphatic groups like isopropyl do not show a negative influence. Furthermore, the catalyst showed good tolerance to a variety of functional groups at the *meta* position to the nitro group, especially prone towards side reactions.<sup>67</sup> These include boron groups, which are highly relevant for coupling reactions.<sup>68–70</sup> Additionally, the catalyst is not poisoned by sulfur atoms in the substrate, which is a common problem in heterogeneous hydrogenation catalysis.<sup>71,72</sup>

A very interesting selectivity feature was observed during the substrate screening: if the molecule offered more than one nitro group, only one nitro moiety was reduced in all cases. To the best of our knowledge, the system presented here is the first cobalt-based catalytic system to display this type of selectivity. There are only a few examples of heterogeneous catalysts for selective hydrogenation of only one nitro group when two are present in the same molecule, and a number of them use NaBH<sub>4</sub> as a reducing agent.<sup>73–76</sup> There are only a few examples where hydrogen is used instead, and all of them rely on rare and expensive metals like ruthenium,<sup>77</sup> platinum–palladium alloy,<sup>78</sup> or gold.<sup>79,80</sup> Recently, our group developed a silver-based system also using rice husk ashes as a support, with the same selectivity.<sup>20</sup> Interestingly, all these systems, except the silver-based, exhibit apparent activity for kinetic product control. This does not seem to be the case for the RH based systems as no diamino species could be detected even with prolonged reaction time, higher pressure, and increased reaction temperature. However, to provide an explanation for this behavior, a comprehensive mechanistic investigation must be undertaken.

The above-mentioned trend of giving slightly lower yields when another substituent is present in the *ortho* position to

the nitro groups also holds for dinitro compounds, giving the lowest 1,2-dinitrobenzene yield among all three isomers (93%). Interestingly, aromatic nitro groups were preferably hydrogenated over aliphatic nitro groups, as demonstrated by the synthesis of 4-(2-methyl-2-nitropropyl)aniline.

To prove the versatility of Co1@RH-E1 as a hydrogenation catalyst, a range of aliphatic substrates was investigated (Fig. 7). It was shown that both small and polar as well as long-chain lipophilic substrates could be hydrogenated in almost complete yields. However, with increasing chain length, the yield decreased proportionally. The catalyst also showed good performance in the conversion of cyclic aliphatic nitro compounds into the corresponding amines, indicating that it is not a problem to hydrogenate the oxime-nitroso intermediate (stabilized by mesomerism), as previously observed.<sup>20</sup>

Furthermore, the applicability of the synthesized catalyst in late-stage drug modification was demonstrated (Fig. 7). Nimesulide,<sup>81</sup> which is used as a non-steroidal anti-inflammatory drug and selective cyclooxygenase-2 inhibitor,<sup>82</sup> was converted into the corresponding amine without

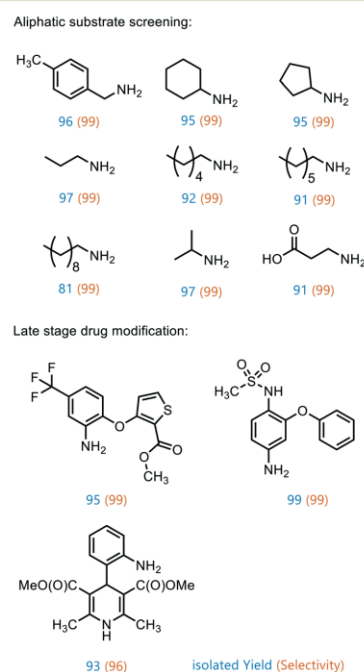


Fig. 7 Products of aliphatic substrate screening and late-stage drug modification using Co1@RH-E1. Reaction conditions: 120 °C, 10 bar H<sub>2</sub>, 1 mmol substrate, 12 h, in 1 ml of isopropanol/H<sub>2</sub>O, 20 mg catalyst (1.8 mol% of Co).





reducing the sensitive sulfone moiety in excellent yield. Moreover, the selective synthesis of 4-(2-methyl-2-nitropropyl) aniline was achieved in good yield (93%) and with excellent selectivity (96%), regardless of the redox sensitive dihydropyridine core. This has so far only been described using stoichiometric amounts of  $\text{Na}_2\text{S}$  in moderate yields of 70%.<sup>83</sup>

### Recycling experiments

A major advantage of heterogeneous catalytic systems over their homogeneous counterparts is the possibility of easy recycling. After reaction, the catalyst can be removed by simple filtration or centrifugation, or by action of a magnetic field if the material has a magnetic moment,<sup>84</sup> which is the case with the material presented here. Thus, the catalyst could be easily recovered from the reaction solution with a magnet.

Recycling experiments with the untreated (before etching) catalyst **Co1@RH** showed that a yield drops from nearly 100% down to 70% after five runs and stabilized at that level. However, the recycling stability of the base-etched catalyst **Co1@RH-E1** turned out to be superior to **Co1@RH**, as no decrease in activity was observed over 10 runs (Fig. 8). The better recycling stability of **Co1@RH-E1** was also indicated by the fact that the reaction solution after the separation of the catalyst was clear after every cycle, whereas the reaction solution obtained when **Co1@RH** was used was cloudy after a couple of cycles, suggesting a mechanical deterioration of the material. This is indeed visible in SEM measurements. The particle morphology changes drastically during the recycling process for both un-etched and etched materials (Fig. S9†). However, the type of change is very different; while particles of **Co1@RH** are fractured into smaller ones, around 1 to 10  $\mu\text{m}$ , the particle size of **Co1@RH-E1** after recycling is

considerably bigger, between 10 and 20  $\mu\text{m}$ . This suggests that the etched material has an enhanced mechanical stability, which contributes significantly to the higher recycling stability.

Perhaps correlated to the lower mechanical stability is the drastic increase of the oxygen-carbon ratio during the recycling of **Co1@RH**, which is higher than that of **Co1@RH-E1**, (Fig. S14†). Additionally, XPS revealed that the amount of CoN bonding is just slightly decreased from 67% to 58% in the un-etched material, compared to a stronger decrease of 66% to 47% in the etched catalyst. This suggests that the oxidation stability of the support is critical to the recycling stability of the material, while the amount of cobalt nitrogen bonding plays a lesser role. The general oxidation stability of the nitrogen species at the surface seems to be also of relevance since the amount of NOx bonding is slightly higher in the un-etched material with 11% compared to 7% in the etched material.

### Kinetic studies and reaction mechanism

Kinetic investigations on the hydrogenation of nitrobenzene revealed a zeroth order dependence with respect to the substrate at high concentrations for both **Co1@RH** and **Co1@RH-E1**. Previous kinetic studies interpreted similar results by applying the Langmuir-Hinshelwood model,<sup>85–87</sup> identifying the reaction of hydrogen and nitrobenzene at the catalyst surface as the rate determining step, and therefore the adsorption of all reaction partners on the catalyst surface as well.<sup>88</sup> For **Co1@RH-E1** and **Co1@RH**, initial reaction rates ( $r$ ) of 1938 and 290 [ $\text{mol}^{\text{aniline}}$  per  $\text{mol}^{\text{cobalt}}$  h], respectively, were calculated. This demonstrates the superiority of the base-etched catalyst over the untreated material. The initial rate calculated for **Co1@RH** is lower than for a  $\text{Pd-Al}_2\text{O}_3$  based system (473 [ $\text{mol}^{\text{aniline}}$  per  $\text{mol}^{\text{palladium}}$  h]) reported by Shi *et al.*,<sup>85</sup> which is in turn outperformed by **Co1@RH-E1**. An activation energy of  $28.0 \pm 1.1$  [ $\text{kJ mol}^{-1}$ ] for the reaction using the etched material was calculated based on the Arrhenius equation (Fig. S74†). This energy is lower than the 44.8 [ $\text{kJ mol}^{-1}$ ] determined for the highly active etched cobalt-based system by Zhou *et al.*<sup>52</sup> and the 67.2 [ $\text{kJ mol}^{-1}$ ] observed by Gomez *et al.* for an  $\text{Au/ZrO}_2$  catalyst.<sup>89</sup>

Comparing the concentration-time profile of **Co1@RH** and **Co1@RH-E1**, it is clearly visible that the reaction is significantly faster with the etched catalyst: the reaction is completed after 10 h using **Co1@RH** and after 3 h using **Co1@RH-E1** (Fig. 9). It is noted that all reactions show an induction time within the first ten minutes. This phenomenon is most likely caused by insufficient or inhomogeneous heating of the reaction mixture while placing the autoclave in the preheated aluminum block.

A major challenge in understanding heterogeneous catalysts is to achieve an accurate description of the catalytic active center. XPS has proven to be a well-suited tool for this purpose in previous studies. The apparent correlation between higher CoN bonding fractions and higher catalytic

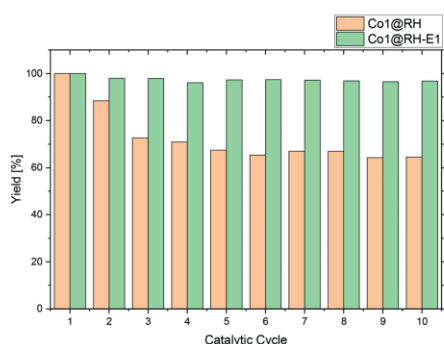


Fig. 8 Catalyst recycling test over 10 runs using un-etched (**Co1@RH**) and etched (**Co1@RH-E1**) catalysts. Reaction conditions: 120  $^{\circ}\text{C}$ , 10 bar  $\text{H}_2$ , 200 mg of catalyst, nitrobenzene (8 mmol), isopropanol (0.5 ml) and water (0.5 ml).



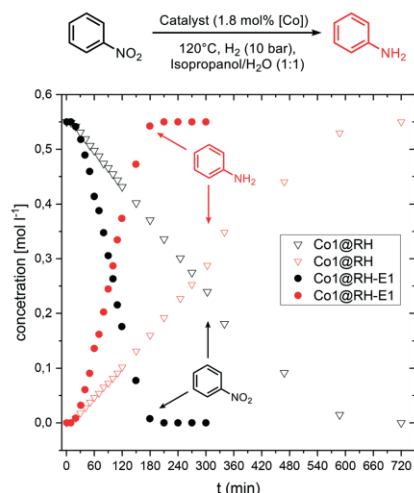


Fig. 9 Concentration-time profile in kinetic experiments using Co1@RH-E1 (filled circles) and Co1@RH (hollow triangles). Reaction conditions: 120 °C, 10 bar H<sub>2</sub>, 8 mmol nitrobenzene, in 8 ml of isopropanol/H<sub>2</sub>O, 100 mg catalyst (1.8 mol% of Co).

activities (with Co1@RH-E1 compared to the less active Co2@RH-E1) as shown in Fig. 5 is consistent with previous studies. They propose a coordination interaction between

pyridinic nitrogen atoms at the surface with adsorbed hydrogen, leading to easier activation/cleavage by the cobalt centers.<sup>55</sup> However, as mentioned before, the nature of CoN bonding is not the only measure to describe the activity of the present system, since the CoN bonding fraction in the more active material is approx. 10% lower after several recycling runs. Nevertheless, it is generally accepted that the Co–N–C interaction is key to achieve highly active and chemoselective heterogeneous Co-catalysts on a carbon matrix.<sup>35,90</sup> The data obtained in this study do not suggest otherwise. However, we see an increased fraction of N-pyrrol bonding at the expense of CoN binding, indicating a change in the cobalt–nitrogen interplay without negative effects on the catalytic activity. Additionally, the amount of cobalt in the bulk material compared to the amount of cobalt on the surface must be considered. It is noted that the most active catalyst, Co1@RH-E1, has the lowest cobalt content (5.5 m%) but with 2.6 mol% on the surface, almost twice as much compared with Co2@RH-E1. This indicates that the distribution of cobalt on the carbon matrix is highly relevant for the catalytic activity as well.

The mechanism of hydrogenation of nitro compounds over heterogeneous cobalt catalysts is well known,<sup>64</sup> as has been shown to occur through at least two competitive pathways: the “direct” double hydrogenation of the nitro group *via* hydroxylamine (Fig. 10, path A) or through a condensation reaction between the nitroso and hydroxylamine intermediates, to yield a hydrazo compound which is rapidly reduced to yield the final amine product (Fig. 10, path B). In our system, whilst not much can be said

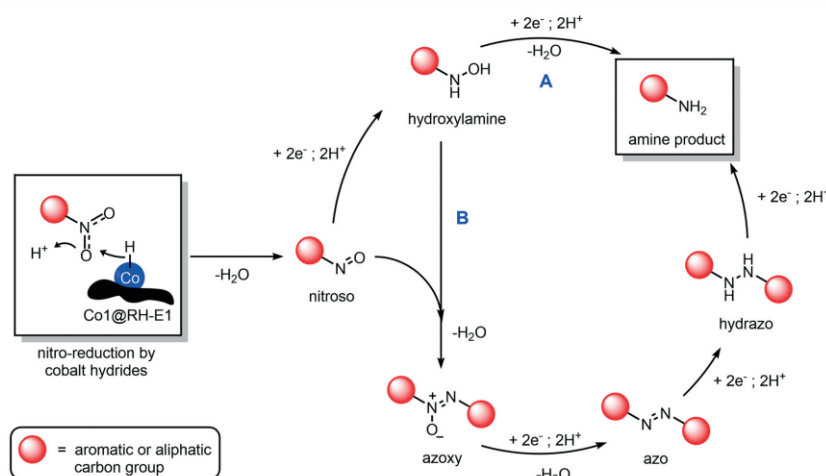


Fig. 10 Proposed reaction mechanism of the hydrogenation of nitro compounds using cobalt-based heterogeneous catalysts supported on rice husk ashes (Co1@RH-E1). The two competitive pathways are shown: direct amine formation by reduction of a hydroxylamine intermediate (A) and through condensation of hydroxylamine and nitroso intermediate to generate azo and hydrazo dimeric species (B).



about the role of path A, we could prove the occurrence of path B, as the intermediacy of azoxy and azo compounds was observed, as they quickly accumulate and disappear in the reaction mixture (Fig. S75†). In any case, independent from the preferred reaction pathway, the hydrogenation of aromatic and aliphatic nitro compounds proceeded with exquisite yields and selectivity in our hands, as no side products in relevant amounts were detected.

## Experimental

### Catalyst preparation

The rice husk was dried under the sun at the harvesting sites in Vietnam by local farmers (see the ESI† for further details). All samples were shredded with a SM 200 (1000 rpm, 2 mm sieve sizes) cutting mill and milled for 3 h in a ball mill PM 200 in steel cups using steel balls at 400 rpm.

**General procedure.** Preparation of Co1@RH-E1. For details on the synthesis of the other complexes and catalysts please see the ESI†. 0.5 g (2.1 mmol) of  $\text{Co}(\text{n})\text{Cl}_2 \cdot 6\text{H}_2\text{O}$  was dissolved in 50 mL of ethanol and 0.5 g (1.0 mmol) of phthalocyanine was added, followed by 2 g of ground RH. The suspension was stirred for 24 h at 21 °C. After that, the solvent was removed *in vacuo* with a rotary evaporator. The dried sample was pyrolyzed under a  $\text{N}_2$  atmosphere at 600 °C in an  $\text{Al}_2\text{O}_3$  pot inside a quartz tube furnace at a heating rate of 10 °C  $\text{min}^{-1}$ . After reaching the aspired temperature it was maintained for 1 h. The quartz tube was flushed using nitrogen at 50  $\text{ml min}^{-1}$  and after cooling down to room temperature the prepared material was stored under ambient conditions. For the base etching, a sample of the material was suspended in an aqueous 1 M NaOH solution, stirred at room temperature for 24 h, filtered, washed with water, and dried in an oven.

### Characterization methods

A detailed description of the used analytical methods for catalyst characterization and characterization of the products from the catalytic experiments as well as from the kinetic experiments is given in the ESI† including NMR, GC, GC-MS, IR, ICP-OES, EA (for C, H, N and S), BET, XRD, XPS and SEM imaging.

### Catalytic experiments

**General procedure.** For details on each specific substrate please see the ESI†. The organic substrate (1 mmol), 25 mg of Co1@RH-E1, isopropanol (0.5 ml) and water (0.5 ml) were mixed in a 12 ml vial equipped with a magnetic stirrer. The lid of the vial was pierced through with a steel cannula (0.45 × 12 mm) to equalize the pressure and ensure gas exchange. The prepared vial was placed in a steel autoclave. The autoclave was flushed three times with 10 bar of hydrogen and the required reaction pressure was adjusted. The pressurized autoclave was placed in an aluminium heating block. After completing the desired reaction time, the system

was cooled down using an ice bath. The crude mixture was filtered through a syringe filter after adding 2 ml of ethyl acetate. Finally, the crude product was purified by flash-column chromatography.

### Recycling and hot filtration experiment

200 mg of Co1@RH-E1, nitrobenzene (816  $\mu\text{l}$ , 8 mmol), isopropanol (7 mmol, 0.5 ml) and water (28 mmol, 0.5 ml) were used following a general procedure. For the hot filtration experiment 50 mg of catalyst, nitrobenzene (204  $\mu\text{l}$ , 2 mmol), isopropanol (14 mmol, 1 ml) and water (56 mmol, 1 ml) were added and used as described in the general procedure for catalytic experiments. After 2 h, the autoclave was abruptly cooled down to 70 °C and the pressure was lowered. The reaction solution was filtered through a filter and a Celite plug, and a sample was taken for GC analysis. The filtered reaction mixture (without a catalyst) was transferred in a fresh vial and the reaction continued under the conditions described above.

### Kinetic experiments

All kinetic experiments were conducted in a 200 ml autoclave using nitrobenzene (12.3 ml, 120 mmol), isopropanol (10.5 ml, 75 mmol) and water (42 ml, 75 mmol), equipped with a Teflon-coated magnetic stirrer and a riser pipe of 0.2 mm diameter for taking samples. The sealed autoclave was flushed three times with hydrogen at 10 bar and placed in the preheated aluminium block. The riser pipe was flushed each time before taking samples and the pressure was adjusted if necessary. All experiments have been measured in triplicate.

## Conclusions

Herein we present a novel heterogeneous cobalt-based catalyst for the highly chemoselective hydrogenation of nitro compounds, prepared from agricultural biowaste. The catalyst was synthesized by impregnating waste rice husk with cobalt complexes containing nitrogen ligands. The obtained material is mainly composed of carbon, silica and cobalt–nitrogen centers, which were identified by XPS. The catalytic performance of the material is enhanced by base etching, which removed a significant amount of the silica domains, resulting in a larger surface area, increased activity, and excellent recycling stability. Furthermore, the catalyst shows a broad substrate scope, being active towards both aliphatic and aromatic substrates, yielding the corresponding amines even in the presence of easily reducible groups, including additional nitro groups in the same molecule (thus reducing only one), which is an outstanding feature compared to other highly active hydrogenation catalysts.

We foresee that the implementation of this methodology within a bio-refinery concept in rice-farming communities is feasible within a reachable timescale (which is the overall goal of the consortium this project belongs to). The success



## Paper

## Catalysis Science &amp; Technology

of the said bio-refinery can be used to effectively meet some of the most relevant sustainable development goals (SDGs) of agricultural societies, addressing economic growth, innovation, industrialization, and improvement of production and recycling patterns, while reducing the nefarious footprint of human activities on the planet.

## Author contributions

F. Unglaube conceptualised the work, planned the experiments, conducted most of them, and co-wrote the manuscript. J. Schlapp conducted and evaluated various experiments. A. Quade conducted and evaluated the XPS measurements. J. Schäfer conducted and evaluated the SEM measurements. E. Mejia conceptualised and planned the research, supervised the work, and co-wrote the manuscript. All authors revised and authorized the final version of the manuscript.

## Conflicts of interest

There are no conflicts to declare.

## Acknowledgements

We would like to thank all the Vietnamese farmers and local authorities at the sample collection sites for their help and hospitality. We would like to acknowledge Dr. Abel Salazar for helpful discussions and inspiration. Also, thanks to Dr. Hendrik Lund and Kathleen Schubert, as well as Reinhard Eckelt for performing the XRD and BET-surface measurements (respectively), and for their helpful comments and discussions. This work has been supported by the RoHan Project funded by the German Academic Exchange Service (DAAD, No. 57315854) and the Federal Ministry for Economic Cooperation and Development (BMZ) inside the framework "SDG Bilateral Graduate school programme". Furthermore, we would like to acknowledge the funding for the SUVALIG project from the German Federal Ministry of Education and Research (BMBF, 031B0707B).

## Notes and references

- 1 U. N. General Assembly, *Resolution adopted by the General Assembly on 6 July 2017, A/RES/71/313*, 2017.
- 2 B. Lomborg, *Global Policy*, 2016, 7, 109–118.
- 3 V. Masson-Delmotte, P. Zhai, A. Pirani, S. L. Connors, C. Péan, S. Berger, N. Caud, Y. Chen, L. M. I. G. Goldfarb, M. Huang, K. Leitzell, E. Lonnoy, J. B. R. Matthews, T. K. Maycock, T. Waterfield, R. Y. O. Yelekçi and B. Zhou, *IPCC, Climate Change 2021: The Physical Science Basis. Contribution of Working Group I to the Sixth Assessment Report of the Intergovernmental Panel on Climate Change*, Cambridge University Press, 2021.
- 4 H. P. Makkar, *Anim. Prod. Sci.*, 2016, 56, 519–534.
- 5 H.-y. Wang, L. Shen, L.-m. Zhai, J.-z. Zhang, T.-z. Ren, B.-q. Fan and H.-b. Liu, *J. Integr. Agric.*, 2015, 14, 158–167.
- 6 Z. Mengqi, A. Shi, M. Ajmal, L. Ye and M. Awais, *Biomass Convers. Biorefin.*, 2021, 1–24.
- 7 K. Foo and B. Hameed, *Renewable Sustainable Energy Rev.*, 2010, 14, 1445–1452.
- 8 S. Jung, N. P. Shetti, K. R. Reddy, M. N. Nadagouda, Y.-K. Park, T. M. Aminabhavi and E. E. Kwon, *Energy Convers. Manage.*, 2021, 236, 114038.
- 9 D. Cheng, Y. Liu, H. H. Ngo, W. Guo, S. W. Chang, D. D. Nguyen, S. Zhang, G. Luo and Y. Liu, *Bioresour. Technol.*, 2020, 313, 123683.
- 10 K. Obileke, H. Onyeaka and N. Nwokolo, *Int. J. Energy Res.*, 2021, 45, 3761–3779.
- 11 J. He, S. Kawasaki and V. Achal, *Sustainability*, 2020, 12, 6971.
- 12 K. Foo and B. Hameed, *Adv. Colloid Interface Sci.*, 2009, 152, 39–47.
- 13 C. d. M. S. Rios, V. Simone, L. Simonin, S. Martinet and C. Dupont, *Biomass Bioenergy*, 2018, 117, 32–37.
- 14 V. S. Bhat, P. Kanagavalli, G. Sriram, N. S. John, M. Veerapandian, M. Kurkuri and G. Hegde, *J. Energy Storage*, 2020, 32, 101829.
- 15 V. Singh, S. Chatterjee, M. Palecha, P. Sen, B. Ateeq and V. Verma, *Carbon Lett.*, 2021, 31, 117–123.
- 16 R. Bharati and S. Suresh, in *Biofuels and bioenergy (BICE2016)*, Springer, 2017, pp. 25–32.
- 17 M. Fan, H. Wu, M. Shi, P. Zhang and P. Jiang, *Green Energy Environ.*, 2019, 4, 322–327.
- 18 N. Nakatani, H. Takamori, K. Takeda and H. Sakagawa, *Bioresour. Technol.*, 2009, 100, 1510–1513.
- 19 H. M. Salvi and G. D. Yadav, *ACS Omega*, 2020, 5, 22940–22950.
- 20 F. Unglaube, C. R. Kreyenschulte and E. Mejia, *ChemCatChem*, 2021, 13, 2583–2591.
- 21 P. F. Vogt and J. J. Gerulis, in *Ullmann's Encyclopedia of Industrial Chemistry*, Wiley-VCH Verlag GmbH & Co. KGaA, 2000, p. 699, DOI: 10.1002/14356007.a02\_037.
- 22 P. Roose, K. Eller, E. Henkes, R. Rossbacher and H. Höke, in *Ullmann's Encyclopedia of Industrial Chemistry*, Wiley-VCH Verlag GmbH & Co. KGaA, 2015, pp. 1–55, DOI: 10.1002/14356007.a02\_001.pub2.
- 23 C. G. S. Gopinathan, J. Kuruvilla, S. A. Pardhy and P. Ratnasamy, *US Pat.*, US5856575A, 1997.
- 24 D.-Q. Xu, Z.-Y. Hu, W.-W. Li, S.-P. Luo and Z.-Y. Xu, *J. Mol. Catal. A: Chem.*, 2005, 235, 137–142.
- 25 P. Baumeister, H. Blaser and W. Scherrer, in *Studies in Surface Science and Catalysis*, Elsevier, 1991, vol. 59, pp. 321–328.
- 26 G. Wu, M. Huang, M. Richards, M. Poirier, X. Wen and R. W. Draper, *Synthesis*, 2003, 2003, 1657–1660.
- 27 H.-J. Arpe, *Industrial Organic Chemistry*, Wiley-VCH, Weinheim, 2010.
- 28 R. Gao, L. Pan, Z. Li, X. Zhang, L. Wang and J.-J. Zou, *Chin. J. Catal.*, 2018, 39, 664–672.
- 29 P. Ryabchuk, G. Agostini, M.-M. Pohl, H. Lund, A. Agapova, H. Junge, K. Junge and M. Beller, *Sci. Adv.*, 2018, 4, eaat0761.





- 30 H.-U. Blaser, H. Steiner and M. Studer, *ChemCatChem*, 2009, **1**, 210–221.
- 31 L. R. Pokhrel and B. Dubey, *Crit. Rev. Environ. Sci. Technol.*, 2013, **43**, 2352–2388.
- 32 F. Griffiths and O. Brown, *J. Phys. Chem.*, 1937, **41**, 477–484.
- 33 F. A. Westerhaus, R. V. Jagadeesh, G. Wienhöfer, M.-M. Pohl, J. Radnik, A.-E. Surkus, J. Rabeah, K. Junge, H. Junge, M. Nielsen, A. Brückner and M. Beller, *Nat. Chem.*, 2013, **5**, 537–543.
- 34 X. Sun, A. I. Olivos-Suarez, D. Osadchii, M. J. V. Romero, F. Kapteijn and J. Gascon, *J. Catal.*, 2018, **357**, 20–28.
- 35 Y. Dai, C. Jiang, M. Xu, B. Bian, D. Lu and Y. Yang, *Appl. Catal., A*, 2019, **580**, 158–166.
- 36 W. Li, J. Artz, C. Broicher, K. Junge, H. Hartmann, A. Besmehn, R. Palkovits and M. Beller, *Catal. Sci. Technol.*, 2019, **9**, 157–162.
- 37 M. Elfinger, T. Schönauer, S. Thomä, R. Stäglich, M. Drechsler, M. Zobel, J. Senker and R. Kempe, *ChemSusChem*, 2021, **14**, 2360–2366.
- 38 Z. Yuan, B. Liu, P. Zhou, Z. Zhang and Q. Chi, *J. Catal.*, 2019, **370**, 347–356.
- 39 J. Wu, A. Mehmood, G. Zhang, S. Wu, G. Ali and A. Kucernak, *ACS Catal.*, 2021, 5035–5046, DOI: 10.1021/acscatal.0c05701.
- 40 B. Sahoo, A. E. Surkus, M. M. Pohl, J. Radnik, M. Schneider, S. Bachmann, M. Scalone, K. Junge and M. Beller, *Am. Ethnol.*, 2017, **129**, 11394–11399.
- 41 B. Sahoo, D. Formenti, C. Topf, S. Bachmann, M. Scalone, K. Junge and M. Beller, *ChemSusChem*, 2017, **10**, 3035–3039.
- 42 T. Song, P. Ren, Y. Duan, Z. Wang, X. Chen and Y. Yang, *Green Chem.*, 2018, **20**, 4629–4637.
- 43 Y. Zou and T. Yang, in *Rice Bran and Rice Bran Oil*, Elsevier, 2019, pp. 207–246.
- 44 K. Mochizuki and M. Fujimoto, *Bull. Chem. Soc. Jpn.*, 1985, **58**, 1520–1523.
- 45 S. M. Soliman, M. A. Abu-Youssef, J. Albering and A. El-Faham, *J. Chem. Sci.*, 2015, **127**, 2137–2149.
- 46 P. Ray, *Chem. Rev.*, 1961, **61**, 313–359.
- 47 M. A. Al-Omair, *Arabian J. Chem.*, 2019, **12**, 1061–1069.
- 48 D. Ziegler, F. Boschetto, E. Marin, P. Palmero, G. Pezzotti and J.-M. Tulliani, *Sens. Actuators, B*, 2021, **328**, 129049.
- 49 V. Malhotra, *Concr. Int.*, 1993, **15**, 23–28.
- 50 T.-H. Liou, *Mater. Sci. Eng., A*, 2004, **364**, 313–323.
- 51 F. Zhang, C. Zhao, S. Chen, H. Li, H. Yang and X.-M. Zhang, *J. Catal.*, 2017, **348**, 212–222.
- 52 P. Zhou, L. Jiang, F. Wang, K. Deng, K. Lv and Z. Zhang, *Sci. Adv.*, 2017, **3**, e1601945.
- 53 D. Nicholls, *The chemistry of iron, cobalt and nickel: comprehensive inorganic chemistry*, Elsevier, 2013.
- 54 D. Formenti, R. Mocchi, H. Atia, S. Dastgir, M. Anwar, S. Bachmann, M. Scalone, K. Junge and M. Beller, *Chem. – Eur. J.*, 2020, **26**, 15589–15595.
- 55 D. Formenti, F. Ferretti, C. Topf, A.-E. Surkus, M.-M. Pohl, J. Radnik, M. Schneider, K. Junge, M. Beller and F. Ragaini, *J. Catal.*, 2017, **351**, 79–89.
- 56 T. Senthamarai, V. G. Chandrashekar, M. B. Gawande, N. V. Kalevaru, R. Zbořil, P. C. Kamer, R. V. Jagadeesh and M. Beller, *Chem. Sci.*, 2020, **11**, 2973–2981.
- 57 N. Morlanés, W. Almaksoud, R. K. Rai, S. Ould-Chikh, M. M. Ali, B. Vidjayacoumar, B. E. Al-Sabhan, K. Albahily and J.-M. Basset, *Catal. Sci. Technol.*, 2020, **10**, 844–852.
- 58 M. Ladouceur, G. Lalande, D. Guay, J. Dodelet, L. Dignard-Bailey, M. Trudeau and R. Schulz, *J. Electrochem. Soc.*, 1993, **140**, 1974.
- 59 X. Zhang, Z. Wu, X. Zhang, L. Li, Y. Li, H. Xu, X. Li, X. Yu, Z. Zhang and Y. Liang, *Nat. Commun.*, 2017, **8**, 1–8.
- 60 R. L. Arechederra, K. Artyushkova, P. Atanassov and S. D. Minteer, *ACS Appl. Mater. Interfaces*, 2010, **2**, 3295–3302.
- 61 N. Soltani, A. Bahrami, M. Pech-Canul and L. González, *Chem. Eng. J.*, 2015, **264**, 899–935.
- 62 X. Lan and T. Wang, *ACS Catal.*, 2020, **10**, 2764–2790.
- 63 R. A. Sheldon, *Green Chem.*, 2005, **7**, 267–278.
- 64 D. Formenti, F. Ferretti, F. K. Scharnagl and M. Beller, *Chem. Rev.*, 2018, **119**, 2611–2680.
- 65 J. Song, Z.-F. Huang, L. Pan, K. Li, X. Zhang, L. Wang and J.-J. Zou, *Appl. Catal., B*, 2018, **227**, 386–408.
- 66 T. Vincent, S. Spinelli and E. Guibal, *Ind. Eng. Chem. Res.*, 2003, **42**, 5968–5976.
- 67 M. Pietrowski, *Curr. Org. Synth.*, 2012, **9**, 470–487.
- 68 M. D. Aparece, C. Gao, G. J. Lovinger and J. P. Morken, *Angew. Chem.*, 2019, **131**, 602–605.
- 69 S. Bera and X. Hu, *Angew. Chem.*, 2019, **131**, 13992–13997.
- 70 J. W. Fyfe, C. P. Seath and A. J. Watson, *Angew. Chem.*, 2014, **126**, 12273–12276.
- 71 L. M. Baldyga, S. O. Blavo, C.-H. Kuo, C.-K. Tsung and J. N. Kuhn, *ACS Catal.*, 2012, **2**, 2626–2629.
- 72 F. Pinna, F. Menegazzo, M. Signorello, P. Canton, G. Fagherazzi and N. Pernicone, *Appl. Catal., A*, 2001, **219**, 195–200.
- 73 M. J. Nasab and A. R. Kiasat, *RSC Adv.*, 2016, **6**, 41871–41877.
- 74 M. Pashaei and E. Mehdipour, *Appl. Organomet. Chem.*, 2018, **32**, e4226.
- 75 P. K. Verma, M. Bala, K. Thakur, U. Sharma, N. Kumar and B. Singh, *Catal. Lett.*, 2014, **144**, 1258–1267.
- 76 M. Azaroon and A. R. Kiasat, *Catal. Lett.*, 2018, **148**, 745–756.
- 77 J. Hou, Y. Ma, Y. Li, F. Guo and L. Lu, *Chem. Lett.*, 2008, **37**, 974–975.
- 78 G. Vile, N. Almora-Barrios, N. r. López and J. Perez-Ramirez, *ACS Catal.*, 2015, **5**, 3767–3778.
- 79 S.-S. Liu, X. Liu, L. Yu, Y.-M. Liu, H.-Y. He and Y. Cao, *Green Chem.*, 2014, **16**, 4162–4169.
- 80 C. C. Torres, V. A. Jiménez, C. H. Campos, J. B. Alderete, R. Dinamarca, T. M. Bustamente and B. Pawelec, *Mol. Catal.*, 2018, **447**, 21–27.
- 81 S. Durgadas, V. K. Chatare, K. Mukkanti and S. Pal, *Appl. Organomet. Chem.*, 2010, **24**, 680–684.
- 82 L. I. Roberts, *Analgesic-antipyretic and anti-inflammatory agents and drugs employed in the treatment of gout*, 2001.
- 83 D. Huber, G. Andermann and G. Leclerc, *Tetrahedron Lett.*, 1988, **29**, 635–638.
- 84 Q. Zhang, X. Yang and J. Guan, *ACS Appl. Nano Mater.*, 2019, **2**, 4681–4697.
- 85 H. Wu, L. Zhuo, Q. He, X. Liao and B. Shi, *Appl. Catal., A*, 2009, **366**, 44–56.



[View Article Online](#)

## Paper

## Catalysis Science &amp; Technology

- 86 J. Relvas, R. Andrade, F. G. Freire, F. Lemos, P. Araújo, M. J. Pinho, C. P. Nunes and F. R. Ribeiro, *Catal. Today*, 2008, **133**, 828–835.
- 87 C. Rode, M. Vaidya, R. Jaganathan and R. Chaudhari, *Chem. Eng. Sci.*, 2001, **56**, 1299–1304.
- 88 R. Baxter and P. Hu, *J. Chem. Phys.*, 2002, **116**, 4379–4381.
- 89 S. Gomez, C. Torres, J. L. Garcia Fierro, C. R. Apesteguia and P. Reyes, *J. Chil. Chem. Soc.*, 2012, **57**, 1194–1198.
- 90 M. Li, S. Chen, Q. Jiang, Q. Chen, X. Wang, Y. Yan, J. Liu, C. Lv, W. Ding and X. Guo, *ACS Catal.*, 2021, **11**, 3026–3039.

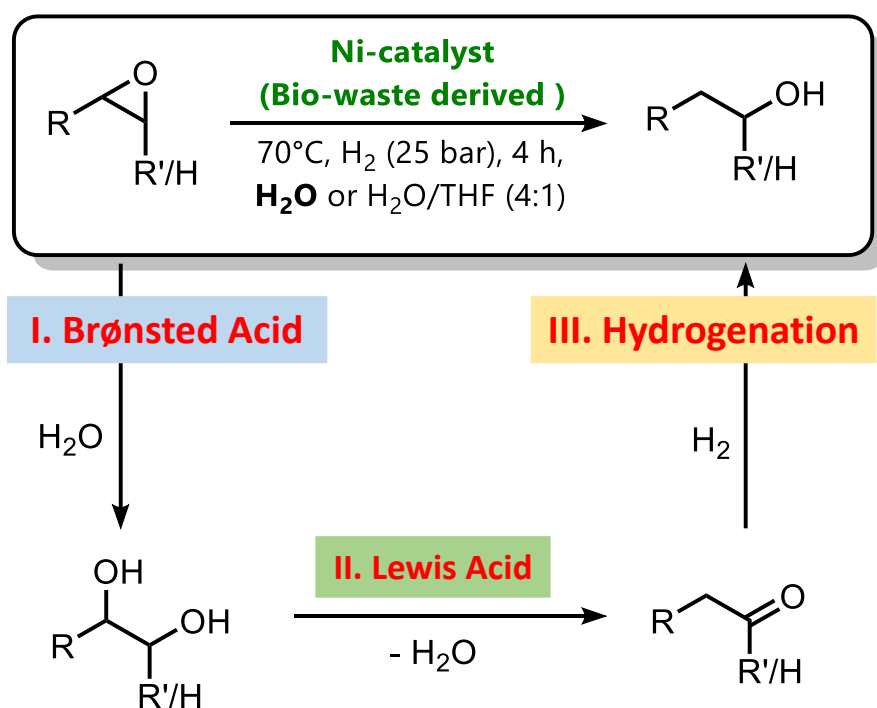
Open Access Article. Published on 14 February 2022. Downloaded on 5/1/2023 2:30:51 PM.  
This article is licensed under a Creative Commons Attribution-NonCommercial 3.0 Unported Licence.



## Hydrogenation of Epoxides to Anti-Markovnikov Alcohols over a Nickel Heterogenous Catalyst Prepared from Biomass (Rice) Waste

F. Unglaube, H. Atia, S. Bartling, C. Kreyenschulte and E. Mejia. *Helvetica Chimica Acta* (2022), e202200167

DOI: 10.1002/hlca.202200167



**Abstract:** The synthesis of primary alcohols (from olefins) is an important and challenging transformation, as most of the current methods suffer from regioselectivity issues. This work describes the utilization of rice husk (RH) from agricultural waste as support for the preparation of a catalyst for the conversion of olefin oxides to primary alcohols. The catalyst was synthesized by pyrolysis of RH impregnated with nickel, and characterized by IR, AAS, XRD, BET, XPS, TEM, and TPD technics. The catalyst shows excellent activity and selectivity towards anti-Markovnikow alcohols, acting simultaneously as Brønsted acid, solid Lewis acid, and as hydrogenation catalyst. A substrate screening was done, the catalyst's recycling stability was assessed, and a plausibly reaction mechanism was proposed.

## RESEARCH ARTICLE

# Hydrogenation of Epoxides to Anti-Markovnikov Alcohols over a Nickel Heterogenous Catalyst Prepared from Biomass (Rice) Waste

Felix Unglaube,<sup>[a]</sup> Hanan Atia,<sup>[a]</sup> Stephan Bartling,<sup>[a]</sup> Carsten R. Kreyenschulte<sup>[a]</sup> and Esteban Mejía<sup>\*[a]</sup>

Dedicated to Prof. Janine Cossy for her contributions to the advancement of organic synthesis and catalysis

[a] F. Unglaube, Dr. H. Atia, Dr. S. Bartling, Dr. C. R. Kreyenschulte, Dr. E. Mejía  
Leibniz-Institut für Katalyse e. V. an der Universität Rostock,  
Albert-Einstein-Str. 29 A, 18059 Rostock, Germany  
E-mail: Esteban.mejia@catalysis.de

Supporting information for this article is given via a link at the end of the document.

**Abstract:** The synthesis of primary alcohols (from olefins) is an important and challenging transformation, as most of the current methods suffer from regioselectivity issues. This work describes the utilization of rice husk (RH) from agricultural waste as support for the preparation of a catalyst for the conversion of olefin oxides to primary alcohols. The catalyst was synthesized by pyrolysis of RH impregnated with nickel, and characterized by IR, AAS, XRD, BET, XPS, TEM, and TPD technics. The catalyst shows excellent activity and selectivity towards anti-Markovnikov alcohols, acting simultaneously as Brønsted acid, solid Lewis acid, and as hydrogenation catalyst. A substrate screening was done, the catalyst's recycling stability was assessed, and a plausible reaction mechanism was proposed.

## Introduction

Rice is one of the most important food crops for human consumption, leaving after harvesting approximately 800 million tons of biomass waste each year, mainly straw and husk.<sup>[1, 2]</sup> The management of this amount of waste represents a challenge for most communities, being the current "solution" the open-field burning of the biomass, resulting in huge amounts of green-house gas and particulate emissions to the atmosphere, which is associated with major health issues.<sup>[3, 5]</sup> With the aim of finding a more sustainable use of these residues, our group recently developed ways to valorize rice husk waste (RH) to prepare new materials with bio-medical,<sup>[6]</sup> and catalytic applications.<sup>[7, 8]</sup> Our general strategy is to exploit the ability of pyrolyzed RH to act simultaneously as Brønsted- and Lewis-acid, and supporting metal nanoparticles onto its surface, thus conferring these composites antimicrobial and catalytic properties. The work presented herein discloses the synthesis of nickel-containing materials from rice husk, and their use as catalyst for the reductive ring-opening of epoxides to yield alcohols with anti-Markovnikov selectivity; a straightforward way to obtain primary alcohols from terminal olefin oxides.

Primary alcohols are widely used building blocks, both in chemical and pharmaceutical industries. They play a key role in various synthetic transformations like alkylation,<sup>[9]</sup> oxidation,<sup>[10]</sup>

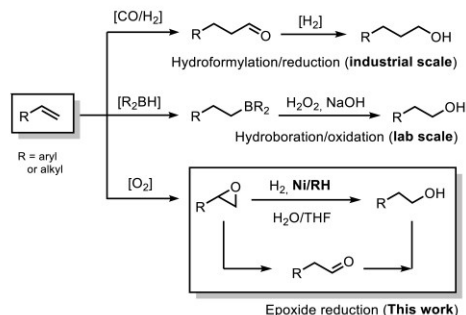
amination,<sup>[11, 12]</sup> etc., and in energy technologies like hydrogen utilization,<sup>[13]</sup> and storage.<sup>[14]</sup> Currently, the two leading approaches to prepare primary alcohols are through derivatization of olefins, namely via hydroformylation and consecutive reduction,<sup>[15, 16]</sup> and hydroboration followed by oxidation (Scheme 1).<sup>[17]</sup> On the one hand, the hydroformylation pathway is used by industry in large scale thanks to the high turnover numbers of the used catalysts.<sup>[16]</sup> However, these reactions often suffer from selectivity issues regarding the Markovnikov/anti-Markovnikov product distribution and inevitably requires noble metals like Rh and Ru.<sup>[18, 19]</sup> On the other hand, hydroboration reactions are applied only in lab scale since the required borane reagents are required in stoichiometric amounts and are difficult to recover. Thus, there is a need for more selective and sustainable catalytic approaches for the synthesis of primary alcohols from olefines.

A viable alternative that has caught much attention in recent years, due to good atom economy and advantageous reaction conditions is through the olefin oxide (epoxide). It can easily be prepared by oxidation of the corresponding olefin,<sup>[20, 21]</sup> which can be ring-opened in a reductive fashion to yield anti-Markovnikov alcohols. The second, more difficult step can be done by hydrosilylation,<sup>[22-24]</sup> hydrolysis<sup>[25]</sup> and transfer hydrogenations.<sup>[26, 27]</sup> The conversion via direct hydrogenation, is more attractive, as it has a higher atom utilization, as demonstrated by some groups in recent years.<sup>[26, 28, 29]</sup> Homogenous catalytic systems have shown good regioselectivity in the ring opening reaction, which is the bottleneck towards anti-Markovnikov alcohols. Nevertheless, most homogenous catalysts are based on noble metals like Ru,<sup>[30, 31]</sup> or Rh,<sup>[32]</sup> and still suffer from poor selectivity (not only regarding the regioselectivity) as they produce as well deoxygenated side products. Similar problems are observed when heterogenous catalysts are employed. The majority of state-of-the-art heterogenous systems for the direct hydrogenation for epoxides is based on Pd,<sup>[33-35]</sup> and Ni.<sup>[36]</sup>

Nickel-based catalysts offer a cheaper alternative to noble metal-based systems for the direct hydrogenation of epoxides, although the "classical" Raney-Ni has proven to be difficult to handle.<sup>[37]</sup> Thus, Ni-catalysts have been prepared using various supports,<sup>[38, 39]</sup> including MgO-Al<sub>2</sub>O<sub>3</sub>, MgO,<sup>[40, 41]</sup> and saponites.<sup>[42]</sup> A major drawback of these heterogenous systems is that high catalyst

## RESEARCH ARTICLE

loadings are required, and their tolerance to functional groups is limited, reducing their substrate scope mostly to styrene oxide,<sup>[43, 44]</sup>



**Scheme 1.** Synthetic approaches towards primary alcohols from terminal olefins. In this work, we describe the use of a nickel catalysts (Ni/RH) prepared from rice husk (RH) waste

In this contribution, nickel-containing hydrogenation catalysts have been prepared successfully from waste RH. Nickel nanoparticles are generated on the catalysts surface by coordinating Ni(II) ions on the RH followed by pyrolysis, where carbothermal reduction leads to catalytically active nickel species.<sup>[7]</sup> We have applied this catalyst for the reductive ring-opening of epoxides to the corresponding anti-Markovnikov alcohols with excellent yield and selectivity. The generality of the developed method was demonstrated by using it for the reduction of carbonyl compounds, also with excellent results.

## Results and Discussion

### Catalysts Synthesis and Characterization

The sun-dried RH was collected at rice harvesting sites at the Red River and Mekong Delta in Vietnam, and then shredded, and grounded in a ball mill (see ESI for details). In preliminary experiments, the plant material was first washed with 1 M HCl in order to eliminate eventual metal impurities, especially iron oxide which is naturally present in RH in amounts of up to 0.2 wt%.<sup>[49]</sup> However, catalytic experiments revealed that there is no significant advantage (in terms of catalytic performance) if the acidic treatment was made. Thus, this step was later omitted, significantly lowering the amount of acidic wastewater generated in the process.

The supported nickel catalyst (Ni/RH) was prepared by wet impregnation of RH with Ni(NO<sub>3</sub>)<sub>2</sub> followed by pyrolysis at 700 °C under inert atmosphere. In preliminary experiments, different catalysts were synthesized at different pyrolysis temperatures from 400 to 1000 °C (Figure S17), but later catalytic performance assessments showed that the material pyrolyzed at 700 °C gave the best results. Thus, all analysis and catalytic experiments presented here were obtained with this material.

The prepared material is a composite of carbon and silica with nickel nanoparticles at the surface, as attested by EDX measurements (Figures 1E-F and S1-S4). XRD measurements

(Figure 1A) showed a broad peak from 16 to 30° corresponding to amorphous silica and graphite, respectively. Rice husk is well known for containing up to 20 wt% of silica,<sup>[46, 47]</sup> although, elemental analysis (EA) revealed a content of only 11.4 wt% Si in the prepared material (for details see Table S2). Further reflexes at 44, 51 and 76° which can be correlated with cubic Ni<sup>0</sup>. An average crystallite size of 27 nm was calculated using the Scherrer equation after whole powder fitting (Table S3).

XPS was applied for further material characterization (Figures 1B, and S5-S9), showing that the majority of the surface appears to be composed of carbon (77.1 at.%) (see XPS quantification Table S1 for details). The XPS survey (Figure S5) shows a strong C 1s peak at 284.6 eV as well as satellite features at 290.3 eV and 293.9 eV, suggesting sp<sup>2</sup> hybridized carbon but also the coexistence of sp<sup>3</sup> hybridized carbon to a minor extent is possible. Additionally, oxygenated carbon moieties are visible in the C 1s signal at 285.7 eV, 286.8 eV, and 287.8 eV as well as in the O 1s signal at 530.6 eV. The Si 2p signal at 103.8 eV and a O 1s signal at 533.3 eV are associated with amorphous SiO<sub>2</sub>. This suggests that the ligno-cellulosic silica matrix of the RH epidermis is completely converted into graphene and other carbonaceous materials with low amounts of oxygenated carbon species like carbonyl or acetal functionalities along with silica particles. EDX mapping shows that the nickel particles are located only on the carbon domains, while the SiO<sub>2</sub> support is embedded in the carbon matrix (Figure 1E). The XPS N 1s signal shows pyridinic and pyrrolic nitrogen at 398.1 eV and 401 eV, respectively as well as oxidized pyridinic nitrogen at 402.7 eV (Figure S9).<sup>[48]</sup>

Interestingly, the determined nickel oxidation states by XPS differs from those observed in XRD analysis. XPS measurements revealed that, together with Ni 2p signals at 852.9 and 870.0 eV<sup>[48]</sup> matching Ni<sup>0</sup>, a second nickel species is present at the surface. Strong Ni 2p<sub>3/2</sub> signal at 856.4 eV with corresponding satellite peaks at 861.4 eV and 864.3 eV can be correlated with Ni(OH)<sub>2</sub>,<sup>[50]</sup> due to the shift to higher binding energies as well the characteristic peak shape rather than with NiO.<sup>[51]</sup> This findings suggest a Ni<sup>0</sup> core surrounded with a Ni<sup>+2</sup> layer. This hypothesis was confirmed by TEM measurements. The Ni particles indeed consist of a metal core surrounded by an oxide shell, clearly visible in the HAADF-STEM (Figures 1H and G). Interestingly, the Ni particles are not covered by a layer of graphitic carbon, which was previously observed in similar cobalt<sup>[52-54]</sup> and silver-based systems.<sup>[7]</sup>

Temperature programmed reduction experiments (H<sub>2</sub>-TPR) showed that the nickel species on the catalyst surface can be reduced by hydrogen (Figure 1C). The TPR profile of Ni/RH shows three peaks with an offset at 188, 342 and 562 °C, due to the presence of nickel in different binding states.<sup>[55]</sup>

The surface structure was further investigated using BET-isotherm measurements (Figures S11 and S12). A surface area of 301 m<sup>2</sup>·g<sup>-1</sup> was found. The sorption isotherms showing a type IV shape suggesting a porous structure. The biggest share of pore area is with 242 m<sup>2</sup>·g<sup>-1</sup> accounted to micro pores with a pore width of 0.5 to 2 nm and only 58 m<sup>2</sup>·g<sup>-1</sup> are accounted to the external surface area. A sorption with a type H3 (IUPAC classification) hysteresis loop was found, which is known from silica containing materials<sup>[56]</sup> like clay<sup>[57, 58]</sup> and silica-based catalysts prepared by sol-gel methods,<sup>[59]</sup> indication the existence of slit pores and capillary condensation of adsorption gas in interstices between silica and the carbon matrix.<sup>[58]</sup>



## RESEARCH ARTICLE

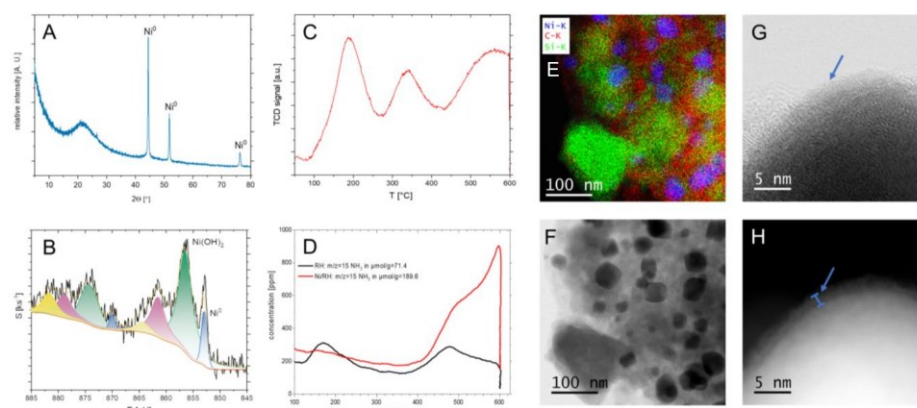


**Figure 1.** Solid state characterization of Ni/RH: XRD (A), Ni2p peak from XPS (B), H<sub>2</sub>-TPR (C), NH<sub>3</sub>-TPD (D), EDX mapping (E) and its corresponding HAADF image (F), and ABF (G), as well as HAADF STEM image (H) of Ni<sup>2+</sup> particles with oxide shell (blue arrow and bar)

Furthermore, TGA-MS analysis were used to determine the thermal stability of the prepared material (Figure S13). The catalyst Ni/RH shows surprisingly good thermal stability under non oxidizing atmosphere up to 500 °C. The minimal mass loss of 3 wt% can be explained by desorption of water and atmosphere gases (O<sub>2</sub> and N<sub>2</sub>) from the material surface. At 660 °C an endothermic process occurs, resulting in a mass loss of approx. 2 wt%. The MS assigns this mass loss to a molecule of 44 g mol<sup>-1</sup>, suggesting the emission of propane (C<sub>3</sub>H<sub>8</sub>) or CO<sub>2</sub>. The emission of propane from biomass is usually accompanied by the emission of other members of the homologous series, of which only methane was detectable in trace amounts. Thus, the emission of CO<sub>2</sub> seems to be more likely since it could result from the decomposition of oxygenated carbon species on the surface. The acidic nature of the catalyst was assessed by TPD-NH<sub>3</sub> experiments, showing that the bare support (RH) has mainly acidic centers in the weak range, with a signal peak around 160 °C (Figure 1D), while the catalyst Ni/RH contains a significantly higher share of acidic centers in the stronger range, with a strong signal from 400 to 600 °C. Additionally, the nature of these acidic centers was investigated using the decomposition of 2-(1-bromoethyl)-2-phenyl-1,3-dioxolane, as probe, as described by Coma and co-workers.<sup>[60,67]</sup> The obtained relative amounts of products revealed that Ni/RH offers both soft Lewis, and Brønsted acidic sites, and that the acidity of Ni/RH is mainly associated with the support (RH), and not with the nickel particles (for details see Table S5).

### Hydrogenation Catalysis

The prepared material (Ni/RH) was tested as catalyst for the hydrogenation of styrene oxide. Preliminary screening of reaction conditions (Table 1, Figures S15 and S16) showed that the product distribution (**1**, **2** and **3**) largely depends on the different variables (temperature, pressure, and solvent). The conditions were thus optimized towards the formation of the primary alcohol 2-Phenylethan-1-ol (2-PEA) (**3**), using 20 mg of the Ni/RH catalyst

(1.5 mol% of Ni) and 2 mmol of substrate. Interestingly, the Markovnikov/anti-Markovnikov selectivity of the reductive ring opening reaction was not affected by the choice of the reaction parameters, resulting always only in the formation of the anti-Markovnikov product.

**Table 1.** Optimization of reaction conditions for the reduction of styrene oxide using Ni/RH as hydrogenation catalyst.<sup>[6]</sup>

$\text{Ph-CH(O)} + \text{H}_2 \xrightarrow[1.5 \text{ mol\% [Ni]}]{4 \text{ h}} \text{Ph-CH(OH)-CH}_2\text{OH} + \text{Ph-CH=O} + \text{Ph-CH}_2\text{OH}$					Yield [%]		
Entr y	T [°C]	P [bar]	Solvent		1	2	3
1	120	10	H <sub>2</sub> O	-	-	87	12
2	120	25	H <sub>2</sub> O	-	-	-	98
3	70	25	H <sub>2</sub> O	-	-	-	99
4	50	10	H <sub>2</sub> O	93	4	-	-
5	70	10	H <sub>2</sub> O	-	-	81	15
6 <sup>[a]</sup>	50	10	H <sub>2</sub> O/THF	90	5	-	-
7 <sup>[a]</sup>	50	25	H <sub>2</sub> O/THF	82	-	-	15
8 <sup>[a]</sup>	70	10	H <sub>2</sub> O/THF	-	-	86	12
9 <sup>[a]</sup>	70	25	H <sub>2</sub> O/THF	-	-	-	99
10 <sup>[b,c]</sup>	70	25	H <sub>2</sub> O/THF	-	-	-	99
11 <sup>[b,d]</sup>	70	25	H <sub>2</sub> O/THF	-	-	95	4

## RESEARCH ARTICLE

12	70	25	CH <sub>3</sub> OH	45	-	30
13	70	25	CH <sub>3</sub> CN	86	-	3

[a] Reaction conditions: 2 mmol of substrate, 2 ml of solvent, 4 h reaction time, and 20 mg catalyst (Ni/RH, corresponding to 1.5 mol % Ni). Yield was determined by GC using n-octane as internal standard. [b] H<sub>2</sub>O/THF mixture 4:1. [c] catalyst prepared with RH without acidic treatment. [d] using pyrolyzed RH without nickel (no Ni(NO<sub>3</sub>)<sub>2</sub> was added).

The reaction was initially performed using pure water as solvent (Table 1, entries 1 to 5), resulting in the quantitative formation of **3** under 25 bar of H<sub>2</sub> at 70 °C (entry 3). Lower pressure and temperature (10 bar, 50 °C) resulted in the almost exclusive formation of diol **1** (entry 4). Increasing the temperature while keeping the lower pressure (70 °C, 10 bar) resulted on preferential formation of the corresponding aldehyde **2** (entry 5). Since water might be an unsuitable solvent for more hydrophobic substrates, the addition of different organic solvents like THF and 1,4-dioxane to the aqueous reaction mixture was assessed (Figure S15). However, the best results were obtained with a water/THF (4:1) mixture, which was then used for the subsequent substrate scope experiments (see below). Further strategies to increase the availability of non-polar substrates in the aqueous media, like the addition of micelle-forming amphiphiles,<sup>[68]</sup> were not investigated. The recyclability of the catalyst was also investigated (Figure S17). To our delight no significant reduction in yield was found over ten catalytic runs (Figure S18). Additionally, by means of a "hot filtration" experiment the heterogeneous character of the process was attested, since no further product formation was found after removing the Ni/RH catalyst from the reaction mixture under catalysis conditions (see ESI for further details).

Finally, the substrate scope of the reductive ring opening of epoxides was investigated (Figure 2). The developed catalyst could successfully reduce several epoxides into the corresponding anti-Markovnikov alcohols regardless of the nature of the epoxide (terminal or internal). As expected, terminal epoxides gave invariably the corresponding primary alcohols with complete selectivity. Moreover, the system showed to be selective even in presence of sensitive groups (which can react under the reaction conditions), like aryl halides and nitriles, remaining these groups untouched in every case, in strong contrast to other nickel catalysts known to be active in the hydrogenation of nitriles to amines.<sup>[69-71]</sup>

Aliphatic epoxides could also be converted to the corresponding alcohols in good yields, although higher temperatures (120 °C) were necessary to achieve good conversions. In general, even though the yields of aliphatic alcohols were lower than those for aromatic substrates, the anti-Markovnikov selectivity was not affected.

The generality of the developed methodology was tested by performing the reduction of several ketones and aldehydes under the same conditions. All the tested substrates were almost quantitatively converted into the corresponding alcohols (Figure 3). As in the case of the epoxides, substrates containing reducible groups (halide, nitrile) or unprotected hydroxyls, were tolerated by the catalysts under the selected conditions.

Importantly, it was observed during substrate screening that the catalyst loses its selectivity towards epoxides in the presences of nitro as well as carbonyl functions like aldehydes and ketones.

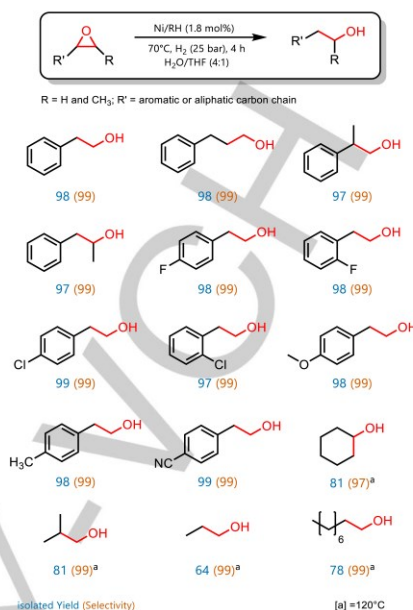


**Figure 2:** Products of epoxide hydrogenation using Ni/RH. Reaction conditions (if not state differently): 70 °C, 25 bar H<sub>2</sub>, 2 mmol substrate, 4 h, in 2 ml of H<sub>2</sub>O/THF (4:1), 20 mg catalyst (1.8 mol % of Ni).

Considering these experimental observations as well as previous literature reports, a feasible reaction mechanism has been proposed (Scheme 2). The overall reductive ring-opening of epoxides can be divided in three major steps: I. Brønsted acid catalyzed ring opening, II. Lewis acid catalyzed diol dehydration, and III. Nickel catalyzed hydrogenation.

The Brønsted acid catalyzed ring opening yields a vicinal diol as reaction product. This is promoted by acidic sites at the catalyst support (RH) and is effective for both, terminal as well as internal epoxides, as proved by the isolation of both intermediates when the corresponding reactions were prematurely interrupted. The conversion of epoxides to diols has been previously described with other catalysts,<sup>[72]</sup> showing similar reactivity trends and solvent effects as those described here, so it can be assumed that our system follows the accepted reaction mechanism.<sup>[72]</sup> The second step is either a Lewis acid catalyzed semi-pinacol rearrangement of diols, or, as previously reported by other groups, a classical Meinwald rearrangement.<sup>[73-76]</sup> In this step, the elimination of water is followed by keto-enol tautomerization which leads to the ketone or aldehyde, respectively. The rearrangement is usually catalyzed by the addition of a homogenous Lewis acid like BF<sub>3</sub>,<sup>[73]</sup> InCl<sub>3</sub>,<sup>[77]</sup> or by carbocations.<sup>[78]</sup> In 2015, Graham and co-workers reported the use of heterogeneous nanoporous aluminosilicates for this reaction.<sup>[79]</sup> As described above, the prepared Ni/RH also offers Lewis acidic sites, which enable the material to catalyze this rearrangement.

## RESEARCH ARTICLE

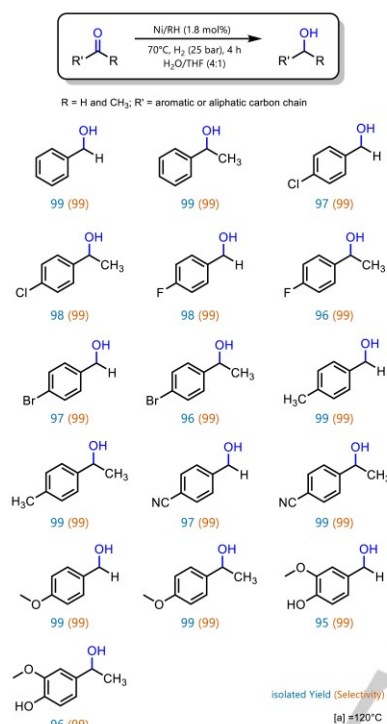
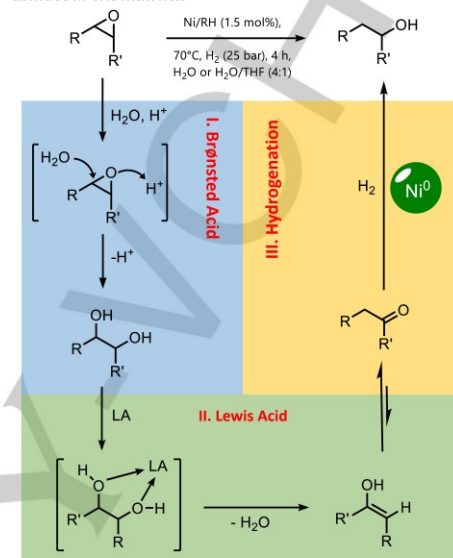


**Figure 3:** Products of carbonyl reduction using Ni/RH. Reaction conditions (if not state differently): 70 °C, 25 bar H<sub>2</sub>, 2 mmol of substrate, 4 h, in 2 ml of H<sub>2</sub>O/THF (4:1), 20 mg catalyst (1.8 mol% of Ni).

The strong selectivity towards the anti-Markovnikov alcohol can be explained by the proposed reaction mechanism (Scheme 2). In the Lewis acid catalyzed step, a carbocationic intermediate is formed after one hydroxy moiety is eliminated.<sup>[73]</sup> This cation is better stabilized when localized closer to strong electron donating groups, being thus no preferred localization in cyclohexane-1,2-diol, while there is a marked regioselectivity in 1-phenylethane-1,2-diol due to the strong inductive effect of the phenyl group.<sup>[73]</sup> Additionally, various carbonyl intermediates were isolated, strongly suggesting that the reaction follows this pathway. The last reaction step is the hydrogenation of the carbonyl groups catalyzed by the nickel nanoparticles fixed on the RH support. The ability of nickel catalysts to promote this kind of reaction is well known, and amply described in several publications.<sup>[80-82]</sup> In principle, a direct hydrogenation via hydride transfer from the nickel catalyst (which would make the Lewis/Brønsted sites redundant),<sup>[24]</sup> cannot be easily ruled out. However, it will be equally hard to prove to which extend this direct hydrogenation competes with the acid-mediated alternative, as the latter species are inherent to the nature of the used bio-derived support.

Moreover, all previously reported systems catalyzing the conversion of epoxides to anti-Markovnikov alcohols require of the separate addition of a Brønsted acid, a Lewis acid (or high temperatures for thermal activation) and a hydrogenation catalyst,<sup>[26, 28, 83, 84]</sup> the presented Ni/RH composite offers all three abilities in one material.



**Scheme 2:** Proposed reaction mechanism for the selective conversion of epoxides to anti-Markovnikov alcohols using Ni/RH as catalyst. This catalyst shows a triple reactivity, acting at the same time as Brønsted acid (I), solid Lewis acid (LA, II), and as hydrogenation catalyst (III).

## Conclusions

Herein we report the synthesis and full characterization of an inexpensive catalyst for the selective anti-Markovnikov ring-opening hydrogenation of epoxides. The catalyst was prepared by pyrolysis waste rice husk impregnated with nickel nitrate. The catalyst is highly active, selective, and can be easily recycled without any apparent performance decrease (after 10 runs). Mechanistic investigations suggest an unprecedented triple reactivity of the catalysts, acting at the same time as Brønsted acid, Lewis acid, and as hydrogenation catalyst. These features are attributed to the nickel nanoparticles deposited at the rice husk ashes' surface, as well as to the acidic properties of the bio-derived support.

The generality of this catalyst was showcased with the successful reduction of various carbonyl compounds, also yielding the corresponding anti-Markovnikov alcohols. Furthermore, the intermediacy of an aldehyde in this transformation opens several alternative applications, as this reactive intermediate might be trapped by various nucleophiles, like primary amines, leading to amides or to complex secondary amines.<sup>[85, 86]</sup>



## RESEARCH ARTICLE

Moreover, these results further demonstrate the immense potential of rice biowaste as a source of higher added-value materials, beyond their traditional use as fertilizer and cheap heat source, and posing a utilization alternative to alleviate the toll of its current waste management.

## Experimental

## Materials and methods

Completed details on the materials employed (chemicals, solvents, and rice waste samples), characterization methods (STEM, XPS, XRD, IR, BET, TGA-MS, TPx and NMR spectra of all synthesized substrates), as well as recycling-, hot filtration-, indicator- and Corma's acetal-experiments can be found in the Electronic Supplementary Information (ESI) file.

## Synthetic procedures

**Catalyst Synthesis:** Sun-dried rice husk samples were collected at farming sites in Vietnam (see ESI for further details). The plant material was then shredded with a cutting mill SM 200 (rotation and speed 1000 rpm, 2 mm sieve sizes) and milled in a ball mill PM 200 in steel cups with steel balls at 400 rpm for 3 h to give a fine powder (RH). In a typical experiment 2 g RH were mixed with 368 mg nickel nitrate in 50 ml ethanol by stirring at 21 °C for 24 h. Subsequently, the solvent was removed in a rotary evaporator. The Ni-impregnated RH was pyrolyzed at a rate of 10 K/min in a quartz tube furnace under inert atmosphere (nitrogen at 50 ml/min). After reaching the pyrolysis temperature (400–1000 °C), this was maintained for 1 h. The catalyst was then allowed to cool under nitrogen atmosphere and was stored under ambient conditions.

**Catalytic experiments (General procedure):** The general procedure for the product preparation is given exemplarily for 2-phenylethan-1-ol (**1a**). The other products were synthesized following the general procedure (see ESI file). 2-phenyloxirane (2 mmol, 240 µl), 20 mg of Ni/RH catalyst and 2 ml of a H<sub>2</sub>O/THF mixture (4:1) were added together in a 12 ml vial, equipped with a Teflon coated magnetic stirrer and a steel cannula (0.45 x 12 mm) through the top. The vial was placed in an autoclave and flushed three times with hydrogen at a pressure of 25 bar. The autoclave vessel was heated for 4 hours at 50 °C in an aluminum block. The autoclave was cooled down to room temperature in an ice bath and 2 ml ethyl acetate was added. The mixture was filtered through a syringe filter, the sample was washed two more times with ethyl acetate and filtered. After performing TLC, the product was fixed on silica and purified by column chromatography on silica gel (heptane/ethyl acetate 1:1). The product was collected with a retention time of R<sub>f</sub> = 0.4. The desired product was a yellowish liquid (180 mg; yield 98 %).

## Author Contributions

F. Unglaube conceptualised the work, planned and conducted experiments, and co-wrote the manuscript. H. Atia, S. Bartling, and C. Kreyenschulte performed and interpreted the solid-state analysis of the catalysts. E. Mejia conceptualised and planned the research, supervised the work, and co-wrote the manuscript. All authors revised and authorized the final version of the manuscript.

## Conflicts of interest

There are no conflicts to declare.

## Acknowledgements

We would like to thank all the Vietnamese farmers and local authorities at the sample collection sites for their help and hospitality. We would like to acknowledge Xuewen Guo for helpful discussions and inspiration. Also, thanks to Kathleen Schubert as well as Reinhard Eckelt for performing the XRD and BET-surface measurements (respectively), and for their helpful comments and discussions. This work has been supported by the RoHan Project funded by the German Academic Exchange Service (DAAD, No. 57315854) and the Federal Ministry for Economic Cooperation and Development (BMZ) inside the framework "SDG Bilateral Graduate school programme". Furthermore, we would like to acknowledge the funding for the SUVALIG project from the German Federal Ministry of Education and Research (BMBF, 031B0707B).

**Keywords:** Biomass • Rice Husk • Epoxides • Nickel • Hydrogenation

- [1] Y. Zou, T. Yang, in *Rice Bran and Rice Bran Oil*, Elsevier, 2019, pp. 207–246.
- [2] L. Domínguez - Escribá, M. Porcar, 'Rice straw management: the big waste', *Biofuels, Bioproducts and Biorefining* **2010**, *4*, 154–159.
- [3] K. Lasko, K. Vadrevu, 'Improved rice residue burning emissions estimates: Accounting for practice-specific emission factors in air pollution assessments of Vietnam', *Environmental Pollution* **2018**, *236*, 795–806.
- [4] M. F. Khan, M. T. Latif, W. H. Saw, N. Aml, M. Nadzir, M. Sahani, N. Tahir, J. Chung, 'Fine particulate matter in the tropical environment: monsoonal effects, source apportionment, and health risk assessment', *Atmospheric Chemistry and Physics* **2016**, *16*, 597–617.
- [5] S. You, Y. W. Tong, K. G. Neoh, Y. Dai, C.-H. Wang, 'On the association between outdoor PM<sub>2.5</sub> concentration and the seasonality of tuberculosis for Beijing and Hong Kong', *Environmental Pollution* **2016**, *218*, 1170–1179.
- [6] F. Unglaube, A. Lammers, C. R. Kreyenschulte, M. Laik, E. Mejia, 'Preparation, Characterization and Antimicrobial Properties of Nanosized Silver - Containing Carbon/Silica Composites from Rice Husk Waste', *ChemistryOpen* **2021**, *10*, 1244–1250.
- [7] F. Unglaube, C. R. Kreyenschulte, E. Mejia, 'Development and Application of Efficient Ag - based Hydrogenation Catalysts Prepared from Rice Husk Waste', *ChemCatChem* **2021**, *13*, 2583–2591.
- [8] F. Unglaube, J. Schlapp, A. Quade, J. Schäfer, E. Mejia, 'Highly active heterogeneous hydrogenation catalysts prepared from cobalt complexes and rice husk waste', *Catalysis Science & Technology* **2022**.
- [9] F. Freitag, T. Irgang, R. Kempe, 'Cobalt - Catalyzed Alkylation of Secondary Alcohols with Primary Alcohols via Borrowing Hydrogen/Hydrogen Autotransfer', *Chemistry - A European Journal* **2017**, *23*, 12110–12113.
- [10] R. Ciriminna, V. Pandarus, F. Beland, Y.-J. Xu, M. Pagliaro, 'Heterogeneously catalyzed alcohol oxidation for the fine chemical industry', *Organic Process Research & Development* **2015**, *19*, 1554–1558.
- [11] J. H. Sattler, M. Fuchs, K. Tauber, F. G. Mutti, K. Faber, J. Pfeiffer, T. Haas, W. Kroutil, 'Redox self - sufficient

## RESEARCH ARTICLE

- biocatalyst network for the amination of primary alcohols', *Angewandte Chemie* **2012**, *124*, 9290-9293.
- [12] T. Oishi, K. Yamaguchi, N. Mizuno, 'Catalytic oxidative synthesis of nitriles directly from primary alcohols and ammonia', *Angewandte Chemie* **2009**, *121*, 6404-6406.
- [13] S. Sabater, J. A. Mata, E. Peris, 'Dual catalysis with an Ir(III)-Au heterodimetallic complex: reduction of nitroarenes by transfer hydrogenation using primary alcohols', *Chemistry-A European Journal* **2012**, *18*, 6380-6385.
- [14] A. Friedrich, S. Schneider, 'Acceptorless Dehydrogenation of Alcohols: Perspectives for Synthesis and H<sub>2</sub> Storage', *ChemCatChem* **2009**, *1*, 72-73.
- [15] P. Eilbracht, L. Bärfacker, C. Buss, C. Hollmann, B. E. Kitsos-Rzychon, C. L. Kranemann, T. Rische, R. Roggenbuck, A. Schmidt, 'Tandem reaction sequences under hydroformylation conditions: new synthetic applications of transition metal catalysis', *Chemical reviews* **1999**, *99*, 3329-3366.
- [16] K. Takahashi, M. Yamashita, T. Ichihara, K. Nakano, K. Nozaki, 'High-Yielding Tandem Hydroformylation/Hydrogenation of a Terminal Olefin to Produce a Linear Alcohol Using a Rh/Ru Dual Catalyst System', *Angewandte Chemie* **2010**, *122*, 4590-4592.
- [17] T. Hayashi, Y. Matsumoto, Y. Ito, 'Catalytic asymmetric hydroboration of styrenes', *Journal of the American Chemical Society* **1989**, *111*, 3426-3428.
- [18] C. Li, W. Wang, L. Yan, Y. Ding, 'A mini review on strategies for heterogenization of rhodium-based hydroformylation catalysts', *Frontiers of Chemical Science and Engineering* **2018**, *12*, 113-123.
- [19] R. Franke, D. Selent, A. Bömer, 'Applied hydroformylation', *Chemical reviews* **2012**, *112*, 5675-5732.
- [20] S. Panke, M. Held, M. G. Wubbols, B. Witholt, A. Schmid, 'Pilot-scale production of (S)-styrene oxide from styrene by recombinant *Escherichia coli* synthesizing styrene monooxygenase', *Biotechnology and bioengineering* **2002**, *80*, 33-41.
- [21] Z. Yang, S. Zhang, H. Zhao, A. Li, L. Luo, L. Guo, 'Subnano-FeO<sub>x</sub> Clusters Anchored in an Ultrathin Amorphous Al<sub>2</sub>O<sub>3</sub> Nanosheet for Styrene Epoxidation', *ACS Catalysis* **2021**, *11*, 11542-11550.
- [22] J. Wenz, H. Wadepohl, L. H. Gade, 'Regioselective hydrosilylation of epoxides catalysed by nickel(II) hydride complexes', *Chemical Communications* **2017**, *53*, 4308-4311.
- [23] M. Vayer, S. Zhang, J. Moran, D. Leboeuf, 'Rapid and Mild Metal-Free Reduction of Epoxides to Primary Alcohols Mediated by HFIP', *ACS Catalysis* **2022**, *12*, 3309-3316.
- [24] K. A. Steiniger, T. H. Lambert, 'Primary Alcohols via Nickel Pentacarboxycyclopentadienyl Diamide Catalyzed Hydrosilylation of Terminal Epoxides', *Organic Letters* **2021**, *23*, 8013-8017.
- [25] G. Dong, P. Teo, Z. K. Wickens, R. H. Grubbs, 'Primary alcohols from terminal olefins: formal anti-Markovnikov hydration via triple relay catalysis', *Science* **2011**, *333*, 1609-1612.
- [26] X. Liu, L. Longwitz, B. Spiegelberg, J. Tönjes, T. Beweries, T. Werner, 'Erbium-Catalyzed Regioselective Isomerization-Cobalt-Catalyzed Transfer Hydrogenation Sequence for the Synthesis of Anti-Markovnikov Alcohols from Epoxides under Mild Conditions', *ACS Catalysis* **2020**, *10*, 13659-13667.
- [27] S. Thiagarajan, C. Gunanathan, 'Catalytic Hydrogenation of Epoxides to Alcohols', *Chemistry-An Asian Journal* **2022**.
- [28] W. Liu, W. Li, A. Spannenberg, K. Junge, M. Beller, 'Iron-catalysed regioselective hydrogenation of terminal epoxides to alcohols under mild conditions', *Nature Catalysis* **2019**, *2*, 523-528.
- [29] C. Yao, T. Dahmen, A. Gansäuer, J. Norton, 'Anti-Markovnikov alcohols via epoxide hydrogenation through cooperative catalysis', *Science* **2019**, *364*, 764-767.
- [30] S. Muru, K. M. Nicholas, R. S. Srivastava, 'Ruthenium(II) sulfoxides-catalyzed hydrogenolysis of glycols and epoxides', *Journal of Molecular Catalysis A: Chemical* **2012**, *363*, 460-464.
- [31] T. N. Plank, J. L. Drake, D. K. Kim, T. W. Funk, 'Air-Stable, Nitrile-Ligated (Cyclopentadienone)iron Dicarboxyl Compounds as Transfer Reduction and Oxidation Catalysts', *Advanced Synthesis & Catalysis* **2012**, *354*, 597-601.
- [32] H. Fujitsu, S. Shirahama, E. Matsumura, K. Takeshita, I. Mochida, 'Catalytic hydrogenation of styrene oxide with cationic rhodium complexes', *The Journal of Organic Chemistry* **1981**, *46*, 2287-2290.
- [33] M. Duval, V. Deboos, A. Hallonet, G. Sagorin, A. Denicourt-Nowicki, A. Roucoux, 'Selective palladium nanoparticles-catalyzed hydrogenolysis of industrially targeted epoxides in water', *Journal of Catalysis* **2021**, *396*, 261-268.
- [34] T. Yamada, W. Teranishi, K. Park, J. Jiang, T. Tachikawa, S. Furusato, H. Sajiki, 'Development of Carbon-Neutral Cellulose-Supported Heterogeneous Palladium Catalysts for Chemoselective Hydrogenation', *ChemCatChem* **2020**, *12*, 4052-4058.
- [35] I. Kim, F. Medina, X. Rodríguez, Y. Cesteros, P. Salagre, J. Sueiras, 'Preparation of 2-phenylethanol by catalytic selective hydrogenation of styrene oxide using palladium catalysts', *Journal of Molecular Catalysis A: Chemical* **2005**, *239*, 215-221.
- [36] M. S. Newman, G. Underwood, M. Renoll, 'The reduction of terminal epoxides', *Journal of the American Chemical Society* **1949**, *71*, 3362-3363.
- [37] R. C. Sun, M. Okabe, '(2S,4S)-2,4,5-Trihydroxypentanoic acid, 5-Acetonide Methyl Ester: D-erythro-Pentonic acid, 3-deoxy-4,5-O-(1-methylethylidene)-, methyl ester', *Organic Syntheses* **2003**, *72*, 48-48.
- [38] I. Vicente, P. Salagre, Y. Cesteros, 'Ni nanoparticles supported on microwave-synthesised hectorite for the hydrogenation of styrene oxide', *Applied Catalysis A: General* **2011**, *408*, 31-37.
- [39] S. K. Kanojia, G. Shukla, S. Sharma, R. Dwivedi, P. Sharma, R. Prasad, M. Satakar, S. Kane, 'Hydrogenation of Styrene Oxide to 2-Phenylethanol over Nanocrystalline Ni Prepared by Ethylene Glycol Reduction Method', *International Journal of Chemical Engineering* **2014**, *2014*.
- [40] O. Bergadá, P. Salagre, Y. Cesteros, F. Medina, J. E. Sueiras, 'High-selective Ni-MgO catalysts for a clean obtention of 2-phenylethanol', *Applied Catalysis A: General* **2004**, *272*, 125-132.
- [41] A. Sasu, B. Dragoi, A. Ungureanu, S. Royer, E. Dumitriu, V. Hulea, 'Selective conversion of styrene oxide to 2-phenylethanol in cascade reactions over non-noble metal catalysts', *Catalysis Science & Technology* **2016**, *6*, 468-478.
- [42] I. Vicente, P. Salagre, Y. Cesteros, 'Ni nanoparticles supported on microwave-synthesised saponite for the hydrogenation of styrene oxide', *Applied clay science* **2011**, *53*, 212-219.
- [43] T. Yamada, A. Ogawa, H. Masuda, W. Teranishi, A. Fujii, K. Park, Y. Ashikari, N. Tomiyasu, T. Ichikawa, R. Miyamoto, 'Pd catalysts supported on dual-pore monolithic silica beads for chemoselective hydrogenation under batch and flow reaction conditions', *Catalysis Science & Technology* **2020**, *10*, 6359-6367.
- [44] T. Hattori, A. Tsubone, Y. Sawama, Y. Monguchi, H. Sajiki, 'Systematic evaluation of the palladium-catalyzed hydrogenation under flow conditions', *Tetrahedron* **2014**, *70*, 4790-4798.
- [45] T. G. Chuah, A. Jumasiah, I. Azni, S. Katayon, S. T. Choong, 'Rice husk as a potentially low-cost biosorbent for heavy metal and dye removal: an overview', *Desalination* **2005**, *175*, 305-316.
- [46] Y. Shen, K. Yoshikawa, 'Tar conversion and vapor upgrading via in situ catalysis using silica-based nickel nanoparticles embedded in rice husk char for biomass



## RESEARCH ARTICLE

- pyrolysis/gasification', *Industrial & Engineering Chemistry Research* **2014**, *53*, 10929-10942.
- [47] Y. Shen, P. Zhao, Q. Shao, 'Porous silica and carbon derived materials from rice husk pyrolysis char', *Microporous and Mesoporous Materials* **2014**, *188*, 46-76.
- [48] B. J. Matoso, K. Ranganathan, B. K. Mutuma, T. Lerotholi, G. Jones, N. J. Coville, 'Time-dependent evolution of the nitrogen configurations in N-doped graphene films', *RSC advances* **2016**, *6*, 106914-106920.
- [49] M. Bihani, P. P. Bora, M. Nachtegaal, J. B. Jasinski, S. Plummer, F. Gallou, S. Handa, 'Microballs containing Ni (0) Pd (0) nanoparticles for highly selective micellar catalysis in water', *ACS Catalysis* **2019**, *9*, 7520-7526.
- [50] N. Danilovic, R. Subbaraman, D. Strmcnik, K. C. Chang, A. Paulikas, V. Stamenkovic, N. M. Markovic, 'Enhancing the alkaline hydrogen evolution reaction activity through the bifunctionality of Ni(OH) 2/metal catalysts', *Angewandte Chemie* **2012**, *124*, 12663-12666.
- [51] J.-C. Dupin, D. Gonbeau, P. Vinatier, A. Levasseur, 'Systematic XPS studies of metal oxides, hydroxides and peroxides', *Physical Chemistry Chemical Physics* **2000**, *2*, 1319-1324.
- [52] D. Formenti, F. Ferretti, C. Topf, A.-E. Surkus, M.-M. Pohl, J. Radnik, M. Schneider, K. Junge, M. Beller, F. Ragaini, 'Co-based heterogeneous catalysts from well-defined  $\alpha$ -imine complexes: Discussing the role of nitrogen', *Journal of Catalysis* **2017**, *351*, 79-89.
- [53] B. Sahoo, D. Formenti, C. Topf, S. Bachmann, M. Scalone, K. Junge, M. Beller, 'Biomass - Derived Catalysts for Selective Hydrogenation of Nitroarenes', *ChemSusChem* **2017**, *10*, 3035-3039.
- [54] D. Formenti, R. Mocci, H. Atia, S. Dastgir, M. Anwar, S. Bachmann, M. Scalone, K. Junge, M. Beller, 'A State - of - the - Art Heterogeneous Catalyst for Efficient and General Nitrile Hydrogenation', *Chemistry - A European Journal* **2020**, *26*, 15589-15595.
- [55] M. Zielinski, R. Wojcieszak, S. Monteveddi, M. Mercy, M. Bettahar, 'Hydrogen storage in nickel catalysts supported on activated carbon', *International Journal of Hydrogen Energy* **2007**, *32*, 1024-1032.
- [56] K. Sing, D. Everett, R. Haul, L. Moscou, R. Pierotti, J. Rouquerol, T. Siemieniowska, 'Physical and biophysical chemistry division commission on colloid and surface chemistry including catalysis', *Pure Appl. Chem* **1985**, *57*, 603-619.
- [57] K. A. Carrado, R. Csencsits, P. Thiyagarajan, S. Seifert, S. M. Macha, J. S. Harwood, 'Crystallization and textural porosity of synthetic clay minerals', *Journal of Materials Chemistry* **2002**, *12*, 3228-3237.
- [58] Z. Qian, G. Hu, S. Zhang, M. Yang, 'Preparation and characterization of montmorillonite-silica nanocomposites: A sol-gel approach to modifying clay surfaces', *Physica B: Condensed Matter* **2008**, *403*, 3231-3238.
- [59] F. Adam, L. Muniandy, R. Thankappan, 'Ceria and titania incorporated silica based catalyst prepared from rice husk: adsorption and photocatalytic studies of methylene blue', *Journal of Colloid and Interface Science* **2013**, *406*, 209-216.
- [60] M. V. Baldoval, A. Corma, V. Fornés, H. García, A. Martínez, J. Primo, 'Soft and hard acidity in ion-exchanged Y zeolites: rearrangement of 2-bromopropiophenone ethylene acetal to 2-hydroxyethyl 2-phenylpropanoate', *Journal of the Chemical Society, Chemical Communications* **1992**, 949-951.
- [61] F. Algarra, A. Corma, V. Fornés, H. García, A. Martínez, J. Primo, in *Studies in Surface Science and Catalysis*, Vol. 78, Elsevier, 1993, pp. 653-660.
- [62] A. Corma, H. García, M. A. Miranda, J. Primo, M. J. Sabater, 'Modification of the photochemical reactivity of the cyclic ethylene acetal of  $\alpha$ -bromopropiophenone by adsorption within zeolites. A combined contribution of Lewis acidity and cage effect in the formation of a 2-phenylpropanoate via 1, 2-phenyl shift', *The Journal of Organic Chemistry* **1993**, *58*, 6892-6894.
- [63] A. Corma, H. García, A. Primo, A. Domenech, 'A test reaction to assess the presence of Brønsted and the softness/hardness of Lewis acid sites in palladium supported catalysts', *New Journal of Chemistry* **2004**, *28*, 361-365.
- [64] A. Corma, P. Serna, 'Chemoselective Hydrogenation of Nitro Compounds with Supported Gold Catalysts', *Science* **2006**, *313*, 332-334.
- [65] M. Boronat, P. Concepción, A. Corma, S. González, F. Illas, P. Serna, 'A Molecular Mechanism for the Chemoselective Hydrogenation of Substituted Nitroaromatics with Nanoparticles of Gold on TiO2 Catalysts: A Cooperative Effect between Gold and the Support', *Journal of the American Chemical Society* **2007**, *129*, 16230-16237.
- [66] A. Corma, P. Concepción, P. Serna, 'A Different Reaction Pathway for the Reduction of Aromatic Nitro Compounds on Gold Catalysts', *Angewandte Chemie International Edition* **2007**, *46*, 7266-7269.
- [67] A. Dhakshinamoorthy, M. Alvaro, A. Corma, H. García, 'Delineating similarities and dissimilarities in the use of metal organic frameworks and zeolites as heterogeneous catalysts for organic reactions', *Dalton Transactions* **2011**, *40*, 6344-6360.
- [68] B. H. Lipshutz, S. Ghorai, A. R. Abela, R. Moser, T. Nishikata, C. Duplais, A. Krasovskiy, R. D. Gaston, R. C. Gadwood, 'TPGS-750-M: A Second-Generation Amphiphile for Metal-Catalyzed Cross-Couplings in Water at Room Temperature', *The Journal of Organic Chemistry* **2011**, *76*, 4379-4391.
- [69] P. Ryabchuk, G. Agostini, M.-M. Pohl, H. Lund, A. Agapova, H. Junge, K. Junge, M. Beller, 'Intermetallic nickel silicide nanocatalyst—A non-noble metal-based general hydrogenation catalyst', *Science advances* **2018**, *4*, eaat0761.
- [70] M. Verhaak, A. Van Dillen, J. Geus, 'The selective hydrogenation of acetonitrile on supported nickel catalysts', *Catalysis Letters* **1994**, *26*, 37-53.
- [71] J. Krupka, J. Pasek, 'Nitrile hydrogenation on solid catalysts—New insights into the reaction mechanism', *Current Organic Chemistry* **2012**, *16*, 988-1004.
- [72] Z. Wang, Y.-T. Cui, Z.-B. Xu, J. Qu, 'Hot water-promoted ring-opening of epoxides and aziridines by water and other nucleophiles', *The Journal of Organic Chemistry* **2008**, *73*, 2270-2274.
- [73] J.-L. Wang, H.-J. Li, H.-S. Wang, Y.-C. Wu, 'Regioselective 1, 2-Diol Rearrangement by Controlling the Loading of BF3·Et2O and Its Application to the Synthesis of Related Nor-Sesquiterene- and Sesquiterene-Type Marine Natural Products', *Organic Letters* **2017**, *19*, 3811-3814.
- [74] V. L. Mamedova, Z. K. Gul'naz, 'The Meinwald rearrangement in tandem processes (microreview)', *Chemistry of Heterocyclic Compounds* **2017**, *53*, 976-978.
- [75] J. Xu, Y. Song, J. He, S. Dong, L. Lin, X. Feng, 'Asymmetric Catalytic Vinylogous Addition Reactions Initiated by Meinwald Rearrangement of Vinyl Epoxides', *Angewandte Chemie International Edition* **2021**.
- [76] Z.-L. Song, C.-A. Fan, Y.-Q. Tu, 'Semipinacol rearrangement in natural product synthesis', *Chemical Reviews* **2011**, *111*, 7523-7556.
- [77] A. K. Pandey, A. Ghosh, P. Banerjee, 'Lewis-acid-catalysed tandem meinwald rearrangement/intermolecular [3+ 2]-cycloaddition of epoxides with donor-acceptor cyclopropanes: synthesis of functionalized tetrahydrofurans', *Eur. J. Org. Chem* **2015**, 2517, 2523.
- [78] J. Bah, V. R. Naidu, J. Teske, J. Franzén, 'Carbocations as Lewis acid catalysts: Reactivity and scope', *Advanced Synthesis & Catalysis* **2015**, *357*, 148-158.
- [79] T. E. Davies, S. A. Kondrat, E. Nowicka, J. L. Kean, C. M. Harris, J. M. Socci, D. C. Apperley, S. J. Taylor, A. E. Graham, 'Nanoporous alumino- and borosilicate-mediated Meinwald rearrangement of epoxides', *Applied Catalysis A: General* **2015**, *493*, 17-24.

## RESEARCH ARTICLE

- [80] D. Formenti, F. Ferretti, F. K. Schamagl, M. Beller, 'Reduction of nitro compounds using 3d-non-noble metal catalysts', *Chemical reviews* **2018**, *119*, 2611-2680.
- [81] Y. Zhang, H. Yang, Q. Chi, Z. Zhang, 'Nitrogen - Doped Carbon - Supported Nickel Nanoparticles: A Robust Catalyst to Bridge the Hydrogenation of Nitriles and the Reductive Amination of Carbonyl Compounds for the Synthesis of Primary Amines', *ChemSusChem* **2019**, *12*, 1246-1255.
- [82] M. Heitbaum, F. Glorius, I. Escher, 'Asymmetric heterogeneous catalysis', *Angewandte Chemie International Edition* **2006**, *45*, 4732-4762.
- [83] A. Gansäuer, C. A. Fan, F. Keller, P. Karbaum, 'Regiodivergent epoxide opening: a concept in stereoselective catalysis beyond classical kinetic resolutions and desymmetrizations', *Chemistry-A European Journal* **2007**, *13*, 8084-8090.
- [84] J. Jiang, S. Yoon, 'An aluminum (iii) picket fence phthalocyanine-based heterogeneous catalyst for ring-expansion carbonylation of epoxides', *Journal of Materials Chemistry A* **2019**, *7*, 6120-6125.
- [85] P.-Q. Huang, Y.-H. Huang, K.-J. Xiao, Y. Wang, X.-E. Xia, 'A General Method for the One-Pot Reductive Functionalization of Secondary Amides', *The Journal of Organic Chemistry* **2015**, *80*, 2861-2868.
- [86] C. L. Allen, S. Davulcu, J. M. J. Williams, 'Catalytic Acylation of Amines with Aldehydes or Aldoximes', *Organic Letters* **2010**, *12*, 5096-5099.

## Curriculum Vitae

### Personal Data:

Name	Felix Unglaube
Date of birth	12.12.1993, in Bad Saarow-Pieskow
Civil status	unwed

### Educational and Academic Training:

2012	Abitur at catholic high school Bernhardinum, Fürstenwalde/Spree
2012 to 2016	Studies in chemistry (Bachelor of Science) at University of Rostock. Thesis with Prof. Martin Köckerling
2016 to 2018	Studies in chemistry (Master of Science) at University of Rostock. Thesis with Prof. Udo Kragl
2018 to 2022	Doctorate with Prof. Udo Kragl and Dr. habil. Esteban Mejia at Leibniz Institute for Catalysis

### Professional Experience:

2014 to 2016	Student assistant at University of Rostock, Institute for chemistry, Department for solid state chemistry
2016 to 2017	Internship at Leibniz Institute for Catalysis
2017 to 2018	Seminar facilitator: „Basis of chemistry for physicians“
2017 to 2018	Student assistant at Leibniz Institute for Catalysis
2018 to 2020	Seminar facilitator: „Chemistry for agricultural engineers and agronomist“
2018 to 2022	Research assistant at Leibniz Institute for Catalysis
Since 2022	Development Engineer at CORTRONIK GmbH

## Publications

### Peer-Reviewed scientific publications:

- [1] R. Brišar, F. Unglaube, D. Hollmann, H. Jiao and E. Mejía (2018). Aerobic Oxidative Homo-and Cross-Coupling of Amines Catalyzed by Phenazine Radical Cations. *The Journal of organic chemistry*, 83(21), 13481-13490.
- [2] F. Unglaube, P. Hünemörder, X. Guo, Z. Chen, D. Wang and E. Mejia (2020). Phenazine Radical Cations as Efficient Homogeneous and Heterogeneous Catalysts for the Cross-Dehydrogenative Aza-Henry Reaction. *Helvetica Chimica Acta*, 103(12),e2000184
- [3] F. Unglaube, C. R. Kreyenschulte and E. Mejia (2021). Development and Application of Efficient Ag-based Hydrogenation Catalysts Prepared from Rice Husk Waste. *ChemCatChem*, 13(11), 2583-2591
- [4] F. Unglaube, A. Lammers, C. R. Kreyenschulte, M. Lalk and E. Mejia (2021). Preparation, Characterization and Antimicrobial Properties of Nanosized Silver-Containing Carbon/Silica Composites from Rice Husk Waste. *ChemistryOpen*, 10(12), 1244.
- [5] F. Unglaube, J. Schlapp, A. Quade, J. Schafer and E. Mejia (2022) Highly Active Heterogenous Hydrogenation Catalysts Prepared from Cobalt Complexes and Rice Husk Waste *Catalysis Science & Technology*, 12, 3123-3136
- [6] F. Unglaube, H. Atia, S. Bartling, C. Kreyenschulte and E. Mejia. *Helvetica Chimica Acta* (2022), Hydrogenation of Epoxides to Anti-Markovnikov Alcohols over a Nickel Heterogenous Catalyst Prepared from Biomass (Rice) Waste *Helvetica Chimica Acta* e202200167

### Book chapter:

- [7] F. Unglaube and E. Mejia, (2020). Aerobic Oxidations Reactions. *Catalytic Aerobic Oxidations*, Chapter 5: Aerobic oxidations reactions using metal-free homogeneous systems, RSC Catalysis Series, Royal Society of Chemistry, ISSN 17576733

---

Lectures at international conferences:

[8] F. Unglaube, R. Brisar, D. Hollmann and E. Mejia: Phenazine as a Metal Free Catalyst, 2nd RoHan DAAD SDG Workshop **2018**, Hanoi, Vietnam, 2018

[9] F. Unglaube, R. Brisar, D. Hollmann, H. Jiao and E. Mejia: Phenazine Radical Cations as a Metal Free Oxidation Catalyst, 52. Jahrestreffen Deutscher Katalytiker, Weimar, Germany, **2019**

[10] F. Unglaube and E. Mejia: Development and tuning of a bio derived heterogeneous catalyst from agricultural waste, 54. Jahrestreffen Deutscher Katalytiker, Weimar (digital), Germany, **2021**

Poster at international conferences:

[11] F. Unglaube and E. Mejia: Aerobic Oxidative Homo-and Cross-Coupling of Amines Catalyzed by Radical Cations, 7th EuCheMS Chemistry Congress, Liverpool, United Kingdom, **2018**

[12] F. Unglaube, R. Brisar, D. Hollmann and E. Mejia: Phenazine as a Metal Free Catalyst, 2nd RoHan DAAD SDG Workshop 2018, Hanoi, Vietnam, **2018**

[13] R. Brisar, F. Unglaube, D. Wang and E. Majía: Persistent Radical Cations as Catalysts for Aerobic Oxidative Amine Coupling Reactions, Hanse Chemistry Symposium 2019, Rostock, Germany, **2019**

[14] F. Unglaube and E. Mejia: Development and tuning of a bio derived heterogeneous catalyst from agricultural waste, 54. Jahrestreffen Deutscher Katalytiker, Weimar (digital), Germany, **2021**

[15] F. Unglaube and E. Mejia: Heterogenous rice husk based catalyst tuned by silica leaching, 10th International Symposium on Silicon Chemistry, Toulouse (digital), French, **2021**